



City Research Online

City, University of London Institutional Repository

Citation: Papageorgiou, G. N. (1997). A computer-aided design approach to the modelling of sound energy radiation in bounded spatial systems. (Unpublished Doctoral thesis, City, University of London)

This is the accepted version of the paper.

This version of the publication may differ from the final published version.

Permanent repository link: <https://openaccess.city.ac.uk/id/eprint/31102/>

Link to published version:

Copyright: City Research Online aims to make research outputs of City, University of London available to a wider audience. Copyright and Moral Rights remain with the author(s) and/or copyright holders. URLs from City Research Online may be freely distributed and linked to.

Reuse: Copies of full items can be used for personal research or study, educational, or not-for-profit purposes without prior permission or charge. Provided that the authors, title and full bibliographic details are credited, a hyperlink and/or URL is given for the original metadata page and the content is not changed in any way.

City Research Online:

<http://openaccess.city.ac.uk/>

publications@city.ac.uk

A COMPUTER-AIDED DESIGN
APPROACH TO THE
MODELLING OF SOUND
ENERGY RADIATION IN
BOUNDED SPATIAL SYSTEMS

by

George Nathaniel Papageorgiou

A thesis submitted in partial fulfilment of
the requirements for the degree of

Doctor of Philosophy

City University

Department of Mechanical Engineering
and Aeronautics

June 1997

TABLE OF CONTENTS

ABSTRACT	1
1. INTRODUCTION.....	3
2. THEORETICAL BACKGROUND	10
2.1. INTRODUCTION.....	10
2.2. GENERAL DESCRIPTION OF SOUND	10
2.3. PROPAGATION OF SOUND WAVES	11
2.3.1. <i>Sound Power, Pressure, Intensity, Loudness and Sound Level</i>	11
2.3.2. <i>Speed of Sound</i>	13
2.3.3. <i>Reflection of Sound Waves</i>	13
2.3.4. <i>Reflection from a Curved Surface</i>	14
2.3.5. <i>Scattering of Sound</i>	15
2.3.6. <i>Refraction and Transmission of Sound</i>	15
2.3.7. <i>Interference and Standing Waves</i>	16
2.3.8. <i>Diffraction</i>	17
2.3.9. <i>Sound Wave Equation</i>	18
2.4. GEOMETRICAL ACOUSTICS APPROACH.....	19
2.3.10. <i>Validity of the Geometrical Approach</i>	20
2.4. ARCHITECTURAL ACOUSTICS PARAMETERS.....	20
2.4.1. <i>Free Sound Field</i>	21
2.4.2. <i>Diffuse Sound Field</i>	21
2.4.3. <i>Mean Free Path</i>	21
2.4.4. <i>Reflection Density</i>	22
2.4.5. <i>The Combined Direct and Diffuse field</i>	23
2.4.6. <i>Coupled Rooms</i>	23
2.5. CRITERIA FOR ASSESSMENT	24
2.5.1. <i>Reverberation Time (RT_{60})</i>	24
2.5.2. <i>Early Decay Time (EDT)</i>	24
2.5.3. <i>Definition</i>	24
2.5.4. <i>Clarity</i>	24
2.5.5. <i>Sound Spatial Impression</i>	25
2.6. ACOUSTICAL SIGNAL THEORY	25
2.6.1. <i>Dirac Delta Function</i>	25
2.6.2. <i>Impulse Response</i>	26
2.6.3. <i>Sampling</i>	26
2.6.4. <i>Decimation-Interpolation</i>	27
2.6.5. <i>Schroeder's Integrated Impulse Response</i>	27
2.6.6. <i>Spectrum - Frequency Response - Room Transfer Function</i>	28
2.6.7. <i>Auralization, the Ultimate Goal</i>	28
3. MODELLING OF SOUND FIELDS IN BOUNDED SPATIAL SYSTEMS	31
3.1. INTRODUCTION.....	31
3.2. PHYSICAL ACOUSTICAL MODELLING	32
3.2.1. <i>Water-Wave Models and Sound Pulse Photography</i>	32
3.2.2. <i>Light-Ray Models</i>	32
3.2.3. <i>Three-dimensional Scale Acoustical Models</i>	33
3.3. EMPIRICAL MODELS (SABINE).....	33
3.4. STATISTICAL MODELLING	34

3.4.1. Eyring's Model.....	34
3.5. WAVE THEORETICAL MODEL (FINITE ELEMENT METHOD).....	34
3.6. NUMERICAL MODELLING.....	35
3.6.1. The Mirror Image Source Method.....	35
3.6.2. The Ray-Tracing Method.....	36
3.6.3. Discussion on the mirror image source and ray-tracing methods.....	38
3.6.4. Applications of numerical modelling.....	40
3.7. MAIN ACOUSTICS SOFTWARE AVAILABLE ON THE MARKET.....	42
3.7.1. The ODEON Acoustics Program.....	42
3.7.2. The Computer Array Design Program (CADP2).....	43
3.7.3. The EPIDAURE-EBINAUR Software Package.....	43
3.7.4. EASE, EASE JR, and EARS.....	44
3.7.5. ACOUSTA CADD.....	44
3.7.6. BOSE MODELER.....	44
3.7.7. RAYNOISE.....	45
3.8. CONCLUSION.....	45
4. THE PROPOSED MODEL.....	48
4.1. GENERAL DESCRIPTION.....	48
4.1.1. Assumptions and Specifications of the Proposed Model.....	49
4.2. THE SOUND SOURCE.....	50
4.3. TRACING THE SOUND PARTICLE.....	51
4.4. DETERMINATION OF THE REFLECTING SURFACE-OBJECT.....	52
4.4.1. Collision Calculations.....	52
4.4.2. A Sound Particle Colliding with a Planar Object.....	52
4.4.3. A Sound Particle Colliding with a Ring Type of Object.....	53
4.4.4. A Sound Particle Colliding with a Polygon Object.....	54
4.4.5. A Sound Particle Colliding with a Spherical Object.....	55
4.4.6. A Sound Particle Colliding with a Quadric Type of Object.....	55
4.5. CALCULATION OF THE REFLECTED SOUND PARTICLE DIRECTION.....	58
4.5.1. Sound Particle Reflected from a Planar Object.....	59
4.5.2. Sound Particle Reflected from a Ring Type of Object.....	59
4.5.3. Sound Particle Reflected from a Polygon Object.....	59
4.5.4. Sound Particle Reflected from a Spherical Object.....	60
4.5.5. Sound Particle Reflected from a Quadric Type of Object.....	60
4.6. CONSIDERING SCATTERING AND DIFFRACTION.....	61
4.7. CALCULATION OF THE SOUND PARTICLE ENERGY.....	62
4.7.1. Surface Absorption.....	62
4.7.2. Atmospheric absorption.....	62
4.8. THE RECEIVER.....	63
4.8.1. Calculation of the Sound Energy Received.....	65
4.9. THE USE OF EXPANDING RECEIVERS.....	66
5. SOFTWARE DESIGN, DEVELOPMENT AND COMPUTER IMPLEMENTATION OF THE PROPOSED MODEL.....	70
5.1. INTRODUCTION.....	70
5.2. SOFTWARE DESIGN ISSUES.....	70
5.3. PRE-PROCESSING, MODELLING, DATA INPUT.....	71
5.4. PROCESSING, SIMULATION.....	72
5.5. OBJECT-ORIENTED PROGRAMMING.....	73
5.6. IMPLEMENTATION.....	75
5.7. TRACING THE SOUND PARTICLE.....	79
5.8. POST-PROCESSING, PRESENTATION OF THE RESULTS.....	85
6. THE CADAЕ PROGRAM DESCRIPTION LANGUAGE.....	88

6.1. INTRODUCTION.....	88
6.2. LANGUAGE BASICS.....	88
6.2.1. <i>Comments</i>	89
6.2.2. <i>Float Expressions</i>	89
6.2.3. <i>Vector Expressions</i>	89
6.3. THE CADAE CO-ORDINATE SYSTEM.....	90
6.4. DEFINING THE SOUND SOURCE.....	90
6.5. PLACING A RECEIVER.....	91
6.6. DESCRIBING A SURFACE-OBJECT.....	91
6.6.1. <i>Describing a Parallelepiped Object</i>	92
6.6.2. <i>The Spherical Object</i>	93
6.6.3. <i>The Cone</i>	93
6.6.4. <i>The Polygon</i>	94
6.6.5. <i>The Ring</i>	95
6.6.6. <i>The plane</i>	95
6.6.7. <i>Quadric</i>	96
6.7. CONSTRUCTIVE SOLID GEOMETRY.....	97
6.8. THE ACOUSTICAL PROPERTIES OF A SURFACE-OBJECT.....	98
6.8.1. <i>Absorption</i>	98
6.8.2. <i>Diffuse Reflection Items</i>	100
6.8.3. <i>Sound Transmission</i>	100
7. COMPUTER EXPERIMENTS AND ACOUSTICAL MEASUREMENTS.....	102
7.1. INTRODUCTION.....	102
7.2. COMPUTER EXPERIMENTS.....	102
7.2.1. <i>Apparatus</i>	102
7.2.2. <i>The computer experimental procedure</i>	102
7.3. ACOUSTICAL MEASUREMENTS.....	104
7.3.1. <i>Apparatus</i>	104
7.3.1.1. <i>Sound Level Meter</i>	104
7.3.1.2. <i>Microphone</i>	105
7.3.1.3. <i>Sound Level Calibrator</i>	105
7.3.1.4. <i>Hygrometer</i>	105
7.3.1.5. <i>Sound Power Source</i>	105
7.3.1.6. <i>The Computer</i>	106
7.3.2. <i>Procedure for the Acoustical Measurements</i>	106
8. APPLICATION OF THE PROPOSED COMPUTER MODEL RESULTS - DISCUSSION.....	109
8.1. INTRODUCTION.....	109
8.2. BOX-SHAPED ENCLOSURES.....	109
8.3. A TEST ROOM COMPARISON.....	112
8.4. LONG ENCLOSURES.....	113
8.5. ENCLOSURES WITH TILTED WALLS.....	115
8.6. COUPLED ROOMS.....	116
8.7. ENCLOSURES WITH CURVED BOUNDARIES.....	118
8.7.1. <i>Cylindrical Boundaries</i>	118
8.7.2. <i>A Barrel Shape Room</i>	120
8.8. ST. PAUL'S CATHEDRAL.....	122
8.8.1. <i>General Description</i>	122
8.8.2. <i>Modelling</i>	124
8.8.3. <i>Sound Path analysis</i>	124
8.8.4. <i>Reverberation Test</i>	125
8.8.5. <i>Echogram Analysis</i>	126
8.8.6. <i>Sound Pressure Level Results</i>	127

8.8.7. <i>Speech Intelligibility</i>	127
8.8.8. <i>Acoustically Coupled Spaces</i>	128
8.9. WHISPERING GALLERIES.....	128
9. FINAL DISCUSSION – CONCLUSIONS – FUTURE WORK	133
9.1. DISCUSSION – CONCLUSIONS.....	133
9.2. SUGGESTIONS FOR FUTURE WORK.....	136
APPENDIX.....	139
A.1. TABLES.....	140
A.2. FIGURES.....	180
REFERENCES.....	262

LIST OF TABLES

<i>Number</i>	<i>Page</i>
TABLE 1: THE CADAÆ PROGRAM GENERAL FLOWCHART.	141
TABLE 2: THE CONTENTS OF A SAMPLE DATA OUTPUT FILE.....	142
TABLE 3: RECTANGULAR ROOM CASE, LISTING OF THE CADAÆ DATA INPUT FILE.	143
TABLE 4: TEST ROOM CASE, LISTING OF THE CADAÆ DATA INPUT FILE.....	144
TABLE 5: CORRIDOR CASE, MEASURED REVERBERATION TIMES IN SECONDS.....	151
TABLE 6: CORRIDOR CASE, PREDICTED REVERBERATION TIMES IN SECONDS.	151
TABLE 7: CORRIDOR CASE, COMPARISON BETWEEN PREDICTED AND MEASURED REVERBERATION.	151
TABLE 8: AUDITORIUM CASE, LISTING OF THE CADAÆ DATA INPUT FILE.....	152
TABLE 9: AUDITORIUM WITH TILTED WALLS CASE, COMPARISON BETWEEN COMPUTER RESULTS AND THEORETICAL CALCULATIONS.	153
TABLE 10: CYLINDRICAL BOUNDARY CASE, CADAÆ DATA INPUT FILE.	154
TABLE 11: ST. PAUL'S CATHEDRAL, LISTING OF THE CADAÆ DATA INPUT FILE.	156
TABLE 12: ST. PAUL'S CATHEDRAL, MEASURED REVERBERATION TIMES IN SECONDS.	177
TABLE 13: ST. PAUL'S CATHEDRAL, PREDICTED REVERBERATION TIMES IN SECONDS.....	177
TABLE 14: ST. PAUL'S CATHEDRAL, COMPARISON BETWEEN SIMULATED AND MEASURED REVERBERATION TIMES.	178
TABLE 15: ST. PAUL'S CATHEDRAL, MEASURED SOUND PRESSURE LEVEL IN dB	178
TABLE 16: ST. PAUL'S CATHEDRAL, PREDICTED SOUND PRESSURE LEVEL IN dB	179
TABLE 17: ST. PAUL'S CATHEDRAL, COMPARISON BETWEEN SIMULATED AND MEASURED SPL RESULTS.	179

LIST OF FIGURES

<i>Number</i>	<i>Page</i>
FIGURE 1: SOUND DIVERGENCE, NEAR AND FAR ACOUSTIC FIELDS.	181
FIGURE 2: SOUND PROPAGATION, REFLECTION, AND SCATTERING OF SOUND.	182
FIGURE 3: STANDING WAVES.	183
FIGURE 4: DIRECT AND DIFFUSE SOUND FIELDS.	184
FIGURE 5: IMPULSE RESPONSE, REVERBERATION.	185
FIGURE 6: WATER WAVE MODELS AND SOUND PULSE PHOTOGRAPHY.	186
FIGURE 7: THE MIRROR IMAGE SOURCE AND THE RAY TRACING METHODS, SYSTEMATIC ERRORS.	187
FIGURE 8: THE SOUND SOURCE - SOUND PARTICLE EMISSION METHODS.	188
FIGURE 9: CONSTRUCTION OF AN OMNI-DIRECTIONAL SOURCE BY SUBDIVISION OF THE SPHERE SURFACE AREA INTO A NUMBER OF EQUAL AREA SURFACES.	189
FIGURE 10: APPARATUS USED FOR THE ACOUSTICAL MEASUREMENTS.	190
FIGURE 11: RECTANGULAR ROOM CASE, SOUND PARTICLE SPATIAL DISTRIBUTION, SOURCE AND RECEIVER POSITIONS.	191
FIGURE 12: RECTANGULAR ROOM CASE, THE DIRECT SOUND FIELD.	192
FIGURE 13: RECTANGULAR ROOM CASE, THE DIRECT AND DIFFUSE SOUND FIELD.	193
FIGURE 14: RECTANGULAR ROOM CASE, SOME OF THE SOUND PATHS THAT REACH THE RECEIVER.	194
FIGURE 15: RECTANGULAR ROOM CASE, A HEDGEHOG DIAGRAM INDICATING THE SPATIAL DIFFUSIVITY.	195
FIGURE 16: RECTANGULAR ROOM CASE, MEAN FREE PATH.	196
FIGURE 17: RECTANGULAR ROOM CASE, IMPULSE RESPONSE.	197
FIGURE 18: RECTANGULAR ROOM CASE, ENERGETIC IMPULSE RESPONSE.	198
FIGURE 19: RECTANGULAR ROOM CASE, INTEGRATED IMPULSE RESPONSE.	199
FIGURE 20: RECTANGULAR ROOM CASE, DECIMATED SOUND DECAY CURVE.	200
FIGURE 21: RECTANGULAR ROOM CASE, SOUND DECAY CURVE USING REGRESSION ANALYSIS.	201
FIGURE 22: RECTANGULAR ROOM CASE, AVERAGE ENERGY DECAY USING ENSEMBLE AVERAGES.	202
FIGURE 23: TEST ROOM CASE CONFIGURATION (A), SOUND PARTICLE SPATIAL DISTRIBUTION.	203
FIGURE 24: TEST ROOM CASE CONFIGURATION (A), 2-D NOISE CONTOUR MAP.	204
FIGURE 25: TEST ROOM CASE CONFIGURATION (B), SOUND PARTICLE SPATIAL DISTRIBUTION.	205
FIGURE 26: TEST ROOM CASE, THE SOUND PRESSURE LEVEL VERSUS RECEIVER POSITION, PREDICTED AND MEASURED RESULTS, (A) EMPTY ROOM, (B) FITTED ROOM.	206
FIGURE 27: CORRIDOR CASE, SOUND PARTICLE SPATIAL DISTRIBUTION AND SOUND PATH ANALYSIS.	207
FIGURE 28: CORRIDOR CASE, MATERIALS DISTRIBUTION.	208
FIGURE 29: CORRIDOR CASE, GRAPHICAL COMPARISON OF SOUND PRESSURE LEVEL BETWEEN COMPUTATIONAL AND EXPERIMENTAL RESULTS.	209
FIGURE 30: CORRIDOR CASE, SIMULATED REVERBERATION TRACE USING SCHROEDER'S BACKWARDS INTEGRATION METHOD.	210
FIGURE 31: CORRIDOR CASE, SPATIAL DIFFUSIVITY AT A RECEIVER POSITION 18.2 M FROM THE SOURCE.	211
FIGURE 32: CORRIDOR CASE, HEDGEHOG DIAGRAMS REVEALING THE DIFFUSIVITY OF THE SOUND FIELD ALONG THE ROOM.	212
FIGURE 33: CORRIDOR CASE, DIFFUSION MAP FOR A RECEIVER 6 M FROM THE SOURCE.	213
FIGURE 34: CORRIDOR CASE, DIFFUSION MAP FOR A RECEIVER 18 M FROM THE SOURCE.	214

FIGURE 35: CORRIDOR CASE, DIFFUSION MAP FOR A RECEIVER 30 M FROM THE SOURCE.....	215
FIGURE 36: TYPICAL AUDITORIUM WITH TILTED WALLS CASE, SOUND PARTICLE SPATIAL DISTRIBUTION.	216
FIGURE 37: AUDITORIUM WITH TILTED WALLS CASE, SPATIAL DIFFUSIVITY.	217
FIGURE 38: AUDITORIUM WITH TILTED WALLS CASE, MEAN FREE PATH.	218
FIGURE 39: AUDITORIUM WITH TILTED WALLS CASE, ENERGY DECAY USING ENSEMBLE AVERAGES.	219
FIGURE 40: AUDITORIUM CASE, INTEGRATED SOUND DECAY CURVE.....	220
FIGURE 41: COUPLED ROOMS CASE, SOUND PARTICLE SPATIAL DISTRIBUTION.	221
FIGURE 42: COUPLED ROOMS CASE, SOUND DECAY IN THE SOURCE AND ADJACENT ROOMS, THEORETICAL AND PREDICTED RESULTS.....	222
FIGURE 43: CYLINDRICAL BOUNDARY, THEORETICAL RESULTS.	223
FIGURE 44: CYLINDRICAL BOUNDARY (FLAT SURFACES), SOUND PARTICLE SPATIAL DISTRIBUTION.	224
FIGURE 45: CYLINDRICAL BOUNDARY (CURVED SURFACES), SOUND PARTICLE SPATIAL DISTRIBUTION.	225
FIGURE 46: CYLINDRICAL BOUNDARY, SOUND ENERGY COMPARISON BETWEEN THE FLAT AND CURVED SURFACE MODELS.	226
FIGURE 47: BARREL-SHAPED ROOM (FLAT SURFACES), SOUND PARTICLE SPATIAL DISTRIBUTION.	227
FIGURE 48: BARREL-SHAPED ROOM (CURVED SURFACES), SOUND PARTICLE SPATIAL DISTRIBUTION.	228
FIGURE 49: BARREL-SHAPED ROOM, SOUND LEVEL COMPARISON BETWEEN THE FLAT AND CURVED SURFACE MODELS.	229
FIGURE 50: ST. PAUL'S CATHEDRAL, CROSS SECTION LOOKING FROM THE EAST AND ISOMETRIC VIEW.	230
FIGURE 51: ST. PAUL'S CATHEDRAL, SECTIONAL ISOMETRIC VIEW.	231
FIGURE 52: ST. PAUL'S CATHEDRAL, PLAN VIEW INDICATING THE VARIOUS PARTS OF THE CATHEDRAL (THE RECTANGLES INDICATE THE SEATING AREAS).	232
FIGURE 53: ST. PAUL'S CATHEDRAL, SOUND PARTICLE SPATIAL DISTRIBUTION.	233
FIGURE 54: PRELIMINARY MODEL OF ST. PAUL'S CATHEDRAL MADE IN AUTOCAD.	234
FIGURE 55: ST. PAUL'S CATHEDRAL, SOUND PATH ANALYSIS.	235
FIGURE 56: ST. PAUL'S CATHEDRAL, AVERAGE ENERGY DECAY WHEN THE CATHEDRAL IS EMPTY.	236
FIGURE 57: ST. PAUL'S CATHEDRAL, AVERAGE ENERGY DECAY WHEN THE CATHEDRAL IS FULL.....	237
FIGURE 58: ST. PAUL'S CATHEDRAL, COMPARISON BETWEEN SIMULATED AND MEASURED REVERBERATION RESULTS (FULL AND EMPTY).....	238
FIGURE 59: ST. PAUL'S CATHEDRAL, SOURCE AND RECEIVER POSITIONS FOR THE REVERBERATION TEST.	239
FIGURE 60: ST. PAUL'S CATHEDRAL, SAMPLE MEASURED REVERBERATION TRACES FOR RECEIVER 4 AT 1 KHZ.	240
FIGURE 61: ST. PAUL'S CATHEDRAL, PREDICTED RESPONSE FOR RECEIVER 4 AT 1 KHZ.	241
FIGURE 62: ST. PAUL'S CATHEDRAL, PREDICTED, INTEGRATED IMPULSE RESPONSE FOR RECEIVER 4 AT 1 KHZ.	242
FIGURE 63: ST. PAUL'S CATHEDRAL, SOUND DECAY CURVE USING REGRESSION ANALYSIS FOR RECEIVER 4 AT 2 KHZ.	243
FIGURE 64: ST. PAUL'S CATHEDRAL, REVERBERATION TIME WITH RESPECT TO FREQUENCY FOR RECEIVER 1, MEASURED AND SIMULATED RESULTS.....	244
FIGURE 65: ST. PAUL'S CATHEDRAL, REVERBERATION TIME WITH RESPECT TO FREQUENCY FOR RECEIVER 4, MEASURED AND SIMULATED RESULTS.....	245
FIGURE 66: ST. PAUL'S CATHEDRAL, SOURCE AND RECEIVER POSITIONS FOR THE SOUND PRESSURE LEVEL TEST.....	246
FIGURE 67: ST. PAUL'S CATHEDRAL, MEASURED SOUND PRESSURE LEVEL RESULTS.....	247
FIGURE 68: ST. PAUL'S CATHEDRAL, PREDICTED SOUND PRESSURE LEVEL RESULTS.....	248

FIGURE 69: ST. PAUL'S CATHEDRAL, SOURCE AND RECEIVER POSITIONS FOR THE SPEECH INTELLIGIBILITY TEST.....	249
FIGURE 70: ST. PAUL'S CATHEDRAL, SPEECH INTELLIGIBILITY, COMPARISON BETWEEN A SUBJECTIVE TEST, RASTI MEASUREMENTS, AND COMPUTER RESULTS.	250
FIGURE 71: ST. PAUL'S CATHEDRAL, SOURCE AND RECEIVER POSITIONS FOR THE COUPLED SPACES TEST.	251
FIGURE 72: ST. PAUL'S CATHEDRAL, MEASURED RESPONSE FOR THE RECEIVER IN THE CHOIR (1 KHz).....	252
FIGURE 73: ST. PAUL'S CATHEDRAL, MEASURED RESPONSE FOR THE RECEIVER UNDER THE DOME (1 KHz).....	253
FIGURE 74: ST. PAUL'S CATHEDRAL, COUPLING BETWEEN THE CHOIR AND THE AREA UNDER THE DOME (1 KHz).	254
FIGURE 75: WHISPERING GALLERY – DOME, SOUND PARTICLE SPATIAL DISTRIBUTION.....	255
FIGURE 76: WHISPERING GALLERY – DOME, SOUND RAY PATHS (HORIZONTAL VIEW).....	256
FIGURE 77: WHISPERING GALLERY – DOME, SOUND RAY PATHS (VERTICAL VIEW).	257
FIGURE 78: WHISPERING GALLERY, HEDGEHOG DIAGRAM INDICATING THE DIFFUSIVITY OF THE FIELD.	258
FIGURE 79: WHISPERING GALLERY, DIFFUSION MAP.....	259
FIGURE 80: WHISPERING GALLERY, COMPARISON BETWEEN THEORETICAL AND SIMULATED RESULTS.	260
FIGURE 81: WHISPERING GALLERY, THE EFFECT OF HAVING A SPHERICAL DOME.	261

ACKNOWLEDGMENTS

The author wishes to express his sincere thanks to his supervisor Dr. J.S. Anderson who provided assistance, encouragement, guidance and valuable advice throughout the years of research. Thanks to the staff and research students of the Mechanical Engineering and Computer Science Departments of the City University for the help and support. Grateful thanks to the administration of the St. Paul's Cathedral for permission to carry out measurement tests in the Cathedral.

DECLARATION

“ I grant powers of discretion to the University Librarian to allow this thesis to be copied in whole or in part without further references to me. This permission covers only single copies made for study purposes, subject to normal conditions of acknowledgment”.

ABSTRACT

The thesis is concerned with the modelling of sound fields in large enclosed spaces. Although the subject is necessarily complex, today's computer systems provide a unique opportunity to develop numerical models for the analysis of acoustic behaviour in such spaces.

Based on the findings of a survey on the modelling of sound fields a computer model is implemented. The model is capable of predicting accurately the acoustic environment of bounded spatial systems of any particular geometry including rooms with curved surfaces. Note that in buildings with curved surfaces there are often serious problems with speech intelligibility and the appreciation of music. The proposed model given the name CADAЕ (Computer-Aided Design of Acoustical Environments) is developed based on the geometrical acoustics approach and computer programs are written in C++ an object-oriented language and MATLAB, a fourth generation mathematical language. The pre-processing, that is the data input is carried out in the model's description language, which could be assisted by a computer-aided design package such as Autodesk's AutoCAD.

The CADAЕ model is applied successfully to a variety of acoustical environments including rectangular rooms, fitted rooms, long enclosures, rooms with tilted walls, coupled rooms, spaces with curved walls and a very complex case, namely London St. Paul's Cathedral. The model is validated for various acoustical parameters including Sound Pressure Level, Speech Intelligibility and Reverberation. Further, the significance of using curved surfaces is appreciated by direct comparison to the flat surface approximation. As shown using the exact curved surface model improves the accuracy by up to 90% especially around the focal region.

The computer model presented in this thesis will assist noise control engineers, architects, sound contractors, acousticians etc., to meet the acoustic requirements when designing an enclosure, help in choosing the most appropriate materials, location for the sound source(s), receiver(s) and generally aid in diminishing any acoustical problems. Further, the work presented contributes to the ongoing research of virtual reality and telepresence by approaching the virtual auditory environment.

Chapter 1

INTRODUCTION

1. INTRODUCTION

The work done aims to satisfy the need for accurate prediction and optimisation of sound in bounded spatial systems¹, such as auditoriums, indoor sports halls, concert halls, churches, factories and large enclosed spaces in general. This is accomplished by contributing to the current state of research in the modelling of sound fields in living environments. Thereby, the quality of human life is improved in terms of an optimum, well-monitored acoustical environment.

The analysis of sound in large enclosed spaces or bounded spatial systems is necessarily complex. As sound is being reflected once or several times from six or several limiting surfaces in a room, together with the direct sound from the source, a sound field is built up. This field involves so many complicated patterns of interference and standing waves that even the simplest case is practically impossible to describe completely.

Due to this complexity, a practical solution to the problem should be concerned with methods for the calculation and description of the important features of a sound field in real rooms. And for finding areas in which calculated variables must lie within if the rooms are to fulfil certain acoustical functional demands. As within other parts of engineering, the attempt is to try to define parameters and procedures, which can give a practical and accurate solution to the problem.

The recent rapid development of computer technology in the last decades gave the opportunity to apply numerical methods for computer simulation of sound fields. Further developments in computer technology allow the use of more sophisticated methods resulting in a more accurate and lower cost modelling. This is why computer modelling is becoming the ultimate tool for the accurate prediction, optimisation, and monitoring of acoustic performance in industry, architecture, and the environment.

After carrying out an evaluative review on the aspect of modelling sound fields in enclosed spaces a few interesting facts have been revealed.

1. Classical room acoustics theory cannot represent the acoustic field accurately enough.
2. Developing physical models compared to computer models is expensive, difficult, and time consuming, while the accuracy of the results would be comparable to that of a computer model².
3. The rapid development of computer technology opened up new horizons to the implementation of tedious numerical methods. This is the main reason as to why the last two decades have seen an increasing number of developments of computer models for the prediction of sound fields in enclosed spaces.
4. The main numerical methods are the finite element method based on the wave approach, and the image source method and ray-tracing based on the geometrical acoustics approach.
5. The finite element method, which represents the wave theoretical approach, is only applicable to rooms with very simple geometry³.
6. The mirror image source method and ray-tracing have been successfully applied to various rooms with much more complicated geometry. Both methods have their advantages and disadvantages, but research has shown^{4, 5} that the ray-tracing method is more efficient and applicable for the same accuracy, and more promising for future development⁶.
7. There have been suggestions by researchers such as Kuttruff⁷ and Schroeder⁸ that curved surfaces should be used to represent curved walls and thereby calculate the exact reflection of sound. Despite that, looking at the acoustical computer models developed up to date (see Chapter 3) all represent the room to be modelled as a series of flat or planar surfaces. Generally these surfaces

must have many edge vertices but must be contained in a single plane. That means that curved walls are required to be represented by a finite number of flat planar segments.

8. The quality of the overall simulation process is directly related to the three-dimensional geometrical and acoustical model and obviously the restriction of flat surface representation is a negative factor leading to significant errors⁹. In fact Kuttruff⁷ concludes that it is preferable to compute the exact sound paths without approximating the curved boundary with flat surfaces since such an approximation inevitably leads to significant errors especially near the focal region of the curved wall. Further the use of a large number of planar surfaces to represent a curved surface is inefficient, as the number of calculations increases in proportion to the surfaces.
9. Researchers use some kind of mathematical or empirical formulae^{10, 11, 12} to match the reduction in energy due to the spherical wave propagation with the sound particle density as moving away from the source. Since it is known that the spherical wave propagation depends strictly on the geometry of the enclosure none of these formulae will be generally applicable.

The above facts have led to the formulation of the purpose of this thesis. This is to implement a computer model that will be able to predict accurately and efficiently the acoustic environment of closed or partially closed spaces. The model should be able to tolerate curved surfaces without approximating them into planes, as contemporary models do. The main applications of the proposed computer model would be in relation to churches with domes, indoor sports halls with curved ceilings but also any large enclosure of any particular geometry.

The computer model is mainly to be used for research purposes, but generally it should be able assist noise control engineers, architects, sound contractors, acousticians etc., to meet the acoustic requirements when designing an enclosure. That includes, predicting the necessary objective or subjective properties of the

sound field, analyse the results, help in choosing the best sound source receiver location, and generally aid in diminishing any acoustical problems.

For this purpose the program of research involved:

1. Review of the existing theoretical background on room acoustics.
2. Review of all previous work on the subject of computer modelling of sound fields
3. Prepare a simple preliminary computer model. Check the results of this pilot computer model by applying it to a room of simple geometry.
4. Depending on the results and experience gained by the pilot computer model implementation, develop the main computer model, after choosing the appropriate programming language and efficient and accurate algorithms.
5. Design a friendly user – computer interface for data input as well as for result analysis.
6. Check the validity of the main computer model by applying it to various types of enclosed spaces. These should include various shapes such as regular enclosures, long enclosures, spaces with tilted walls, rooms involving barriers, coupled rooms, and enclosed spaces with curved boundaries.
7. Finally validate the proposed computer model by applying it to an appropriate existing building. Check the accuracy by comparing with measurements, on both subjective and objective properties such as reverberation, speech intelligibility, and sound pressure level.

The work carried out based on the above research program is described in detail in the following Chapters. Chapter 2 gives a brief review on the basic theory of sound, aiming to get the reader acquainted with the context. The wave and geometrical acoustics approaches are discussed, giving reasons as to why

geometrical acoustics approach is more appropriate, as well as its validity limitations. Further, some useful parameters and concepts used in the thesis are outlined. Next, Chapter 3 presents a survey on the acoustical computer models, how these gained ground over physical modelling, which are the main numerical methods, advantages and shortcomings of these, main features of the main models etc.

In Chapter 4 the proposed model suggested by the author is formulated. First a general description of the proposed model is given, where the basic operations, assumptions and specifications are stated. Then specific issues are examined, such as, the sound source, tracing the sound paths with respect to surfaces of various geometry, sound energy calculation, as well as calculation of the total sound energy at a receiver position.

Chapter 5 describes how the formulated proposed model is transformed into a computer program. The Chapter starts with a general description of the proposed computer model given the name CADAЕ (Computer-Aided Design of Acoustical Environments), and how the plan for the development of the program was designed. Then three main sections are followed, the pre-processing, processing and post-processing, where the actual development of the computer model is described. Chapter 6 describes in more detail the pre-processing part of CADAЕ that is the program's data input language. This involves the language basics, three-dimensional co-ordinate system employed, defining the sound source, placing the receiver, describing the various surface-objects the enclosed space is made from, as well as declaring the acoustical properties of the various surface objects.

Next Chapter 7 gives a description of the computer experiments and acoustical measurements carried out. The equipment used for each case is outlined as well as the procedures followed. Chapter 8 discusses the validity of the proposed computer model in relation to subjective and objective sound field properties, as applied to a variety of room shapes.

The thesis ends with the main conclusions drawn and a speculation of any possible future work.

Chapter 2

THEORETICAL BACKGROUND

2. THEORETICAL BACKGROUND

2.1. Introduction

The problem of sound in rooms, or bounded spatial systems¹, can be analysed theoretically by several ways. These include mainly the wave theoretical model, the geometrical acoustics model, the use of statistical methods, and the psychoacoustics approach^{13,14,15,16,17,18}. Further, signal theory is quite useful to the analysis of sound^{19,20}.

Before getting on to the main part of this thesis it would be wise to describe briefly the basic theory for the analysis of sound. This Chapter aims to get the reader acquainted with the basic mathematical tools and concepts used in the main context. The next Chapter (Chapter 3) reviews acoustical modelling which is based on the theory described here.

2.2. General Description of Sound

Sound is one of those phenomena of nature that human beings have known and used since prehistoric times. We have two ears that can receive sound, and we have a voice that can produce sound. The interaction between hearing and speaking has contributed to the development of mental abilities of humans. Besides, human beings have always used sound to communicate aesthetic values through music.

It should be noted that sound is a wave phenomenon. An object that vibrates in space sets the air around it into vibration. Then, these vibrations are spread in a wave type of motion in all directions. When the waves reach the ear, the tympanic membrane starts to vibrate, transmitting the waves to the sense organs that are perceived as sound by the brain. This is what happens in a typical microphone as well as in a human ear. The effect can be made visible with a cathode ray oscilloscope.

2.3. Propagation of Sound Waves

Sound in air is a longitudinal type of wave. If several points are studied on the direction of the wave propagation it can be observed that the fluid particles oscillate along the direction of propagation of the wave. For a sound wave the air particles carry out mechanical oscillations, and therefore the particles carry energy. The energy follows with the wave front and therefore sound radiation is in fact an energy radiation. The energy transport in the direction of the wave is associated with the cycle of changes of the potential energy into kinetic energy and vice versa.

The energy is delivered by the wave source and spreads after a while outwards. For the wave source to continue to send out waves then a constant supply of energy should be given to the source. Usually a sound wave will propagate with the same velocity c_0 in all directions. All the points that are a distance $r = c_0 t$ (t is time) from the wave source, lie on a spherical surface (see Figure 1a) that actually represents the wave front. For example, when a firework explodes in the air sound travels as spherically shaped waves from the position of explosion that represents the sound source. This means that the wave surface is an expanding sphere having as centre the sound source.

At a certain distance from the sound source it can be assumed that a small part of the wave front is plane. The space where this assumption can be made is known as the far acoustic field (see Figure 1b) and it is in this region where most conventional sound measurements are made.

2.3.1. Sound Power, Pressure, Intensity, Loudness and Sound Level

A sound source radiates power into a room and the effect is sound pressure. The sound pressure is dependent on the distance from the source and on the acoustical environment, that is the geometry, absorption and environmental conditions of the room. On the other hand, sound power is independent of the environment.

From a simple point wave source the power radiates evenly in all directions, and it disperses on sphere surfaces of increasing radius r and therefore area, as moving away from the source (see Figure 1a). Thus

Eq. 1

$$I = \frac{W}{4\pi r^2} .$$

Therefore the power is constant and equal to the power at the wave source and Intensity I of the wave is proportional to the power W and inversely proportional to the square of the distance to the wave source.

Sound Intensity is power per area, but that is not the same as what the ear hears as sound loudness because the loudness is related to the ear's sensitivity. This relationship is not quite simple, because the ear is not equally sensitive to all frequencies. Two sounds could have the same intensity but can be heard with different loudness when the sounds have different frequencies.

For humans sound is audible from about 20 Hz to 20 kHz. The sensitivity of the ear varies quite a lot in this range. The sensitivity is greatest within the range from 1 kHz to 5 kHz. At 1 kHz sound can be heard with intensities as low as $I_{ref} = 10^{-12} W / m^2$. This is close to the threshold of hearing at 1 kHz. When the intensity increases, the sound will eventually be so strong that it hurts the ear. Then it is said that the threshold of pain has been reached. At 1 kHz the threshold of pain is $1 W / m^2$. The relationship between the threshold of hearing and the threshold of pain gives the range of intensities that the ear can detect which is at the order of $10^{12} W / m^2$. This shows that the ear is an excellent sense organ. Due to this vast range of intensity a logarithmic scale is used so that this range is reduced. Therefore, the sound level in terms of intensity is given by:

Eq. 2

$$IL = 10 \log_{10} \frac{I}{I_{ref}} \text{ dB.}$$

Or the sound level in terms of pressure is given by:

Eq. 3

$$SPL = 20 \log_{10} \frac{P_{rms}}{P_{ref}} \text{ dB.}$$

It can be shown that the sound intensity level is almost equivalent to the sound pressure level¹³:

Eq. 4

$$IL = SPL - 0.2 \text{ dB.}$$

2.3.2. Speed of Sound

The speed of sound in gases increases with temperature. It can be shown¹³ that for a perfect gas the velocity of sound is given by:

Eq. 5

$$c_0^2 = \gamma RT,$$

where c_0 is the speed of sound, γ is the ratio of specific heats, R is the specific gas constant, and T is the atmospheric temperature.

2.3.3. Reflection of Sound Waves

When a wave hits a solid wall it is reflected in some direction. To illustrate the behaviour of sound waves, water waves can be utilised as an analogy such as the case of water wave models (see page 32). This can be seen at an open reservoir of water. Waves can be created with a pin that dips up and down into the water and creates circular waves. If a perpendicular wall is positioned to the water surface near the wave source it can be seen that the waves in front of the wall are composed of two circular wave fronts. The one wave front has its centre at the wave source that represents the incident wave. The reflected wave front has its centre at a point behind the wall. It can be shown that the centre of the reflected wave front lies on the direction of the perpendicular from the original wave source to the wall, and that it is positioned equally far behind the wall as the wave source lies in front of the wall. The centre for the reflected wave lies in the mirror image of the wave source.

If the plane approximation is assumed (far acoustic field), the reflected wave will be also planar. When plane waves hit a vertical wall with an oblique angle, these are reflected with an oblique angle too. Experiments have shown that the incident wave front and the reflected wave front form identical angles with the wall (see Figure 2a and 2b). This is the well-known law that the angle of incidence equals the angle of reflection.

2.3.4. Reflection from a Curved Surface

The reflection law applies to curved surfaces as well but after reflection sound concentrates at certain positions creating a focus as seen on Figure 2c.

Rayleigh²³ realised that there is a great deal of similarity between the oscillations of circular membrane and the oscillation of the cross-section of a curved surface such as a cylinder. So he suggested that the reflection of sound waves from curved surfaces could be analysed mathematically by the use of Bessel functions.

The final solution of the wave equation in terms of pressure, as related to the transverse vibrations of a stretched membrane, is given by:

$$p = J_n(kr) \cos(kc_0t - n\theta), \quad \text{Eq. 6}$$

where p is the sound pressure, n is any integer, J_n is a Bessel function of order n , k is the wave number ($k=2\pi/\lambda$), λ is the sound wavelength, r , θ denote the polar co-ordinates.

The squared sound pressure in a sound wave which is reflected from a hollow rigid cylinder when this is irradiated by a spherical wave originating uniformly from a point on the cylinder axis is given by⁷:

$$P_{rms}^2 = \frac{\rho_0 c_0 k a^4}{4(a^2 + z^2/4)^{5/2}} \left[J_0 \left(\frac{kar}{(a^2 + z^2/4)^{1/2}} \right) \right]^2 W, \quad \text{Eq. 7}$$

where a is the relative distance from the centre of curvature, r, φ are the cylindrical coordinates of the receiving point, and W is the power of the source

2.3.5. Scattering of Sound

Scattering of sound could be classified to take place in two ways. These are either when meeting an obstacle (see Figure 2d) or due to surface irregularities, (see Figure 2e).

If there are a great many irregularities on a reflecting wall, the sizes of which are comparable with the wavelength the incident sound energy is diffracted or scattered into an extended solid angle according to Lambert's Law¹⁵. Scattering of sound due to surface irregularities is sometimes desirable and it can be achieved with specially made diffusors²¹.

Scattering due to meeting an obstacle can be explained as follows. When a plane wave strikes a body in its path, part of it spreads out from the obstacle in all directions according to the sound wavelength.. As seen in Figure 2d when a sound wave, indicated by the arrow, meets a rigid cylinder of circumference $2\pi\alpha$, indicated by the small dark circle, it is scattered depending on the magnitude relation μ of its wavelength with the cylinder's circumference as indicated by the polar plots²².

2.3.6. Refraction and Transmission of Sound

When the wave passes the surface border between two media the wave front changes its direction of propagation. Then it is said that the wave has been refracted. When a plane wave hits obliquely the surface between two fluids of different density it is refracted at an angle usually less than the incident wave front angle. It can be shown that there is a relationship between the refraction of waves and the change in the wave velocity, which is known as Snell's Law and is given by:

Eq 8

$$\frac{c_1}{c_2} = \frac{\sin \alpha_1}{\sin \alpha_2},$$

where α_1 is the incident angle, α_2 is the refracted angle c_1 is the velocity of the wave in the more dense fluid and c_2 is the velocity in the less dense fluid. Refraction of sound occurs in a room usually where there are differences in temperatures. Especially above the audience area it is known that sound moves at grazing angles.

Refraction occurs also when sound waves move normally against a thick wall. Some of the sound energy is reflected, some energy absorbed by the wall and some is refracted or transmitted through the wall. This transmission of sound is indicated by a sound transmission coefficient, which is defined in the following relationship¹³:

Eq. 9

$$\alpha_r + \alpha_t + \alpha_d = 1,$$

where α_r is the sound absorption coefficient, α_t is the sound transmission coefficient, and α_d is coefficient representing the loss of sound energy. The transmission coefficient then obviously depends on the type of material and thickness of the wall.

2.3.7. Interference and Standing Waves

A phenomenon typical for sound waves is interference. This happens when two or more waves mix. Two bodies cannot be at the same place simultaneously but two waves can, and this is called interference.

A classic example of interference in sound is the standing waves phenomenon. Imagine two waves coming towards each other with the same frequency wavelength and amplitude. This can be achieved by creating plane waves striking a wall that is parallel to the wave fronts. The waves are reflected straight back. Then the incoming and reflected waves have the same frequency wavelength and

amplitude but the waves travel in opposite directions. The peculiarity of this form of interference is that the resultant waves do not move which is the reason they are called standing waves. Standing waves can easily be made visible, in a spring driven by a rigid vibrating support as seen in Figure 3a.

A similar effect occurs, if a vibrating piston creates sound waves in a tube as shown in Figure 3b. Sound concentrates in some areas creating peaks of sound pressure called antinodes, and pressure minima called nodes. Standing waves are not like ordinary waves where the oscillations move in the direction of propagation. In standing waves the phase is always the same everywhere between two nodes, but the amplitude increases from the node lines to the antinode. In two neighbour antinodes the phase is opposite. The wavelength for the resultant wave is equal to the wavelength of the two opposite waves.

2.3.8. Diffraction

If a sound source, which is generating plane waves, is placed in front of a wall with an opening which is smaller than the wavelength of sound an interesting phenomenon can be observed. When the waves reach the wall they stop. Behind the wall though, waves are generated with centre the opening on the wall. Behind the wall the waves are no longer plane. This is what is known as diffraction.

Diffraction can be explained by Huygen's principle. Huygen's principle states that the cause for a wave can be a close row of wave sources, or a continuous wave front. When the cause is a wave front, every point in the wave front functions as the starting point for a new wave. In both these cases it is interference between the new waves that create the resultant wave.

The waves create oscillations at the opening. These oscillations are the source of waves that spread on the other side of the wall. It does not matter where the opening is.

2.3.9. Sound Wave Equation

After applying the law of conservation of mass momentum and energy, for a homogeneous isotropic and source free medium it can be shown¹³ that:

$$\frac{\partial^2 p}{\partial x^2} = c_0^2 \frac{\partial^2 p}{\partial t^2}. \quad \text{Eq. 10}$$

This is the one-dimensional acoustic wave equation in terms of pressure p (c_0 is the velocity of sound and t is time). A similar second-order partial differential equation can be derived in terms of particle displacement ξ ,

$$\frac{\partial^2 \xi}{\partial x^2} = c_0^2 \frac{\partial^2 \xi}{\partial t^2}. \quad \text{Eq. 11}$$

And the three-dimensional wave equation in terms of pressure is given by:

$$\frac{\partial^2 p}{\partial t^2} = c_0^2 \left(\frac{\partial^2 p}{\partial x^2} + \frac{\partial^2 p}{\partial y^2} + \frac{\partial^2 p}{\partial z^2} \right). \quad \text{Eq. 12}$$

From the solution of the wave equation for a simple rectangular room, it can be shown that²³:

$$f = \frac{c_0}{2} \sqrt{\frac{n_x^2}{l_x^2} + \frac{n_y^2}{l_y^2} + \frac{n_z^2}{l_z^2}}, \quad \text{Eq. 13}$$

where, f represents the frequencies of the modes of vibration, c_0 is velocity of sound, n_x, n_y, n_z are integers 0, 1, 2, 3, ... etc., and l_x, l_y, l_z are the length width and height of the room.

The solution to the sound wave equation in a room would consist of thousands of natural modes of vibration that even the simplest case of room configuration is

impossible to analyse completely. Weyl in the beginning of the century developed a formula for the approximate number of individual eigen-frequencies N within the frequency range from 0 to f :

Eq. 14

$$N = \frac{4}{3} \pi V \frac{f^3}{c_0^3},$$

where V is the volume of the room, f is the frequency, c_0 is velocity of sound. For example the number of individual normal modes for a simple rectangular room $30 \times 20 \times 10 \text{ m}^3$ would be about 5 million up to 2 kHz. Actually, this number is even greater according to Kinsler and Frey¹⁸.

The large number of modes makes the sound wave approach unsuitable for the analysis of sound fields in large enclosed spaces. On the other hand, the previously described concepts of sound propagation can be incorporated in a simpler approach, the geometrical acoustics approach. Although the geometrical approach is less accurate it is more practical and useful for the description of sound behaviour in large spaces.

2.4. Geometrical Acoustics Approach

The geometrical acoustics approach is an approximation to the wave approach discussed in the preceding sections. The assumption of the geometrical acoustics approach is that sound is spread as rays, rather than wave fronts, which can be defined as lines perpendicular to the surfaces of constant phase. Sound energy is carried along the rays that follow the law of reflection and Snell's law for refraction. That means that phase and wave sphericity are ignored. By following possible sound wave paths one can get a picture of the spatial distribution of sound intensity.

The geometrical approach is not specific to acoustics and is mainly derived from optics²⁴. Optical analogies can therefore be used (see page 32). One disadvantage is that information about interference and resultant sound pressure distribution is

not easily obtained. Further, the practical use is limited mainly to situations where the surfaces both in size and property can be assumed to give specular reflections.

2.3.10. Validity of the Geometrical Approach

In bounded spatial systems or enclosed spaces in which the dimensions are large compared with the wavelength of sound, sound can be regarded as similar to light. When meeting an obstacle, part of the sound energy will be reflected and part of it absorbed. However, when the sound wavelength is larger than the dimensions of the obstacle it meets then part of the sound will be diffracted. That is sound will be heard behind the obstacle although being in a shadow region.

If the obstacle has an irregular surface and those irregularities are large compared to the wavelength then the result will be that sound is reflected in all directions. This phenomenon is called scattering, which results to diffusion. Diffusion occurs always at rough surfaces for light rays whereas it always depends on the degree of roughness and the magnitude of the wavelength in the case of sound (see also page 15).

Another property adopted from geometrical optics is refraction. Refraction is based on the fact that, every wave propagates from the source to the receiver by taking the fastest path, which is not necessarily the shortest. The fastest would be the shortest as long as the speed of sound in the medium of transmission is uniform. Otherwise, the direction of the wave front or the sound ray will change in order to take the fastest path (see also page 15).

Low frequency sound usually is diffracted when meeting most surfaces but it could also be reflected specularly when meeting a zig-zag wall¹⁴. High frequency sound is specularly reflected when the surface is smooth and diffusely reflected when the surface is rough.

2.4. Architectural Acoustics Parameters

Architectural or room acoustics is the study of the generation, propagation, and transmission of sound in bounded spatial systems or enclosures. It uses theory

from different branches of acoustics, but mostly from the geometrical, statistical, and psychological acoustics as well as signal processing. It deals with reverberation control, noise insulation and reduction, sound distribution and absorption, the richness of music and the intelligibility of speech.

A description of a few important concepts and parameters useful for architectural acoustics includes the following.

2.4.1. Free Sound Field

Such a sound field would occur in free space (open air) where there are no reflections. It is possible though to have no reflections in an enclosure such as an anechoic chamber (see Figure 4a). The free sound field propagation follows the inverse square law (see page 11). Further the intensity level and sound pressure level are equivalent in the free field.

2.4.2. Diffuse Sound Field

The diffuse field (see Figure 4b) represents the other extreme where sound is reflected so many times that it travels in all directions with equal magnitude and probability thus giving a net sound intensity of zero at any position in the room. Such a field can be created in a reverberation chamber.

2.4.3. Mean Free Path

The concept of the mean free path was taken from the kinetic theory of gases²⁵. In acoustics the mean free path²⁶ is defined as the average distance between points of collision of a sound wave with the walls of the enclosure. That means that diffraction effects in the sound propagation are ignored. It was verified^{27, 15} that the mean free path for regular rectangular enclosures is given by:

Eq. 15

$$l = \frac{4V}{S},$$

where l is the mean free path, V is the volume of the enclosure, and S the surface area. Based on this expression, reverberation formulas such as Sabine's (see page 33), Eyring's (see page 34) may be derived¹⁵.

Further to the mean free path, useful is the notion of the average reflection frequency¹⁵ n , that is the average number of wall reflections per second which is given by:

Eq. 16

$$n = \frac{c_0}{l},$$

where c_0 is the velocity of sound and l is the mean free path (as defined above).

2.4.4. Reflection Density

Assume that a brief pressure impulse (see page 25) is generated at some point inside a room. At some other point an installed microphone acts as a receiver. The response at the receiver location will be similar to the one in Figure 5. Primary sound arrives first at the receiver location, followed by a series of reflections (represented by vertical lines) that have only once encountered one of the walls enclosing the room (first order reflections). Then higher order reflections arrive at the receiver location while their density per unit time increases rapidly.

The density of reflections per unit time increases as the square of the elapsed time after a short impulse (see page 25), as formulated by Cremer¹⁴:

Eq. 17

$$N_r = \frac{4\pi c_0^3}{V} t^2,$$

where N_r is the number of reflections per second, c_0 is the velocity of sound, V is the volume of the room, and t is the time elapsed.

2.4.5. The Combined Direct and Diffuse field

Using statistical room acoustics theory it can be shown¹³ that the sound pressure level in an enclosed space is given by:

$$SPL = L_w + 10 \log \left(\frac{Q}{4\pi r^2} + \frac{4}{R_c} \right) + 10 \log \left(\frac{\rho_0 c_0}{400} \right), \quad \text{Eq. 18}$$

where L_w is the sound power level of the sound source, Q is a directivity factor, R_c is the room constant based on the average sound absorption, $\rho_0 c_0$ specific acoustic resistance.

2.4.6. Coupled Rooms

Sound fields in rooms, which are subdivided architecturally into a number of smaller subspaces, show interesting characteristics. It can be shown using statistical room acoustics that the decay slopes of two rooms separated by a small open area, such as a door is given by¹⁴:

$$E_1 \approx \frac{4W_1}{c_0 A_{11}} \left(e^{-2\delta_1 t} + k^2 \frac{\delta_1^2}{(\delta_1 - \delta_2)^2} e^{-2\delta_2 t} \right), \quad \text{Eq. 19}$$

$$E_2 \approx \frac{4W_1}{c_0 A_{11}} k_2 \left(\frac{\delta_2}{\delta_2 - \delta_1} e^{-2\delta_1 t} - \frac{\delta_1}{\delta_2 - \delta_1} e^{-2\delta_2 t} \right),$$

where E_1, E_2 represent the sound energy density in each of the two rooms, W_1 is the power of the sound source in room 1, c_0 is the velocity of sound, A_{11} is the sum of the coupling area of the opening and the total equivalent absorption area of the source room, k is the coupling coefficient, δ_1, δ_2 are the damping constants

for each room, t is the time interval from the impulsive excitation (see page 25) in seconds. Further details are given by Cremer and Muller¹⁴.

2.5. Criteria for Assessment

Some important parameters of assessment are summarised as follows:

2.5.1. Reverberation Time (RT_{60})

The time required for the sound pressure level to decrease by 60 dB in a bounded spatial system after a pulse or steady state excitation (see page 25). The reverberation time is estimated by the rate of decay given by the linear least squares regression of the measured or computed decay curve from a level of 5 dB below the initial level to 35 dB below the initial level.

2.5.2. Early Decay Time (EDT)

The time required for the sound pressure level to decrease by an equivalent of 60 dB in a bounded spatial system after a pulse excitation. The reverberation time is estimated by the rate of decay given by the linear least squares regression of the measured or computed decay curve from the initial level to 10 dB below the initial level.

2.5.3. Definition

The Definition²⁸ (D50) relates the sound energy (squared pressure) reaching the receiver in the first 50ms to the total energy received and is given by:

$$D = \frac{\int_0^{50} p^2(t) dt}{\int_0^{\infty} p^2(t) dt}.$$

Eq. 20

2.5.4. Clarity

The Clarity²⁹ (C80) is the decimal logarithm of the arrival sound energy in the first 80ms and the total energy from 80ms and onwards.

Eq. 21

$$C = \log_{10} \left(\frac{\int_0^{80} p^2(t) dt}{\int_{80}^{\infty} p^2(t) dt} \right).$$

2.5.5. Sound Spatial Impression

For the sound spatial impression the most relevant factors are the origin and sequence of the reflections and the arrival angle of the signal to the receiver. The lateral energy factor³⁰ which is the quotient between the value of lateral energy on the ear axis from 5 to 80 ms and the total energy of the first 80 ms is given by:

Eq. 22

$$LEF = \frac{\int_5^{80} p_{lat}^2(t) dt}{\int_0^{80} p^2(t) dt}.$$

2.6. Acoustical Signal Theory

A signal is a physical quantity or quality, which conveys information³¹. The practical importance to acoustics is related to the fact that, since sound is a type of signal, many useful analytical tools from signal theory can be utilised. There are various transformations that can be applied to sound signals, but these do not affect the amount of information that is known about the sound signals, they rather change only the point of view.

Some important concepts and mathematical tools from acoustical signal analysis and processing are described as follows.

2.6.1. Dirac Delta Function

An important special function used in acoustical signal processing and consequently in the work done in this thesis is the unit impulse or Dirac delta function which is equal to unity only at a particular time and elsewhere is zero. Its importance depends on the fact that any signal can be represented by a series of

short pulses and the delta function is quite appropriate for the representation of these pulses.

2.6.2. Impulse Response

The impulse response³² as the name implies is the system's response to an impulse. In acoustics the impulse response is the sound pressure function of the room resulting from its excitation by a Dirac delta function. Ideally the impulse response is related to the transfer function between sound pressure received and the volume velocity transmitted by the source. In practice source volume velocity and directivity are not known and the impulse response represents the sound pressure function with respect to time.

The impulse response is the signature of the system, since knowing the impulse response a full description of the system may be attained. The impulse response of an existing room can be easily measured using many different methods, however its predictive calculation is a very complicated task.

There exist not one single impulse response for a room but there are corresponding impulse responses for different sound source locations and receiver positions.

2.6.3. Sampling

A digitised signal is not represented as a function of a continuous variable, but rather as a function of discrete values of time. It is assumed that the samples are uniformly spaced in time.

When watching a movie a stream of separate, discrete photographs is displayed on the screen at a particular rate but what is seen by the human eye is the illusion of the continuous motion. This is a result of digitising the original analogue scene at a sufficient sampling rate. If the sampling rate was less than sufficient the motion would appear discontinuous. The aim of the sampling process is to accurately represent the section of the analogue signal, which was digitised.

The sampling theorem states that a sampled time signal must contain components at frequencies above half the sampling rate, called the Nyquist frequency. Thus in order to represent an analogue signal accurately with digital samples, the sampling frequency should be at least two times greater than that of the highest frequency component of the original signal. For example, to be able to digitise a sound signal for hearing purposes accurately enough, a sampling frequency of above 40 kHz should be used since it is known that the human ear can detect sound of up to about 20 kHz.

2.6.4. Decimation-Interpolation

Decimation is the signal processing operation used to change from a high sample rate to a lower sample rate. The decimation algorithm³³ involves filtering the data with a low-pass filter and then re-sampling the resulting smoothed signal at a lower rate. Decimation can be used to smooth out the reverberation decay curve.

Interpolation on the other hand is opposite to decimation. Interpolation is the operation used to change from a low sample rate to a higher sample rate. The interpolation algorithm³⁴ can be used to smooth out a series of data values such as for the construction noise maps, diffusion maps and so on.

2.6.5. Schroeder's Integrated Impulse Response

Once the pressure impulse response of the room has been determined, by applying a method called reverse-time integration³⁵, the sound decay curve may be obtained. This sound decay curve is what is known as the integrated impulse response. According to Schroeder, for ergodic systems the logarithmic integrated impulse response is identical with the noisy decay curve obtained after infinite ensemble averaging.

Based on Schroeder's method Kolowski³⁶ demonstrates a technique for the determination of the reverberant response of a room from superposition of its impulse response. The energy versus time curve $E_d(t)$ describing the reverberant response of a room is given by³⁶:

Eq. 23

$$E_d(t) = \int_0^{t_z} p(t)dt - \int_0^t p(t)dt = E_s - \int_0^t p(t)dt, \quad 0 \leq t \leq t_z,$$

where t_z total duration of the impulse response, $p(t)$ is the power density versus time curve describing the impulse response, E_s is the energy density of the steady state response.

2.6.6. Spectrum - Frequency Response - Room Transfer Function

The spectrum of a signal is its frequency response and it can be estimated by using a Fourier transform algorithm³⁷. The frequency response, which is equivalent to the room transfer function, may be obtained from the room squared sound pressure impulse response, since the two represent a Fourier transform pair.

Interesting to mention is the finding of Schroeder and Kuttruff³⁸ that above a certain lower frequency limit the frequency response shows statistical features. As a result according to Schroeder and Kuttruff the reverberation time T is related to the average spacing between the maxima Δf_{max} of the frequency curve:

Eq. 24

$$T = \frac{3.91}{\Delta f_{max}}$$

2.6.7. Auralization, the Ultimate Goal

The work done and presented in this thesis can be thought of as being part of the auralization³⁹ process, which is equivalent to audible simulation. The concept is based on the possibility of creating aural impressions from simulated room responses. Auralization can be based on geometric and acoustical data of both existing and non-existing enclosures and it can be a result of computer modelling.

The idea of auralization is not new. Attempts to simulate sound fields have been documented in technical papers dating back to the 1930's⁴⁰ using scale models. The availability of computer power in recent years, has given a new momentum

to the subject to allow audible simulations to be calculated in minutes instead of days.

The auralization process can be described in four individual parts:

1. Building an acoustical computer model of the enclosure.
2. Calculation of the monaural impulse response.
3. Calculation of the binaural or multi-channel impulse response by taking into consideration the directional information of the reflected sound rays.
4. Convolution of the resulting impulse response with an anechoic signal.

The first and second steps involve modelling and analysis of the sound field in an enclosed space, which is what is done in this thesis. The third and fourth steps involve further analysis of the results with aim of producing a signal, which will give the same acoustical impression to a potential listener as if she or he was situated in the real building.

Chapter 3

MODELING OF SOUND FIELDS IN BOUNDED SPATIAL SYSTEMS

3. MODELLING OF SOUND FIELDS IN BOUNDED SPATIAL SYSTEMS

3.1. Introduction

There are two ways to simulate a natural phenomenon. That is, by means of a physical model or by means of a mathematical model. Therefore to simulate sound fields either a scale model should be built or a mathematical model should be implemented.

Physical modelling usually involves building a scale model and carrying out acoustical experiments in order to predict the sound characteristics of the prototype. The results of physical modelling are quite acceptable in many cases but the overall method is expensive, difficult, and time consuming.

On the other hand, the situation is not so bad when considering mathematical modelling. The practical tool for the implementation of a mathematical model is essentially the computer. The recent rapid technological development of computer software and hardware made the process of numerical modelling relatively easy, economic and time saving as compared to scale modelling. Computer models have been widely used for many scientific and engineering simulations for the last fifty years or so and more recently for acoustical simulations. Further comparisons between physical scale models and computer models² give good agreement indicating that computer modelling can be used with confidence.

This Chapter reviews the main methods for the modelling of sound fields in enclosures. These include physical acoustical modelling, the wave theoretical model, statistical models, and the mirror image source and ray-tracing methods, which are derived from the geometrical acoustics approach and are implemented as numerical models by means of computer codes.

3.2. Physical Acoustical Modelling

Physical acoustical modelling is carried out in various ways including water wave models and sound pulse photography, light ray models, and the most popular type which are the physical scale models. These are reviewed as follows.

3.2.1. *Water-Wave Models and Sound Pulse Photography*

Water wave models⁴¹ comprise a plane parallel glass plate that represents the longitudinal section of the room to be examined. The plate is framed to a certain depth 7-8 mm so that the whole plate can be covered with water. Further it is illuminated from below in order that the wave fronts will be visible. Absorption is accomplished by placing a wedge-shaped strip of felt in front of the surface of interest. Waves are excited by a drop of water upon the surface of the water where the sound source is supposed to be. The low propagation speed of the wave fronts makes it easy to use photography for subsequent investigation.

Sound pulse photography^{41, 42} represents an improvement to the water wave models in the sense that the wave fronts can be seen more clear. The two methods are rarely used nowadays for the prediction of sound fields but it can be claimed that are good for demonstrations although they are applicable only in two dimensions. An example can be seen in Figure 6.

3.2.2. *Light-Ray Models*

It is a fact that the propagation of sound and light waves is similar. This concept led to the use of light-ray models^{43, 44} to simulate sound fields. These models are constructed by using light sources and optical mirrors. Therefore, the paths and reflections of sound are simulated. To make the light rays visible smoke can be inserted into the model.

The purpose of light-ray models is to trace the paths of rays of light and thereby the paths that the sound wave fronts are taking on their way from the source to the receiver. This nowadays can be accomplished easier by numerical methods such as ray-tracing with the aid of the computer.

3.2.3. Three-dimensional Scale Acoustical Models

The most widely used physical models are the scale models^{45, 46, 47}. The idea is to build a smaller three-dimensional model similar to the original building or proposed room, both in terms of geometry and materials. Then the sound pressure and other parameters can be measured at the locations of interest in the model, which correspond to the original room.

Although scale models give satisfactory results, they are quite expensive. Furthermore, during the design of a new building such as a concert hall the plans may have to change and consequently, the scale model should be rebuilt or modified.

3.3. Empirical models (Sabine)

At the turn of the century W.C. Sabine⁴², in order to describe the sound field in an enclosure, developed in an empirical fashion a simple formula for the reverberation time. After carrying out considerable amount of research on several auditoria his work led to the following relationship:

$$T = \frac{55.3V}{c_0 S \bar{a}},$$

Eq. 25

where, T is the reverberation time in seconds, V is the volume of the room in m^3 , c_0 is the velocity of sound, S is the total surface area of the room in m^2 , \bar{a} is the average absorption coefficient of room surfaces.

Sabine's equation assumes that the sound in the enclosure is diffuse and that all directions of propagation are equally probable. It neglects very important factors such as room modes, position of absorptive material, and the shape of the room. Sabine's formula gives a good estimation of the reverberation time for reverberant rooms with uniform absorption.

It should be mentioned that Sabine's equation could be derived analytically by considering the balance of sound energy in a room which has a diffuse field.

3.4. Statistical Modelling

After having accepted that an accurately deterministic description of sound fields in rooms is practically impossible or may be not even wanted, it is natural to look for statistical methods. The statistical models are usually used in conjunction with the main numerical models (ray-tracing and image source methods), to simulate diffusion or diffraction and generally to estimate the later part of the impulse response.

3.4.1. Eyring's Model

In order to improve Sabine's estimation of the reverberation time, Eyring⁴⁸ developed the following formula by making use of the concept of the mean free path (see page 21) and the same assumptions as the Sabine's model.

$$T = \frac{55.3V}{c_0 S [-\ln(1 - \bar{a})]},$$

Eq. 26

where, T is the reverberation time in seconds, V is the volume of the room in m^3 , c_0 is the velocity of sound, S is the total surface area of the room in m^2 , \bar{a} is the average absorption coefficient of room surfaces.

The above formula gives a value of zero when the average absorption coefficient is unity while the Sabine formula would give a finite value.

3.5. Wave Theoretical Model (Finite Element Method)

In this model attempts are made to solve the three-dimensional wave equation (see page 18) with given initial conditions. Analytical solutions are only useful for a limited number of simple geometrical shapes.

Numerical solving methods can be used among which is the finite element method³. The wave theoretical method is the only exact method but the amount of data becomes vast and it is difficult to study time varying fields and the influence of room parameters on this. The limiting conditions of hard surfaces can be solved by mirror images. As a way of approaching the problem with

mirror images to see important transient features of the sound field, statistical theory can be used to gain an understanding of the influence of the approximations which must be carried out in wave theoretical calculations.

3.6. Numerical Modelling

The main numerical models are concerned with the geometrical representation of the spherical sound wave propagation, that is to say that phase and wave sphericity are ignored. In general, analytic models assume an omni-directional source, reverberant absorption coefficients, specularly reflecting surfaces, and air absorption quantified by the air absorption exponent.

The most important methods for the numerical modelling of sound fields in enclosures are the Mirror Image Source Method and the Ray-tracing Technique (RTT). Both these methods are derived from geometrical acoustics (see page 19) and give an approximate description for the sound behaviour in an enclosure.

The two methods are based on the assumption that the sound wavelength is smaller than the thickness of the wall structures so that reflections occur as would happen with light. The path of the energy propagation is traced in both methods, the main difference being that for the Mirror Image Source method the starting point is the receiver while for the Ray Method the source represents the beginning of tracing the rays.

The aim of both methods is to determine the impulse response at a receiver point. From the impulse response other acoustical responses may be calculated such as the steady state response, the reverberation response, and the sound build up phenomenon³⁶.

3.6.1. The Mirror Image Source Method

The basic principle of the Mirror Image Source Method is to trace the sound path that connects a receiver to a source by finding the image sources in this path, as shown in Figure 7. The sound path is represented by straight lines, which

symbolise the reflections due to the various surfaces in the room. According to Kuttruff¹⁵ the total number of images N of order up to i_0 is given by:

Eq. 27

$$N(i_0) = N \frac{(N-1)^{i_0} - 1}{N-2}.$$

For regular rooms such as rectangular enclosures the method can be applied quite easily but the more the complexity of the geometry the more the difficulty of application. The problem becomes more severe when the source might not be visible from every position in the room due the finite size of the surfaces.

The Image source method was first used as a computer modelling technique by Allen and Berkley⁴⁹, but the geometry of their model was limited to rectangular rooms. Later on Barron⁵⁰ extended the method to include more complicated shapes but retaining some geometrical restrictions and limited his model to two reflections. Baxa⁵¹ improved the method by extending the number of reflections to five. The major improvement of the image source method was achieved by Borish⁵² who extended the model to arbitrary polyhedra eliminating the restriction imposed by the size of core memory, but the practical application of the model is still limited by the computation time.

Further, in order to overcome some of the problems of the Image Source method, Vorlander⁵³, suggested using a combined ray-tracing/image source algorithm. In this hybrid approach Vorlander uses ray particles to determine the visible image source and therefore calculate the impulse response where the listening conditions in a room are based. With this combined method calculation times are improved, but not at the expense of accuracy.

3.6.2. *The Ray-Tracing Method*

The principle of the ray-tracing method is that the spherical wave energy that sound sources emit is represented by certain tokens, which could be rays⁵⁴, cones⁵⁵ or pyramids⁵⁶. Further the tokens could be used merely to find the sound

propagation paths and therefore do not correspond to any physical quantity. These tokens propagate in straight lines running at the speed of sound and they obey the laws of geometrical acoustics when hitting a surface. The response at a point in the room is determined by specifying the position of a particular object (surface or volume) as being the receiver.

The method was first used by, Allred and Newhouse⁵⁷ in the form of ray-tracing programs as early as 1958. A more advanced ray-tracing algorithm was used by Krokstad *et al*⁵⁴ with several applications in research and in real life room acoustics consulting projects. Those involved the Acoustical Design of the Multi-Purpose 'Hjertnes' Hall in Sandefjord^{58,59}, the design of a large broadcasting studio⁵⁹, a sound reinforcement system⁵⁹, the Acoustical Design of the Grieg Memorial Hall in Bergen^{59,60}.

According to Krokstad *et al*⁵⁹ a ray-tracing program represents a fair compromise between initial cost of programming, cost of use, flexibility of use and precision in modelling rooms and sound fields. The benefits of the ray-tracing method as compared with the scale modelling include the following. Easier to setup and change room shapes and wall materials, easy to simulate various full scale sound sources and microphone directivities, easy to facilitate evaluation by analysing and visualising the results in a variety of ways, no necessity for laboratory facilities or special equipment.

Although Krokstad *et al* were pioneers in applying the ray-tracing technique in the late 1960s other researchers contributed to the development of the method. Schroeder⁸ used the ray-tracing method to estimate the reverberation in simple geometry rooms. Santon⁶¹ used the ray method for the prediction of speech intelligibility by the use of predicted echograms. The method was applied for a conference room and the results were satisfactory. Later on Rietschote *et al*¹⁰ used a ray-tracing computer model for the prediction of speech intelligibility from the modulation transfer function. The model was able to calculate the Speech Transmission Index (STI) in an auditorium.

3.6.3. Discussion on the mirror image source and ray-tracing methods

It is very difficult to develop programs for the Mirror Image Source Model especially for complex room geometry and the computation time increases rapidly with increasing order of reflections in a simulation. For example, for a hall made up of eight plane walls with a total area of 3800 m^2 and therefore volume 12000 m^3 a sound ray or sound particle would undergo 27 reflections per second on average according to Eq. 16 (see page 21). Consequently to compute only the first 500 ms of the impulse response, images sources of at least up to the 14th order must be considered. So for a 14th order of reflection and 8 plane surfaces 9×10^{11} image sources must be constructed according to Eq. 27. Further to that, all of these image sources must be checked for visibility from a given receiver position since only a small fraction of these are valid, due to the finite size of the plane surfaces.

This has limited the practical applications of the Image Source method especially for generalised cases of very complicated geometrical shapes. Further it should be mentioned that the visibility problem makes it impossible to model curved surfaces using the mirror image source method while this would be feasible by the ray-tracing technique, as will be demonstrated in this thesis.

Further the diffraction and diffusion phenomena can be implemented with the Ray-tracing Method while these cannot be taken into account with the Mirror Image Source Method.

On the other hand the Ray-tracing Method is not error free. The main error of the method especially when using rays is at the receiver place and was analysed by Kulowski¹¹. The probability of hitting a point by a sound ray is zero, therefore the observation region should be an area or a volume. Thus the results obtained are not of deterministic nature and therefore are of limited accuracy. Of course the smaller the volume or area of the receiver the more accurate the results.

To minimise errors Krokstad presented a formula for determining the number of rays that should be sent to obtain at least one hit on a receiver region after the last reflection.

Eq. 28

$$I = \left[\frac{2\bar{l} - \ln k}{r \ln(1 - \bar{\alpha})} \right],$$

where I is the number of rays sent from the source, \bar{l} is the mean free path, k is a factor of energy decay range where each ray is being traced (e.g. $k = 10^6$ corresponds to 60 dB), r is the radius of the sphere which represents the listener region, $\bar{\alpha}$ is the mean sound absorption coefficient.

Lehnert⁶² classifies the errors of the ray-tracing method into two categories, errors due to a detection problem and errors due to limited spatial resolution (see Figure 7 A,B,C). The detection problem is caused by the fact that the receiver represents a surface or a volume instead of a point. The limited spatial resolution is caused due to the limited number of rays traced from the source.

The detection problem category comprises the multiple detections error and the detection of invalid paths error. The multiple detections error occurs when many rays from a source or a reflection point hit the detector which is either a two or a three dimensional object. The invalid path error occurs when for example the sound source is shaded, the reflection point is not located within the wall, the receiver is on the rear of the wall. The limited spatial resolution error arises due to long ray paths or small number of rays emitted. As a result the number of rays emitted are not enough to achieve sufficient coverage of the sound field to be modelled.

Overall though the ray-tracing method with the same accuracy represents a considerably more efficient and hence faster algorithm⁵. Further it is much more promising for future development as computer technology improves⁶.

3.6.4. Applications of numerical modelling

The 1980s and 1990s until today have seen an increase in developing numerical models based on the methods discussed earlier. Some of the models have been developed for specific applications such as for industry or for concert halls but most are for general application. The most important of these models are summarised as follows.

Shield⁶³ in 1980 presented a computer model for predicting noise. The model is a computational-empirical hybrid which is based on the first sound reflection from each surface and uses an index for sound decay, caused by the fittings, which depends on their density and on the user's experience. The model has been applied successfully to factory spaces.

The Mehta⁶⁴ model uses the ray-tracing technique and attempts to compensate for edge diffraction by scattering the rays within a quarter of a wavelength from the edge and decay according to a constant derived from the Eyring formula. The model was used to study the non-uniform distribution of absorption in a rectangular enclosure.

Hodgson⁴ describes and compares various models created specially for industrial applications among which are the following. The Jovicic⁶⁵ model employs the image source method and ignores phase and wave sphericity. The shapes of the rooms considered are flat rooms of infinite length and width and duct rooms of infinite length and width equal to height. The Hodgson⁶⁶ model is also based on the image source method and is an extension of the Jovicic model. It can consider any long rectangular parallelepiped room with any source and receiver positions. The Lindqvist^{67, 68} model is based on the method of images and the use of statistical methods. The model can tolerate arbitrary rectangular-parallelepiped rooms, any source and receiver positions, and arbitrary absorption coefficients. The Lemire and Nicolas⁶⁹ model is also based on the mirror image source method with some differences such as the energy contribution of higher order images and is evaluated⁷⁰ by an analytic expression. The Kurze⁷⁰ model is based on

the method of images approach. It can employ room shapes of infinite length and width. The RAYSCAT model developed by Ondet and Barby⁷¹ is based on a ray-tracing technique and takes into account the real geometry of the room and areas with different fittings. The modelling of the fittings is carried out by using a statistical approach. The model was applied quite successfully in workshops and factories.

From the above models Hodgson⁴ finds the Ondet and Barby model, which is based on the ray-tracing method as the most appropriate in terms of accuracy and applicability. Later on, Hodgson⁷² developed a model based on the ray-tracing method whereby the geometry considered was much more complicated and the accuracy was quite good when applied to a machine shop.

Dance¹², has extended the Ondet and Barby model to provide a more detailed representation of the space. The extensions, according to Dance, involved rewriting and restructuring the program to enable the inclusion of source directivity, and a more efficient receiver zone generating system. Furthermore, Dance validated the new model for various industrial applications.

Moore⁷³ and later on Lewers⁵⁶ used ray-tracing with pyramids to model the specular reflections and a radiant exchange method to model diffuse reflection. By determining form factors between surfaces the distribution of path lengths is estimated. By tracing rays from the receiver to all the surfaces, incidence angle and arrival time distributions are formed. A random process is then initiated which propagates sound from surface to surface and to the receiver, where path lengths and receiver incidence angles are sampled by random numbers. The model is restricted to rooms of simple geometry since the method employed imposes very long calculation times.

More recently developed models for general application include the following. The RAMSETE⁷⁴ model is based on the ray-tracing method and employs a pyramid tracer as an improvement to the conical beam tracer. It should be mentioned that the conical beam tracer has problems of overlapping cones, and

multiple detection of the same image source. The SOPRAN⁷⁵ (Sound particle Program for Room Acoustics and Noise emission) is applicable both for concert room acoustics and factory halls. The model employs a sound particle simulation method, which is a type of ray-tracing method. Sound particles as exact points and as carriers of a quantum of sound energy are emitted from point sources. While tracing their paths through the room with all reflections taking absorption into account, they are detected if crossing a grid of cubic volumes where their relative energies are summed up. The RAYON⁷⁶ model is based on the Gaussian beam method, which is an extension of the ray-tracing method. It allows calculations of sound levels, speech intelligibility, and rooms criteria such as reverberation time and clarity. Further, it employs statistical techniques for the modelling of fitted rooms.

Comparisons^{4, 5, 77, 78, 79} between the most popular models have shown that the models that incorporate the ray-tracing method are more suitable for the purpose of prediction of sound fields in rooms which are not rectangular or of simple geometry.

3.7. Main Acoustics Software Available on the Market

Although acoustical software packages are priced quite high, it can be stated that the software development for acoustical design is fairly stagnant. This is basically due to the high development costs needed to dramatically improve the available programs.

The main commercial acoustical computer programs are based on the two methods of the image sources and ray-tracing and are described as follows.

3.7.1. The ODEON Acoustics Program

The ODEON^{80, 81, 82} program was developed at the Acoustics Laboratory at the Technical University of Denmark and it can be used as a tool for the basic evaluation of large rooms. It uses a hybrid approach that is a ray-tracing-image source method, as Vorlander⁵³ suggested. The model was applied relatively successfully to a variety of enclosed spaces⁸³. The main features of ODEON

include predictions of reverberation times, energy parameters, reflectograms, reflection paths and reflector coverage. Further, the program involves auralization.

3.7.2. The Computer Array Design Program (CADP2)

The CADP2^{84, 85} software is made by JBL and it can be used mainly to predict the performance of complex multi-loudspeaker sound reinforcement systems in real spaces. The program has the advantage that it is running on the Microsoft Windows operating system, which makes it flexible to run and user friendly. The algorithm used is of an image source type for polyhedral spaces and statistical room acoustics. The built-in library of manufacturers loudspeakers, makes it mainly suitable for checking the uniformity of coverage, maximum sound levels, predicting RASTI measurements with the room empty and full. Further the program is useful for estimating reverberation times and for producing high quality binaural audio.

CADP2 is quite good for saving and recalling arrays. This feature gives the program the advantage that complicated systems can be treated as single speaker devices which means that the array can be positioned aimed and controlled as a single unit. Auralization can be achieved by exporting room impulse response files in ASCII text format to "Hyperception". Subsequently, this can be used to perform the auralization process by incorporating third party programs such as "Hypersignal" provided a DSP (Digital Signal Processing) board is available.

3.7.3. The EPIDAURE-EBINAUR Software Package

The EPIDAURE⁸⁶ software was developed by Maercke & Martin and can be used as an efficient design tool in room acoustics. The program uses an algorithm involving ray, beam, and cone tracing. Its main features include prediction of objective acoustical criteria from the estimated energy responses. Auralization based on impulse responses is possible with EBINAUR⁸⁷.

3.7.4. EASE, EASE JR, and EARS

EASE^{88, 89}, EASE JR⁹⁰, and EARS⁹¹ are produced by Renkus-Heinz. EASE is quite a powerful program operating in a windows-like environment, is capable of modeling complex rooms providing the necessary information for sound system design. EASE JR is just a smaller version of EASE. EARS, which stands for Electronically Auralized Room Simulation, performs the binaural auralization process.

3.7.5. ACOUSTA CADD

ACOUSTA CADD⁹² is made by Altec Lansing. The program includes binaural auralization considering the direction of the listeners face and the loudspeaker's off axis transient response. Another main feature of ACOUSTA CADD is the inclusion of the effect of the diffusion scattering response of reflecting surfaces. Further ACOUSTA CADD is specially used for multiple speaker arrangements.

3.7.6. BOSE MODELER

Unlike the other acoustics and sound system design programs running on the PC platform, BOSE MODELER⁹³ made by BOSE is working on the Mac platform. Further the BOSE MODELLER is suitable for indoor as well as outdoor sound system design

The developers of BOSE presented a paper at the 91st AES Convention which points out that none of the existing auralization systems had been scientifically quantitatively proved as being accurate. Research in BOSE is concentrated in binaural impulse response synthesis, algorithm efficiency, synthesis algorithm diagnostics, and simulation system authentication.

On the synthesis algorithm diagnostics research, BOSE attempted to prove that BOSE MODELER software and auralization system is reliable. The results were at least convincing as binaural recordings since the listeners were unable to tell whether the simulations were synthetic or real. On the simulation system authentication, BOSE is planning to test the ability of BOSE Modeler auralization system to simulate the speech intelligibility of sound systems in large

rooms. Further, D'Antonio⁹⁴ at BOSE developed a way to characterise diffusion and determine the necessary directional scattering coefficients, as well as computational algorithms, which utilise these data in image model/ray-tracing programs.

3.7.7. RAYNOISE

RAYNOISE^{95, 96} is a computer program that gives capabilities in the analysis of room acoustics, industrial noise control and environmental noise.

The mathematical model used by RAYNOISE is that of geometrical acoustics based on the assumption that sound waves can be treated as rays following the same reflection laws as light rays in geometrical optics. The model embodies the conical beam method⁹⁷ and combines the advantages of the ray-tracing and mirror image source method.

Some of the analysis features of RAYNOISE are echogram calculation, and calculation of several acoustical criteria such as Definition, Clarity-index, Early Decay Time, Lateral Efficiency and RASTI-index.

3.8. Conclusion

This Chapter has reviewed different methods and models used for the prediction of sound fields in enclosures. The most important and practical of these methods and models are the scale modelling from the physical modelling category and the Mirror image source and ray-tracing methods from numerical modelling.

The advantages that numerical modelling enjoys due to the recent rapid development of computer software and hardware is making the use of physical models relatively rare. These advantages include easier build of the model, greater economy, and time saving, while the accuracy of both physical and numerical models lies at the same level.

As far as the choice between, the mirror image source and ray-tracing models is concerned, research has shown that ray-tracing is more appropriate because of

numerous advantages. These include the possibility to model complex room geometry, the possibility to model refraction, diffraction, and diffusion. Further, an important advantage, more relevant to the work done in this thesis, is the possibility of using ray-tracing to model sound fields interacting with curved walls while this would not be possible with the mirror image source method.

Although suggested by researchers such as Schroeder⁸ and Kuttruff⁷ that it would be wise to make use of curved surfaces in the development of acoustical numerical models, all the contemporary acoustical computer models represent the room to be modelled as a series of flat or planar surfaces.

Chapter 4

THE PROPOSED MODEL

4. THE PROPOSED MODEL

4.1. General Description

The proposed model is concerned with the geometrical representation of the spherical sound wave propagation in closed or partially closed spaces. This is done by tracing the reflected waves in three dimensions with the aid of the computer. The method employed makes use of the ray-tracing method and the idea of a sound particle. The modelling is directed towards enclosures of any shape including spaces with curved surfaces. This is accomplished by using an object-oriented approach (see page 73) and utilising solid body modelling techniques such as constructive solid geometry (see page 97).

The energy of a single spherical wave after a short duration sound burst emitted by a source in a room is divided into elements which are assumed to be discrete objects. These elements, called sound particles, move with the speed of sound and obey the laws of geometrical acoustics. Sound particles propagate through the enclosure and are reflected at the boundaries. Because of the sound absorbing properties of the walls and the air, the energy of a sound particle decays with time. Each sound particle is traced until its energy decreases below a certain negligible value or up to a certain order of reflection.

The ultimate aim is to obtain a diagram of sound energy Vs time for a particular receiver position. The receiver position, which represents a microphone registering pressure fluctuations, could be represented by any kind of object, surface or solid. The diagram obtained represents the energy of the sound particles penetrating the particular object and the time elapsed before penetration for each sound particle. Further the direction of attack of the sound particles hitting the receiver can be registered.

If a room is excited by an impulsive sound the diagram obtained could be interpreted as a series of echoes (see page 22). From this echogram (reflectogram)

the delays of reflections and the intelligibility of speech can be determined. The directivity of the sound field may also be obtained. The reverberation time early decay time and the steady state energy at the receiver position can be determined from the reverberant curve obtained from the reflectogram. Further audible simulation can be achieved by convolution of the room impulse response with an anechoic signal.

4.1.1 Assumptions and Specifications of the Proposed Model

Any model is an idealisation of reality and this idealisation should be based on several reasonable assumptions that make the model feasible to be created. Further any model should have some specifications to ensure that the model will be useful enough for its purpose.

The assumptions and specifications of the proposed model include the following:

1. The sound source is a point source. Directivity characteristics can be applied to the source accordingly.
2. Phase and wave sphericity is ignored.
3. The receiver could be represented by a two or three-dimensional object. Any directivity characteristics can be accomplished according to the shape of the object.
4. The receiver is sound transparent in order not to interfere with the sound field, that is sound particles pass through the receiver as though it does not exist.
5. The surfaces or objects in the model are assumed to be rigid.
6. Complex curved surfaces are modelled using the Constructive Solid Geometry technique and quadric algebraic objects.
7. In the case of perfect reflections the size or radii of curvature of the reflecting surface-object are large compared with the sound wavelength.
8. The absorption of the surfaces is considered to be independent of the angle of incidence, so that published reverberant absorption coefficients can be

used (It would be easy for the model to accommodate absorption coefficients depending on the angle of incidence but there is not much data about such coefficients).

9. Diffusion, diffraction, and transmission of sound are roughly considered using randomised processes.
10. Absorption of sound in the air is accounted by the model for the various frequency bands.
11. The reduction in energy due to the spherical wave propagation is realised by the reduction in the sound particle density.

4.2. The Sound Source

Although real sources are usually strongly directional, the source in the model is assumed to be an omni-directional point source giving rise to a spherically expanding wave front. This is due to the fact that in practice sources that radiate uniformly in all directions are used in order not to bias measurements.

In geometrical acoustics the source of a spherical wave may be represented by a set of lines originating from one point. Since the source is assumed to be omni-directional, the directions of the lines are uniformly distributed around that point and therefore the initial sound energy E_m of a sound particle after a short sound burst is given by:

$$E_m = \frac{W}{N},$$

Eq. 29

where W is the sound source power, and N is the total number of sound particles sent by the source.

The most useful equation to represent the sound particle path is the equation of a straight line in vectorial form given by:

$$\mathbf{P} = \mathbf{P}_0 + \mathbf{u}t,$$

Eq. 30

where \mathbf{P} are the co-ordinates of a running point on the line representing a sound ray or a sound particle path (see Figure 8a), \mathbf{P}_0 are the co-ordinates of the sound source or the reflecting position, t is the current value of the parameter which is equal to the distance between points \mathbf{P} and \mathbf{P}_0 , and \mathbf{u} is the unit direction vector parallel to the line indicating the direction of the sound particle.

There are two ways of obtaining the uniform directions distribution of the vectors around the sound source. Those are the deterministic and the statistical. In the deterministic method an algebraic formula is used which gives the regular net of vector vertices (see Figure 8b) that make up a sphere surrounding the source^{54, 98}.

In the statistical way (see Figure 8c) the vector vertices are randomly distributed on the sphere surface. In order to calculate the randomly distributed vertices two random numbers are generated from 0 to 2π and from 0 to π to represent the azimuth ϕ and elevation θ angles respectively. Then the direction vector \mathbf{u} is given by:

$$\{\cos \phi \cos \theta, \sin \phi \cos \theta, \sin \theta\}. \quad \text{Eq. 31}$$

It should be noted that an important advantage occurs in favour of the statistical method when the number of sound particles to be emitted is not known. If the statistical method is employed the distribution of points is uniform irrespective of their number. Thus, when there is a need to enlarge the sound particle number to obtain sufficient reliable results the calculations, which have already been made keep their validity.

4.3. Tracing the Sound Particle

In numerical form the space is represented by a set of equations which describe the set of surface-objects that the enclosure is made of in three dimensions. Flat surfaces, can be represented by polygons and/or planes, while curved surfaces

may be represented by quadric (represented by a quadratic function) type of objects.

The reflection subroutine consists of a determination of the reflecting object, calculation of the reflected sound particle path direction, and calculation of the reflected sound particle energy.

4.4. Determination of the Reflecting Surface-object

Each object in the enclosed space is tested to determine, whether is intersected by a sound particle path. If the sound particle path intersects the object, the distance from the origin of the sound particle path to the object-intersection point is calculated. The smallest calculated intersection distance identifies that object as being the nearest and therefore as being the reflecting object.

4.4.1. Collision Calculations

A sound particle path can be described with an initial position \mathbf{P}_0 and a unit vector \mathbf{u} , as explained earlier (see Eq. 30). The co-ordinates of any point \mathbf{P} along the sound particle path at a distance t from \mathbf{P}_0 is computed from Eq. 30 as:

$$\mathbf{P} = \mathbf{P}_0 + t\mathbf{u}.$$

Initially \mathbf{P}_0 can be set to the position of the sound source and then at the position of each reflection. The unit vector \mathbf{u} is initially obtained from the direction of the primary sound particle from the sound source and afterwards from the direction of each reflection. At each reflecting object, vectors \mathbf{P}_0 and \mathbf{u} are updated for the secondary sound particle paths at each sound particle-surface collision point. To locate surface collisions, the sound particle path equation (Eq. 30) and the surface equation are simultaneously solved for each of the individual objects in the room.

4.4.2. A Sound Particle Colliding with a Planar Object

The plane is the simplest surface that can be used to describe enclosed spaces and therefore is used quite extensively in the development of acoustical models by many researchers such as Kolowski⁹⁹ and Ondet and Barby⁷¹.

The plane is a two dimensional figure having an infinite extent. In a three-dimensional world, the plane cuts across the three dimensional space dividing it into two parts, one inside the plane and the other outside it. The equation of a plane is:

$$Ax + By + Cz + D = 0. \tag{Eq. 32}$$

The coefficients A , B and C compose the normal to the plane. If the vector $\{A, B, C\}$ is normalised, $|D|$ is the distance from the origin to the nearest point on the plane.

Inserting the equation of the sound particle path (Eq. 30) into the equation of the plane (Eq. 32) the collision point can be obtained by determining t :

$$A(p_x + tu_x) + B(p_y + tu_y) + C(p_z + tu_z) + D = 0, \tag{Eq. 33}$$

$$t = \frac{-D - Ap_x - Bp_y - Cp_z}{Au_x + Bu_y + Cu_z}. \tag{Eq. 34}$$

4.4.3. *A Sound Particle Colliding with a Ring Type of Object*

Rings are planar objects with a centre, an inner radius, and an outer radius. The area between the inner and outer radii is considered to be inside the ring. An example where a ring object may be used for modelling is the whispering gallery of St Paul's Cathedral (see page 128).

Checking for collision between a sound particle and a ring involves first intersecting with the ring's plane and then computing the distance of the intersection point to the centre of the ring. Then the distance is compared with the minimum and maximum radii to determine if there is a real collision between the sound particle and the ring.

4.4.4. A Sound Particle Colliding with a Polygon Object

The polygon collision algorithm¹⁰¹ should be as efficient as possible, since polygon objects are used extensively when preparing a particular model. A polygon is actually a collection of points in a plane. It is usually specified by a list of endpoints, and the points enclosed are inside the polygon.

A polygon is considered to lie in a plane, and one of the many values pre-computed for a polygon is the plane equation. As explained earlier the normal to a plane is part of the plane equation. Given that the vertices are in clockwise order when viewed from a direction the normal is facing, the normal vector can be computed from the first three vertices v_0, v_1, v_2 as follows:

$$\mathbf{N} = (v_0 - v_1) \times (v_2 - v_1).$$

Eq. 35

If \mathbf{N} has length zero, then the three vertices are collinear and do not define a plane. Also, if there are more than four vertices they might not lie in a plane. Once \mathbf{N} has been computed the value D for the plane equation can be calculated from any one of the points.

The sound particle polygon collision point calculation can be divided into two parts. First, check the plane that the polygon resides in, and second, check to see whether the intersection point on the plane lies within the polygon.

Determining whether the intersection point with the plane of the polygon lies within the polygon can be reduced from a three-dimensional problem to a two dimensional problem by applying a parallel projection to the polygon vertices onto one of the co-ordinate planes. This operation amounts to ignoring one of the x, y, z components of each vertex. Then a line is extended from the intersection point, in an arbitrary direction and count the number of line segments that it crosses. If the number is odd the point in question is within the polygon if it is even the point in question is outside the polygon.

4.4.5. A Sound Particle Colliding with a Spherical Object

The equation for a sphere is given by:

$$(x - x_0)^2 + (y - y_0)^2 + (z - z_0)^2 = r^2, \quad \text{Eq. 36}$$

where x_0, y_0, z_0 is the centre of the sphere and r is the radius. Inserting the equation of the sound particle path into the equation of the sphere gives the following:

$$(p_x + tu_x - x_0)^2 + (p_y + tu_y - y_0)^2 + (p_z + tu_z - z_0)^2 = r^2. \quad \text{Eq. 37}$$

This is in fact is only a quadratic equation to solve for t :

$$At^2 + Bt + C = 0, \quad \text{Eq. 38}$$

where $A = \mathbf{u} \cdot \mathbf{u}$, $B = \mathbf{p} \cdot \mathbf{p}$, $C = \mathbf{u} \cdot \mathbf{u} - r^2$.

If the sound particle direction is normalised, then A equals 1. Once the B and C coefficients are calculated, the quadratic equation can be solved. If the roots are imaginary, the sound particle does not hit the sphere. If one of the roots is positive, that root corresponds to a collision of the sound particle with the sphere. If both the roots are positive then the smallest of those is the object's nearest collision along the sound particle path.

4.4.6. A Sound Particle Colliding with a Quadric Type of Object

A quadric is second degree implicit surface. An implicit surface is one whose points can be expressed as an equation in x, y, z . A general quadric is expressed in the following equation:

$$Ax^2 + By^2 + Cz^2 + 2Dxy + 2Eyz + 2Fxz + 2Gx + 2Hy + 2Jz + K = 0. \quad \text{Eq. 39}$$

With the above general equation many familiar shapes may be modelled such as spheres, cylinders, ellipsoids, conic surfaces, paraboloids, hyperboloids.

The equation of a cylinder is given by:

$$\frac{x^2}{a^2} + \frac{y^2}{c^2} - 1 = 0,$$

Eq. 40

where $2a$ and $2c$ are the principal axis lengths.

The equation of a cone is given by:

$$\frac{x^2}{a^2} + y^2 + \frac{z^2}{c^2} = 0,$$

Eq. 41

where principal axis lengths $2a$ and $2c$ are at a unit distance from the apex.

The equation of a paraboloid is given by:

$$\frac{x^2}{a^2} + \frac{y^2}{c^2} - 4fz = 0,$$

Eq. 42

where principal axis lengths $2a$ and $2c$ at twice the focal length f .

The equation of an ellipsoid is given by:

$$\frac{x^2}{a^2} + \frac{y^2}{b^2} + \frac{z^2}{c^2} - 1 = 0,$$

Eq. 43

where axis lengths of a, b, c are along the principal directions of x, y, z .

In order to economise memory and computation time for the computer a more simplified general quadric equation can be generated by having the origin of the

co-ordinate system at the centre of the generated surface; and the shapes generally oriented as surfaces of revolution about the z -axis. Then the quadric equation will have the much simpler form:

$$Ax^2 + By^2 + Cz^2 + Dz + E = 0.$$

Eq. 44

However, the constraints imposed will not reduce the applicability of the model. First, the global co-ordinate system can be transformed to the quadric centred co-ordinate system before performing mathematical operations such as the collision test. Then, transformed back after the computations have finished. Second, the shape can be rotated to any desired position before the mathematical operations and then rotated back afterwards.

For the calculation of the collision point between a sound particle and quadric the equation of motion of the sound particle is inserted into the equation of the particular quadric and the resulting equation solved for t .

Suppose the sound particle path is a straight line with an origin $\{x_c, y_c, z_c\}$ and direction $\{x_d, y_d, z_d\}$. Any point along the line may be represented in parametric form by:

$$x_p = x_c + tx_d, y_p = y_c + ty_d, z_p = z_c + tz_d.$$

Eq. 45

If the line intersects the quadric, there is some value of t for which that point on the line is also on the surface of the quadric. To find the value of t the above equation (Eq. 45) is inserted into the general simplified quadric equation (Eq. 44) as follows.

$$A(x_c + tx_d)^2 + B(y_c + ty_d)^2 + C(z_c + tz_d)^2 + D(z_c + tz_d) + E = 0.$$

Eq. 46

This is a quadratic equation and it can be solved for t using the quadratic formula:

Eq. 47

$$t = \frac{-b \pm \sqrt{b^2 - 4ac}}{2a},$$

where a is the coefficient of the squared term, b is the coefficient of the first power term, and c is the constant term:

Eq. 48

$$a = Ax_d^2 + By_d^2 + Cz_d^2,$$

Eq. 49

$$b = 2(Ax_c x_d + By_c y_d + Bz_c z_d) + Dz_d,$$

Eq. 50

$$c = Ax_c^2 + By_c^2 + Cz_c^2 + Dz_c + E.$$

If the line that represents the sound particle path intersects the particular quadric then the quadratic equation has two solutions which represent the front and back of the quadric surface. The nearest to the line origin represents obviously the collision point.

4.5. Calculation of the Reflected Sound Particle Direction

The sound particle is reflected off the reflecting surface along the specular path where the angle of reflection equals the angle of incidence (see page 13 and Figure 2a). If sound is transmitted through the object a sound particle could be sent through the surface in the transmission direction (see page 15). Further the sound particle could be reflected to a random direction or to a direction according to a probability distribution in order to simulate scattering (see page 15).

The procedure is repeated for each secondary sound particle path that is for paths of higher order reflections. Objects are tested for collision, and the nearest surface along a secondary sound particle path is used to recursively produce the next generation of reflection paths. The level of repetition of this procedure can

be determined by, the reflection order, the current sound particle energy, or even the time value.

In order to calculate the reflected sound particle path the collided surface normal needs to be calculated. The normal will indicate which way the incoming sound particle is facing the collided surface in order to calculate the reflected sound particle path. For objects such as polygons and planes the normal always points out in one direction. While for curved surfaces such as general quadrics, spheres, cylindrical shapes etc., the normal is different at each point on the surface.

Knowing the normal at the collision point the reflected sound particle direction can be evaluated by:

$$\mathbf{R} = 2(-\mathbf{I} \cdot \mathbf{N})\mathbf{N} + \mathbf{I}, \quad \text{Eq. 51}$$

where \mathbf{R} is the reflected sound particle direction, \mathbf{I} is the incident sound particle direction, and \mathbf{N} is the direction of the normal to the surface object at the collision point.

4.5.1. Sound Particle Reflected from a Planar Object

The normal for a plane always points in one direction and is pre-computed by the program. It is given by the coefficients A, B, C , from the equation of the plane.

4.5.2. Sound Particle Reflected from a Ring Type of Object

The normal to be computed is the normal of the plane where the ring exists.

4.5.3. Sound Particle Reflected from a Polygon Object

The sound particle will be reflected with respect to the surface normal of the polygon which is given by the first three vertices as follows:

$$\mathbf{N} = (\mathbf{v}_0 - \mathbf{v}_1) \times (\mathbf{v}_2 - \mathbf{v}_1). \quad \text{Eq. 52}$$

4.5.4. Sound Particle Reflected from a Spherical Object

For objects such as a sphere, the direction of the normal is given by the gradient of the function for the surface¹⁷. The normal is found by converting to a unit vector the gradient to the sphere at the point of collision between the sound particle and the object. The gradient which is a vector whose components are the partial derivatives of the sphere evaluated at the point of collision, is given by:

$$\nabla = \frac{\partial f}{\partial x} i + \frac{\partial f}{\partial y} j + \frac{\partial f}{\partial z} k, \quad \text{Eq. 53}$$

where i, j, k are unit vectors along the axes of the co-ordinate system.

$$\begin{aligned} \frac{\partial}{\partial x} [(x)^2 + (y)^2 + (z)^2 - r^2] &= 2x \\ \frac{\partial}{\partial y} [(x)^2 + (y)^2 + (z)^2 - r^2] &= 2y \\ \frac{\partial}{\partial z} [(x)^2 + (y)^2 + (z)^2 - r^2] &= 2z \end{aligned}$$

Therefore, the normal at the collision point, is given by the following vector:

$$\mathbf{N} = \{2x, 2y, 2z\}. \quad \text{Eq. 54}$$

4.5.5. Sound Particle Reflected from a Quadric Type of Object

In order to compute there are two things that are needed. The sound particle path direction, which is known and the normal to the surface at the collision point. The normal is computed by normalising the gradient to the quadric at the collision point.

The normal to a quadric surface or any implicit surface is equal to the gradient at the point of interest. The gradient of function $f(x, y, z)$ is a vector given by:

$$\left\{ \frac{\partial f}{\partial x}, \frac{\partial f}{\partial y}, \frac{\partial f}{\partial z} \right\}.$$

Hence, the gradient of the quadric is given by:

$$\begin{aligned}\frac{\partial}{\partial x}(Ax^2 + By^2 + Cz^2 + Dz + E) &= 2x \\ \frac{\partial}{\partial y}(Ax^2 + By^2 + Cz^2 + Dz + E) &= 2y \\ \frac{\partial}{\partial z}(Ax^2 + By^2 + Cz^2 + Dz + E) &= 2z + D\end{aligned}$$

Therefore the normal at a particular point, is given by the vector:

$$\mathbf{N} = \{2x, 2y, 2z + D\}.$$

Eq. 55

4.6. Considering Scattering and Diffraction

As mentioned in Chapter 2 (see pages 15 and 20) sound will not always be reflected in the specular direction when meeting a surface. In real life sound will be reflected in the specular direction but also be scattered in all directions and be diffracted (see page 17). This is mainly due to the edge effects created by the finite sizes of the various objects in an enclosed space.

The actual scattering and diffraction process is rather impossible to predict for each particular case of surface object, so a statistical process is used as an alternative method. By assigning a scattering coefficient from 0 to 1 to a surface-object during the modelling stage this will represent the diffusion of sound in relation to the perfect reflection. Therefore, a sound particle will have a probability equal to this scattering coefficient of being reflected in a random direction rather than in the specular direction as explained in the preceding sections.

An even more approximate way to model scattering and diffraction is to assign an order of reflection after which all sound reflection directions become random. Although this method is approximate, it represents a practical and efficient way of achieving a good mix of sound or a diffuse field.

4.7. Calculation of the Sound Particle Energy

As the sound particle propagates through the enclosed space its energy is reduced due to collisions with the various surface-objects and absorption by air.

4.7.1. Surface Absorption

At each reflection the incidence angle of the sound particle is known. That enables the decrease of the reflected sound particle energy to be considered as proportional to a physical sound absorption coefficient. This kind of coefficient describes sound absorption of a material as a function of an incidence angle of a sound wave and therefore it is seldom published due to the complicated measurement procedure. However, when incidence sound particles are numerous enough and their directions are uniformly distributed in the hemisphere at the front of each object in the room a sound field may be considered to be diffuse. This allows the use of reverberant coefficients, which are available in the literature, instead of physical ones.

In most cases of considered rooms, a primary sound particles number of only about 500 the sound particles field may be considered to be sufficiently diffuse to justify the use of reverberant coefficients.

Therefore, the energy decrease due to surface absorption is given by:

$$E = E_0(1 - a), \quad \text{Eq. 56}$$

where E and E_0 is the energy before and after the sound particle hits the reflecting surface, and a is the material reverberant absorption coefficient.

4.7.2. Atmospheric absorption

Besides the energy decrease due to the surface absorption the energy due to atmospheric absorption is accounted for in the model. The sound particle energy is attenuated by air according to the following equation:

Eq. 57

$$E = E_0 e^{-\alpha s},$$

where E_0 and E represent the energy between two points on the sound particle path and s is the distance between them. The coefficient α is given by¹⁰¹:

Eq. 58

$$\begin{aligned} \alpha = & f^2 [1.84 \times 10^{-11} (p_s / p_{s0})^{-1} (T / T_0)^{1/2} \\ & + (T / T_0)^{-5/2} \{1.278 \times 10^{-2} e^{(-2239.1/T)} / (f_{r,O} + (f^2 / f_{r,O})) \\ & + 1.068 \times 10^{-1} e^{-3352/T} / (f_{r,N} + (f^2 / f_{r,N}))\}] \end{aligned}$$

$$f_{r,O} = (p_s / p_{s0}) \{24 + 4.41 \times 10^4 h \times [(0.05 + h) / (0.391 + h)]\}$$

$$f_{r,N} = (p_s / p_{s0}) (T / T_0)^{-1/2} (9 + 350 h e^{-6.142[(T/T_0)^{-1/3} - 1]})$$

where f is the acoustic frequency in Hz, p_s is the atmospheric pressure in Pa, p_w is the reference atmospheric pressure which equals to 101.325 kPa (1 atm), T atmospheric temperature in K, T_0 reference ambient atmospheric temperature which equals to 293.15 K (20 C). $f_{r,O}$ and $f_{r,N}$ are the vibrational relaxation frequencies for the substances of oxygen and nitrogen respectively. h is the molar concentration of water vapour in percent, or, for a given temperature 100 times the ratio of the number of moles of water present in an atmospheric sample.

4.8. The Receiver

The curve of the sound energy decay, which is obtained by means of the proposed model, is composed from the individual sound particle energies. There are various ways in which the curve can be calculated. For example the sound particle energy may be stored in the computer memory: (a) at each reflection point, (b) at equidistant points of the sound particle path, (c) each time a sound particle hits a sound transparent object which is located inside the modelled room.

The first two ways allow the calculation of the sound decay curve averaged in the interior of the whole room. The curve obtained by means of the third way corresponds to a much smaller region of observation, that is, to the single object

or to a solid sound transparent object placed inside the room. This curve can then be considered to be equivalent to the measured response of the room. It gives also the possibility to investigate the space distribution of the acoustical parameters determined from the curve.

The numerical to represent a receiver with a specified object, requires only the indication of this object in the data describing the room to be modelled. At each reflection of a sound particle, it is checked whether the reflecting object is the indicated one. When this happens, the value of the sound particle's actual energy and its time delay are stored. One can find that using a particular surface-object to represent a receiver is very convenient from the viewpoint of both the memory space and the calculation time economising. However this will depend on the type of object, that is how efficient is to perform the collision test for the particular type of object.

It is a general practice when taking measurements, to use a microphone much smaller than the wavelength of sound under investigation so that the microphone will not interfere and influence the measurement. Therefore the use of a sound transparent sphere as the observation region makes the correspondence between the modelling results and the measurement results more obvious. Further the use of the sphere takes advantage of the fact that the numerical values for intensity and energy are identical when measured of unit area and this area is viewed as a circle by the sound particle from all directions. Finally the collision test is very efficient since the calculations involved are minimal.

It is convenient to store the sound energy decay in the form of a histogram, known as the energetic impulse response. This response is composed from individual sound particle energies by their summation in the appropriate intervals of a histogram. A time interval of 10 ms is generally used since this is usually what the human ear can detect.

4.8.1. Calculation of the Sound Energy Received

The total energy received by a potential listener will be the energy due to the direct sound field plus the early reflections plus the energy due to the diffuse sound field.

The energy density flow due to the direct sound field can be calculated exactly from the well known inverse square law (see Eq. 1 on page 11) and therefore:

$$I_d = \frac{W}{4\pi r^2}, \quad \text{Eq. 59}$$

where I_d is the energy density flow due to the direct field, W is the power of the sound source, r is the distance between source and receiver.

The energy density flow due to the diffuse sound field will be the sum of the individual energies of the sound particles received:

$$I_r = \frac{W}{\Delta S N} \sum_{i=1}^{N_m} E_i, \quad \text{Eq. 60}$$

where I_r is the energy density flow or intensity due to the reflected sound, W is the power of the sound source, ΔS is the projected area of the receiver as viewed by the sound particle, N is the number of primary sound particles emitted by the source, N_m is the number of sound particles penetrating the receiver, E_i is the fraction of the energy of single sound particle that reached the receiver.

Thus the total energy density flow received by a potential listener:

$$I_{tot} = I_d + I_r. \quad \text{Eq. 61}$$

One of the assumptions of the proposed model is that the reduction in energy due to the spherical wave propagation is realised in the reduction of the sound

particle density as it moves away from the source. This relationship between the reduction of the sound particle density and sound wave propagation should be adjusted by choosing an appropriate receiver volume and a number of sound particles emitted. However there will always be errors involved due to the complexity of the space considered. The attempt therefore is to choose a receiver size to minimise the errors. The size should not be too high to register invalid paths nor too low to miss valid sound paths. Similarly the sound particles number should be appropriate so that sufficient coverage of the sound field is achieved.

Researchers are using various formulae to calculate the receiver size sound particle number combination to minimise the errors, such as¹⁰²:

$$R = l_{\max} \sqrt{2\pi N}, \quad \text{Eq. 62}$$

where R is the radius of spherical receiver and l_{\max} is the maximum length of a ray and N is the number of sound particles emitted. Dance and Shield¹⁰³ use the following relationship:

$$N = 10 \frac{V_s}{V_r}, \quad \text{Eq. 63}$$

where V_s is the volume of the enclosure, and V_r is the volume of the receiver. Van Rietchote *et al* use:

$$\frac{NR^2}{4m^2l^2} > 1, \quad \text{Eq. 64}$$

where m is the reflection order and l is the mean free path.

4.9. The use of Expanding Receivers

To minimise the detection errors and achieve satisfactory coverage of the sound field, a new method is utilised. Instead of having a fixed sized receiver, the

receiver is expanded according to the propagating sound particle. The idea, suggested by Lenhart⁶², is equivalent to emitting bundles of sound particles in the form of beams or cones depending on the receiver type of object. In beam tracing instead of sending a sound particle which follows a straight line path a solid object is sent such as a pyramid or a cone and therefore full coverage is accomplished.

If a spherical receiver is used and its radius is varied to match the density of primary sound particles sent by the sound source, this would be equivalent to cone tracing. Suppose a source is emitting N sound particles in all directions then the radius of the spherical receiver is varied so that there is only one chance to achieve a collision. This variation obviously depends on the number of particles N and the distance r from the source to the receiver. It can be shown that the radius R for still one particle arriving at the spherical receiver is given by the following equation:

$$\pi R^2 = \frac{4\pi r^2}{N}$$

Eq. 65

The validity of the method is based on the assumption that the specular reflection density growth is quadratic with respect to time (see page 22). This has been verified for rectangular rooms by Cremer¹⁴, and more recently by Vorlander¹¹⁴ for more complex enclosures.

The distance r between the source and receiver can be expressed as:

$$r = c_0 t$$

Eq. 66

Therefore,

Eq. 67

$$\pi R^2 = \frac{4\pi c_0^2 t^2}{N} \quad \text{or} \quad R = \frac{2c_0 t}{\sqrt{N}}$$

The accuracy of the model is obviously related to the number of primary sound particles emitted and the reverberation time of the enclosure considered. The radius of the spherical receiver increases by the time but decreases the higher the number of primary particles. If 10000 primary sound particles are used then the diameter of the sphere will be about 13 meters at one second. If 100000 will be about 5 meters, while if a million primary sound particles are emitted the receiver diameter or spatial uncertainty becomes about 1 meter at one second.

As any model or method cannot be perfect, applying the technique of expanding receivers causes errors in some situations. The first thing to be aware is that the source must be strictly omni-directional. The second is that if receivers are placed very near a surface they could become directional. The third is the multiple detection error.

Although it is very difficult to get a perfectly omni-directional source, it can be approximated by dividing the surface of the sphere into equal square patches as shown in Figure 9. The problem of directional receivers can be overcome by moving the receiver away from the surface as it expands, so that it stays within the bounded system. The multiple detection error is dealt with by checking the surfaces involved in the total sound particle path.

Chapter 5

SOFTWARE DESIGN, DEVELOPMENT AND COMPUTER
IMPLEMENTATION OF THE PROPOSED MODEL

5. SOFTWARE DESIGN, DEVELOPMENT AND COMPUTER IMPLEMENTATION OF THE PROPOSED MODEL

5.1. Introduction

This Chapter describes the development of the CADAЕ computer program, which is based on the previously described proposed model. CADAЕ is a name given to the program, which stands for Computer-Aided Design of Acoustical Environments. The mathematics of the program is based on the proposed model (see Chapter 6). The CADAЕ sound prediction program was developed by the author and was applied to several cases of bounded spatial systems, some of which are described in Chapter 8.

The first section of this Chapter gives a general description of the CADAЕ program, and how the development plan for the program was designed. The next section describes the pre-processing stage, which includes the data input. Afterwards, in the processing stage, the main classes and functions of the program are analysed. Finally, the last section gives a description of the post-processing stage, which includes presentation and further analysis of the results.

A flowchart of the main operations of the CADAЕ program is provided on Table 1. The flowchart can be used as general guide throughout this Chapter in order to get a better picture as to how the computer model works.

5.2. Software Design Issues

To implement the proposed model, apart from coding, involved researching algorithms and designing the structure of the software. Once the design was determined, the algorithms, data structures, and modules have been chosen, coding the program was fairly straightforward.

First of all the programming needs had to be identified. For this reason a simple procedural preliminary implementation of the model was carried out in

MATLAB¹⁰⁵, which is quite suitable for drafting programs. Soon it was realised that the development of the program could be broken down into three parts, each of which could be taken care of by an entirely different system.

1. The pre-processing part, which involves modelling, data input.
2. The processing part, which involves the actual simulation.
3. The post-processing part that is the presentation of the results.

5.3. Pre-processing, Modelling, Data Input

Modelling is the process of describing the enclosed space that is to be investigated. This is the step where the various surfaces, the source, the receiver(s) and other acoustical parameters of the overall process are determined.

In more detail, during the data preparation the following must be defined:

1. The number of primary sound particles emitted by the source.
2. The geometry of the enclosure, that is in terms of objects.
3. The three-dimensional sound source position.
4. The three dimensional receiver position.
5. The enclosure's surface absorption properties, that is the reverberant absorption coefficients at the various frequency bands.
6. The atmospheric conditions in order to calculate the sound absorption at different frequencies.
7. Information about scattering or transmission.

The above information is composed in a data input file for further processing. The data input file is prepared according to the CADAЕ program description

language (see Chapter 7) with the assistance of a good computer-aided design program such as AutoCAD¹⁰⁶.

5.4. Processing, Simulation

Once the model is clearly defined in the pre-processing stage, the program should be ready to carry out the simulation. The pilot computer model in MATLAB made the author realise that a very important factor is the geometry of the enclosed space in relation to the distribution of materials, upon which the sound field created is greatly dependent. Based on this, it was recognised that the program should be able to execute a few main functions, which had to be repeated with slight variations. These functions are described as follows (see also Table 1).

Simulation starts by sending sound particles carrying energy, from the source to the internal space of the enclosure as explained in the previous Chapter. Each time a sound particle hits a solid surface it is reflected and its intensity value is reduced by an amount proportional to the absorption coefficient of that surface. Once a sound particle reaches the receiver the time, direction and energy are recorded. Transformations from global to local (surface) co-ordinate systems and vice-versa are used for the purpose of determining the collision point between a sound particle and a surface. Then the normal at a surface point is computed in order to calculate the reflected sound particle path.

The main function, which had to be constantly repeated, is that each sound particle has to scan a list of surfaces to determine which is closest to the origin of the sound particle path. The way in which the surface and sound particle collision point is computed differs, depending upon the type of surface.

From the experience gained in developing the pilot computer program, it was understood that to use traditional procedural programming for the simulation part, would be very tedious, inefficient and quite accessible to inaccuracies. On the other hand a new style of programming used nowadays, called object-oriented

programming (see next section) seem to be ideal for the implementation of the CADAЕ program.

Having each surface defined as an object and each object defined as a derived class, a generic collision determination function can be called and the program will automatically take care of using the proper function for each particular object class. That is to say that instead of designing the software by procedure, the software is designed by data structure. This has the advantage that object-dependent information can be hidden in data structures local to each file and the procedure interfaces can be very simple and generic. With this approach adding new surface-objects to the scheme becomes easy and efficient.

The question of how to implement the object-oriented programming approach was given the answer, C++^{107, 108}. A general purpose programming language well suited for implementing many different types of application. C++ is a static language, which means all the data types, function parameters, and other elements of the program must be described at compile time. It is a strongly typed language, that is, only compatible types can be intermingled in expressions. Further, C++ is an object-oriented language, that is, programming with objects which are instances of classes and using the concepts of encapsulation, data hiding, inheritance, polymorphism and templates, that is, parameterised data types.

All the above features made the C++ programming language ideal for the implementation of the processing or simulation part of sound prediction model.

5.5. Object-oriented Programming

Object-Oriented Programming^{109, 110} (OOP), is a method of implementation in which programs are organised as a co-operative collection of objects, each of which represents an instance of some class. The classes are all members of a hierarchy of classes united via inheritance relationships. This implementation model uses objects not algorithms as building blocks. Further, each object is an instance of some class and classes are related to one another through inheritance relationships.

The basic concepts of Object-Oriented Programming are abstraction, encapsulation, modularity, hierarchy, inheritance, polymorphism, objects and classes.

An abstraction denotes the essential characteristics of an object that distinguish it from all other kinds of objects. Encapsulation allows programs to be modified reliably, easily and efficiently. Abstraction and encapsulation are complementary concepts. Abstraction focuses on the observable behaviour of an object while encapsulation is concerned on the implementation that gives rise to this behaviour. Encapsulation is the process of separating the elements of an abstraction that constitutes its structure from those representing its behaviour. C++ encapsulation mechanisms include the private, public and protected labels that control access to class members.

Modularity should be the characteristic of every good program. The act of partitioning a program into modular components helps to reduce complexity. Modularization consists of dividing a program into modules which can be separately compiled but which have connections with other modules. In the implementation of the proposed model two modular components were used. The first one was where all the vector operations are declared and the second where the main functions are implemented.

In most real world problems and systems, too many abstractions exist at any one time. A set of abstractions usually forms a hierarchy. Hierarchy is a ranking or ordering of abstractions. Two types of hierarchies can be identified in most problem domains; class hierarchies and object hierarchies. The relationships amongst classes in a class hierarchy is termed an "is a" or "kind of" relationship. The relationship amongst objects is termed a "has a" or "part of" relationship. For example a dome which can be represented by a quadric which is a "kind of" surface and this surface "has a" sound absorption coefficient.

Inheritance is the main characteristic of Object-Oriented Programming. Inheritance defines a relationship amongst classes such that one class shares the

structure and/or behaviour of one or more classes. Inheritance can be said to represent a hierarchy of abstractions in which a derived class inherits from one or more base classes and refines the existing structure or behaviour of the base class to represent a more specific abstraction. In the proposed computer model there are many derived classes, one for each different object (plane, polygon, quadric, etc.), which inherit from the base class called "Object" (see next section).

5.6. Implementation

Several classes and functions make up the CADAЕ computer model. The primary function of CADAЕ is to go through a list of surface-objects that make up the enclosed space and determine whether or not a sound particle path intersects any of them (see Table 1). If so, the program then registers the nearest object for which an intersection takes place as the collision object and calculates the sound energy loss according to the absorption coefficient assigned to that object. Further the program calculates the path that the sound particle will follow after collision according to perfect reflection or to the scattering coefficient assigned to that object. This process is repeated for each sound particle emitted by the source and for all the collisions that follow until the sound particle energy becomes insignificant.

To begin the process an object class must be set up and its contents must be defined.

```
class Object
{
public:
unsigned char  type, name[16];
Vector<float>  vertex[8], lower, upper, norm;
Material      *material;
Object        *nextobj;
Differ        *Differ_list;
Object();
virtual void  get_data(void);
virtual int   CollisionTest(Line * line, float *t);
};
```

An object description begins with a number defining the object type. Next come 8 position vectors. If the primitive object is a polygon, as many position vectors

as needed are used to define the vertices that make up the polygon. For other types of objects this space is used to store other quantities that are required in computations using the objects. For example a spherical object such as a receiver uses “vertex[0]” to define the location of the centre and “vertex[1].x” to define the radius.

The next vectors give lower and upper bounds of the object and the surface normal “norm”. Some types of objects have a surface normal that remains the same over the entire surface. For such cases, the normal is computed when information from the data input file is entered into the program, and is not changed there after. Other objects have different surface normals at different points on the object. For these when a collision between a sound particle and the object is detected, the normal at that point is computed and stored in “norm” for the object.

Then several addresses that are part of the object data structure are defined. The address “*material” contains the location of a data structure for material acoustical information that is attached to the object. The address “*next_object” contains the location of the next object in a list of primitive objects to be examined. The address “*Differ_list” contains the address of a group of shapes that are to be used for constructive solid geometry.

The remaining items of the object class are functions that are used with the object. The first of these “Object()” defines the following constructor that is used to determine the contents of the object data items each time an object is created.

```
Object::Object()
{
  int i;
  type = 0;
  name[0] = NULL;
  for(i=0; i<8; i++)
    vertex[i] = Vector<float>();
  lower = Vector<float>();
  upper = Vector<float>();
  norm = Vector<float>();
  material = NULL;
  nextobj = NULL;
  child = NULL;
  Differ_list = NULL;
}
```

The object constructor can be used to set up any initial values. Whenever a class member is defined the program calls the constructor function automatically to allocate memory for the class member and to initialise its data items.

It is possible in C++ that the same function can perform differently for various situations due to its object-oriented nature. This is known as overriding the function. Suppose a model of an auditorium consists of a number of surface-objects whose addresses are stored in a list. What is to determine, is that if a sound particle emitted by a source in some direction will collide with one or more of these objects in the list and which is the closest collision. The task is to achieve that by a single function called "Collision" for all the different types of objects that comprise the hall under examination. The problem is that the mathematics is different for each type of object.

By calling the generic function "obj->Collision" at the appropriate time in the program, the program automatically determines what type of object is being processed and selects the proper function to do the mathematics. The way this procedure is used is to define the generic function as a virtual function in the preceding listing of the object contents.

There are two virtual functions as seen in the listing of the object class. The first "get_data()" is used to load data from the data input file for a particular type of object. The second "CollisionTest()" tests for the collision of a point with an object. The generic definition of the "CollisionTest()" function is carried out as follows.

```
int Object :: CollisionTest(Line *, float *)
{
  cout<<"Computer doesn't know object type..."<<endl;
  return(FALSE);
}
```

Only the class needs to be specified followed by a pair of colons as shown in the listing. This particular generic class function is used only when the class has not

been identified as one of the derived classes. Since the program does not know what to do with such an unclassified object, it simply reports a FALSE for no collision.

The "Collision_Test()" function is redefined under all derived classes that represent the different types of objects. For example the derived class for the Receiver object is defined by

```
class Receiver: public Object
{
public:
Receiver();
void get_data(void);
int CollisionTest(Line * line, float *t);
};
```

The class "Receiver" is derived from the class "Object" as indicated by the colon followed by public object at the beginning of the definition. That means that the class "Receiver" contains all of the data items that are contained in the class "Object". Below this defined as available for public access, are the two functions that were defined as virtual functions under the "Object" class. If any of these were left out of the "Receiver" class definition, the program would use the generic Object function when the particular function was called for a receiver. Once the prototype function is defined for a derived class, as shown in the definition of the "Receiver" class, a replacement function must be defined. The one for the "Receiver" class for the function "Collision_Test()" is the following.

```
int Receiver :: CollisionTest(Line * line, float *t)
{
float b ,c ,d ,t0 ,t1;
Vector<float> temp, position;
temp = line->loc - vertex[0];
vertex[1].x = 2.0*(ST+length(temp))/sqrt(nrays);
rad_sq = pow(vertex[1].x,2.0);
c = (temp % temp) - rad_sq;
b = ~(line->dir) % temp;
d = b*b - c;
if (d<0.0)
return(FALSE);
d=sqrt(d);
t0 = -b-d;
t1 = -b+d;
if (t1 > SMALL)
{
position = ~(line->dir) * t1 + line->loc;
*t = t1;
}
```

```

norm = ~(position - vertex[0]);
return(TRUE);
}
if (t0 > SMALL)
{
position = ~(line->dir) * t0 + line->loc;
*t = t0;
norm = ~(position - vertex[0]);
return(TRUE);
}
return(FALSE);
}

```

The function begins with a line that is very much like the first line of the generic function, except that the class is the derived class “Receiver” rather than the base class “Object”. It is essential that the parameters passed to this function be the same as the parameters for the virtual function defined under the base class. The mathematics used for objects of the derived “Receiver” class then follow.

In a similar way the “Collision_Test()” function is redefined under all derived classes that represent the different types of objects only the mathematics is different each time.

5.7. Tracing the Sound Particle

A sound particle emitted from the source follows a direction specified by the directivity of the source. If the source is omni-directional then the sound particle path will be parallel to a straight line starting from the position of the source passing through a position on the surface of a unit sphere. Then the sound particle will continue on this path until it meets the nearest wall, which is represented by a certain type of object. At this point the sound particle loses some of its energy according to sound absorption and is reflected specularly, or randomly, indicated by a scattering and/or a transmission coefficient. A new path is assigned to the sound particle and the process is repeated until the sound particle energy is reduced by a factor of 10^6 of its initial energy or the reflection order reaches a certain level. In the meanwhile each time a sound particle encounters a receiver its travel time, energy, position of the surface it came from, direction, order of reflection are registered (see Table 2).

What follows gives a description of the main functions that are used to accomplish the above scheme. First of all the main function of the program is shown below.

```

void main(void)
{
  Line line;
  int type;
  char filename[20];
  fstream in_file;
  int ch;
  float theta, phi;
  float f, T, h, To, ps, pso;
  float frO;
  float frN;

  cout << "\nEnter name of input file ? ";
  cin.get(filename, 20);
  in_file.open(filename, ios::in);
  if (! in_file)
  {
    cout << "\nUnable to open file " << filename << ':' << strerror(errno);
  }
  cout << "\nFile " << filename << " opened OK; contents are: " << endl;
  while ((ch = in_file.get()) != EOF) cout.put(ch);
  fget = fopen(filename,"rb");
  hall.stack=get_data();
  fclose(fget);

  clrscr();

  f=62.5;
  T=hall.temperature;
  h=hall.humid;
  T=T+273.0;
  To=293.0;
  ps=101300.0;
  pso=101300.0;

  frO=(ps/pso)*(24.0+4.41*pow(10.0,4.0)*h*((0.05+h)/(0.391+h)));
  frN=(ps/pso)*sqrt(T/To)*9.0+350.0*h*exp(-6.142*(pow(T/To,-1.0/3.0)-1.0));

  for (i=1; i<=7; i++)
  {
    f=2.0*f;
    ALPHA[i]=f*f*(1.84*pow(10.0,-11.0)*1/(ps/pso)*sqrt(T/To) +
    pow(T/To,5.0/2.0)*(1.278*pow(10,-
    2)*exp(2239.1/T))/(frO+(f*f/frO))+1.068/10*exp(-3352.0/T)/(frN+(f*f/frN)));
    ALPHA[i]=ALPHA[i]*869.0;
    cout<<ALPHA[i]<<endl;
  }

  cout<<"Reflection Order ?"<<endl;
  cin>>REFORDER;
  cout<<"Transition Order ?"<<endl;
  cin>>TRANORDER;

  for (y=1; y<=sqrt(nrays); y++)
  {
    theta= 360.0 * rand()/(32767+1.0)-180.0;
    for (x=0; x<=sqrt(nrays); x++)
    {
      phi= 180.0 * rand()/(32767+1.0)-90.0;
      line.dir.x = cos(th)*cos(ph);
      line.dir.z = cos(ph)*sin(th);
    }
  }
}

```

```

line.dir.y = sin(ph);

line.loc = hall.source;

POSITION=line.loc;
order = 0;
I=1.0, I1=1.0, I2=1.0, I3=1.0, I4=1.0, I5=1.0, I6=1.0, I7=1.0;
ST=0.0;
TIME=0.0;
trace_particle(&line);
clrscr();
cout<<"Number of Sound Particles = " << hall.particles_traced;
}
}
}

```

The main function begins by asking the user for the name of data input file. That is where all the information is stored concerning the enclosed space to be investigated. The function then reads the file context and makes any required remarks. Then a “for loop” is entered where the function calculates the air absorption coefficients for each frequency band. This is done using the set of equations shown (see also Eq. 58 on page 62), according to the atmospheric pressure, temperature and relative humidity of the hall, defined in the data input file.

Then the function asks the user to input a number for the maximum reflection order that the program will trace a sound particle. This number could be as high as required but obviously this means longer calculation times. Usually a number of 50 reflections would be sufficient to accurately simulate the sound field. Next to that is the transition order number. The transition order is the order of reflection after which the program will send the sound particle in a diffused direction according to Lambert’s law (see page 15). This will allow a good mixing of sound bringing the simulation process closer to reality.

The function next enters a pair of for loops that perform the tracing of each sound particle emitted by the source until all are emitted. Then the “trace_particle function is called to subsequently simulate the collisions and energy losses that occur as the sound particle propagates in the enclosure.

```

void trace_particle(Line * line)
{
Line newline;
Object * nearest_obj;

```

```

Vector<float> position, norm, S;
float dist, cos_in_angle, temp, So;
Material *material;

order++;
if (order < REORDER)
{
nearest_obj = Intersect(hall.stack, line, &dist, FALSE, TRUE, NULL);

position = line->loc + ~(line->dir) * dist;
norm = nearest_obj->norm;
if ((norm % line->dir) > 0.0)
norm = -norm;

POS[order] = position;
So = length(position-POS[order-1]);
ST = ST + So;
TIME = ST/co;

for (j=0; j<=7; j++)
{
I[j]=I[j]*(1.0-nearest_obj->material->absorption[j]) *
exp(2.0*ALPHA[j]*So/869.0);
}

cos_in_angle = -(line->dir % norm);
if (order > TRANORDER | (nearest_obj>material>scattering*1000.0)
>(1+int(1000.0*rand()/(32767+1.0))))
{
cos_in_angle = 0.001 + 0.999 * rand()/(32767+1.0);
}
if ((nearest_obj>material>transmission*1000.0)
>(1+int(1000.0*rand()/(32767+1.0))))
{
cos_in_angle = -(0.001 + 0.999 * rand()/(32767+1.0));
}

newline.dir = line->dir + norm * ( 2.0 * cos_in_angle);
newline.loc = position;

trace_particle(&newline);
}

return(0);
}

```

The “trace_particle” function begins by incrementing the global parameter order. This parameter indicates the order of reflection of the “trace_particle” function. That is the number of times the “trace_particle” function is going to call itself provided the energy of the sound particle is higher than a factor of 10^6 of its initial value.

Next the function calls “Intersect”. This function scans the lists of objects that comprise the enclosure and returns the address of the nearest object on the sound particle path. It also sets the parameter “dist” to the value required to

compute the collision point of the sound particle with the nearest object. The function next computes the collision point and places that in position. It also places the object's surface normal at the collision point in the parameter "norm". Next the current position is placed in the array "POS" for each order of reflection for further analysis of the mean free path and of the overall path the sound particle follows. Then the length of sound particle path "So" is calculated for the current order of reflection. And this is added to the total path from the moment of its emission. In this way the total time passed is calculated by dividing the total sound particle path length by the velocity of sound "co".

Next the function enters a for loop where the sound energy is calculated at the collision point for each frequency band (125, 250, ..., 8 KHz). As seen the air material sound absorption and air absorption are taken into consideration. The result is stored into an array each term of which stands for each octave band.

In order to calculate the direction of reflection for the sound particle a new vector newline is computed whose origin is at the current collision point. Then the incident angle between the incoming sound particle path and the surface normal is calculated, doubled and multiplied by the surface normal. The result is added to the incoming sound particle direction to obtain the reflected direction, which is stored to "newline" (see Eq. 51 on page 59). Meanwhile there are two conditional loops one for diffusion and the other for transmission of sound. Both of them manipulate the parameter "cos_in_angle" and therefore the direction of the reflected sound particle according to the pre-defined scattering or transmission coefficient using a random process. Finally the process calls itself with the new sound particle path direction, and the whole process is repeated until the specified order of reflection or sound energy loss level.

As mentioned above the "trace_particle" function calls the "intersect" function to determine the nearest collision point for a sound particle. The "intersect" function listed below, scans the list of objects to find possible intersections

between these objects and the current sound particle path, among which the shortest is the collision point.

```
Object * Intersect(Object * Current_obj, Line * line,
float *Shortest_dist, char init_flag)
{
static Object * Closest_object;
short collision;
float dist;

obj = Current_obj;
if (init_flag)
{
*Shortest_dist=3e30;
Closest_object=NULL;
}
for (obj=Current_obj; obj !=NULL; obj=obj->nextobj)
{
collision = obj->CollisionTest(line,&dist);

if (collision && (dist>SMALL) && (dist!=0))
{
if (obj->type==RECEIVER && (dist<*Shortest_dist))
{
write_data(obj->receiver_number)
}
if ((dist<*Shortest_dist) && (obj->type!=RECEIVER))
{
*Shortest_dist = dist;
Closest_object = obj;
}
}
}
return(Closest_object);
}
```

First, the function sets “obj” to the address of “Current_obj”. The address passed in “Current_obj” is that of the first in the list of objects. The function then checks if this is the first pass through the function. If so the value of “Shortest_dist” is made very high and the address for “Closest_object” is set to NULL indicating that no intersection has been found yet. The function then enters a while loop which continues to repeat until the entire lists of objects is exhausted. First the function “CollisionTest” is called to determine if the sound particle path passed to “Intersect” in the parameter “line” intersects with the current object. An intersection is reported if “dist” is not too small or the collision object is not a receiver since the receiver is a transparent object and has no influence on the sound field. If the collision object is a receiver then the “write_data” function is called where an output file is created or updated with

information about the sound particle path, order of reflection, the sound energy and time of collision (see Table 2).

To find the "closest_object" the value of "dist" is checked against the current value of "Shortest_dist". If "dist" is smaller a closer object is found, so the value of "Shortest_dist" is set to "dist" and set the address of "closest_object" to the object just checked. The address of the current object is then set to the next object in the list and another pass proceeds through the loop. When all objects have been checked the function is complete. It returns the address of the closest object and the value of "dist" for this object to the "trace_particle" function.

5.8. Post-processing, Presentation of the Results

The post-processing of the output data from the main CADAЕ program (described above) is performed in the form of small programs written in MATLAB.

The results from the simulation test come in output files written by the CADAЕ program. A sample of this output data can be seen on Table 2. As shown on the various columns of Table 2 the data output file contains information concerning the time arrival, sound energy, position of reflections, direction of sound particles and order of reflection.

There are various ways to analyse the output of the computer simulation. The most important data obtained from the simulation is that concerning the sound energy impulse response which is the squared sound pressure impulse response. Equally important is the information concerning the directionality of the sound particles hitting the receiver.

From the energy impulse response other acoustical responses may be calculated such as the steady state response, the reverberant response and the sound build up phenomenon. Further, the energy impulse response is just the squared sound pressure impulse response. By calculating the sound pressure impulse response

and taking its Fourier transform the room transfer function may be obtained. Since the room transfer function for particular source receiver positions can be estimated, an auralization filter can be constructed. Then audible simulation may be attained, by convolving the room transfer function with an anechoic signal.

The other way to examine how sound behaves in the room under investigation is by various assessment criteria and graphical presentations. These include sound particle spatial distribution diagrams, receiver sound path tracing, spatial diffusivity plots, noise level maps, impulse response reflectograms, sound decay curves and so on.

A very useful program written in MATLAB calculates the integrated impulse response suggested by Schroeder (see page 27). Another one calculates the sound decay slope by using the least squares method. A third program uses decimation or interpolation (see page 27) accordingly to construct noise level or diffusion maps as seen in some of the figures in the appendix. The Gram program displays the response at the receiver in four graphs a sound level echogram, sound decay curve, squared pressure impulse response, and pressure impulse response. Further MATLAB is used for calculating the reflection of a sound wave from a cylindrical surface (see page 13) using Bessel functions. Another program written applies ensemble averages⁸ to calculate average reverberation times for the various frequency bands.

The programs developed in MATLAB were used to analyse both the results from the simulation and the results from the acoustical measurements. In that sense the programs written in MATLAB can be used as a software toolbox for general acoustical result analysis.

Chapter 6

THE CADAЕ PROGRAM DESCRIPTION LANGUAGE

6. THE CADAE PROGRAM DESCRIPTION LANGUAGE

6.1. Introduction

Considering the requirements of the proposed computer model (CADAЕ) it was decided that the problem of describing complex geometries would be solved by parametrically specified data, written in a programming-like format. This programming-like format which constitutes the CADAЕ description language is based on C++ since this is the language used for the computer implementation of the proposed model. The choice of features to include in CADAЕ was mainly guided by its intended use as an acoustical environment description language. That is to describe a bounded spatial system with respect to its internal geometry, acoustical properties of the walls and the atmospheric conditions.

The CADAЕ program language allows the user to describe the bounded spatial system to be investigated in a readable and convenient way. Files are created in plain ASCII text using an editor of the user's choice. CADAЕ reads the file, processes it, carries out the simulation, and produces the result in the form of output files for each receiver location.

This Chapter describes how an acoustical model of an enclosure is created using CADAЕ's programming language.

6.2. Language Basics

The CADAЕ language consists of reserved keywords, floating point literals, string literals, special symbols and comments. The text of a CADAЕ data input file is free format. Users may put statements on separate lines or on the same line as desired. Users may add blank lines, spaces, or indentations as long as there is not any split in keywords.

6.2.1. Comments

Comments are text in the data input file included to make the file easier to read or understand. They are ignored by the main program and are there for humans to read. The two types of comments used in the CADAЕ description language are similar to the comments used in the C++ programming language.

Two slashes are used for single line comments. Anything on a line after a double slash // is ignored by the program. For example:

```
// This line is ignored
```

The other type of comment is used for multiple lines. This type of comment starts with /* and ends with */ everything in-between is ignored. For example:

```
/* These lines  
   are ignored  
   by the  
   CADAЕ program */
```

This can be useful if the user wants to temporarily remove elements from a perspective model.

6.2.2. Float Expressions

Many parts of the CADAЕ program language require the user to specify one or more floating point numbers. A floating point number is a number with a decimal point. Float literals are represented by an optional sign (-), some digits, an optional decimal point, and more digits. If the number is an integer the user may omit the decimal point and trailing zero. If it is all fractional the user may omit the leading zero. The following are all valid float literals:

```
1.0  -2.0  -4   34  .3  0.6
```

6.2.3. Vector Expressions

CADAЕ operates in a 3D x, y, z co-ordinate system. Often the user needs to specify x, y and z values. A "vector" is a set of three float values used for such

specification. Vectors consist of three float expressions that are bracketed. The three terms are separated by comma as follows:

```
(1.0, 3.0, 2.0)
```

6.3. The CADAE Co-ordinate System

In order to carry out simulation, CADAE should know where is the sound source, receiver positions, and the geometry and acoustical properties of the enclosure under investigation.

To do this, 3D co-ordinates are used. The usual co-ordinate system for the CADAE sound particle program has the positive x-axis pointing to the right, the positive y-axis pointing into the paper and the positive z-axis pointing up.

The negative values of the axes point at exactly the opposite directions. Further, it should be mentioned that for the units of measurement the SI system is used.

6.4. Defining the Sound Source

The source (see also page 50) declaration describes where and how the sound source is placed. It gives x, y, z co-ordinates to indicate the position of the source and its orientation. x, y, z co-ordinates are described using a 3-part "vector". A vector is specified by putting 3 numeric values in brackets, and separating the values with commas as shown below.

```
Source  
location =(1, 2, .5)  
orientation =(0, 0, 0)  
PWL =100  
end
```

Briefly, "location =(1, 2, .5)" places the sound source 1 metre longitudinally 2 meters laterally and 50 centimetres up from the origin of the co-ordinate system which is at (0, 0, 0). "Orientation =(1, 0, 0)" rotates the sound source to point at x, y, z co-ordinates (1, 0, 0), a point along the positive x-axis of the co-ordinate

system. The orientation parameter is used when the sound source is not omnidirectional.

Next is the Sound Power Level (PWL) definition. PWL =100 indicates the Sound Power Level of the source in dB. The “end” indicates that the sound source declaration is completed.

6.5. Placing a Receiver

Once the sound source is set up, the receiver(s) (see also Chapter 3) should be placed into the model. To declare a receiver the following should be typed in the data input file:

```
Receiver
location =(6.1,1.25,1.5)
receiver_number 1
end
```

The “location” vector specifies the centre of the expanding sphere, the expanded radius is calculated at run-time to match the time passed from the emission of a sound particle. The keyword “receiver_number” gives the receiver an identification number so that the output (results) file “r1.out” corresponds to “receiver_number 1”, “r2.out” to “receiver_number 2” and so on.

To be flexible a receiver can be assigned to any object, spherical, cubical, etc. This is accomplished by inserting the “receiver_number” keyword into the declaration for the particular object. For example a fixed radius spherical receiver is defined as follows:

```
Sphere
location =(6.1,1.25,1.5); radius .25
receiver_number 2
end
```

6.6. Describing a Surface-object

Objects are the means to describe the surface-geometry and the acoustical features of the enclosure to be examined. There are eight different types of

objects supported by the CADAЕ sound particle program. Four of them are finite solid primitives, 4 are finite patch primitives and one is specialised object that is the receiver. The solid primitives supported are: the parallelepiped, cone, sphere, and the quadric. These have a well defined “inside” and can be used for Constructive Solid Geometry.

The basic syntax of an object is a keyword describing its type, some floats, vectors or other parameters, which further define its location and some object modifiers such as material, and constructive solid geometry operations (see page 97).

The material keyword describes the acoustical characteristics of the object. By specifying the material the object is made from, sound absorption properties are given to the object. This is accomplished by looking in the material database and assignment of sound absorption coefficients is carried out for the 125 Hz, 250 Hz, 500 Hz, 1 kHz, 2 kHz, 4 kHz and 8kHz octave frequency bands. The scattering and transmission modifiers, which are under the material category, give the object diffusive and refractive properties. The degree of diffusion and transmission for the particular object is specified by a floating point number from zero to one.

Constructive solid geometry is used to glue or cut parts of surfaces in order to get the required shape for best geometrical representation of part of the enclosure model.

6.6.1. Describing a Parallelepiped Object

A simple parallelepiped can be defined by listing its two corners as follows:

```
Parallelepiped  
lower (corner); upper (corner);
```

Where “lower” and “upper” corners are vectors defining the x,y,z co-ordinates of opposite corners of the parallelepiped. For example:

```
Parallelepiped
lower (0, 0, 0); upper (1, 1, 1)
```

Note that all parallelepipeds are defined with their faces parallel to the co-ordinate axes. Each element of “lower” corner should always be less than the corresponding element in “upper” corner. Parallelepipeds are useful for representing columns as well as inside walls. They are also efficient to use in constructive solid geometry with quadrics to create surfaces such as curved ceilings.

6.6.2. The Spherical Object

Spheres are usually used to represent fixed radius receivers or curved surfaces when used with other surfaces using constructive solid geometry. The syntax to describe a spherical object is the following:

```
Sphere
Location= (85, 35, 29); radius = 17
Material
etc.
```

Where location is a vector specifying the x, y, z co-ordinates of the centre of the sphere and radius is a float value specifying the radius. The sphere can be used to construct a series of curved surfaces by constructive solid geometry operations. For example, the following declaration represents a spherical dome.

```
Sphere
location 85 35 29; radius 17
Differ_plane
location 85 35 29; normal 0 0 1
Material
etc.
```

6.6.3. The Cone

A finite length cone or a frustum (a cone with the point cut off) may be defined by:

```
Cone
base (85,35,51); apex (85,35,80); min_radius 3;max_radius 14
Material
Etc.
```

Where base and apex are vectors defining the x, y, z co-ordinates of the centre of each end of the cone and “min_radius” and “max_radius” are float values for the radius of the base and apex respectively.

If neither radius is zero then the result is a tapered cylinder or a cone with the point cut off. If both the radius are equal then the cone becomes a cylindrical object. The ends of a cone are closed by flat planes, which are parallel to each other and perpendicular to the length of the cone. Adding the optional constructive solid geometry keyword “Differ_plane” as shown below the end caps are removed and the result is a tapered hollow tube such as part of the dome of St. Paul’s Cathedral.

```
Cone
apex (85,35,80); base (85,35,51); min_radius 3; max_radius 14
Differ_plane
location 85 35 63; normal (0,0,1)
Differ_plane
location (85, 35, 63); normal (0,0,1)
Material
Etc.
```

6.6.4. *The Polygon*

The polygon belongs to the finite patch primitive family of objects. It is available in order to construct approximately more complex objects than the solid objects will permit. Polygons can either be created by hand, or converted to the CADAЕ language from files created in computer-aided design packages such as AutoCAD. A polygon is defined by:

```
Polygon
vertex =(0,20,0); vertex =(0,50,0); vertex=(0,50,30); vertex =(0,20,30)
Material
Etc.
```

where the three floats in parenthesis represent a vector defining the x,y,z co-ordinates of each vertex of the polygon. Because polygons are perfectly flat surfaces it would require extremely large numbers of them to approximate a curved surface. For this reason they should only be used for flat walls.

6.6.5. The Ring

The ring is the other flat, finite patch object type available in the CADAЕ program. Note that a ring is infinitely thin. A ring with thickness can be simulated with a short cone. A ring shape may be defined by:

```
Ring
location =(85,35,29);normal (0,0,1);min_radius 15;max_radius 17
Material
Etc.
```

The vector location defines the x,y,z co-ordinates of the center of the ring. The normal vector describes its orientation by describing its surface normal vector. This is followed by two floating point numbers specifying the inner and outer radius of the ring. If the inner (`min_radius`) is zero then the ring becomes a circle.

6.6.6. The plane

The plane primitive is a fast, efficient way to define an infinite flat surface. The plane is specified as follows:

```
Plane
normal (0,1,0); distance 8
Material
Etc.
```

The “normal” vector defines the surface normal of the plane. A surface normal is a vector which points up from the surface at a 90 degree angle. This is followed by a float value that gives the distance along the normal that the plane is from the origin. For example:

The plane in the above listing is defined in the positive y direction. The plane is 8 metres in that direction away from the origin. The plane extends infinitely in the x and z directions.

By definition the normal vector points to the outside of the plane while any points away from the vector are defined as inside. This inside/outside distinction is important when using planes in CSG as seen in the previous sections.

6.6.7. Quadric

Quadric surfaces can produce shapes like spheres, cones, cylinders, paraboloids, or nearly any implicit curved surface. A quadric is defined in the CADAE language as follows:

```
Quadric
location =(85,35,65); A=1,B=1,C=0,D=0,E=14,
xmin -100, xmax 100; ymin -100, ymax 100; zmin -14, zmax 0
Material
Etc.
```

where location is the origin, A through E are float expressions. The minimum and maximum values define the limits where the quadric exists.

The quadric defines a surface of x, y, and z points, which satisfy Eq. 44 (see page 57):

$$Ax^2 + By^2 + Cz^2 + Dy + E = 0$$

Different values of A, B, C, D, E will give different shapes. So, if any three-dimensional point is taken and insert its x, y, and z co-ordinates in the above equation, the answer will be 0 if the point is on the surface of the object. The answer will be negative if the point is inside the object and positive if the point is outside the object. Here are some examples:

1. $x^2 + y^2 + z^2 - 1 = 0$

2. $x^2 + y^2 - 1 = 0$

3. $x^2 + y^2 - z^2 = 0$

The first example represents a sphere, the second is an infinitely long cylinder along the z-axis, and the third is an infinitely long cone along the z-axis.

6.7. Constructive Solid Geometry

Constructive Solid Geometry¹¹¹ (CSG) is a method of creating models of physical objects. The method is based on the notion that the physical object can be divided into a set of primitives that can be combined in a certain order following a set of rules to form the object. Each primitive is bounded by a set of surfaces. The primitive's surfaces are combined via a boundary evaluation process to form the boundary of an object.

The main building operations in the CSG method are achieved by the set operators also known as boolean operators: union which corresponds to the logical "or", intersection corresponds to the logical "and", and difference corresponds to "not and". Some less formal but popular building operators are "Assemble" and "Glue". These operators do not really combine primitive objects but the primitive objects involved are merely assembled or glued to represent a composite object, which consists of them.

Constructive Solid Geometry allows the user to define shapes which are the union, intersection, or difference of other shapes or clip sections of objects revealing their hollow interiors. Unions superimpose two or more shapes. This has the same effect as defining two or more separate objects, but is simpler to create and/or manipulate. Intersections define the space where the two or more surfaces overlap. Differences allow you to cut one object out of another.

CSG is used in the CADAЕ program in order to make the shape definition abilities more powerful and thereby describe enclosed spaces more accurately and efficiently. The difference operation is employed since this would be enough to satisfy the representation any necessary surface. Difference means that an object exists if it is within a specified set of boundaries. A cone (cylinder) can be used to bore a hole through a parallelepiped and thereby get a barrel shape ceiling as follows:

```
Parallelepiped  
lower =(0.0,-10.0,0.0); upper =(30.0,30.0,20.0)  
Differ_out_cone
```

```

apex =(30,10,10); base (0,10,10); min_radius 10; max_radius 10
Material
absorb .2
end

Cone
apex =(30,10,0); base =(0,10,0); min_radius 20; max_radius 20
Differ_in_Parallelepiped
base =(0.0,-10,0.0); apex =(30.0,30.0,20.0)
Differ_plane
location =(15,10,0); normal =(0,0,1)
Material
absorb .2
end

```

As seen difference is symbolised by the keyword “differ_in” or “differ_out” which can be used after the object definition and before the material assignment. First the parallelepiped is defined with the cone cut out and then the cone is defined which is cut inside the parallelepiped.

6.8. The Acoustical Properties of a Surface-object

Once the location and size and type of a surface-object are defined the surface acoustical properties of that object should be defined as well before the data input file is ready to be read by the main CADAЕ program. The Material block of statements specifies these parameters. Material blocks describe the absorption, scattering and transmission properties of a surface-object.

6.8.1. Absorption

By specifying the material the surface is made of, the program looks up in the internal material database and assigns the values of the reverberant absorption coefficients for each frequency band (125, 250, ... 8 kHz) to the particular object-surface. In the following example the plane surface-object which represents the floor is assigned the material marble.

```

Plane
normal (0,0,1); distance 0
Material
MARBLE
end

```

Then each time a sound particle contacts the floor its sound energy is reduced by the absorption coefficient for each frequency band as seen below.

```
case MARBLE:
material->type = MARBLE;
material->absorption[1] = .01;
material->absorption[2] = .01;
material->absorption[3] = .015;
material->absorption[4] = .02;
material->absorption[5] = .02;
material->absorption[6] = .02;
material->absorption[7] = .02;
```

A few of the materials in CADAЕ's database include the following:

```
case MOSAIC:
material->type = MOSAIC;
material->absorption[1] = .14;
material->absorption[2] = .1;
material->absorption[3] = .06;
material->absorption[4] = .04;
material->absorption[5] = .04;
material->absorption[6] = .03;
material->absorption[7] = .03;
```

```
case PLASTER:
material->type = PLASTER;
material->absorption[1] = .02;
material->absorption[2] = .02;
material->absorption[3] = .02;
material->absorption[4] = .03;
material->absorption[5] = .03;
material->absorption[6] = .04;
material->absorption[7] = .05;
```

```
case PORTLAND_STONE:
material->type = PORTLAND_STONE;
material->absorption[1] = .08;
material->absorption[2] = .03;
material->absorption[3] = .06;
material->absorption[4] = .09;
material->absorption[5] = .1;
material->absorption[6] = .22;
material->absorption[7] = .22;
```

If the purpose is to run the simulation for only one particular frequency band then the keyword `absorb` can be declared in the material block. For example an absorption coefficient 0.2 can be assigned to a plane surface-object as shown below.

```
Plane
normal (0,0,1); distance 0
Material
absorb 0.2
```

6.8.2. Diffuse Reflection Items

When sound reflects off a surface, the law of specular reflection states that it should leave the surface at the exact same angle it came in (see page 13). This is similar to the way a billiard ball bounces off a bumper of a pool table. However this is not always the case since reflection depends on the size and shape of the object with respect to the sound wavelength (see page 15 and 20). Most of the time, sound reflects and is scattered in all directions. This scattering may be called "diffuse reflection" because sound diffuses or spreads in a variety of directions.

The keyword "scattering", used in the Material block of statements, controls how much sound is reflected via diffuse reflection. For example:

```
Material  
portland_stone; scattering 0.6
```

means that 60% of the sound energy that hits the object will be scattered while the remaining 40% will be reflected specularly.

6.8.3. Sound Transmission

When sound passes through a surface either into or out of a dense medium, the path of a sound particle of sound is bent and loses some of its energy. This phenomenon is called refraction or transmission (see page 15).

The "transmission" keyword is used in the Material block of statements to specify the amount of sound that passes through a particular object-surface. For example:

```
transmission 0.3
```

Means that 30% of the sound energy of a sound particle passes through the surface object.

Chapter 7

COMPUTER EXPERIMENTS AND ACOUSTICAL MEASUREMENTS

7. COMPUTER EXPERIMENTS AND ACOUSTICAL MEASUREMENTS

7.1. Introduction

This Chapter describes the apparatus, preparation, and procedure followed, for both the acoustical measurements and computer experiments carried out.

7.2. Computer Experiments

The purpose of the computer experiments was to use the CADAЕ computer program, in order to produce results to compare with theoretical calculations and experimental measurements.

7.2.1. Apparatus

1. A microcomputer Pentium 120MHz employed with a 16 bit sound card.
2. HP LaserJet 5L printer.
3. Autodesk's AutoCAD, a computer-aided design package.
4. Mathwork's MATLAB, a fourth generation mathematical programming language.
5. Microsoft Excel, a spreadsheets program.

7.2.2. The computer experimental procedure

This section describes how the results are obtained from computer simulation using the CADAЕ program. The following steps were used to get the acoustical results on the various enclosures studied in this thesis.

First of all the data input file for a particular enclosed space had to be prepared. The data input file, as explained in the preceding Chapter, is a standard ASCII text file that contains the description for a three-dimensional bounded spatial system. The data input file text describes sources, receivers and the objects with their particular acoustical properties that make up the enclosure to be studied. The files have the file extension .DAT and can be created by any word processor or editor that can save in standard ASCII text format.

A few aspects considered during the modelling process, that is preparation of the data input file, included the following:

1. Absorption coefficients of the major surface-objects are well approximated.
2. Numerous small surfaces are avoided since these increase calculation times and might even influence negatively the accuracy of the results.
3. The number of primary sound particles emitted by the source is chosen according to the volume and shape of the perspective enclosed space.
4. Since the exact process of scattering for the various surface-objects is unknown a scattering coefficient of unity is assigned for all the cases.
5. To allow a good mixing of sound the transition from the early stage to the late stage (transition order) was assumed to take place after the 5th order reflection. In other words after the 5th reflection sound is reflected randomly according to Lambert's Law.

Some data input files for the investigated enclosures of this thesis can be viewed in the appendix. The investigated enclosures illustrate the diversification of the CADAЕ program in terms of its applicability to bounded spatial systems of nearly any geometry including that of curved surfaces. These files range from very simple such as the description of a simple rectangular room, to very complex such as the description of St Paul's cathedral. They have been created by the author, in order to give an indication of the validity of the CADAЕ sound prediction program.

The procedure followed to get the results for each of the investigated examples is summarised as follows. The TEST sub-program is executed by typing <test> and <enter> at the DOS prompt followed by entering the name of the data input file. The TEST executable is used to verify that the data input file describes the geometry of the bounded spatial system well enough. The first test is dealing with

the syntax of the data input file so that if any errors are present there is an immediate response on the screen. The second test is the water-tightness of the geometrical model, that is, if there are any undefined surfaces, which is verified directly by the program in the same way. The third test is the verification of the geometry of the enclosure with the positions of the receivers and sources. This third test is carried out in MATLAB by viewing the sound particle spatial distribution, after importing the TEST.OUT file produced by the TEST executable by running it for about a minute.

Once everything is checked up, CADAЕ which is the name of the main is executable is run.

CADAЕ reads in, the tested data input file and begins working to calculate the results for the particular receivers. It writes the results to files called R1.OUT, R2.OUT, R3.OUT, etc. corresponding to the various receiver positions. The file R*.OUT contains information about the sound energy arrival time and direction from which it arrived. The analysis of the information is carried out in MATLAB to derive important results such as the reverberation time, the impulse response, speech intelligibility sound pressure levels maps, and directionality of the receiver and so on.

7.3. Acoustical Measurements

The objective was to carry out measurements most accurately in order to compare with the corresponding computer experiments.

7.3.1. Apparatus

The apparatus used were mainly made by BRUEL & KJAER.

7.3.1.1. Sound Level Meter

The sound level meter (SLM) used was a modular precision BRUEL & KJAER Type 2231, shown in Figure 10a. A system of interchangeable application modules allows it to perform a variety of measurements not possible with a single

hand-held instrument. The BZ 7110 integrating module was used for the measurement tests.

The external filter used by the modular precision sound level meter was the octave filter set Type 1624. The filter is connected directly to the bottom of the sound level meter, as shown in Figure 10a.

7.3.1.2. Microphone

The microphone used was a BRUEL & KJAER type 4155. This is a ½ inch free field microphone of the pre-polarised kind. The mechanism is quite stable, so a calibration chart can be relied upon for a long time, but it should be noted that it is very fragile because of the thin diaphragm. The microphone has a uniform frequency response over a wide range (4 Hz – 16 kHz).

7.3.1.3. Sound Level Calibrator

Sound level calibration is an essential part of all occupational acoustical measurements. Acoustical instruments must be calibrated and this was done by a handy portable sound level calibrator which gives a pressure calibration directly and emits a pure tone source of 93.8 dB at 1000 Hz. The calibrator used was a BRUEL & KJAER Type 4230.

7.3.1.4. Hygrometer

The Hygrometer used was of whirling type Gallenkamp Griffin, HYT-610-030Y. This is a device, which measures the temperature and humidity in a room. The procedure to achieve that was to put some distilled water into the instrument so as to wet one of the bulbs and then whirl it vigorously within the measurement area. In this way the two thermometers of the instruments record two temperatures, wet and dry. From these two readings the relative humidity in a room can be calculated.

7.3.1.5. Sound Power Source

The sound power source used for the measurements was BRUEL & KJAER Type 4205. This is a calibrated sound source whose sound power level can be

varied continuously between 40 and approximately 100 dB re 1 pW. The output may be wide band pink noise in the frequency range 100 Hz to 10000 Hz or may be octave band filtered noise by employing one of the 7 built-in octave band pass filters.

The sound power source Type 4205 consists of two separate units: the generator, containing all the controls, filters, battery pack amplifiers and meter etc., and the sound source HP 1001 containing two loudspeakers and the associated crossover networks. Figure 10b shows a simplified block diagram of the complete instrument. The sound power level used for the measurements was 100 dB for the 125 Hz, 250 Hz, 500 Hz, 1 kHz, 2 kHz, 4 kHz and 8 kHz octave frequency bands. The sound source is overall omni-directional on the horizontal plane but has some directionality on the vertical plane as shown in Figure 10c.

7.3.1.6. The Computer

The computer used for the measurements was a portable IBM compatible employed with Pentium processor and a sound card with an application software. As seen in Figure 10a it was connected via wiring to the output of the sound level meter.

7.3.2. Procedure for the Acoustical Measurements

First of all, it was made certain that all the apparatus were in good condition and that the batteries for the instruments were sufficiently charged. Then in order to achieve precise and accurate results calibration was carried out.

The sound level meter was calibrated by placing the portable acoustic calibrator directly over the microphone. The calibrator provided the precisely defined sound pressure level to which the sound level meter was adjusted. To calibrate the sound source, the microphone attached to the sound level meter was inserted into a special slot in the loudspeaker. Then the sound source was adjusted for each octave band. The computer - sound level meter interface was checked and the sampling frequency of the digitised signal was set to 44100 Hz, which should be sufficient according to the sampling theorem (see page 26).

In addition to these some general precautions were taken during the measurement tests. Avoid the presence of a person near the sound level meter. Beware of excessive background noise and use the protective shield on the microphone of the sound level meter.

Three types of measurements were taken. Sound pressure level measurements, impulse response measurements and steady state measurements.

During the sound pressure level measurement test the sound level meter was held at each position and the value was read and recorded. Sound pressure levels were recorded in octave bands from 125 Hz to 4 kHz. Each time the frequency band was changed on the sound source the appropriate filter was set up on the sound level meter.

For the impulse response measurement test the sound source was suddenly switched on and off. The response was stored through the sound level meter into the computer. Impulse responses were taken in octave bands from 125 Hz to 8 kHz. This time the sound level meter was mounted on a tripod at the measurement point. A similar procedure was carried out for the steady state response with the difference that the sound source was switched on for a few seconds to allow sound to build up and then switched off.

Chapter 8

APPLICATION OF THE PROPOSED COMPUTER MODEL

RESULTS - DISCUSSION

8. APPLICATION OF THE PROPOSED COMPUTER MODEL

RESULTS - DISCUSSION

8.1. Introduction

The following examples illustrate several types of acoustical environments that CADAЕ (the computer model developed in this thesis) is capable of investigating. All examples concern the cases where an omni-directional sound source and a spherical observation region are considered. For the calculations, the reverberant coefficients of sound absorption are used which are prescribed in six frequency bands, that is 125, 250, 500, 1000, 2000, 4000, 8000. Air absorption is also accounted for according to the equations on page 62.

The enclosed spaces investigated vary from a simple rectangular room to a long corridor, a typical auditorium, acoustically coupled spaces, rooms with curved boundaries to a complicated existing building with many curved walls exhibiting a variety of acoustical phenomena. The Tables and Figures the text is referring to can be viewed in the appendix starting on page 139.

8.2. Box-shaped Enclosures

In order to demonstrate the basic features of the CADAЕ computer model a simple rectangular enclosure 30×20×10 meters was chosen as the first application. An omni-directional sound source is placed near the centre of one of its walls and a receiver at about 20 meters from the source. The absorption coefficients of all the walls were assigned a value of 0.3.

The data input file is prepared according to the CADAЕ description language as listed on Table 4 (see appendix). As seen the simple rectangular room is modelled using 6 polygons, one for the floor, one for the ceiling, and four for the walls. Simulation is carried out using the CADAЕ executable for 22500 primary sound particles sent by the source and a total calculation time was 7 minutes. The results are analysed in MATLAB using the data output file produced and illustrated with

Figures. Figure 11 shows the geometry of the room in the form of a sound particle spatial distribution. The sound particle distribution is achieved by plotting small dots representing the sound particle collisions with the various surfaces of the enclosed space. The source and receiver positions can be identified by the concentration of sound particles.

In another attempt to visualise the sound field, Figure 12 shows the direct field represented by lines emanating from the position of the source in all directions. The lines or rays symbolise the primary sound particle paths. Such a sound field would exist in open air or in an anechoic chamber. The direct, together with the diffuse field, can be seen in Figure 13 in the form of rays spread all over the room. Such a field would exist in a space with solid surfaces provided these are not completely absorptive.

To examine the directionality of the receiver the sound particle paths that reach the receiver are traced. Some of those are shown in Figure 14. A more intelligent way to illustrate the directionality of the receiver is to draw a hedgehog plot suggested by Thiele²⁸. This is shown in Figure 15, where the individual lines represent the direction and relative sound energy that a receiver will experience. The diffusivity of the field can be examined by the distribution of the length of the free sound paths as shown in Figure 16. The (computer) experimental mean free path is 10.2 m, which is very close to the theoretical value (see page 21), which is 10.9 m.

Figure 17 shows four graphs, which are useful in describing the response at a particular receiver position. The top left graph on Figure 17 shows the impulse response (see page 26) or echogram. This, also called a reflectogram, is generated in the following way. Primary sound arrives first at the receiver location, followed by a series of reflections (represented by vertical lines) that have only once encountered one of the walls enclosing the room (first order reflections). Then higher order reflections arrive at the receiver location while their density per unit time increases rapidly. The upper right graph shows the sound level decay curve.

The lower left graph shows the squared pressure impulse response in a reflectogram form. Finally the lower right graph shows the pressure impulse response.

In order to carry out further analysis of the receiver response the signal must be re-sampled in equal time intervals, as seen in Figure 18. The various graphs show the temporal distribution of the energy received after adding the individual reflections at a specified time interval. This is what is known as the energetic impulse response. As seen in the top left graph of Figure 18, the echogram exhibits an irregular character with almost separable reflection sequences. This might be due to the very simple cuboical form of the room, which provides the possibility of the existence of certain favourable sound propagation paths.

Based on the re-sampled signal, Figure 19 shows the sound decay curve at the receiver position using Schroeder's integrated impulse response method (see page 27). The reverberation time can be extrapolated from the slope of this curve. As seen on Figure 19 the reverberation time is estimated to be 1.4 seconds, which closely agree with Sabine's value, which is 1.46 sec. The agreement is expected since the various requirements for a diffuse field are satisfied.

Further to Schroeder's method, the decay curve slope may be evaluated by the decimation algorithm (see page 27). That is by re-sampling the signal at a lower sampling rate smoothing occurs which helps in the slope extrapolation and thereby in the reverberation time calculation. A plot of the decimated decay curve may be seen in Figure 20. The reverberation time extrapolated by this curve would be about the same as with the one with the integrated impulse response.

An alternative way to represent the sound decay curve is by directly plotting the sound level against time. As long as the decay is exponential then regression analysis can be used to estimate the decay curve and calculate the reverberation time as shown in Figure 21.

The above methods refer to the reverberation time for a particular receiver position. Sometimes though for practical reasons the average reverberation time for the whole room is useful to know. For such a calculation the reverberation times at various receivers spread all over the room can be estimated and then take the mean value of these. Obviously this procedure would be laborious. The average reverberation time for the whole of the room can be calculated much easier using an ensemble average technique suggested by Schroeder⁸, the results of which can be seen in Figure 22. As seen the reverberation time is about 1.4 seconds, which agrees with the above estimated values. This agreement is expected since sound behaviour remains about the same everywhere in the room.

8.3. A Test Room Comparison

For a preliminary validation of CADAЕ in terms of sound pressure level, a comparison is carried out between the experimental results obtained in a test room by Ondet and Barbry⁷¹ and the computer predictions. The test room is an extended parallelepiped, 30 m long, 8 m wide and 3.85 m high. The floor is made of concrete, the walls are made of cellular concrete and the suspended ceiling is made of glass wool panels covered by an aluminium sheet on one side. The sound absorption coefficients for each of the surfaces can be seen in the data input file assigned to each surface object on Table 4. The number of sound particles emitted by the source in both cases was 40000 and the execution times were 16 minutes for the empty test room and about 6 hours when the test room was fitted.

Two configurations of the test room were investigated (a) when the room is empty and (b) when the room is fitted uniformly by eighty fittings made up of $0.5 \times 0.5 \times 3 \text{ m}^3$ obstacles, obtained by stacking $0.5 \times 0.5 \times 1 \text{ m}^3$ polystyrene blocks. An absorption coefficient of 0.3 is assigned to each of the obstacles as well as a scattering coefficient of unity as shown on Table 4. The scattering coefficient of unity means that when a sound particle hits anyone of the obstacles it will be reflected in a random direction.

Figure 23 shows different views of the sound particle spatial distribution for case (a) when the room is empty. The various points indicate sound particles colliding with the surfaces in the room. The spheres represent positions of receivers while the sound source position is easily recognised by the concentration of sound particles. A first observation is that sound is almost uniformly spread all over the room. This can also be seen on the 2-D noise map on Figure 24. On the other hand, for case (b) when the room is fitted the spatial distribution of sound particles, see Figure 25, appears to show the sound energy decreasing with distance from the source.

The computer predictions and experimental results for the ten receiver positions at a 2 kHz frequency band are shown in Figure 26. It seems that the model overestimates the sound pressure level at receiver positions near the source but the difference becomes less from a certain distance and onwards. This might be due to near field (see page 11) effects, which cannot be predicted by the model. As seen the average difference between computer prediction and measurement is in the order of less than 1 dB for both configurations.

8.4. Long Enclosures

Sound fields in long enclosures exhibit unusual characteristics and classical room acoustics is certainly not suitable for analysis since the sound field is non-diffuse. This is why the next application of CADAЕ was to predict the variation of sound pressure level and reverberation along a corridor. The corridor to examine was 2.5 m wide, 2.45 m high and 38 m long as shown in Figure 27. Figure 27 shows the sound particle spatial distribution where sound particles are striking on the boundaries of the corridor. The sound source was placed at the front end of the corridor while receivers were positioned every 6 metres along the corridor. The main materials used for the various surfaces (see Figure 28) were linoleum on concrete for the floor, wood, lignacite and metal, for the walls and acoustic tiles for the ceiling. The number of primary sound particles sent by the source was 36000 and the total calculation time was 11 minutes.

The experimental results¹¹² and the computer results for the sound level at the frequency bands of 1000 and 2000 Hz are shown on Figure 29. It can be observed that at higher frequencies the sound pressure level decays with a faster rate. It seems that the sound pressure level decreases with doubling the distance, but with a lower rate than in a free field. Further, there is some evidence of constant reverberant sound level at the terminated end of the corridor. As seen in the figure the predicted and measured results agree closely with an average difference of about 1 dB.

In addition to the variation of the sound level along the corridor, the reverberation was also investigated at various positions. A typical simulated reverberation trace is shown in Figure 30 for a receiver at a distance of 18 m from the source at the 500 Hz frequency band. The curve was obtained using the Schroeder integrated impulse response method (see page 27). As seen it seems to be composed of slight steps which is probably due to the geometry of the corridor. The reverberation time estimated by the slope of this curve is about 1 second, which is in close agreement with the measured result. The experimentally estimated reverberation times for the different positions at all the frequency bands are shown on Table 5 and the corresponding predicted on Table 6. As seen from the error analysis on Table 7 the average difference between measurement and prediction is in the order of 0.2 seconds. The difference seems to go higher for the low frequencies and lower for the high frequencies. This is probably due to standing waves (see page 16) and interference effects along the corridor, which cannot be predicted by the model.

The other aspect to study was the directional distribution of sound in the corridor. This was achieved by constructing three-dimensional hedgehog diagrams such as the one shown in Figure 31 for a receiver position 18.2 m from the source. It is clear that there is a strong directionality from the front and the rear but the lateral sound is minor. Figure 32 shows the directional sound distribution for the five receivers. This reveals how the diffusivity of the sound field changes as moving away from the source along the corridor. As seen in

Figure 32 for receiver 1 it would be clear where the sound source is positioned, since the hedgehog plot reveals a strong directionality from the front. Going to receiver 2 the sound received from the front decreases while sound from the rear increases. This effect becomes greater until receiver 5 is reached where sound energy from the front and the rear balances. Due to this effect receiver 5 might not recognise where the sound source is placed.

The same effect can be seen in Figure 33, Figure 34, and Figure 35 using another type of diagram called diffusion map. In this diagram the sound energy on the z-axis is plot against azimuth and elevation angle on the x-axis and y-axis, respectively. As seen in Figure 33 which represents receiver number 1 most of the sound energy comes from the front as indicated by the large peaks while the energy from the back is minimal. Going on to receiver 3 as shown in Figure 34 the energy from the back increases until it reaches the stage where it is nearly balancing with the front at receiver 5 as shown in Figure 35.

8.5. Enclosures with Tilted Walls

In this application a computer model is constructed of a simple typical auditorium with tilted walls. The absorption coefficients of all the surfaces were deliberately given the value of 0.2 for all frequency bands and the source and receivers were positioned as shown on the sound particle spatial distribution in Figure 36. The source can be identified by the concentration of sound particles while the receiver is shown as a sphere. Air absorption is taken into account at various frequencies according to the atmospheric conditions, which are assumed to be 20 °C and 50% relative humidity. For 36000 sound particles emitted by the simulated impulsive source the total calculation time was 21 minutes. More details about the model can be viewed on Table 8, in the listing of the data input file.

As seen from Figure 36 the sound energy particles are well spread over the entire volume of the model. By constructing directional diffusion diagrams for several receiver positions such as the one shown in Figure 37, it was verified that the sound field is highly diffused. Further from the distribution of free sound paths

on Figure 38 it can be seen that the mean free path is about 9 metres which is equivalent to the theoretical value ($4V/S$, see Eq. 15 on page 21). This automatically means that Eyring's and Sabine's theory would be applicable for this enclosure.

Therefore, it was decided to compare the acoustical parameters obtained by computer simulation with those obtained from theory. Figure 39 shows the computer results of the average energy decay for the entire hall at the main frequency bands. This was obtained by taking ensemble averages, a method suggested by Schroeder⁸. The reverberation time for 1 kHz at the receiver position (about 20 m from the source, see Figure 36) may be estimated by the slope of the integrated impulse response (see Figure 40). As seen from Figure 40 the reverberation time is about 1.7 seconds, which is in good agreement with the average reverberation obtained above. This verifies the high diffusivity of the field.

By the slopes of the decay curves of Figure 39, the average reverberation times were estimated as seen on Table 9. Table 9 shows the calculated reverberation times using the formulas of Sabine and Eyring and also the estimated reverberation times using the computer generated decay curves. From the error analysis shown on Table 9 it is seen that theory and computer experiments agree quite well.

The theoretical (see Eq. 18 on page 23) and computer predicted results were also compared for sound pressure level as shown on Table 9. As seen, the difference between theory and simulation is marginal which is expected to be due to the diffusivity of the sound field. Actually for a sound power level of 100 dB the theoretical and computer predicted results for the sound pressure level agree closely to be about 81.4 dB.

8.6. Coupled Rooms

The subdivision of enclosed spaces into a number of smaller rooms leads to some interesting acoustical response known as "coupled rooms" phenomenon.

Such a case can occur in large churches with side chapels or where the choir is connected to the nave by a chancel arch, and theatres, which often have many rather deep boxes. The classic case of “coupled rooms” studied by many researchers such as Cremer & Muller¹⁴, and Kuttruff¹⁵ involves two or more rooms coupled by a small area between them. The larger the area the less evident the coupling phenomenon. Further, in order for the coupling phenomenon to occur the room with the sound source has to have a considerably larger sound absorption.

Figure 41 shows the sound particle spatial distribution of this classic case of coupled rooms. The two rectangular rooms are connected by an open doorway 2 m wide and 2.5 m high. A sound source is placed in the corner of the left hand room and one receiver in each of the rooms as shown on Figure 41. The absorption coefficients are 0.5 for all the surfaces in the source room and .1 for all surfaces in the other room. The number of primary sound particles sent by the source was 36000 and the calculation time was 20 minutes.

The theoretical¹⁴ result (see page 23) for the two receivers in each of the coupled rooms is shown in Figure 42 with thin lines while the computer simulation result is shown with thick lines. It can be seen that the curve of the sound decay of the source room consists of two distinctive parts. The first part known as the early stage is characterised by a steep slope, which changes with time while the second part known as the late stage has a constant but less steep slope. It seems that during the early stage sound decays rapidly in the source room as sound energy is given to the highly absorbing boundaries as well as transferred to the next room through the coupling area. The decay rate gradually becomes less while the adjacent room reflects back to the source room some of the energy it was given, and finally, the sound decay rate becomes constant in the late stage. In common terms the source room sound decay curve exhibits a “sagging” appearance. On the other hand, as seen in Figure 42, the sound decay curve of the non-source room exhibits a “ballooned” appearance. Initially it has a gradient of zero and during the early stage sound decays slowly compared with the fast energy decay

rate in the source room. This extra energy that makes the decay slower is obviously supplied by the source room and the decay rate increases gradually as the sound energy is transferred back to the source room. Finally, during the late stage the decay rate becomes constant as the exchange of energy between the two rooms is reduced.

As seen from Figure 42 computer simulation (thick lines) and theoretical solution (thin lines) are in close agreement for both the source and the adjacent room decay curves.

8.7. Enclosures with Curved Boundaries

Buildings with curved walls have usually serious acoustical problems with the intelligibility of speech and appreciation of music. Although in most rooms the sound energy distribution is uniform, the situation is completely changed if some of the room boundaries are curved. The effect is that the reflected waves instead of spreading, usually converge simultaneously causing sound concentrations, provided that the sound wavelength is small compared with the radius of curvature.

It should be noted that contemporary acoustical computer programs use only plane surfaces for modelling. This represents obviously a source of errors since it is rather impossible to predict the sound concentration caused by focussing, by approximating the curvature with a series of flat surfaces.

To be able to realise the significance of the proposed model the same enclosure is modelled first by the use of only flat surfaces, and second by the use of curved surfaces, as seen in the applications that follow.

8.7.1. Cylindrical Boundaries

The first application concerns a long, rigid hollow circular cylinder, with a radius much larger compared to the sound wavelength, having an omni-directional source at its centre line inside the cylindrical room. The solution to the reflection of a sound wave from such a boundary is shown in Figure 43, given by the use of

Bessel functions (see page 14). Figure 43 shows the variation of the value of the squared sound pressure with respect to the relative position from the centre of curvature. As seen there are areas of maxima and minima corresponding to constructive and destructive interference but the important observation is the asymptotic increase in the squared pressure and the maximum value as approaching the centre of curvature, giving evidence that a focus is created. After that the squared sound pressure decreases rapidly symmetrically as the observation point moves away from the centre of curvature.

To be able to realise the significance of the proposed model in its ability to model curved surfaces the cylindrical enclosure described above is (a) approximated by a series of flat surfaces and (b) modelled by the exact cylindrical surface. In both cases 19 receivers are placed on a diameter inside the hollow cylinder. The two data input files preparations can be seen on Table 10. As shown the preparation for the curved surface case involves only one object, which is a cone (cylinder) cut at its ends. On the other the flat surface preparation involves many polygonal objects. This shows directly the efficiency advantage in favour of the curved surface representation.

The sound particle spatial distributions for the two models are shown on Figure 44 and Figure 45. The main observation by looking at the two figures is that in the case of the curved surface model there is a clear definite sound particle concentration along the centre axis, while for the case of the flat surfaces model sound particles seem to spread uniformly.

This observation is reinforced by the sound energy comparison in Figure 46. The 'o' sign stands for the flat surfaces model and the '*' stands for curved surface model. While the curved surface model exhibits a dramatic increase in sound energy near the centre of curvature, the flat surface model gives the impression that the sound level is constant. As seen from Figure 43 and Figure 46 the curved surface model is in good agreement with the theoretical solution while the flat surface model gives false results.

Although cylindrical rooms are seldom used in architecture, the above example indicates that the contemporary acoustical prediction computer models might lead to significant errors when used to model enclosed spaces with curved walls.

8.7.2. A Barrel Shape Room

To enhance the above investigation the next enclosure to be modelled was chosen to be a barrel type of room of simple rectangular shape $30 \times 20 \text{ m}^2$ with a cylindrical ceiling having centre of curvature on the floor. Such a room configuration can be compared to the Congregational Church in Naugatuck, Connecticut, USA. Such a type of enclosure was studied by Sabine⁴². The results of the measurement test with a sound source positioned in the middle of the room near the floor can be seen in reference⁴² in the form of contour plots. The results appear to be quite interesting as the sound level varies quite dramatically just by changing slightly the position of the listener. As Sabine observed it is quite a striking phenomenon since at some positions the sound level is extremely high, while at other positions it is so low that hardly any sound can be heard.

Figure 47 shows the sound particle spatial distribution for the side, elevation and plan views together with an isometric view of the enclosure under investigation, modelled using flat surfaces. Likewise Figure 48 shows the sound particle spatial distribution for the same views using a curved cylindrical surface for the ceiling. The various points represent sound particles hitting the boundaries. Looking carefully at Figure 47 side view one can distinguish the five plane surfaces used for the modelling of the cylindrical ceiling while the same view in Figure 48 shows an exact cylindrical surface.

A first glance at Figure 48 shows that there is strong concentration of sound particles along the longitudinal axis. On the other hand, for the case of the flat surface model (see Figure 47) sound particles seem to be uniformly spread all over the room. Finally, for both models there seems to be some concentration of sound around the sound source as expected.

In both cases 32000 sound particles were emitted in all directions from a source in the middle of the room near the floor. The particles were traced until their energy was reduced by 60 dB. The absorption coefficients of all the surfaces were taken to be 0.2 and the atmospheric conditions were taken to be 20 °C and 50% relative humidity. The sound source was omni-directional and situated at the centre of the room near the floor in both cases. The time required to complete the computer simulation process was about 10 minutes using flat surfaces and 8 minutes using curved surfaces.

Figure 49 shows the predicted sound level results for the curved and flat surfaces model, respectively. The x-axis represents the positions of potential listeners along the lateral (width) axis of the room at a distance of 11 m from the source, while the y-axis is the sound level in (dB) for each particular position. Each receiver number also represents the distance in meters along the lateral axis from the longitudinal wall. The 'o' sign stands for the flat surfaces model while the '*' stands for curved surface model.

Looking first at the flat surface model, the sound level is fairly constant with no dramatic changes. Such a result is entirely different from that of Sabine's measurement test where many fluctuations of sound occur. On the other hand, for the curved surface model the sound level for the same position of receivers varies dramatically with respect to the position especially near the focal area. These results are definitely more acceptable. The peak in the middle represents focussing of sound energy and this could constitute a major acoustical problem in many cases. Such an effect could not be predicted by using the flat surface model. Looking at the two graphs together, it seems that the flat surface model shows just the average of the curved surface model or the real result. That diminishes the real fluctuations of sound and gives the misleading message that sound energy is spread uniformly in the room, which is not the case.

From the above analysis it can be concluded that the use of flat surfaces to represent curved walls leads to noticeable errors especially around the focal

region. Further, attempting to increase the number of plane sections to represent the curved wall decreases the efficiency of the model without any real benefit to the accuracy. On the other hand, using the exact curved surface as opposed to approximating this with a series of flat surfaces represents a more accurate and efficient solution to the simulation of sound fields in spatial systems with curved boundaries.

8.8. St. Paul's Cathedral

Since part of this thesis was to extend the contemporary acoustical numerical methods to enclosed spaces involving curved boundaries a suitable existing building had to be chosen for application of the proposed model. After looking at various buildings including theatres, churches and concert halls, London St. Paul's Cathedral (see Figure 50) seemed to be the ideal building to test the validity of the proposed model due to its many curved walls and ceilings, which produce a variety of acoustical phenomena.

8.8.1. General Description

The architectural style of St. Paul's is called Baroque, a style used in Europe during the 17th and early 18th centuries. The interior of St. Paul's has a volume of 152000 m³, It is 141 m long internally and 69 m wide across the transepts, the nave is 38 m wide and 28 m high. It is the second largest Cathedral in Britain and one of the largest in Europe.

The structure of the Cathedral is quite complex involving many concave surfaces. The roofs are made of numerous saucer domes separated by arches. Some of the arches, in particular those in the nave are made of brick and plaster, while those in the chancel are encrusted with mosaics. The main structure is constructed from Portland stone, a fine limestone, and the floor is made of marble. Every wall in the Cathedral has large windows. The small glass panes are set into lead and iron rods are used to strengthen the window. There are normally 2500 chairs arranged throughout the building and each chair consists of approximately one square metre of 12 mm plywood held in place by a metal frame. The choir stalls and the

organ case in the chancel, are made of oak and pear and form the only concentration of wood.

The most striking feature of the Cathedral is the Dome. Its diameter is 34 m and it rises to a height of 62 m internally. The Dome structure weighs 65000 tonnes and is supported by eight pillars beneath it. It consists of three parts; the painted inner dome is made of brick, the inner cone supporting the lantern also made of brick and the outer dome of wood covered with lead on the outside. The space between the inner dome and the cone is connected to the main interior space of the cathedral by a circular neck. It is possible for sound waves to penetrate into this space and form a Helmholtz resonator with the connecting neck. A particular acoustical feature of the dome interior is a whispering gallery, which stands 30 metres from the floor and where communication in whispers is possible in all parts of the gallery. It should be noted that communication in whispers is impossible at floor level. A distinct and real echo occurs under the dome area with a delay of approximately 0.25 s corresponding to the first reflection of sound to the inner dome.

There are three principal locations from which speakers read or preach, namely the high altar, the pulpit and the lectern (see Figure 52). The pulpit is positioned at the southeast corner of the crossing as shown on Figure 52. It is made of oak and has a canopy, which just covers the lower part of the pulpit in which the preacher stands. The presence of the canopy means that the preacher in the pulpit only has partial sight line to the sides of the dome, but has a good view down the nave. The brass lectern is placed at the north east corner of the crossing and has no canopy to reflect the sound.

A speech reinforcement system was designed for the cathedral, by Parkin and Taylor^{113, 114} about 50 years ago, but in 1981 an entirely new system was introduced. Both systems used, provided delays of the speech signals before transmitting them to column loudspeakers.

There are many opinions as to what are good seats for listening in St. Paul's, but it is clear that the sound of string instruments is poor. Brass only sounds bright when against one of the edges of the dome area. Further, it is often said that the sound from the choir is lost in the dome. The size of the interior of the cathedral is subjectively reinforced by the large reverberation time.

8.8.2. Modelling

The computer model of St. Paul's in the form of sound particle spatial distributions is shown on Figure 53 with the source placed at the pulpit. As seen from the various views, the model is quite complicated involving many walls, columns and arches, and domes in order to describe the actual building in the best possible way. The actual building blocks and materials used to define the model can be seen in the CADAЕ data input file on Table 11. As seen there are about 120 individual surface objects comprising the model. The model was prepared by using data from the architectural drawings¹¹⁵ of St. Paul's Cathedral. A preliminary model was prepared in Autodesk's AutoCAD as seen in Figure 54 and the final modelling was carried out in CADAЕ's description language.

The main materials used for the various surfaces comprising the model, where Portland stone, plaster on brick, mosaic, marble and wood. The seating area as well as the choir area was modelled by large short parallelepipeds assigned a scattering coefficient of unity. The absorption coefficient in this case was varied according to whether the Cathedral was empty or full. The various columns were also given an approximate scattering coefficient depending on their size. The number of sound particles emitted by the source of sound power level 100 dB, was 160000 and the time needed for the computer to complete the calculations was about 15 hours.

8.8.3. Sound Path analysis

By drawing the path of each sound particle, ray diagrams can be constructed (see Figure 55, source at the pulpit). From these diagrams valuable information about the sound field can be drawn. In the case of St. Paul's cathedral, by tracing sound

paths one by one using computer animation, it can be observed that sound particles once they have entered the dome area they do not return back to the audience area. That means that the dome does not contribute any useful reflections. In a similar way, the nave does not produce any useful reflections since not much sound energy will be reflected to the audience.

8.8.4. Reverberation Test

To check the validity of the proposed computer model (CADAЕ) in terms of predicting accurately the reverberation time, a series of measured and predicted results have been compared.

First, the average (over the entire Cathedral) reverberation time was predicted by the computer model, making use of the ensemble averaging technique (see reference 8) described earlier. The results at various frequency bands for when the Cathedral is empty as well as when it is full of people can be seen on Figure 56 and Figure 57 respectively. The predicted results were compared with measured¹¹³ results for the main frequency bands as shown in Figure 58. As seen predicted and measured results agree closely in general but especially for the higher frequencies. The difference at the 125 Hz frequency band is rather high and this is expected due to the fact that diffraction and interference would predominate. Both simulated and measured results for both cases full and empty (especially for full) indicate the relatively higher reverberation times at the low frequencies. This could constitute a great hazard for feedback when using microphones for speech reinforcement.

The reverberation was also measured¹¹⁶ and simulated using the proposed computer model (CADAЕ) at specific locations as shown in Figure 59 with the sound source placed at the ledge of the pulpit. Figure 60 shows a sample measured reverberation trace for receiver 4 at 1 kHz, which was obtained by the steady state method (see page 106, the sound source was allowed to run for a few seconds and then switched off). The reverberation time is given by the slope of a straight line fit as applied to the sound level decay graph (Figure 60), which in this

case is 9.8 seconds. The computer results for receiver 4 at 1kHz are shown in Figure 61. These results are produced as a result of a simulated impulsive source and so this permits the use of Schroeder's integrated impulse response method (see page 27). The reverberation time is extrapolated from the slope of the integrated impulse response of Figure 62, and is about 10 seconds.

The fact that most of the sound curves at the various receiver positions exhibit an exponential decay, permits the use of the use of regression analysis to calculate the slope of the decay curve. The regression analysis is much quicker than constructing the integrated impulse response. An example of using regression to get the decay slope is shown in Figure 63. Figure 63 shows the sound decay at position 4 for the 2 kHz frequency band. As seen the slope of the curve yields to a reverberation time of about 7.4 seconds which in close agreement with the measured result, which was 7.2 seconds (see Table 12).

The measured and simulated variation of reverberation time with respect to frequency for receivers 1 and 4 is shown on Figure 64 and Figure 65 respectively. The reverberation time with respect to frequency for all the receiver positions exhibit a similar appearance as the one for the average reverberation, indicating high low frequency reverberant level. The actual reverberation time with respect to each receiver changes from place to place in the Cathedral. As seen this change is exhibited by both the measured and predicted results, which are in close agreement.

The complete estimated measured and predicted reverberation times for the various positions are quoted on Table 12 and Table 13 respectively. As seen from the error analysis on Table 14 the difference between measurement and prediction is very small (about 0.5 seconds) at the higher frequencies while it becomes greater the lower the frequency band (about 2 seconds).

8.8.5. Echogram Analysis

A good way to check for strong reflections is to analyse the impulse response at a particular receiver position. Looking back at Figure 61 obtained for receiver

position 4 (under the dome) at the 1 kHz frequency band some useful information may be deducted. The echogram exhibits generally a regular character except at the early stage. At this stage a separable reflection is represented by a strong maximum in the reflectograms. The arrival time of this clearly audible strong reflection is about 0.25 seconds after the direct sound arrives and it comes from the dome.

8.8.6. Sound Pressure Level Results

The other type of acoustical parameter to investigate was that of sound pressure level. The various receiver positions investigated were along the central axis of the Cathedral as shown in Figure 66. The source in this case was placed at the entrance to the choir. Table 15 and Figure 67 show the measured sound pressure level results while Table 16 and Figure 68 show the computer prediction. The error analysis on Table 17 shows that the average difference between the measured and predicted results is about 1.5 dB on the low frequencies and only about 0.6 dB at the high frequencies. The maximum difference in fact is 3.3 dB and occurs at 125 Hz. This should be expected by considering that diffraction and interference effects prevail over the lower frequencies (see page 20). Still though from the 500 Hz and upwards the maximum differences are floating around 1 dB.

8.8.7. Speech Intelligibility

The next acoustical factor to study was that of speech intelligibility. The various receiver positions for the test are shown in Figure 69. The sound source was placed at the ledge of the pulpit. The definition criterion (see page 24) was used for this purpose, which was compared with a subjective test¹¹⁶ and RASTI measurements¹¹⁷.

The results of the comparison for the various positions can be seen in graphical form in Figure 70. As seen the results from the three different methods vary slightly but the main trend is the same. It seems that speech intelligibility is dramatically reduced as the distance from the source is increased especially under

the dome area. As seen at receiver position 1 the definition is about 90% and then at position 2 is only 50 %. Passing to the nave the reduction in speech intelligibility decreases slightly and seems to become constant between receivers 5 and 6. This is probably due the various surfaces around giving rise to lateral reflections or perhaps reflection from the back.

8.8.8. Acoustically Coupled Spaces

Often large churches with side chapels or where the choir is connected to the nave by a chancel arch exhibit unusual sound phenomena. So it was decided to check this point in further detail in order to reveal any evidence of coupling. For this purpose the source was placed in the choir with receivers in the choir and under the dome, as shown in Figure 71.

The measured response, using an impulse excitation, for the two receivers at the 1 kHz frequency band can be seen in Figure 72 and Figure 73, while the predicted and measured sound decay curves for the two receiver positions, using Schroeder's method (see page 27) are shown in Figure 74. The heavy lines represent the predicted results while thin lines represent the measured results. The simulated and measured results show that the choir and the dome area are acoustically coupled since the decay curve in the choir, which is the source room, exhibit the "sagging" appearance and the decay curve in the area under the dome exhibits the "ballooned" appearance (see page 116). Simulated and measured results agree, as shown in Figure 74.

8.9. Whispering Galleries

A particular kind of curved reflecting surface is the "whispering gallery". The distinctive characteristic of whispering galleries is that they carry usually high frequency sound such as a whisper over long distances.

The effect occurs mainly in two types of structures. In the simpler type the inside surface of the room is a section of a sphere or an ellipsoid. When a speaker stands at the centre of curvature of the sphere, the spreading sound waves are reflected and focused back to him or her with surprising loudness. If an ellipsoid

is involved, the speaker is at one focus and the listener at the other. Again the curved surface reflects the spreading sound waves and focuses them, this time to the second focal point. In both types of structure sound can travel through a large volume of air and still remain audible because of simple reflection and focusing. An effect of this kind was simulated for a room having a curved ceiling with centre of curvature the floor⁹.

The second type of whispering gallery is also curved but is more difficult to analyse because it involves no focusing. When a speaker whispers along a circular wall the sound is somehow held in a layer adjacent to the wall; it travels along the wall and can be heard by a listener anywhere on the circumference. The most famous gallery of this type is the one at St. Paul's Cathedral.

The gallery is made of an annular platform with a nearly cylindrical outer wall that stands at a height of about 30 metres at the base of the dome as shown in Figure 51. The annular platform is actually a walkway about two metres wide and forms a circle with a diameter of 34 metres. The wall along the side of the walkway belongs to the dome and is inclined slightly inwards. The noticeable effect is that someone whispering along the gallery wall could be heard by anyone who is close to the wall at any point around the walkway.

The whispering gallery phenomenon was first studied by Lord Rayleigh²³ who gave the following explanation. Sound leaves the wall in a cone of rays forming a maximum angle θ with a tangent to the wall. The rays reflect from the curved wall at various points along the circumference in such a way that with each reflection the angle of reflection equals the angle of incidence. Because the rays began in a cone of angle θ they remain in a region bounded on the outside by the wall and on the inside by an imaginary wall with a radius that is the radius of the real wall multiplied by the cosine of θ . The rays are therefore trapped in a layer along the wall and can be heard by a listener in that layer but not by someone outside it. In this model the thickness of the layer is determined by the radius of

curvature of the gallery and by the maximum angle at which the sound leaves the wall when the speaker whispers along it.

Later on Rayleigh carried out further research on the problem and presented a solution by drawing an analogy to the vibrations of a circular membrane^{118, 119}. The solution involves the use of Bessel functions (see page 14). In addition to Rayleigh's explanation, Sabine⁴² supported the view that the presence of the dome leads to an additional increase of sound power due to a vertical collecting of sound.

To investigate Rayleigh's and Sabine's hypotheses a computer model of St. Paul's whispering gallery was constructed. With an omni-directional source and a receiver placed at opposite ends on the annular platform computer simulation was carried out using the CADAE sound particle program. Figure 75 shows sound particles spread uniformly around the annular platform with slight concentration opposite the sound source. Figure 76 and Figure 77 show that the sound paths either follow a circumferential or vertical direction. This confirmed by the hedgehog diagram of Figure 78 and the diffusion map of Figure 79 indicating the directionality of the receiver.

To check the validity of the proposed model computer simulation is carried out using the above model of the whispering gallery. The sound source is placed at the gallery's walkway and 16 receivers are positioned at equal distances along the radius of the gallery opposite the sound source. The theoretical solution using Bessel functions (see page 14) suggested by Rayleigh, and the results from the simulation can be seen in Figure 80. The graph shows the variation of squared sound pressure with respect to radial distance from the whispering gallery centre. The 'o' sign stands for the theoretical solution while the '*' sign stands for the simulated. As seen the sound energy or squared pressure of both the theoretical and simulated results is nearly zero until it approaches the annular platform of the gallery. This is where it begins to increase with an almost exponential ratio indicating that the sound energy gets higher and higher the nearer to the

circumference of the gallery. It should be mentioned that the result will be the same with the sound source placed anywhere around the circumference. The fact that the theoretical and predicted results agree closely gives major confidence to the computer model presented in this thesis.

To see the extent to which the shape of the dome alters the sound field the following computer experiment was conducted using the CADAЕ computer program. The cylindrical wall and the parabolic reflector of the dome in the previous model were replaced by a hemispherical wall having centre of curvature the centre of the annular platform. With an omni-directional source emitting a few thousand sound particles an interesting result occurs as shown on Figure 81. As seen from the distribution of sound particles, sound concentrates on the top periphery of the spherical dome from the source to a location exactly opposite on the annular platform. The highest concentration occurs at the annular platform at the source area and at an area exactly opposite. The same effect was observed in a completely spherical room in the Christian Science Publishing House at Boston, USA.

Chapter 9

FINAL DISCUSSION – CONCLUSIONS – FUTURE WORK

9. FINAL DISCUSSION – CONCLUSIONS – FUTURE WORK

9.1. Discussion – Conclusions

The main objective of the work presented in this thesis was to contribute to the current stage of research in the modelling of sound fields in living or working environments.

Due to the recent rapid development of computer technology, computer simulation of sound fields in enclosed spaces has become the major solution to the problem of acoustical modelling. After a review of all the methods of modelling sound fields it was decided that computer simulation was the best way to achieve the main objective.

A survey on the contemporary acoustical computer models has revealed that there are inaccuracies and inefficiencies in the current models with two main areas having a high potential for improvement. First, all contemporary acoustical computer models treat curved walls approximately with a series of flat surfaces. And second, contemporary models use some kind of statistical or empirical formulae to match the reduction in energy due to the spherical wave propagation with the sound particle density as moving away from the source which usually represents a source of errors.

Based on the above findings a computer model was developed and presented in this thesis with the aim of improving the current state of research. The program given the name CADAЕ (Computer-Aided Design of Acoustical environments) enables one to model acoustical fields in rooms with the aid of personal computers. It should be pointed out that the model does not introduce any limitations on the shape of the enclosure. That is, curved surfaces do not need to be approximated by a series of flat surfaces as in contemporary models.

It has been shown that any acoustical environment may be modelled with high accuracy. The proposed model was applied successfully, to simple rectangular rooms, long corridors, fitted rooms, typical auditoriums and coupled rooms. Further the model was validated in enclosed spaces having curved walls, which included rooms with simple shapes and spaces with complex geometry such as St. Paul's Cathedral, situated in London, UK.

The work done and presented in this thesis has shown that approximating curved walls by planar surfaces (as contemporary models do) leads to errors in the sound field prediction. These errors could be quite high especially around a focal region. As seen on the simple computer experiment of the cylindrical room the theoretical solution (using wave theory) to the problem agrees closely with the simulation when a curved surface is used. On the other hand when a series of flat surfaces is used an error as high as 90% can accumulate around the focal area.

Further it was shown that it is more efficient to use curved surfaces in terms of number of calculations, calculation time, as well as the users time required to prepare a flat surface approximation for a curved wall. For example to model roughly the dome and whispering gallery of St. Paul's Cathedral would require hundreds of flat surfaces. It was shown that the same problem can be solved by only three surface-objects using the proposed model (CADAЕ) with a result that is comparable to the wave theoretical solution.

With regard to matching the reduction in sound energy due to the spherical wave propagation, this thesis applies successfully the concept of the expanding receivers. By varying the size of the receiver according to the flight travel time of a sound particle a perfect match of the reduction in sound energy was achieved.

Thereby, the proposed model can calculate accurately the impulse response, especially during the early part, at any location in the room. Any of the commonly used assessment criteria such as sound pressure level, reverberation time, early decay time, definition etc. can be estimated. Further to that, the directionality of the sound field can be visualised by various three dimensional plots using the

sound particle path information. This visualisation gives the user the ability to see immediately which areas need to be adjusted to get the desired directionality for a receiver in, for example a concert hall.

As seen from the various applications, the proposed model was validated in terms of geometrical applicability since it was proven that any kind of room configuration can be considered, simple or complex, fitted or empty. The model was proven to give valid results in terms of reverberation, sound pressure levels, and speech intelligibility. In fact the average difference between predicted and measured result for the reverberation time was only of the order of 5-10%, while the average difference of the predicted and measured results for the sound pressure levels was less than 1 dB. Further, the proposed computer model was proven to be successful in predicting the sound decay curves in classical coupled rooms but also in identifying coupled spaces, such as was the case of coupling between the choir and the area under the dome in St. Paul's Cathedral. It should be noted that the accuracy of the CADA program was better at the higher frequencies (above 500 Hz).

The way the computer model was developed was to prepare a pilot computer model in order to identify the programming needs. Based on these needs the software development was divided in three stages, each of which can be taken care of by a different system; the pre-processing (modelling part), processing (simulation part) and post-processing (analysis of the results). The appropriate language for the simulation part was identified as the C++ programming language and based on that, an acoustical description language was developed. Further according to the analysis requirements, programs were written for the post-processing stage in MATLAB. Such program organisation allows both computer calculation times and user programming time to be economised with the guarantee of the highest quality in the presented results. Further the object-oriented programming approach employed makes the computer model quite flexible to changes and improvements, apart from being a source for programming optimisation.

In most of the cases of the applications presented herein the calculation time was no longer than 30 minutes and the storage memory needed to produce the output files was within reasonable amounts. Of course as the geometry of the space gets more complicated the calculation time would increase but then again computational time depends on both the primary sound particles sent and the order of reflection, that is the secondary sound particle paths. Only in the case of St. Paul's the computer was left overnight to complete the calculations.

Although the model discussed in this thesis does not pretend to constitute an optimal solution to the problem of simulating sound fields in enclosed spaces, both the results and the calculation times as well as the computer store requirements are quite acceptable. Further improvements in the model will undoubtedly be enhanced by the further development of personal computer software and hardware.

9.2. Suggestions for Future Work

The work done and presented in this thesis describes the basic form of a computer model, concerned with the geometrical approximation of sound wave propagation. Although scattering of sound is accounted for by a diffusion coefficient, which sends the sound particle in a random direction, this coefficient must be pre-defined. By having the various surfaces defined as objects, as it is the case of the proposed computer model, opens the possibility that the distribution of the scattered sound wave can be computed by the program. This calculation will depend directly on the frequency of a modelled sound wave in relation to the object's geometry. Thus, the dispersed sound particles will form the required directional pattern of the scattered wave reflection.

The sound source and receiver are considered to be at fixed positions in the presented work. By appropriately organising the program it is possible to model cases with a moving sound source or a moving receiver. Moreover, it is possible to include the directivity to each source, separately for each frequency.

The CADAЕ program can be used to carry out a complete analysis of a concert hall with a sound reinforcement system on. Several loudspeakers of known directionality could be located on columns and used to reproduce a signal from a particular position. Thus there could be multiple sources with different sound power levels and time delays. Then the program could be used to predict various acoustical criteria at various positions and therefore identify any acoustical problems.

There are two main stages in the design process, that of synthesis and that of analysis. The current computer model carries out the analysis, while the synthesis part is to be carried out by the user. There is a possibility by including artificial intelligence programs in the post-processing stage in MATLAB to make the computer suggest solutions to an acoustical defect. Therefore, an ultimate tool for acoustical design could be developed that can bring all the contemporary knowledge in an acoustical expert system.

As the program was successful in predicting whispering gallery effects it could be directed specially for the design or acoustical treatment of enclosures having curved boundaries such as indoor sports halls or multipurpose halls. The number of these halls is quite large and their acoustical problems are usually severe. The program could then enter the marketplace as a commercial package with a competitive advantage since other programs are not able to predict efficiently or accurately the acoustic field in such buildings.

Further, the proposed model could be used for the design of ultrasonic devices. Also it could be used as a synergetic tool to calculate other similar forms of energy such as heat radiation, or to simulate atomic and molecular collisions. This can be achieved by including the appropriate equations in the current program scheme.

Finally, the possibility of calculating accurate, long and highly resolved impulse responses would allow convolution of the impulse response with anechoic signals

and this would open new opportunities for acoustical modelling such as the auditory part of virtual reality.

The facilities described above may be inserted into the scheme of the current computer program, in some of the cases without a substantial increase on the programming or the computer work-load.

APPENDIX

A.1. TABLES

Table 1: The CADAЕ program general flowchart.

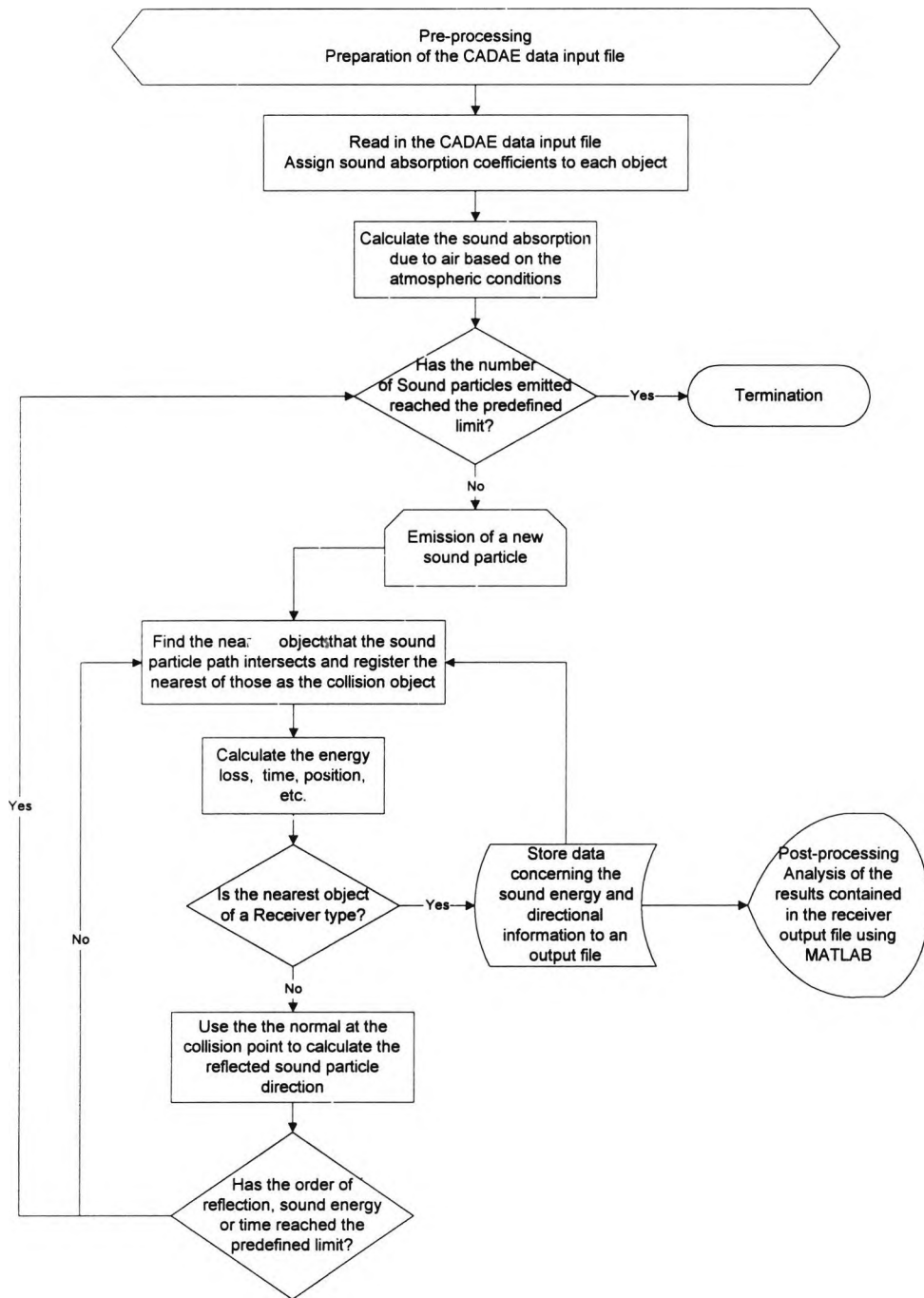


Table 2: The contents of a sample data output file.

Time	Energy	Position where sound comes from			Direction of the sound particle			Reflection Order
0.4973	0.0039	16.2000	0.0000	5.1985	-0.4733	0.8226	-0.3151	16.0000
0.2874	0.0124	9.3720	11.2927	0.0000	0.4186	-0.6087	0.6740	13.0000
0.2333	0.0526	3.3842	20.0000	7.1001	0.5148	-0.7486	-0.4177	9.0000
0.4120	0.0028	7.7435	8.5037	10.0000	0.2931	0.1400	-0.9458	17.0000
0.1544	0.1107	7.5195	8.3968	0.0000	0.7787	0.3719	0.5054	7.0000
0.6233	0.0053	0.0000	1.5565	2.3842	0.7525	0.6556	-0.0629	15.0000
0.4059	0.0058	1.3055	8.3046	10.0000	0.7279	0.1443	-0.6703	15.0000
0.8617	0.0012	23.7004	17.3332	0.0000	-0.8761	-0.4738	0.0893	19.0000
0.1581	0.1105	10.6063	8.9789	0.0000	-0.3525	0.3637	0.8623	7.0000
0.1809	0.1095	8.2546	11.5601	0.0000	0.6306	-0.6506	0.4232	7.0000
0.4490	0.0019	7.5275	12.3103	10.0000	0.2522	-0.2602	-0.9320	18.0000
0.4009	0.0020	9.8894	10.6158	0.0000	0.3012	-0.4375	0.8473	18.0000
0.2508	0.0365	12.2593	15.0553	10.0000	-0.2212	-0.4618	-0.8590	10.0000
0.1350	0.3252	14.6281	20.0000	4.7775	-0.4130	-0.8621	-0.2937	4.0000
0.2332	0.0368	10.1572	10.6674	0.0000	-0.2407	-0.5025	0.8304	10.0000
0.1353	0.3252	14.6281	20.0000	4.6152	-0.4124	-0.8609	-0.2980	4.0000
0.3861	0.0041	10.2270	10.9609	0.0000	-0.1437	-0.4520	0.8804	16.0000
1.1725	0.0010	0.0000	9.1003	2.8130	0.9930	0.0488	-0.1077	19.0000
0.4178	0.0020	7.3419	5.9875	10.0000	0.2871	0.4193	-0.8612	18.0000
0.4819	0.0013	16.9352	1.3094	10.0000	-0.4900	0.6041	-0.6285	19.0000
0.6537	0.0153	0.0000	11.3760	2.4158	0.9778	-0.1807	-0.1057	12.0000
0.4852	0.0013	14.9418	5.8515	10.0000	-0.4758	0.3588	-0.8030	19.0000
0.3020	0.0512	11.9032	20.0000	0.0656	-0.2048	-0.9654	0.1616	9.0000
0.2986	0.0732	11.9032	20.0000	0.8875	-0.2071	-0.9762	0.0639	8.0000
0.3698	0.0059	11.4138	8.5637	10.0000	-0.1658	0.1572	-0.9736	15.0000
0.4649	0.0014	9.8224	10.0720	0.0000	-0.1343	0.1273	0.9827	19.0000
0.1362	0.1115	10.5458	9.3863	0.0000	-0.4552	0.4314	0.7789	7.0000
0.1340	0.3253	0.0000	5.0904	2.0318	0.8958	0.4361	-0.0858	4.0000
0.3928	0.0028	9.9431	9.9306	0.0000	0.3078	0.1498	0.9396	17.0000
0.1838	0.0766	1.8118	5.9724	10.0000	0.6489	0.3159	-0.6922	8.0000
0.4794	0.0019	16.7422	2.1403	10.0000	-0.4792	0.6111	-0.6300	18.0000
0.2875	0.0124	9.0288	9.0279	0.0000	0.4148	0.6117	0.6736	13.0000
0.3851	0.0058	11.8610	20.0000	9.4960	-0.1608	-0.7561	-0.6344	15.0000
0.4283	0.0020	10.6241	10.5547	0.0000	-0.5544	-0.4100	0.7242	18.0000
0.2969	0.0732	23.3951	20.0000	4.0665	-0.7973	-0.5897	-0.1289	8.0000
0.4306	0.0028	11.5145	13.8617	10.0000	-0.1266	-0.4064	-0.9049	17.0000
0.4122	0.0028	10.5306	10.7028	0.0000	-0.1323	-0.4248	0.8956	17.0000
0.3051	0.0175	12.1353	15.8546	10.0000	-0.1794	-0.5758	-0.7976	12.0000
0.2026	0.0760	3.8053	7.2436	10.0000	0.5627	0.2958	-0.7719	8.0000
0.2721	0.0178	4.9755	5.0541	10.0000	0.4379	0.4267	-0.7913	12.0000

**Table 3: Rectangular room case, listing of the
CADAE data input file.**

```
NRAYS =22500

TEMPERATURE =20
HUMIDITY =0.5

SOURCE
location =(29,10,5)
orientation =(0,0,0)
PWL =100
end

/* Receiver Positions */
Receiver
location =(10,10,1.5)
receiver_number =1
end

/* Geometry and Sound Absorption of the Room */

Polygon
vertex =(0,0,0); vertex =(0,0,10); vertex =(0,20,10); vertex =(0,20,0)
Material
absorb =0.3
end

Polygon
vertex =(0,0,0); vertex =(0,0,10); vertex =(30 0 10); vertex =(30 0 0)
Material
absorb =0.3
end

Polygon
vertex =(0,0,0); vertex =(30,0,0); vertex =(30,20,0); vertex =(0,20,0)
Material
absorb =0.3
end

Polygon
vertex =(30,0,0); vertex =(30,0,10); vertex =(30,20,10); vertex =(30,20,0)
Material
absorb =0.3
end

Polygon
vertex =(0,20,0); vertex =(0,20,10); vertex =(30,20,10); vertex =(30,20,0)
Material
absorb =0.3
end

Polygon
vertex =(0,0,10); vertex =(0,20,10); vertex =(30,20,10); vertex =(30,0,10)
Material
absorb =0.3
end
```

Table 4: Test room case, listing of the CADAЕ data input file.

```
NRAYS =40000

TEMPERATURE =20
HUMIDITY =0.5

SOURCE
location =(1.5,1,0.85)
orientation =(0,0,0)
PWL =102.9
end

/* Receiver positions */

Receiver
location =(3,2,1.5)
receiver_number =1
end

Receiver
location =(3,4,1.5)
receiver_number =2
end

Receiver
location =(6,4,1.5)
receiver_number =3
end

Receiver
location =(9,4,1.5)
receiver_number =4
end

Receiver
location =(12,4,1.5)
receiver_number =5
end

Receiver
location =(15,4,1.5)
receiver_number =6
end

Receiver
location =(18,4,1.5)
receiver_number =7
end

Receiver
location =(21,4,1.5)
receiver_number =8
end
```

```

Receiver
location =(24,4,1.5)
receiver_number =9
end

Receiver
location =(27,4,1.5)
receiver_number =10
end

/* Geometry and Sound Absorption of the Room */

/* Floor */
Polygon
vertex =(0,0,0); vertex =(30,0,0); vertex =(30,8,0); vertex =(0,8,0)
Material
absorb =0.05
end

/* Ceiling */
Polygon
vertex =(0,0,3.85);vertex =(0,8,3.85);vertex =(30,8,3.85);vertex =(30,0,3.85)
Material
absorb =0.15
end

/* Walls */

Polygon
vertex =(0,0,0); vertex =(0,0,3.85); vertex =(0,8,3.85); vertex =(0,8,0)
Material
absorb =0.1
end

Polygon
vertex =(0,0,0); vertex =(0,0,3.85); vertex =(30 0 3.85); vertex =(30 0 0)
Material
absorb =0.1
end

Polygon
vertex =(30,0,0); vertex =(30,0,3.85); vertex =(30,8,3.85); vertex =(30,8,0)
Material
absorb =0.1
end

Polygon
vertex =(0,8,0); vertex =(0,8,3.85); vertex =(30,8,3.85); vertex =(30,8,0)
Material
absorb =0.1
end

/* First series of obstacles along the room */

Parallelepiped
lower =(3.5,.75,0); upper =(4,1.25,3);
Material
absorb 0.3; scattering 1.0;
end

Parallelepiped
lower =(5,.75,0); upper =(5.5,1.25,3);
Material
absorb 0.3; scattering 1.0;
end

Parallelepiped

```

```
lower =(6.5,.75,0); upper =(7,1.25,3);
Material
absorb 0.3; scattering 1.0;
end

Parallelepiped
lower =(8,.75,0); upper =(8.5,1.25,3);
Material
absorb 0.3; scattering 1.0;
end

Parallelepiped
lower =(9.5,0.75,0); upper =(10,1.25,3);
Material
absorb 0.3; scattering 1.0;
end

Parallelepiped
lower =(11,0.75,0); upper =(11.5,1.25,3);
Material
absorb 0.3; scattering 1.0;
end

Parallelepiped
lower =(12.5,0.75,0); upper =(13,1.25,3);
Material
absorb 0.3; scattering 1.0;
end

Parallelepiped
lower =(14,0.75,0); upper =(14.5,1.25,3);
Material
absorb 0.3; scattering 1.0;
end

Parallelepiped
lower =(15.5,0.75,0); upper =(16,1.25,3);
Material
absorb 0.3; scattering 1.0;
end

Parallelepiped
lower =(17,0.75,0); upper =(17.5,1.25,3);
Material
absorb 0.3; scattering 1.0;
end

Parallelepiped
lower =(18.5,0.75,0); upper =(19,1.25,3);
Material
absorb 0.3; scattering 1.0;
end

Parallelepiped
lower =(20,0.75,0); upper =(20.5,1.25,3);
Material
absorb 0.3; scattering 1.0;
end

Parallelepiped
lower =(21.5,0.75,0); upper =(22,1.25,3);
Material
absorb 0.3; scattering 1.0;
end

Parallelepiped
lower =(23,0.75,0); upper =(23.5,1.25,3);
Material
absorb 0.3; scattering 1.0;
end
```

```

Parallelepiped
lower =(24.5,0.75,0); upper =(25,1.25,3);
Material
absorb 0.3; scattering 1.0;
end

Parallelepiped
lower =(26,0.75,0); upper =(26.5,1.25,3);
Material
absorb 0.3; scattering 1.0;
end

Parallelepiped
lower =(27.5,0.75,0); upper =(28,1.25,3);
Material
absorb 0.3; scattering 1.0;
end

Parallelepiped
lower =(29,0.75,0); upper =(29.5,1.25,3);
Material
absorb 0.3; scattering 1.0;
end

/* Second Series of obstacles along the room */

Parallelepiped
lower =(0.5,2.75,0); upper =(1,3.25,3);
Material
absorb 0.3; scattering 1.0;
end

Parallelepiped
lower =(2,2.75,0); upper =(2.5,3.25,3);
Material
absorb 0.3; scattering 1.0;
end

Parallelepiped
lower =(3.5,2.75,0); upper =(4,3.25,3);
Material
absorb 0.3; scattering 1.0;
end

Parallelepiped
lower =(5,2.75,0); upper =(5.5,3.25,3);
Material
absorb 0.3; scattering 1.0;
end

Parallelepiped
lower =(6.5,2.75,0); upper =(7,3.25,3);
Material
absorb 0.3; scattering 1.0;
end

Parallelepiped
lower =(8,2.75,0); upper =(8.5,3.25,3);
Material
absorb 0.3; scattering 1.0;
end

Parallelepiped
lower =(9.5,2.75,0); upper =(10,3.25,3);
Material
absorb 0.3; scattering 1.0;
end

Parallelepiped

```

```
lower =(11,2.75,0); upper =(11.5,3.25,3);  
Material  
absorb 0.3; scattering 1.0;  
end
```

```
Parallelepiped  
lower =(12.5,2.75,0); upper =(13,3.25,3);  
Material  
absorb 0.3; scattering 1.0;  
end
```

```
Parallelepiped  
lower =(14,2.75,0); upper =(14.5,3.25,3);  
Material  
absorb 0.3; scattering 1.0;  
end
```

```
Parallelepiped  
lower =(15.5,2.75,0); upper =(16,3.25,3);  
Material  
absorb 0.3; scattering 1.0;  
end
```

```
Parallelepiped  
lower =(17,2.75,0); upper =(17.5,3.25,3);  
Material  
absorb 0.3; scattering 1.0;  
end
```

```
Parallelepiped  
lower =(18.5,2.75,0); upper =(19,3.25,3);  
Material  
absorb 0.3; scattering 1.0;  
end
```

```
Parallelepiped  
lower =(20,2.75,0); upper =(20.5,3.25,3);  
Material  
absorb 0.3; scattering 1.0;  
end
```

```
Parallelepiped  
lower =(21.5,2.75,0); upper =(22,3.25,3);  
Material  
absorb 0.3; scattering 1.0;  
end
```

```
Parallelepiped  
lower =(23,2.75,0); upper =(23.5,3.25,3);  
Material  
absorb 0.3; scattering 1.0;  
end
```

```
Parallelepiped  
lower =(24.5,2.75,0); upper =(25,3.25,3);  
Material  
absorb 0.3; scattering 1.0;  
end
```

```
Parallelepiped  
lower =(26,2.75,0); upper =(26.5,3.25,3);  
Material  
absorb 0.3; scattering 1.0;  
end
```

```
Parallelepiped  
lower =(27.5,2.75,0); upper =(28,3.25,3);  
Material  
absorb 0.3; scattering 1.0;  
end
```

```

Parallelepiped
lower =(29,2.75,0); upper =(29.5,3.25,3);
Material
absorb 0.3; scattering 1.0;
end

/* Third Series of obstacles along the room */

Parallelepiped
lower =(0.5,4.75,0); upper =(1,5.25,3);
Material
absorb 0.3; scattering 1.0;
end

Parallelepiped
lower =(2,4.75,0); upper =(2.5,5.25,3);
Material
absorb 0.3; scattering 1.0;
end

Parallelepiped
lower =(3.5,4.75,0); upper =(4,5.25,3);
Material
absorb 0.3; scattering 1.0;
end

Parallelepiped
lower =(5,4.75,0); upper =(5.5,5.25,3);
Material
absorb 0.3; scattering 1.0;
end

Parallelepiped
lower =(6.5,4.75,0); upper =(7,5.25,3);
Material
absorb 0.3; scattering 1.0;
end

Parallelepiped
lower =(8,4.75,0); upper =(8.5,5.25,3);
Material
absorb 0.3; scattering 1.0;
end

Parallelepiped
lower =(9.5,4.75,0); upper =(10,5.25,3);
Material
absorb 0.3; scattering 1.0;
end

Parallelepiped
lower =(11,4.75,0); upper =(11.5,5.25,3);
Material
absorb 0.3; scattering 1.0;
end

Parallelepiped
lower =(12.5,4.75,0); upper =(13,5.25,3);
Material
absorb 0.3; scattering 1.0;
end

Parallelepiped
lower =(14,4.75,0); upper =(14.5,5.25,3);
Material
absorb 0.3; scattering 1.0;
end

Parallelepiped

```

```
lower =(15.5,4.75,0); upper =(16,5.25,3);  
Material  
absorb 0.3; scattering 1.0;  
end
```

```
Parallelepiped  
lower =(17,4.75,0); upper =(17.5,5.25,3);  
Material  
absorb 0.3; scattering 1.0;  
end
```

```
Parallelepiped  
lower =(18.5,4.75,0); upper =(19,5.25,3);  
Material  
absorb 0.3; scattering 1.0;  
end
```

```
Parallelepiped  
lower =(20,4.75,0); upper =(20.5,5.25,3);  
Material  
absorb 0.3; scattering 1.0;  
end
```

```
Parallelepiped  
lower =(21.5,4.75,0); upper =(22,5.25,3);  
Material  
absorb 0.3; scattering 1.0;  
end
```

```
Parallelepiped  
lower =(23,4.75,0); upper =(23.5,5.25,3);  
Material  
absorb 0.3; scattering 1.0;  
end
```

```
Parallelepiped  
lower =(24.5,4.75,0); upper =(25,5.25,3);  
Material  
absorb 0.3; scattering 1.0;  
end
```

```
Parallelepiped  
lower =(26,4.75,0); upper =(26.5,5.25,3);  
Material  
absorb 0.3; scattering 1.0;  
end
```

```
Parallelepiped  
lower =(27.5,4.75,0); upper =(28,5.25,3);  
Material  
absorb 0.3; scattering 1.0;  
end
```

```
Parallelepiped  
lower =(29,4.75,0); upper =(29.5,5.25,3);  
Material  
absorb 0.3; scattering 1.0;  
end
```

Table 5: Corridor case, Measured Reverberation Times in seconds.

Frequency (Hz)	125	250	500	1000	2000	4000	8000
1	1.0	0.9	1.0	0.8	0.6	0.6	0.5
2	0.8	0.7	0.9	0.8	0.7	0.7	0.5
3	1.4	1.2	1.0	0.7	0.8	0.7	0.6
4	1.4	1.3	1.0	0.9	0.9	0.8	0.7
5	2.0	1.4	1.1	1.0	0.8	0.7	0.7

Table 6: Corridor case, Predicted Reverberation Times in seconds.

Frequency (Hz)	125	250	500	1000	2000	4000	8000
1	1.1	1.0	0.9	1.0	0.8	0.8	0.6
2	1.0	1.2	1.1	0.9	0.8	0.7	0.6
3	1.0	1.3	1.0	1.0	0.9	0.8	0.7
4	1.1	1.1	1.2	1.1	1.1	1.0	0.7
5	1.2	1.2	1.4	1.1	1.0	0.9	0.7

Table 7: Corridor case, Comparison between Predicted and measured Reverberation.

Frequency (Hz)	125	250	500	1000	2000	4000	8000
1	-0.1	0.1	0.1	-0.2	-0.2	-0.2	-0.1
2	-0.2	-0.5	-0.2	-0.1	-0.1	0.0	-0.1
3	0.4	-0.1	0.0	-0.3	-0.1	-0.1	-0.1
4	0.3	0.3	-0.2	-0.2	-0.2	-0.2	0.0
5	0.8	-0.1	-0.3	-0.1	-0.2	-0.2	0.0

**Table 8: Auditorium case, listing of the
CADAЕ data input file.**

```
NRAYS =36000
TEMPERATURE =20
HUMIDITY =0.3

SOURCE
location =(2,0,1)
orientation =(2,4,0.5)
PWL =100
end

/* Receiver Positions */
Receiver
location =(20,0,4)
Material
receiver_number =1
end

/* Geometry and Materials */
Polygon
vertex =(6,-8,0); vertex =(6,8,0); vertex =(0,5,0); vertex =(0,-5,0)
Material
absorb_20
end

Polygon
vertex =(6,-8,0); vertex =(22,-8,2.5); vertex =(22,8,2.5); vertex =(6,8,0)
Material
absorb_20
end

Polygon
vertex =(0,-5,7.5); vertex =(0,5,7.5); vertex =(0,5,0); vertex =(0,-5,0)
Material
absorb_20
end

Polygon
vertex =(0,5,0); vertex =(0,5,7.5); vertex =(6,8,10); vertex =(6,8,0)
Material
absorb_20
end

Polygon
vertex =(6,8,0); vertex =(22,8,2.5); vertex =(22,8,10); vertex =(6,8,10)
Material
absorb_20
end

Polygon
vertex =(0,-5,0); vertex =(0,-5,7.5); vertex =(6,-8,10); vertex =(6,-8,0)
Material
absorb_20
end

Polygon
vertex =(6,-8,0); vertex =(22,-8,2.5); vertex =(22,-8,10); vertex =(6,-8,10)
Material
absorb_20
```

end

```
Polygon  
vertex =(22,-8,2.5); vertex =(22,-8,10); vertex =(22,8,10); vertex =(22,8,2)  
Material  
absorb_20  
end
```

```
Polygon  
vertex =(6,-8,10); vertex =(6,8,10); vertex =(0,5,7.5); vertex =(0,-5,7.5)  
Material  
absorb_20  
end
```

```
Polygon  
vertex =(6,-8,10); vertex =(22,-8,10); vertex =(22,8,10); vertex =(6,8,10)  
Material  
absorb_20  
end
```

**Table 9: Auditorium with tilted walls case,
comparison between computer results and
theoretical calculations.**

Frequency (Hz)	Sabine Rev. Time (s)	Eyring Rev. Time (s)	Simulated Rev. Time (s)	Theoretical SPL (dB)	Simulated SPL (dB)
125	1.9	1.7	1.8	81.4	81.6
250	1.9	1.7	1.7	81.4	81.6
500	1.8	1.6	1.7	81.4	81.5
1000	1.8	1.6	1.7	81.4	81.4
2000	1.7	1.5	1.6	81.4	81.2
4000	1.4	1.3	1.3	81.4	80.3

**Table 10: Cylindrical boundary case, CADAЕ
data input file.**

```
NRAYS =32000
TEMPERATURE =20
HUMIDITY =0.3

Source
location =(0,0,1)
orientation =(0,0,0)
PWL =100
end

/* Receiver Positions */

/* 19 Receivers are placed at equal distances along the radial axis */

/* Geometry and Sound Absorption for the curved surface application */

Cone
apex =(0,0,10); base =(0,0,0); min_radius 10; max_radius 10
clip_plane
location (0,0,0); normal =(0,0,1)
clip_plane
location =(0,0,10); normal =(0,0,-1)
Material
absorb .1
end

/* Geometry and Sound Absorption for the flat surface application */

Polygon
vertex =(10,0,0); vertex =(10,0,10); vertex =(8.1,5.8,10); vertex=(8.1,5.8,0)
Material
absorb .1
end

Polygon
vertex=(3.1,9.5,0);vertex=(3.1,9.5,10);vertex=(8.1,5.8,10);vertex=(8.1,5.8,0)
Material
absorb .1
end

Polygon
vertex=(3.1,9.5,0);vertex=(3.1,9.5,10);vertex=(3.1,9.5,10);vertex=(3.1,9.5,0)
Material
absorb .1
end

Polygon
vertex=(8.1,5.8,0);vertex=(8.1,5.8,10);vertex=(3.1,9.5,10);vertex=(3.1,9.5,0)
Material
absorb .1
end

Polygon
vertex =(-8.1,5.8,0); vertex=(-8.1,5.8,10);vertex =(-10,0,10);vertex=(10,0,0)
Material
absorb .1
```

end

Polygon

vertex=(-8.1,-5.8,0);vertex=(-8.1,-5.8,10);vertex=(-10,0,10);vertex=(10,0,0)

Material

absorb .1

end

Polygon

vertex=(-8.1,-5.8,0); vertex=(-8.1,-5.8,10); vertex=(-3.1,-9.5,10); vertex=(-3.1,-9.5,0)

Material

absorb .1

end

Polygon

vertex=(3.1,-9.5,0); vertex=(3.1,-9.5,10); vertex=(-3.1,-9.5,10)vertex=(-3.1,-9.5,0)

Material

absorb .1

end

Polygon

vertex=(3.1,-9.5,0); vertex=(3.1,-9.5,10); vertex=(8.1,-5.8,10); vertex=(8.1,-5.8,0)

Material

absorb .1

end

Polygon

vertex=(10,0,0); vertex=(10,0,10); vertex=(8.1,-5.8,10); vertex=(8.1,-5.8,0)

Material

absorb .1

end

Table 11: St. Paul's Cathedral, listing of the
CADAE data input file.

```
NRAYS =160000
TEMPERATURE =17.5
HUMIDITY =0.52

/* Sound Source for the Reverberation Test */
SOURCE
location =(99,27,3)
orientation =(0,0,0)
PWL =100
end

/* Sound Source for the Sound Pressure Level Test */
SOURCE
location =(100,31,.5)
orientation =(0,0,0)
PWL =100
end

/* Sound Source for the Coupled Spaces Test */
SOURCE
location =(120,31,.5)
orientation =(0,0,0)
PWL =100
end

/* Receiver Positions for the SPL Test */
Receiver
location =(90,33,2.5)
receiver_number =1
end

Receiver
location =(84,33,2.5)
receiver_number =2
end

Receiver
location =(78,33,2.5)
receiver_number =3
end

Receiver
location =(70,33,2.5)
receiver_number =4
end

Receiver
location =(60,34,2.5)
receiver_number =5
end

Receiver
location =(48,34,2.5)
Material
receiver_number =6
```

```
end

Receiver
location = (35,34,2.5)
Material
receiver_number =7
end

/* Receiver Positions for the Coupled Spaces Test */
Receiver
location = (110,38,1.5)
Material
receiver_number 1
end

Receiver
location = (85,35,1.5)
Material
receiver_number 2
end

/* Receiver Positions for the Reverberation Test */
Receiver
location = (59,38,1.5)
Material
receiver_number 1
end

Receiver
location = (55,30,1.5)
Material
receiver_number 2
end

Receiver
location = (73,45,1.5)
Material
receiver_number 3
end

Receiver
location = (85,35,1.5)
Material
receiver_number 4
end

Receiver
location = (95,45,1.5)
Material
receiver_number 5
end

Receiver
location = (111,35,1.5)
Material
receiver_number 6
end

Receiver
location = (132,35,1.5)
Material
receiver_number 7
end

Receiver
location = (77,7,1.5)
Material
receiver_number 8
```

```

end

Receiver
location =(57,23,1.5)
Material
receiver_number 9
end

/* Geometry and Materials */

/* Floor */
Plane
normal =(0,0,1); distance =0
Material
marble
end

/* Nave Seats*/
Parallelepiped
lower =(30,29,0); upper =(70,34,0.75)
Material
audience; scattering =1.0
end

Parallelepiped
lower =(30,36,0); upper =(70,41,0.75)
Material
audience; scattering =1.0
end

/* Seats Under the Dome */
Parallelepiped
lower =(72,23,0); upper =(84,34,0.75)
Material
audience; scattering =1.0
end

Parallelepiped
lower =(72,36,0); upper =(84,47,0.75)
Material
audience; scattering =1.0
end

Parallelepiped
lower =(86,23,0); upper =(91,34,0.75)
Material
audience; scattering =1.0
end

Parallelepiped
lower =(86,36,0); upper =(91,47,0.75)
Material
audience; scattering =1.0
end

/*South Trancept Seats*/
Parallelepiped
lower =(79,8,0); upper =(84,20,0.75)
Material
audience; scattering =1.0
end

Parallelepiped
lower =(86,8,0); upper =(91,20,0.75)
Material

```

```

audience; scattering =1.0
end

/*North Trancept Seats*/
Parallelepiped
lower =(79,50,0); upper =(84,62,0.75)
Material
audience; scattering =1.0
end

Parallelepiped
lower =(86,50,0); upper =(91,62,0.75)
Material
audience; scattering =1.0
end

/*Choir Seats*/
Parallelepiped
lower =(100,30,0); upper =(130,33,1.75)
Material
audience; scattering =1.0
end

Parallelepiped
lower =(100,37,0); upper =(130,40,1.75)
Material
audience; scattering =1.0
end

/* Western Wall*/
Polygon
vertex =(7.5,20,0); vertex =(7.5,50,0); vertex =(7.5,50,30); vertex
=(7.5,20,30)
Material
portland_stone
end

Parallelepiped
lower =(5,25,0); upper =(15,32,30)
Material
portland_stone
end

Parallelepiped
lower =(5,38,0); upper =(15,45,30)
Material
portland_stone
end

/* Northern Wall */
Polygon
vertex =(70,70,0); vertex =(70,70,30); vertex =(100,70,30); vertex
=(100,70,0)
Material
portland_stone
end

/* Southern Wall */
Polygon
vertex =(70,0,0); vertex =(70,0,30); vertex =(100,0,30); vertex =(100,0,0)
Material
portland_stone
end

/*North Aisle Wall*/
Parallelepiped

```

```

lower =(0,50,0); upper =(70,60,11.5)
differ_out_cone
apex =(36,50,8.5); base =(36,50,0); min_radius 3; max_radius 3
differ_out_cone
apex =(46.5,50,8.5); base =(46.5,50,0); min_radius 3; max_radius 3
differ_out_cone
apex =(57,50,8.5); base =(57,50,0); min_radius 3; max_radius 3
differ_out_sphere
location =(36,50,8.5); radius 3
differ_out_sphere
location =(46.5,50,8.5); radius 3
differ_out_sphere
location =(57,50,8.5); radius 3
Material
portland_stone
end

Cone
apex =(36,50,8.5); base =(36,50,0); min_radius 3; max_radius 3
differ_in_Parallelepiped
base =(0,50,0); apex =(70,60,11.5)
differ_plane
location =(36,50,6); normal =(0,1,0)
Material
portland_stone
end

Sphere
location =(36,50,8.5); radius 3
differ_in_Parallelepiped
base =(0,50,0); apex =(70,60,11.5)
differ_plane
location =(36,50,8.5); normal =(0,0,1)
differ_plane
location =(36,50,8.5); normal =(0,1,0)
Material
plaster
end

Cone
apex =(46.5,50,8.5); base =(46.5,50,0); min_radius 3; max_radius 3
differ_in_Parallelepiped
base =(0,50,0); apex =(70,60,11.5)
differ_plane
location =(46.5,50,6); normal =(0,1,0)
Material
portland_stone
end

Sphere
location =(46.5,50,8.5); radius 3
differ_in_Parallelepiped
base =(0,50,0); apex =(70,60,11.5)
differ_plane
location =(46.5,50,8.5); normal =(0,0,1)
differ_plane
location =(46.5,50,8.5); normal =(0,1,0)
Material
mosaic
end

Cone
apex =(57,50,8.5); base =(57,50,0); min_radius 3; max_radius 3
differ_in_Parallelepiped
base =(0,50,0); apex =(70,60,11.5)
differ_plane
location =(57,50,6); normal =(0,1,0)
Material
portland_stone
end

```

```

Sphere
location =(57,50,8.5); radius 3
differ_in_Parallelepiped
base =(0,50,0); apex =(70,60,11.5)
differ_plane
location =(57,50,8.5); normal =(0,0,1)
differ_plane
location =(57,50,8.5); normal =(0,1,0)
Material
plaster
end

/*North Aisle*/
Parallelepiped
lower =(0,50,8.5); upper =(70,41,20)
differ_out_cone
apex =(70,47,8.5); base =(0,47,8.5); min_radius 3; max_radius 3
differ_out_cone
apex =(36,50,8.5); base =(36,41,8.5); min_radius 3; max_radius 3
differ_out_cone
apex =(46.5,50,8.5); base =(46.5,41,8.5); min_radius 3; max_radius 3
differ_out_cone
apex =(57,50,8.5); base =(57,41,8.50); min_radius 3; max_radius 3
Material
portland_stone
end

Cone
apex =(70,47,8.5); base =(0,47,8.5); min_radius 3; max_radius 3
differ_in_Parallelepiped
base =(0,50,8.5); apex =(70,41,20)
differ_out_cone
apex =(36,50,8.5); base =(36,41,8.50); min_radius 3; max_radius 3
differ_out_cone
apex =(46.5,50,8.5); base =(46.5,41,8.5); min_radius 3; max_radius 3
differ_out_cone
apex =(57,50,8.5); base =(57,41,8.5); min_radius 3; max_radius 3
differ_plane
location =(35,47,8.5); normal =(0,0,1)
Material
plaster
end

Cone
apex =(36,50,8.5); base =(36,41,8.5); min_radius 3; max_radius 3
differ_in_Parallelepiped
base =(0,50,8.5); apex =(70,41,20)
differ_out_cone
apex =(70,47,8.5); base =(0,47,8.5); min_radius 3; max_radius 3
differ_plane
location =(36,45,8.5); normal =(0,0,1)
Material
mosaic
end

Cone
apex =(46.5,50,8.5); base =(46.5,41,8.5); min_radius 3; max_radius 3
differ_in_Parallelepiped
base =(0,50,8.5); apex =(70,41,20)
differ_out_cone
apex =(70,47,8.5); base =(0,47,8.5); min_radius 3; max_radius 3
differ_plane
location =(46.5,45,8.5); normal =(0,0,1)
Material
plaster
end

Cone

```

```

apex =(57,50,8.5); base =(57,41,8.5); min_radius 3; max_radius 3
differ_in_Parallelepiped
base =(0,50,8.5); apex =(70,41,20)
differ_out_cone
apex =(70,47,8.5); base =(0,47,8.5); min_radius 3; max_radius 3
differ_plane
location =(57,45,8.5); normal =(0,0,1)
Material
plaster
end

/*South Aisle Wall*/
Parallelepiped
lower =(0,10,0); upper =(70,20,11.5)
differ_out_cone
apex =(36,20,8.5); base =(36,20,0); min_radius 3; max_radius 3
differ_out_cone
apex =(46.5,20,8.5); base =(46.5,20,0); min_radius 3; max_radius 3
differ_out_cone
apex =(57,20,8.5); base =(57,20,0); min_radius 3; max_radius 3
differ_out_sphere
location =(36,20,8.5); radius 3
differ_out_sphere
location =(46.5,20,8.5); radius 3
differ_out_sphere
location =(57,20,8.5); radius 3
Material
portland_stone
end

Cone
apex =(36,20,8.5); base =(36,20,0); min_radius 3; max_radius 3
differ_in_Parallelepiped
base =(0,10,0); apex =(70,20,11.5)
differ_plane
location =(36,20,6); normal =(0,-1,0)
Material
portland_stone
end

Sphere
location =(36,20,8.5); radius 3
differ_in_Parallelepiped
base =(0,10,0); apex =(70,20,11.5)
differ_plane
location =(36,20,8.5); normal =(0,0,1)
differ_plane
location =(36,20,8.5); normal =(0,-1,0)
Material
plaster
end

Cone
apex =(46.5,20,8.5); base =(46.5,20,0); min_radius 3; max_radius 3
differ_in_Parallelepiped
base =(0,0,0); apex =(70,20,11.5)
differ_plane
location =(46.5,20,6); normal =(0,-1,0)
Material
portland_stone
end

Sphere
location =(46.5,20,8.5); radius 3
differ_in_Parallelepiped
base =(0,0,0); apex =(70,20,11.5)
differ_plane
location =(46.5,20,8.5); normal =(0,0,1)
differ_plane

```

```

location =(46.5,20,8.5); normal =(0,-1,0)
Material
plaster
end

Cone
apex =(57,20,8.5); base =(57,20,0; min_radius 3; max_radius 3
differ_in_Parallelepiped
base =(0,0,0); apex =(70,20,11.5)
differ_plane
location =(57,20,6); normal =(0,-1,0)
Material
portland_stone
end

Sphere
location =(57,20,8.5); radius 3
differ_in_Parallelepiped
base =(0,0,0); apex =(70,20,11.5)
differ_plane
location =(57,20,8.5); normal =(0,0,1)
differ_plane
location =(57,20,8.5); normal =(0,-1,0)
Material
plaster
end

/*South Aisle*/
Parallelepiped
lower =(0,20,8.5); upper =(70,29,20)
differ_out_cone
apex =(70,23,8.5); base =(0,23,8.5); min_radius 3; max_radius 3
differ_out_cone
apex =(36,29,8.5); base =(36,20,8.5); min_radius 3; max_radius 3
differ_out_cone
apex =(46.5,29,8.5); base =(46.5,20,8.5); min_radius 3; max_radius 3
differ_out_cone
apex =(57,29,8.5); base =(57,20,8.5); min_radius 3; max_radius 3
Material
portland_stone
end

Cone
apex =(70,23,8.5); base =(0,23,8.5); min_radius 3; max_radius 3
differ_in_Parallelepiped
base =(0,20,8.5); apex =(70,29,20)
differ_out_cone
apex =(36,29,8.5); base =(36,20,8.5); min_radius 3; max_radius 3
differ_out_cone
apex =(46.5,29,8.5); base =(46.5,20,8.5); min_radius 3; max_radius 3
differ_out_cone
apex =(57,29,8.5); base =(57,20,8.5); min_radius 3; max_radius 3
differ_plane
location =(35,23,8.5); normal =(0,0,1)
Material
plaster
end

Cone
apex =(36,29,8.5); base =(36,20,8.5); min_radius 3; max_radius 3
differ_in_Parallelepiped
base =(0,20,8.5); apex =(70,29,20)
differ_out_cone
apex =(70,23,8.5); base =(0,23,8.5); min_radius 3; max_radius 3
differ_plane
location =(36,23,8.5); normal =(0,0,1)
Material
plaster
end

```

```

Cone
apex =(46.5,29,8.5); base =(46.5,20,8.5); min_radius 3; max_radius 3
differ_in_Parallelepiped
base =(0,20,8.5); apex =(70,29,20)
differ_out_cone
apex =(70,23,8.5); base =(0,23,8.5); min_radius 3; max_radius 3
differ_plane
location =(46.5,23,8.5); normal =(0,0,1)
Material
plaster
end

```

```

Cone
apex =(57,29,8.5); base =(57,20,8.5); min_radius 3; max_radius 3
differ_in_Parallelepiped
base =(0,20,8.5); apex =(70,29,20)
differ_out_cone
apex =(70,23,8.5); base =(0,23,8.5); min_radius 3; max_radius 3
differ_plane
location =(57,23,8.5); normal =(0,0,1)
Material
plaster
end

```

```

/*Under the DOME*/
/* North & South Trancept, Nave & Chancel */
Parallelepiped
lower =(0,0,20); upper =(155,70,29)
differ_out_sphere
location =(85,35,20); radius = 17
differ_out_cone
apex =(85,70,20); base =(85,0,20); min_radius 6; max_radius 6
differ_out_cone
apex =(155,35,20); base =(0,35,20); min_radius 6; max_radius 6
differ_out_cone
apex =(85,35,51); base =(85,35,29);min_radius 14; max_radius 17
differ_out_sphere
location =(85,35,51); radius 14
differ_out_cone
apex =(85,35,80); base =(85,35,63); min_radius 3; max_radius 10
differ_out_sphere
location =(85,35,80); radius 3
Material
portland_stone
end

```

```

/* Under the Whispering Gallery*/
Sphere
location =(85,35,20); radius = 17,
differ_in_Parallelepiped
base =(0,0,20); apex =(155,70,29)
differ_out_cone
apex =(85,70,20); base =(85,0,20); min_radius 6; max_radius 6
differ_out_cone
apex =(155,35,20); base =(0,35,20); min_radius 6; max_radius 6
differ_plane
location =(85,35,20); normal =(0,0,1)
differ_plane
location =(85,35,29); normal =(0,0,-1)
Material
mosaic
end

```

```

/*North & South Trancept */
Cone
apex =(85,70,20); base =(85,0,20); min_radius 6; max_radius 6
differ_in_Parallelepiped

```

```

base =(0,0,20); apex =(155,70,29)
differ_out_sphere
location = =(85,35,20); radius = 17
differ_plane
location =(85,35,20); normal =(0,0,1)
Material
plaster
end

/* Nave and Chancel */
Cone
apex =(155,35,20); base =(0,35,20); min_radius 6; max_radius 6
differ_in_Parallelepiped
base =(0,0,20); apex =(155,70,29)
differ_out_sphere
location = =(85,35,20); radius = 17
differ_plane
location =(85,35,20); normal =(0,0,1)
Material
mosaic
end

/* Dome from the whispering gallery and upwards */
Ring
location =(85,35,29); normal =(0,0,1); max_radius 16; min_radius 14
Material
portland_stone
end

Cone
apex =(85,35,51); base =(85,35,29); min_radius 14; max_radius 16
differ_plane
location (85,35,51); normal =(0,0,-1)
differ_plane
location =(85,35,29); normal =(0,0,1)
Material
portland_stone
end

Quadratic
location =(85,35,65); A=1, B=1, C=0, D=0, E=14,
xmin =-100, xmax =100,
ymin =-100, ymax =100,
zmin =-14, zmax =0
differ_plane
location =(85,35,64.5); normal =(0,0,-1)
Material
plaster
end

Cone
apex 85 35 80; base 85 35 63; min_radius 3; max_radius 10
differ_plane
location 85 35 63; normal 0 0 1
Material
portland_stone
end

Sphere
location 85 35 80; radius 3
differ_plane
location 85 35 80; normal 0 0 1
Material
mosaic
end

/*North Trancept West Aisle Wall*/

```

```

Parallelepiped
lower =(67,50,0); upper =(70,70,11.5)
differ_out_cone
apex =(70,64,8.5); base =(70,64,0); min_radius 3; max_radius 3
differ_out_sphere
location =(70,64,8.5); radius 3
Material
portland_stone
end

Cone
apex =(70,64,8.5); base =(70,64,0); min_radius 3; max_radius 3
differ_in_Parallelepiped
base =(67,50,0); apex =(70,70,11.5)
differ_plane
location =(70,64,6); normal =(-1,0,0)
Material
portland_stone
end

Sphere
location =(70,64,8.5); radius 3
differ_in_Parallelepiped
base =(67,50,0); apex =(70,70,11.5)
differ_plane
location =(70,64,8.5); normal =(0,0,1)
differ_plane
location =(70,64,8.5); normal =(-1,0,0)
Material
plaster
end

/*North Trancept West Aisle*/
Parallelepiped
lower =(70,50,8.5); upper =(79,70,20)
differ_out_cone
apex =(73,70,8.5); base =(73,50,8.5); min_radius 3; max_radius 3
differ_out_cone
apex =(79,64,8.5); base =(70,64,8.5); min_radius 3; max_radius 3
Material
portland_stone
end

Cone
apex =(73,70,8.5); base =(73,50,8.5); min_radius 3; max_radius 3
differ_in_Parallelepiped
base =(70,50,8.5); apex =(79,70,20)
differ_out_cone
apex =(79,64,8.5); base =(70,64,8.5); min_radius 3; max_radius 3
differ_plane
location =(73,60,8.5); normal =(0,0,1)
Material
mosaic
end

Cone
apex =(79,64,8.5); base =(70,64,8.5); min_radius 3; max_radius 3
differ_in_Parallelepiped
base =(70,50,8.5); apex =(79,70,20)
differ_out_cone
apex =(73,70,8.5); base =(73,50,8.5); min_radius 3; max_radius 3
differ_plane
location =(75,64,8.5); normal =(0,0,1)
Material
mosaic
end

/*North Trancept East Aisle Wall*/

```

```

Parallelepiped
lower =(100,50,0); upper =(103,70,11.5)
differ_out_cone
apex =(100,64,8.5); base =(100,64,0); min_radius 3; max_radius 3
differ_out_sphere
location =(100,64,8.5); radius 3
Material
portland_stone
end

```

```

Cone
apex =(100,64,8.5); base =(100,64,0); min_radius 3; max_radius 3
differ_in_Parallelepiped
base =(100,50,0); apex =(103,70,11.5)
differ_plane
location =(100,64,6); normal =(1,0,0)
Material
portland_stone
end

```

```

Sphere
location =(100,64,8.5); radius 3
differ_in_Parallelepiped
base =(100,50,0); apex =(103,70,11.5)
differ_plane
location =(100,64,8.5); normal =(0,0,1)
differ_plane
location =(100,64,8.5); normal =(1,0,0)
Material
plaster
end

```

/*North Trancept East Aisle*/

```

Parallelepiped
lower =(91,50,8.5); upper =(100,70,20)
differ_out_cone
apex =(97,70,8.5); base =(97,50,8.5); min_radius 3; max_radius 3
differ_out_cone
apex =(100,64,8.5); base =(91,64,8.5); min_radius 3; max_radius 3
Material
portland_stone
end

```

```

Cone
apex =(97,70,8.5); base =(97,50,8.5); min_radius 3; max_radius 3
differ_in_Parallelepiped
base =(91,50,8.5); apex =(100,70,20)
differ_out_cone
apex =(100,64,8.5); base =(91,64,8.5); min_radius 3; max_radius 3
differ_plane
location =(97,60,8.5); normal =(0,0,1)
Material
mosaic
end

```

```

Cone
apex =(100,64,8.5); base =(91,64,8.5); min_radius 3; max_radius 3
differ_in_Parallelepiped
base =(91,50,8.5); apex =(100,70,20)
differ_out_cone
apex =(97,70,8.5); base =(97,50,8.5); min_radius 3; max_radius 3
differ_plane
location =(95,64,8.5); normal =(0,0,1)
Material
mosaic
end

```

/*South Trancept West Aisle Wall*/

```

Parallelepiped
lower =(67,0,0); upper =(70,20,11.5)
differ_out_cone
apex =(70,6,8.5); base =(70,6,0); min_radius 3; max_radius 3
differ_out_sphere
location =(70,6,8.5); radius 3
Material
portland_stone
end

Cone
apex =(70,6,8.5); base =(70,6,0); min_radius 3; max_radius 3
differ_in_Parallelepiped
base =(67,0,0); apex =(70,20,11.5)
differ_plane
location =(70,6,6); normal =(-1,0,0)
Material
portland_stone
end

Sphere
location =(70,6,8.5); radius 3
differ_in_Parallelepiped
base =(67,0,0); apex =(70,20,11.5)
differ_plane
location =(70,6,8.5); normal =(0,0,1)
differ_plane
location =(70,6,8.5); normal =(-1,0,0)
Material
plaster
end

/*South Trancept West Aisle*/
Parallelepiped
lower =(70,0,8.5); upper =(79,20,20)
differ_out_cone
apex =(73,20,8.5); base =(73,0,8.5); min_radius 3; max_radius 3
differ_out_cone
apex =(79,6,8.5); base =(70,6,8.5); min_radius 3; max_radius 3
Material
portland_stone
end

Cone
apex =(73,20,8.5); base =(73,0,8.5); min_radius 3; max_radius 3
differ_in_Parallelepiped
base =(70,0,8.5); apex =(79,20,20)
differ_out_cone
apex =(79,6,8.5); base =(70,6,8.5); min_radius 3; max_radius 3
differ_plane
location =(73,10,8.5); normal =(0,0,1)
Material
mosaic
end

Cone
apex =(79,6,8.5); base =(70,6,8.5); min_radius 3; max_radius 3
differ_in_Parallelepiped
base =(70,0,8.5); apex =(79,20,20)
differ_out_cone
apex =(73,20,8.5); base =(73,0,8.5); min_radius 3; max_radius 3
differ_plane
location =(75,6,8.5); normal =(0,0,1)
Material
mosaic
end

/*South Trancept East Aisle Wall*/

```

```

Parallelepiped
lower =(100,0,0); upper =(103,20,11.5)
differ_out_cone
apex =(100,6,8.5); base =(100,6,0); min_radius 3; max_radius 3
differ_out_sphere
location =(100,6,8.5); radius 3
Material
portland_stone
end

Cone
apex =(100,6,8.5); base =(100,6,0); min_radius 3; max_radius 3
differ_in_Parallelepiped
base =(100,0,0); apex =(103,20,11.5)
differ_plane
location =(100,6,6); normal =(1,0,0)
Material
portland_stone
end

Sphere
location =(100,6,8.5); radius 3
differ_in_Parallelepiped
base =(100,0,0); apex =(103,20,11.5)
differ_plane
location =(100,6,8.5); normal =(0,0,1)
differ_plane
location =(100,6,8.5); normal =(1,0,0)
Material
plaster
end

/*South Trancept East Aisle*/
Parallelepiped
lower =(91,0,8.5); upper =(100,20,20)
differ_out_cone
apex =(97,20,8.5); base =(97,0,8.5); min_radius 3; max_radius 3
differ_out_cone
apex =(100,6,8.5); base =(91,6,8.5); min_radius 3; max_radius 3
Material
portland_stone
end

Cone
apex =(97,20,8.5); base =(97,0,8.5); min_radius 3; max_radius 3
differ_in_Parallelepiped
base =(91,0,8.5); apex =(100,20,20)
differ_out_cone
apex =(100,6,8.5); base =(91,6,8.5); min_radius 3; max_radius 3
differ_plane
location =(97,60,8.5); normal =(0,0,1)
Material
mosaic
end

Cone
apex =(100,6,8.5); base =(91,6,8.5); min_radius 3; max_radius 3
differ_in_Parallelepiped
base =(91,0,8.5); apex =(100,20,20)
differ_out_cone
apex =(97,20,8.5); base =(97,0,8.5); min_radius 3; max_radius 3
differ_plane
location =(95,6,8.5); normal =(0,0,1)
Material
mosaic
end

/*North Choir Wall*/

```

```

Parallelepiped
lower =(100,50,0); upper =(145,55,11.5)
differ_out_cone
apex =(113,50,8.5); base =(113,50,0); min_radius 3; max_radius 3
differ_out_cone
apex =(123.5,50,8.5); base =(123.5,50,0); min_radius 3; max_radius 3
differ_out_cone
apex =(134,50,8.5); base =(134,50,0); min_radius 3; max_radius 3
differ_out_sphere
location =(113,50,8.5); radius 3
differ_out_sphere
location =(123.5,50,8.5); radius 3
differ_out_sphere
location =(134,50,8.5); radius 3
Material
portland_stone
end

Cone
apex =(113,50,8.5); base =(113,50,0); min_radius 3; max_radius 3
differ_in_Parallelepiped
base =(100,50,0); apex =(145,55,11.5)
differ_plane
location =(113,50,6); normal =(0,1,0)
Material
portland_stone
end

Sphere
location =(113,50,8.5); radius 3
differ_in_Parallelepiped
base =(100,50,0); apex =(145,55,11.5)
differ_plane
location =(113,50,8.5); normal =(0,0,1)
differ_plane
location =(113,50,8.5); normal =(0,1,0)
Material
mosaic
end

Cone
apex =(123.5,50,8.5); base =(123.5,50,0); min_radius 3; max_radius 3
differ_in_Parallelepiped
base =(100,50,0); apex =(145,55,11.5)
differ_plane
location =(123.5,50,6); normal =(0,1,0)
Material
portland_stone
end

Sphere
location =(123.5,50,8.5); radius 3
differ_in_Parallelepiped
base =(100,50,0); apex =(145,55,11.5)
differ_plane
location =(123.5,50,8.5); normal =(0,0,1)
differ_plane
location =(123.5,50,8.5); normal =(0,1,0)
Material
mosaic
end

Cone
apex =(134,50,8.5); base =(134,50,0); min_radius 3; max_radius 3
differ_in_Parallelepiped
base =(100,50,0); apex =(145,55,11.5)
differ_plane
location =(134,50,6); normal =(0,1,0)
Material
portland_stone
end

```

end

```
Sphere
location =(134,50,8.5); radius 3
differ_in_Parallelepiped
base =(100,50,0); apex =(145,55,11.5)
differ_plane
location =(134,50,8.5); normal =(0,0,1)
differ_plane
location =(134,50,8.5); normal =(0,1,0)
Material
mosaic
end
```

/*North Choir Aisle*/

```
Parallelepiped
lower =(100,41,8.5); upper =(145,50,20)
differ_out_cone
apex =(145,47,8.50; base =(100,47,8.5); min_radius 3; max_radius 3
differ_out_cone
apex =(113,50,8.5); base =(113,41,8.5); min_radius 3; max_radius 3
differ_out_cone
apex =(123.5,50,8.5); base =(123.5,41,8.5); min_radius 3; max_radius 3
differ_out_cone
apex =(134,50,8.5); base =(134,41,8.5); min_radius 3; max_radius 3
Material
portland_stone
end
```

```
Cone
apex =(145,47,8.5); base =(100,47,8.5); min_radius 3; max_radius 3
differ_in_Parallelepiped
base =(100,41,8.5); apex =(145,50,20)
differ_out_cone
apex =(113,50,8.5); base =(113,41,8.5); min_radius 3; max_radius 3
differ_out_cone
apex =(123.5,50,8.5); base =(123.5,41,8.5); min_radius 3; max_radius 3
differ_out_cone
apex =(134,50,8.5); base =(134,41,8.5); min_radius 3; max_radius 3
differ_plane
location =(35,47,8.5); normal =(0,0,1)
Material
mosaic
end
```

```
Cone
apex =(113,50,8.5); base =(113,41,8.5); min_radius 3; max_radius 3
differ_in_Parallelepiped
base =(100,41,8.5); apex =(145,50,20)
differ_out_cone
apex =(145,47,8.5); base =(100,47,8.5); min_radius 3; max_radius 3
differ_plane
location =(113,45,8.5); normal =(0,0,1)
Material
mosaic
end
```

```
Cone
apex =(123.5,50,8.5); base =(123.5,41,8.5); min_radius 3; max_radius 3
differ_in_Parallelepiped
base =(100,41,8.5); apex =(145,50,20)
differ_out_cone
apex =(145,47,8.5); base =(100,47,8.5); min_radius 3; max_radius 3
differ_plane
location =(123.5,45,8.5); normal =(0,0,1)
Material
mosaic
end
```

```

Cone
apex =(134,50,8.5); base =(134,41,8.5); min_radius 3; max_radius 3
differ_in_Parallelepiped
base =(100,41,8.5); apex =(145,50,20)
differ_out_cone
apex =(145,47,8.5); base =(100,47,8.5); min_radius 3; max_radius 3
differ_plane
location =(134,45,8.5); normal =(0,0,1)
Material
mosaic
end

/*South Choir Wall*/
Parallelepiped
lower =(100,10,0); upper =(145,20,11.5)
differ_out_cone
apex =(113,20,8.5); base =(113,20,0); min_radius 3; max_radius 3
differ_out_cone
apex =(123.5,20,8.5); base =(123.5,20,0); min_radius 3; max_radius 3
differ_out_cone
apex =(134,20,8.5); base =(134,20,0); min_radius 3; max_radius 3
differ_out_sphere
location =(113,20,8.5); radius 3
differ_out_sphere
location =(123.5,20,8.5); radius 3
differ_out_sphere
location =(134,20,8.5); radius 3
Material
portland_stone
end

Cone
apex =(113,20,8.5); base =(113,20,0); min_radius 3; max_radius 3
differ_in_Parallelepiped
base =(100,10,0); apex =(145,20,11.5)
differ_plane
location =(113,20,6); normal =(0,-1,0)
Material
portland_stone
end

Sphere
location =(113,20,8.5); radius 3
differ_in_Parallelepiped
base =(100,10,0); apex =(145,20,11.5)
differ_plane
location =(113,20,8.5); normal =(0,0,1)
differ_plane
location =(113,20,8.5); normal =(0,-1,0)
Material
mosaic
end

Cone
apex =(123.5,20,8.5); base =(123.5,20,0); min_radius 3; max_radius 3
differ_in_Parallelepiped
base =(100,10,0); apex =(145,20,11.5)
differ_plane
location =(123.5,20,6); normal =(0,-1,0)
Material
portland_stone
end

Sphere
location =(123.5,20,8.5); radius 3
differ_in_Parallelepiped
base =(100,10,0); apex =(145,20,11.5)
differ_plane
location =(123.5,20,8.5); normal =(0,0,1)
differ_plane

```

```

location =(123.5,20,8.5); normal =(0,-1,0)
Material
mosaic
end

Cone
apex =(134,20,8.5); base =(134,20,0); min_radius 3; max_radius 3
differ_in_Parallelepiped
base =(100,10,0); apex =(145,20,11.5)
differ_plane
location =(134,20,6); normal =(0,-1,0)
Material
portland_stone
end

Sphere
location =(134,20,8.5); radius 3
differ_in_Parallelepiped
base =(100,10,0); apex =(145,20,11.5)
differ_plane
location =(134,20,8.5); normal =(0,0,1)
differ_plane
location =(134,20,8.5); normal =(0,-1,0)
Material
mosaic
end

/*South Choir Aisle*/
Parallelepiped
lower =(100,20,8.5); upper =(145,29,20)
differ_out_cone
apex =(145,23,8.5); base =(100,23,8.5); min_radius 3; max_radius 3
differ_out_cone
apex =(113,29,8.5); base =(113,20,8.5); min_radius 3; max_radius 3
differ_out_cone
apex =(123.5,29,8.5); base =(123.5,20,8.5); min_radius 3; max_radius 3
differ_out_cone
apex =(134,29,8.5); base =(134,20,8.5); min_radius 3; max_radius 3
Material
portland_stone
end

Cone
apex =(145,23,8.5); base =(100,23,8.5); min_radius 3; max_radius 3
differ_in_Parallelepiped
base =(100,20,8.5); apex =(145,29,20)
differ_out_cone
apex =(113,29,8.5); base =(113,20,8.5); min_radius 3; max_radius 3
differ_out_cone
apex =(123.5,29,8.5); base =(123.5,20,8.5); min_radius 3; max_radius 3
differ_out_cone
apex =(134,29,8.5); base =(134,20,8.5); min_radius 3; max_radius 3
differ_plane
location =(35,23,8.5); normal =(0,0,1)
Material
mosaic
end

Cone
apex =(113,29,8.5); base =(113,20,8.5); min_radius 3; max_radius 3
differ_in_Parallelepiped
base =(100,20,8.5); apex =(145,29,20)
differ_out_cone
apex =(145,23,8.5); base =(100,23,8.5); min_radius 3; max_radius 3
differ_plane
location =(113,23,8.5); normal =(0,0,1)
Material
mosaic
end

```

```

Cone
apex =(123.5,29,8.5); base =(123.5,20,8.5); min_radius 3; max_radius 3
differ_in_Parallelepiped
base =(100,20,8.5); apex =(145,29,20)
differ_out_cone
apex =(145,23,8.5); base =(100,23,8.5); min_radius 3; max_radius 3
differ_plane
location =(123.5,23,8.5); normal =(0,0,1)
Material
mosaic
end

```

```

Cone
apex =(134,29,8.5); base =(134,20,8.5); min_radius 3; max_radius 3
differ_in_Parallelepiped
base =(100,20,8.5); apex =(145,29,20)
differ_out_cone
apex =(145,23,8.5); base =(100,23,8.5); min_radius 3; max_radius 3
differ_plane
location =(134,23,8.5); normal =(0,0,1)
Material
mosaic
end

```

```

/* APSE*/
Parallelepiped
lower =(145,20,0); upper =(155,50,26)
differ_out_cone
apex =(145,35,20); base =(145,35,0); min_radius 6; max_radius 6
differ_out_sphere
location =(145,35,20); radius 6
Material
portland_stone
end

```

```

Cone
apex =(145,35,20); base =(145,35,0); min_radius 6; max_radius 6
differ_in_Parallelepiped
base =(145,20,0); apex =(155,50,26)
differ_plane
location =(145,35,10); normal =(1,0,0)
Material
portland_stone
end

```

```

Sphere
location =(145,35,20); radius 6
differ_in_Parallelepiped
base =(145,20,0); apex =(155,50,26)
differ_plane
location =(145,35,20); normal =(0,0,1)
differ_plane
location =(145,35,20); normal =(1,0,0)
Material
mosaic
end

```

```

/* Nave Columns */
Parallelepiped
lower =(28,41,0); upper =(33,44,8.5)
Material
Portland_Stone; scattering =1
end

```

```

Parallelepiped
lower =(28,26,0); upper =(33,29,8.5)
Material
Portland_Stone; scattering =1

```

```

end

Parallelepiped
lower =(41,41,0); upper =(43,44,8.5)
Material
Portland_Stone; scattering =1
end

Parallelepiped
lower =(41,26,0); upper =(43,29,8.5)
Material
Portland_Stone; scattering =1
end

Parallelepiped
lower =(51,41,0); upper =(53,44,8.5)
Material
Portland_Stone; scattering =1
end

Parallelepiped
lower =(51,26,0); upper =(53,29,8.5)
Material
Portland_Stone; scattering =1
end

/* Nave Dome Columns */
Parallelepiped
lower =(60,41,0); upper =(70,44,8.5)
Material
Portland_Stone
end

Parallelepiped
lower =(60,26,0); upper =(70,29,8.5)
Material
Portland_Stone
end

/* Chancel Columns */
Parallelepiped
lower =(100,41,0); upper =(140,44,8.5)
Material
wood
end

Parallelepiped
lower =(100,26,0); upper =(140,29,8.5)
Material
wood
end

/* North Transept Dome Columns */
Parallelepiped
lower =(76,50,0); upper =(79,60,8.5)
Material
Portland_Stone
end

Parallelepiped
lower =(76,10,0); upper =(79,20,8.5)
Material
Portland_Stone
end

/* South Transept Dome Columns */
Parallelepiped

```

```
lower =(91,50,0); upper =(94,60,8.5)
Material
Portland_Stone
end
```

```
Parallelepiped
lower =(91,10,0); upper =(94,20,8.5)
Material
Portland_Stone
end
```

Table 12: St. Paul's Cathedral, measured reverberation times in seconds.

Frequency	125	250	500	1000	2000	4000	8000
1	10.4	10.9	11.3	9.8	6.6	3.3	1.6
2	10.7	11.4	11.2	9.8	7.1	3.8	1.4
3	10.6	11.0	10.8	10.5	7.3	4.1	1.6
4	10.1	11.6	11.2	9.8	7.2	3.6	1.4
5	11.3	11.0	11.3	10.0	6.9	3.6	1.6
6	10.1	10.3	10.2	9.5	5.6	3.6	1.0
7	10.9	11.7	11.3	9.7	6.7	3.4	1.4
8	10.1	11.2	10.7	9.7	8.7	4.8	1.6
9	12.4	11.4	10.8	9.7	7.1	4.0	1.5

Table 13: St. Paul's Cathedral, predicted reverberation times in seconds.

Frequency	125	250	500	1000	2000	4000	8000
1	6.8	10.6	11.1	9.5	7.3	3.6	1.7
2	7.1	11.0	11.6	9.7	7.5	3.7	1.7
3	7.5	11.6	11.9	9.8	7.6	3.7	1.7
4	7.3	11.2	12.0	10.0	7.4	4.0	1.8
5	7.9	12.4	12.5	10.2	7.8	3.8	1.7
6	7.4	11.6	11.8	9.8	7.5	3.7	1.7
7	7.9	12.3	12.5	10.2	7.8	3.8	1.7
8	7.5	11.8	12.0	9.9	7.6	3.7	1.6
9	9.0	13.9	13.7	10.9	8.3	4.0	1.7

Table 14: St. Paul's Cathedral, comparison between simulated and measured reverberation times.

Frequency	125	250	500	1000	2000	4000	8000
1	3.6	0.3	0.2	0.3	-0.7	-0.3	-0.1
2	3.6	0.4	-0.4	0.1	-0.4	0.1	-0.3
3	3.1	-0.6	-1.1	0.7	-0.3	0.4	-0.1
4	2.8	0.4	-0.8	-0.2	-0.2	-0.4	-0.4
5	3.4	-1.4	-1.2	-0.2	-0.9	-0.2	-0.1
6	2.7	-1.3	-1.6	-0.3	-1.9	-0.1	-0.7
7	3.0	-0.6	-1.2	-0.5	-1.1	-0.4	-0.3
8	2.6	-0.6	-1.3	-0.2	1.1	1.1	0.0
9	3.4	-2.5	-2.9	-1.2	-1.2	0.0	-0.2

Table 15: St. Paul's Cathedral, Measured sound pressure level in dB.

Frequency (Hz)	125	250	500	1000	2000	4000
1	77.7	76.1	76.3	74.4	74.6	71.5
2	75.5	74.3	73.3	73.3	71.3	67.8
3	73.8	71.5	73.4	73.6	69.8	67.1
4	72.2	71.6	72.2	73.5	68.5	64.7
5	72.1	71.5	71.6	72.6	66.5	62.3
6	72.0	70.4	70.3	71.1	65.6	60.9
7	71.8	69.9	70.2	71.4	65.4	59.8

Table 16: St. Paul's Cathedral, Predicted Sound Pressure Level in dB.

Frequency (Hz)	125	250	500	1000	2000	4000
1	74.4	75.7	75.2	74.2	73.7	70.3
2	74.2	73.6	73.1	73.0	70.4	66.7
3	74.2	73.8	73.4	73.7	70.3	66.1
4	73.3	73.8	73.2	73.0	69.7	65.2
5	72.6	73.4	73.0	72.2	67.8	63.0
6	71.8	72.8	72.9	71.4	66.4	61.1
7	71.1	71.4	72.4	70.8	65.6	60.9

Table 17: St. Paul's Cathedral, comparison between simulated and measured SPL results.

Frequency (Hz)	125	250	500	1000	2000	4000
1	3.3	0.4	1.1	0.2	0.9	1.2
2	1.3	0.7	0.2	0.3	0.9	1.1
3	-0.4	-2.3	0.0	-0.1	-0.5	1.0
4	-1.1	-2.2	-1.0	0.5	-1.2	-0.5
5	-0.5	-1.9	-1.4	0.4	-1.3	-0.7
6	0.2	-2.4	-2.6	-0.3	-0.8	-0.2
7	0.7	-1.5	-2.2	0.6	-0.2	-1.1

A.2. FIGURES

FIGURE 1: SOUND DIVERGENCE, NEAR AND FAR ACOUSTIC FIELDS.

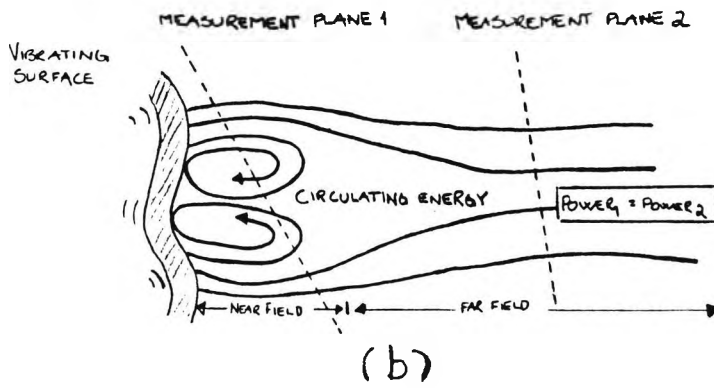
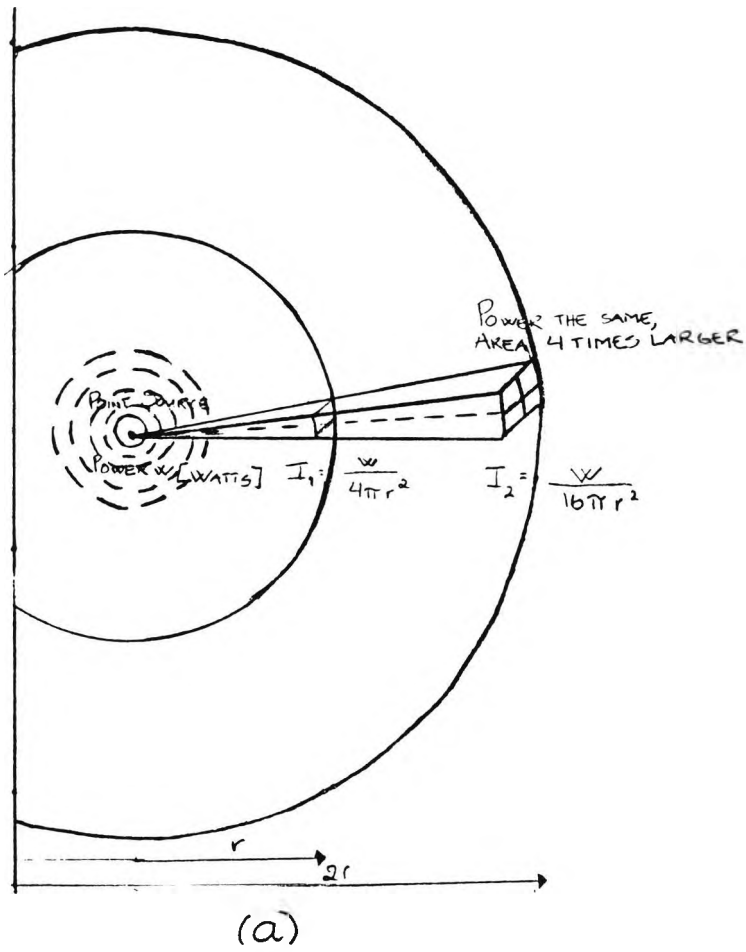


FIGURE 2: SOUND PROPAGATION, REFLECTION, AND SCATTERING²² OF SOUND.

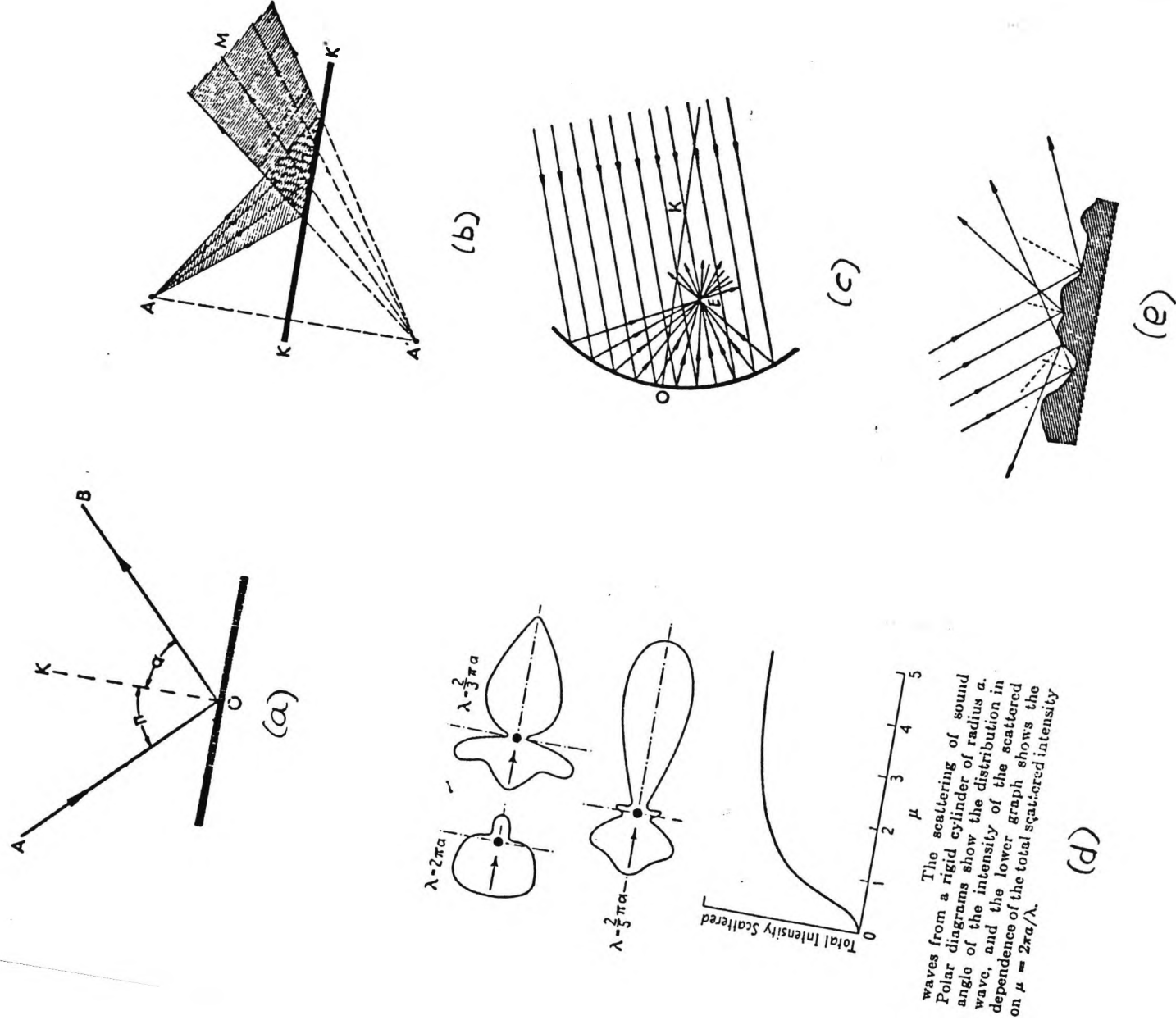


FIGURE 3: STANDING WAVES.

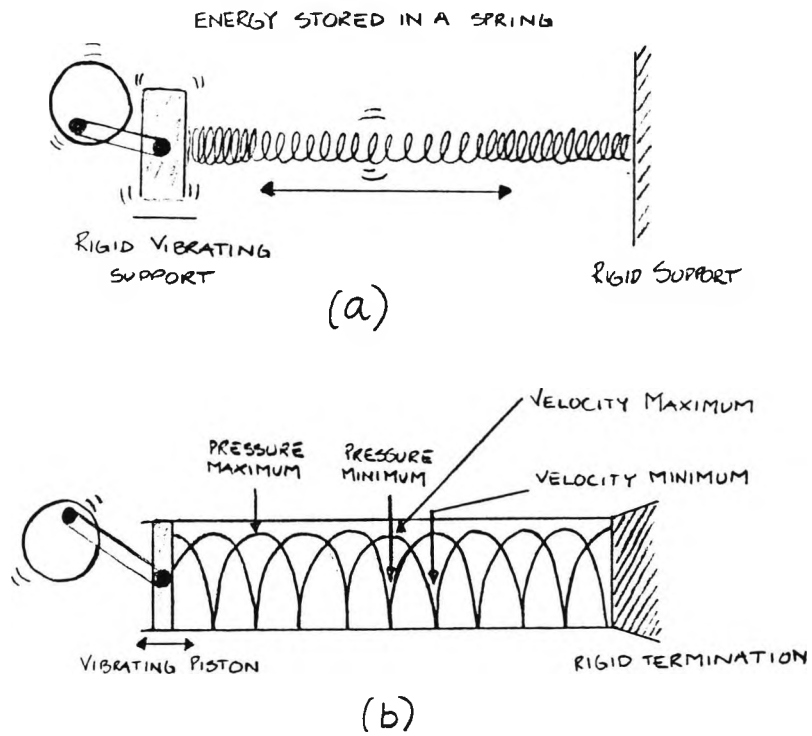


FIGURE 4: DIRECT AND DIFFUSE SOUND FIELDS.

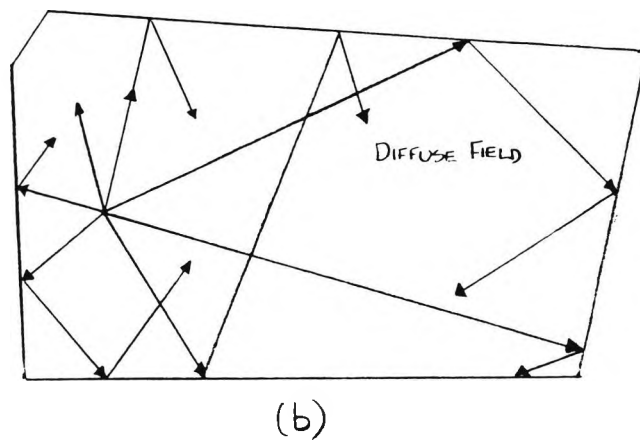
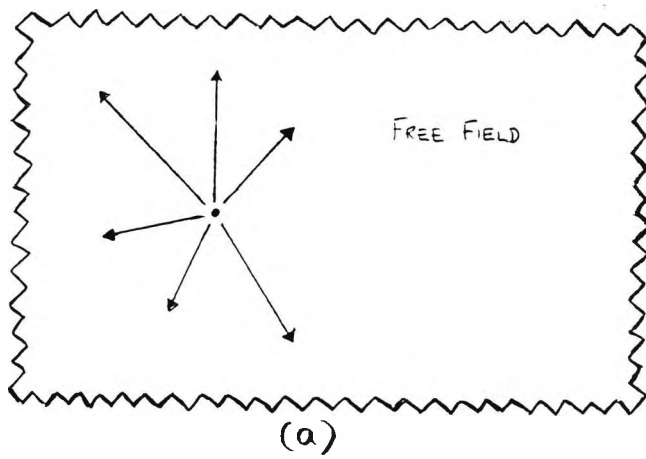


FIGURE 5: IMPULSE RESPONSE, REVERBERATION.

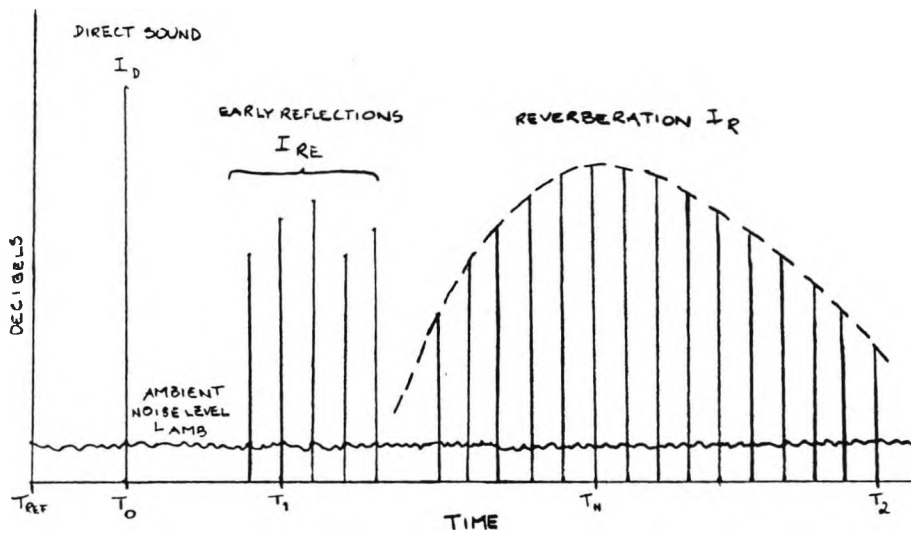


FIGURE 6: WATER WAVE MODELS AND SOUND PULSE PHOTOGRAPHY⁴¹.

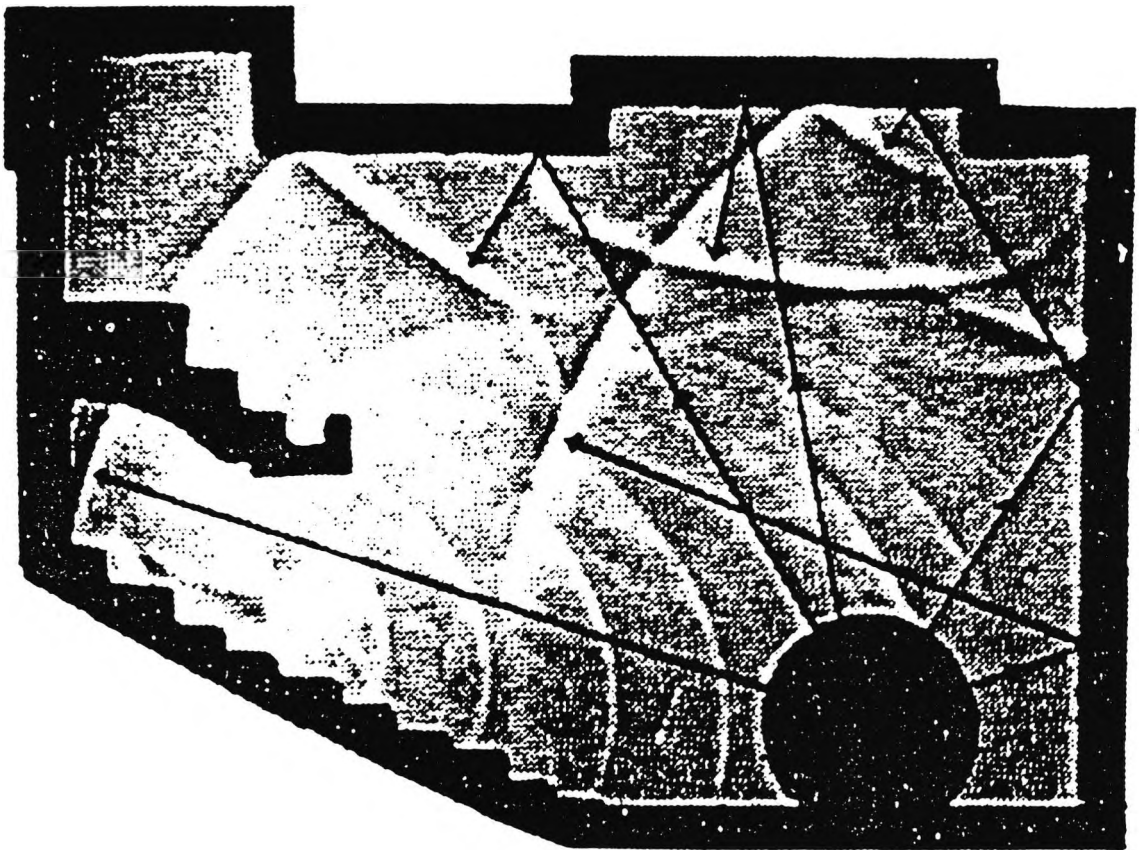
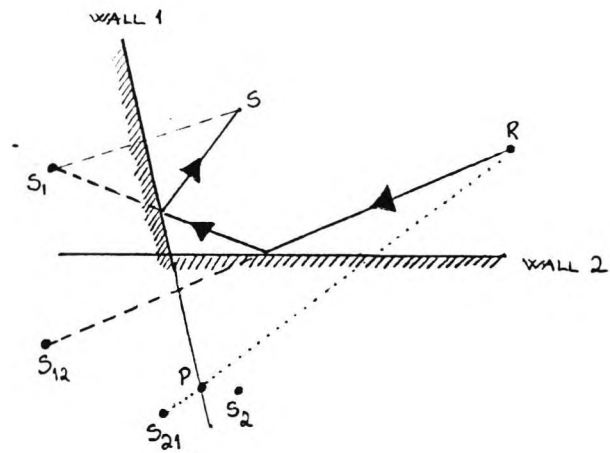


FIGURE 7: THE MIRROR IMAGE SOURCE AND THE RAY TRACING METHODS, SYSTEMATIC ERRORS⁶².

THE IMAGE SOURCE METHOD



THE RAY-TRACING METHOD

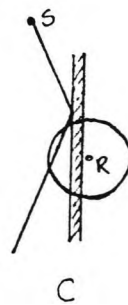
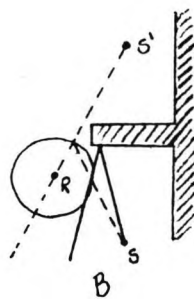
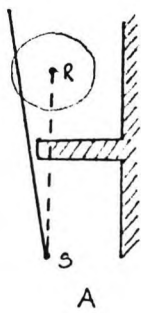
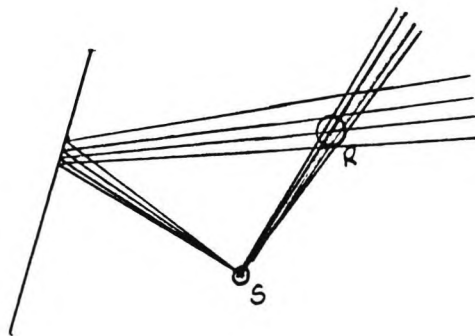
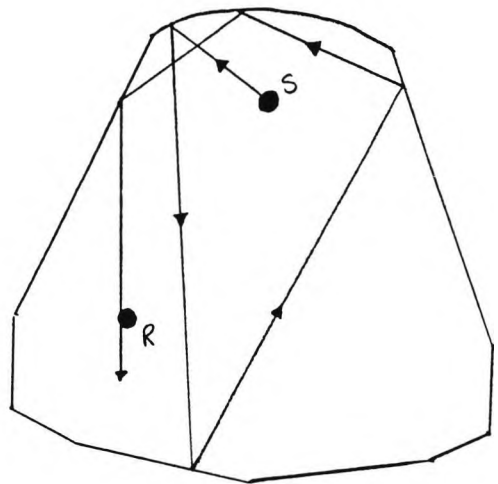
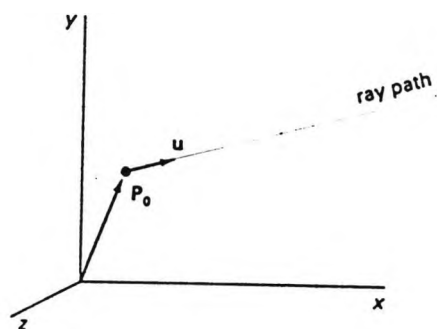


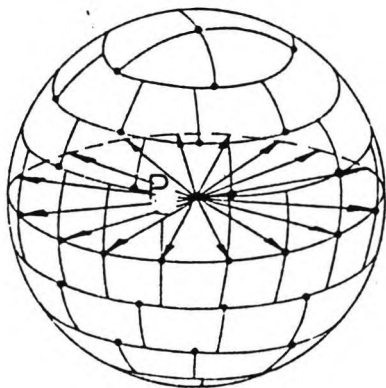
FIGURE 8: THE SOUND SOURCE - SOUND PARTICLE EMISSION METHODS.

(a) The sound source - sound particle emission

$$P = P_0 + tu$$



(b) *Deterministic Method*



(c) *Statistical Method*

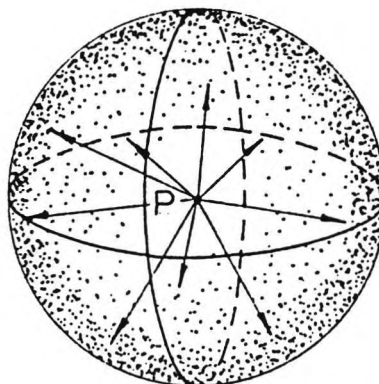


FIGURE 9: CONSTRUCTION OF AN OMNI-DIRECTIONAL SOURCE BY SUBDIVISION OF THE SPHERE SURFACE AREA INTO A NUMBER OF EQUAL AREA SURFACES.

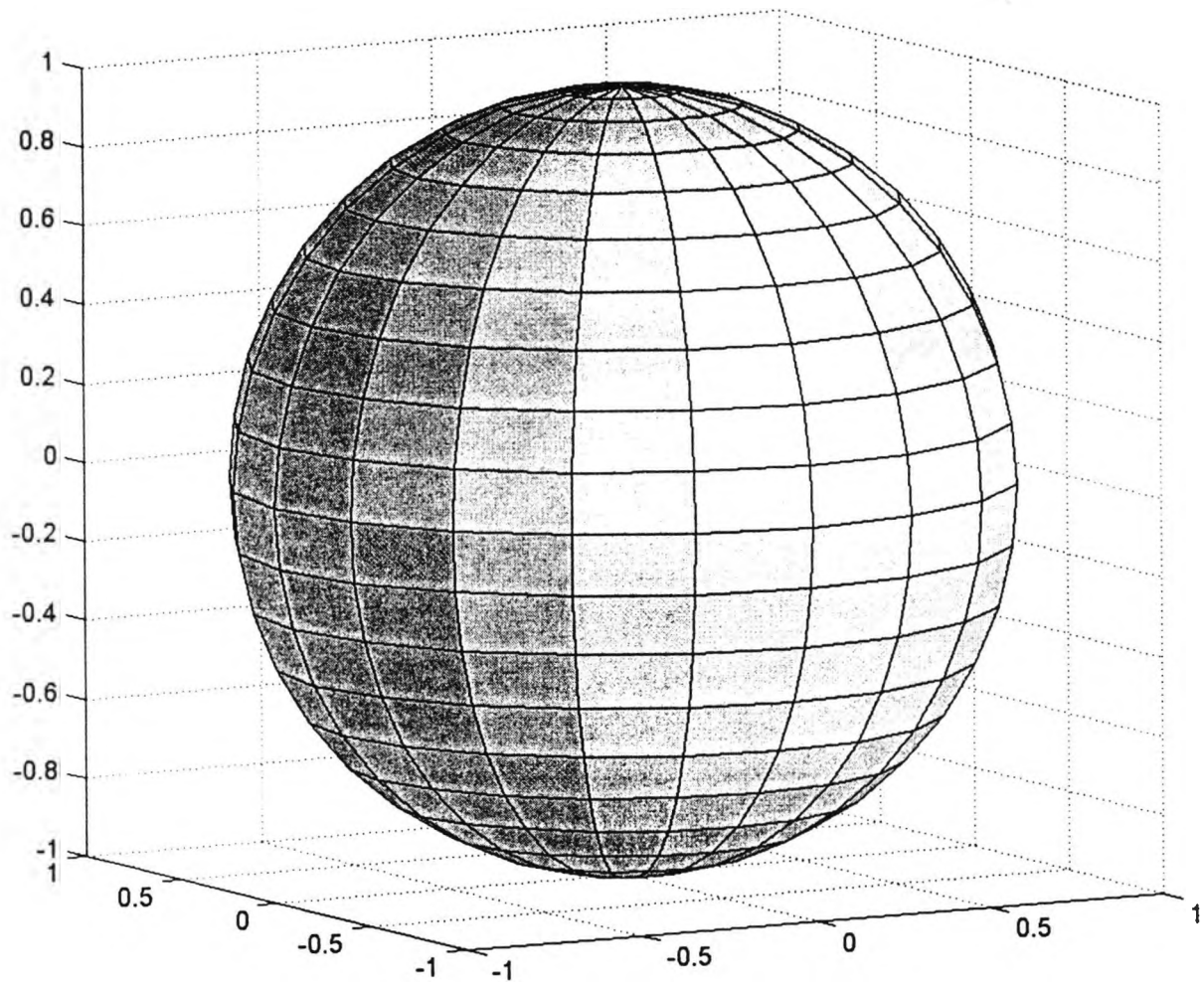
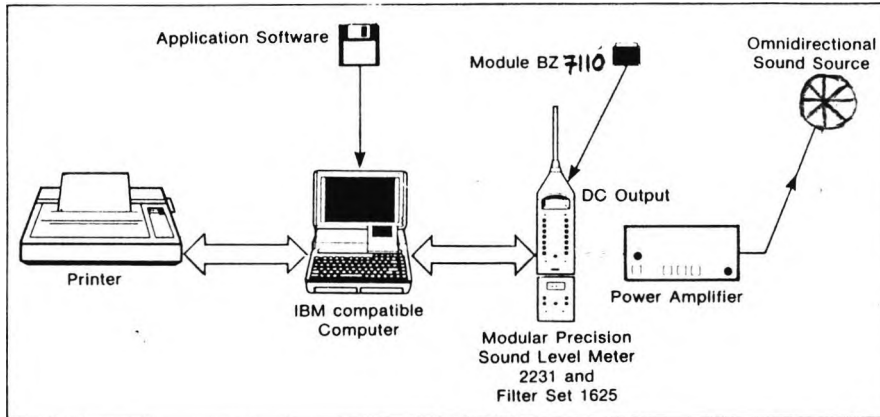
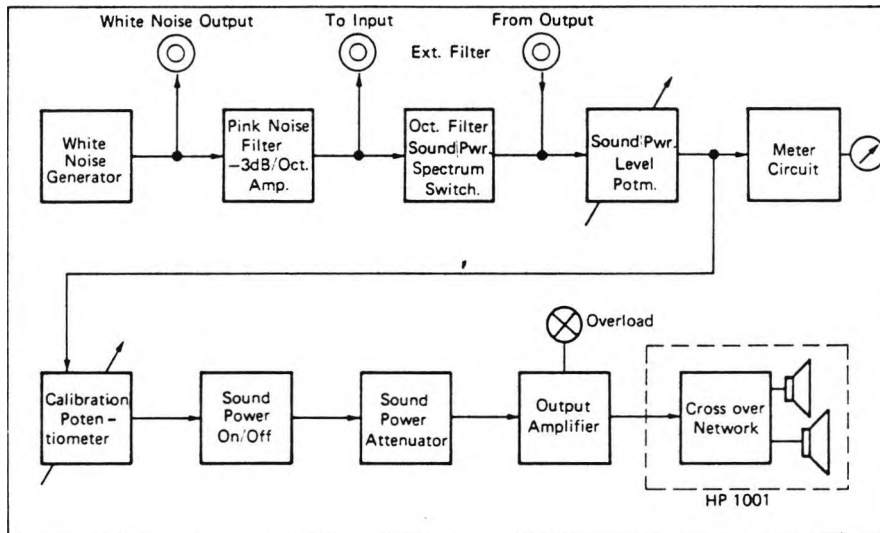


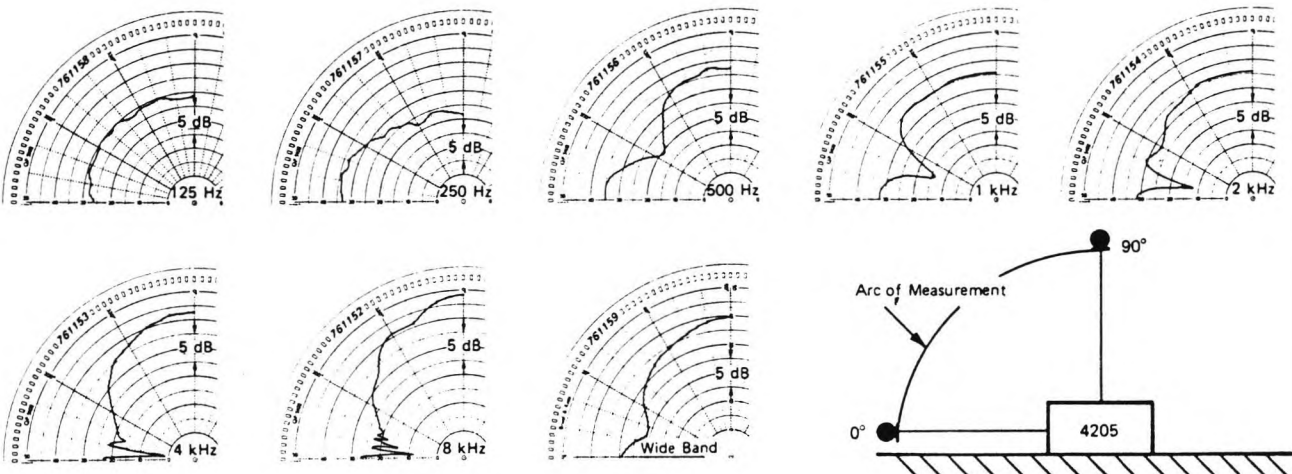
FIGURE 10: APPARATUS USED FOR THE ACOUSTICAL MEASUREMENTS.



(a) Measurement system



(b) Simplified block diagram of Sound Power Source Type 4205



(c) Typical vertical directional characteristics

FIGURE 11: RECTANGULAR ROOM CASE, SOUND PARTICLE SPATIAL DISTRIBUTION, SOURCE AND RECEIVER POSITIONS.

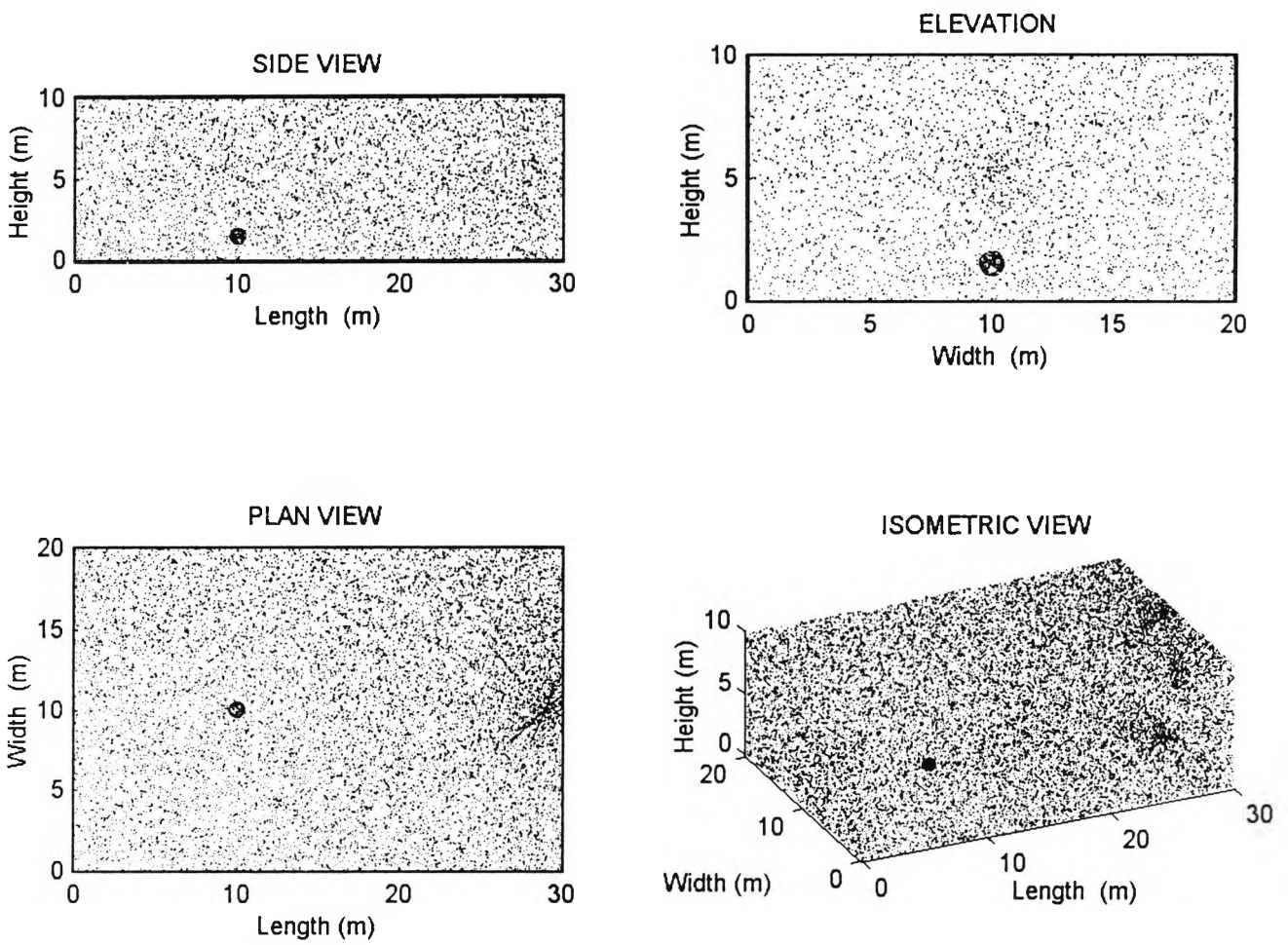


FIGURE 12: RECTANGULAR ROOM CASE, THE DIRECT SOUND FIELD.

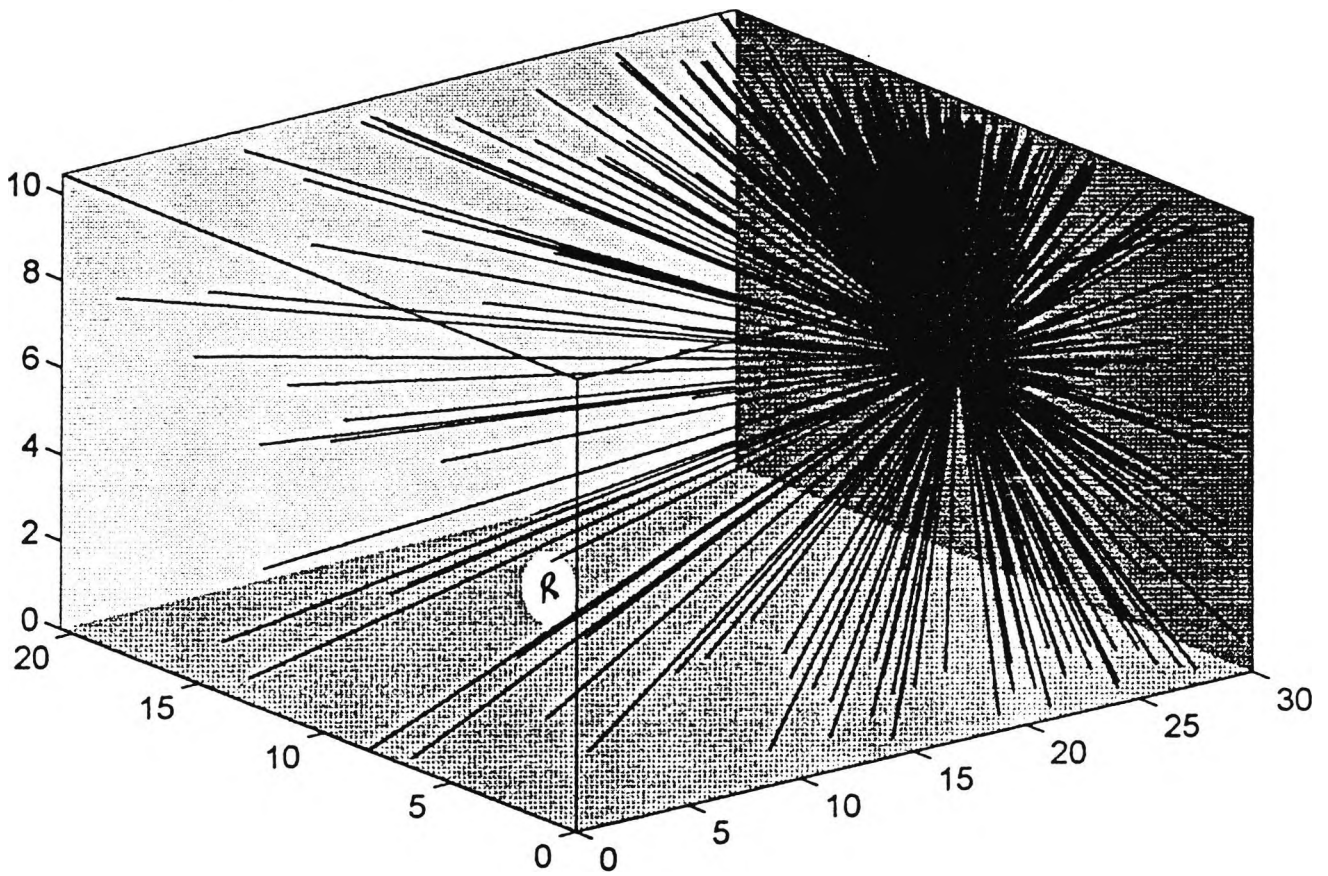


FIGURE 13: RECTANGULAR ROOM CASE, THE DIRECT AND
DIFFUSE SOUND FIELD.

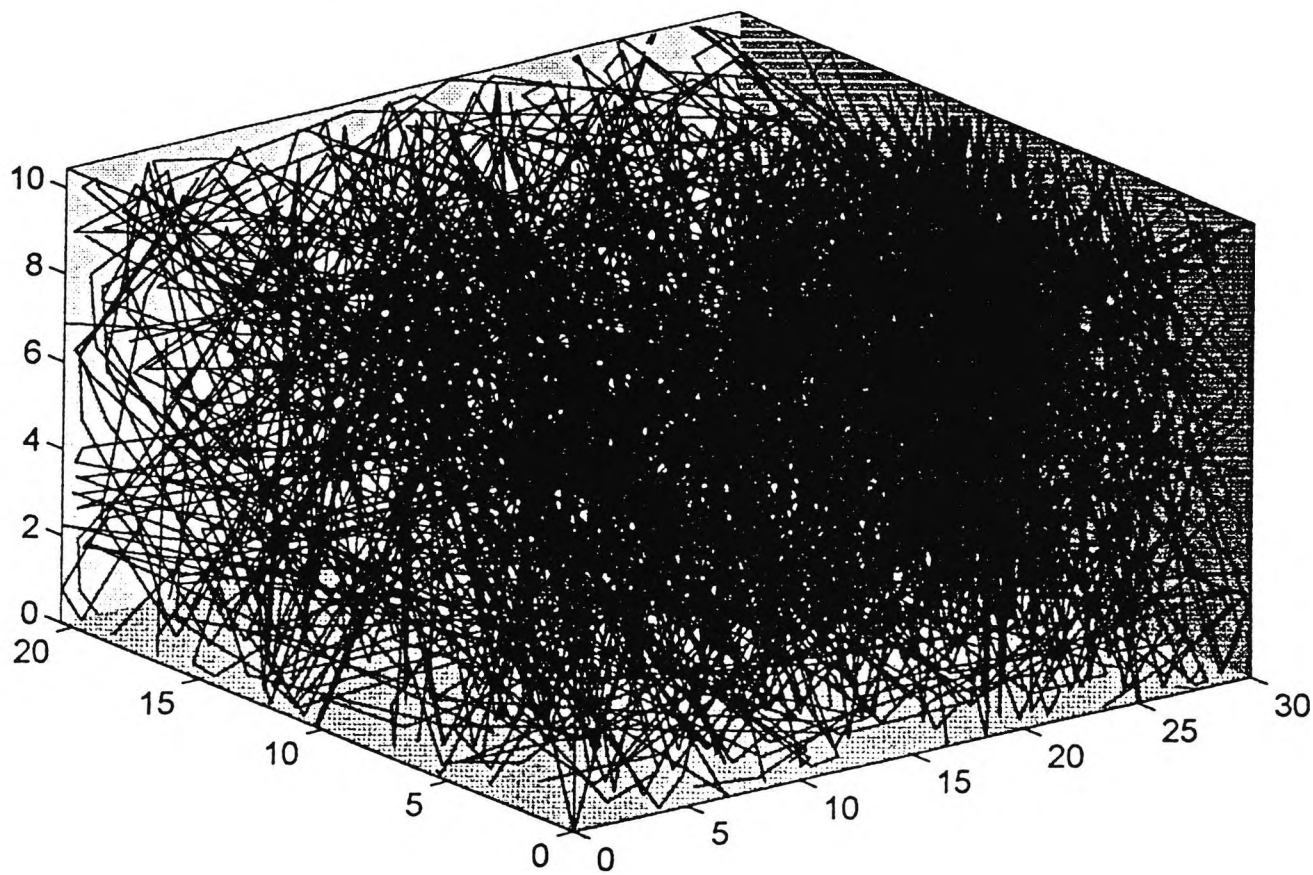


FIGURE 14: RECTANGULAR ROOM CASE, SOME OF THE SOUND PATHS THAT REACH THE RECEIVER.

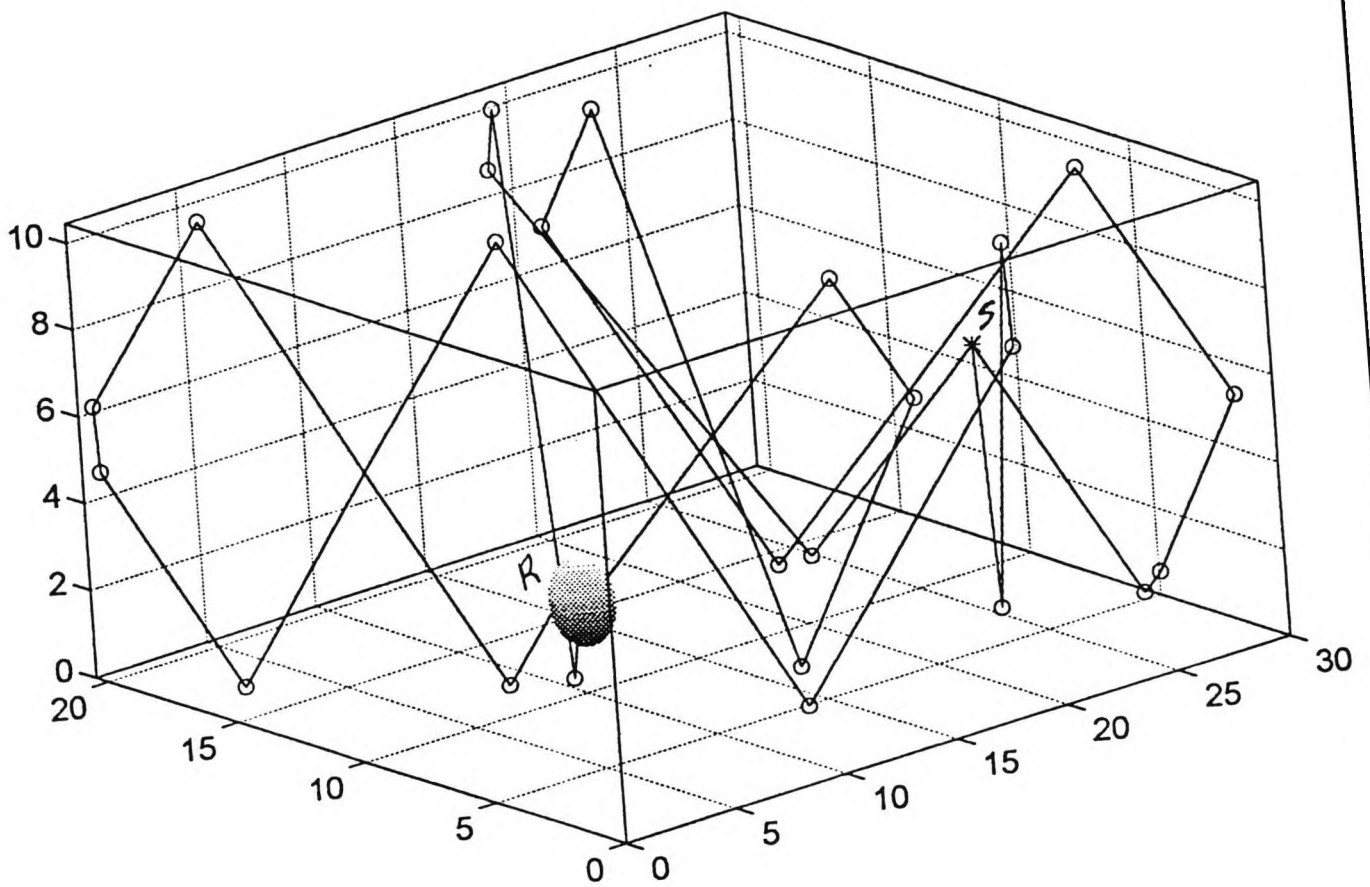


FIGURE 15: RECTANGULAR ROOM CASE, A HEDGEHOG
DIAGRAM INDICATING THE SPATIAL DIFFUSIVITY.

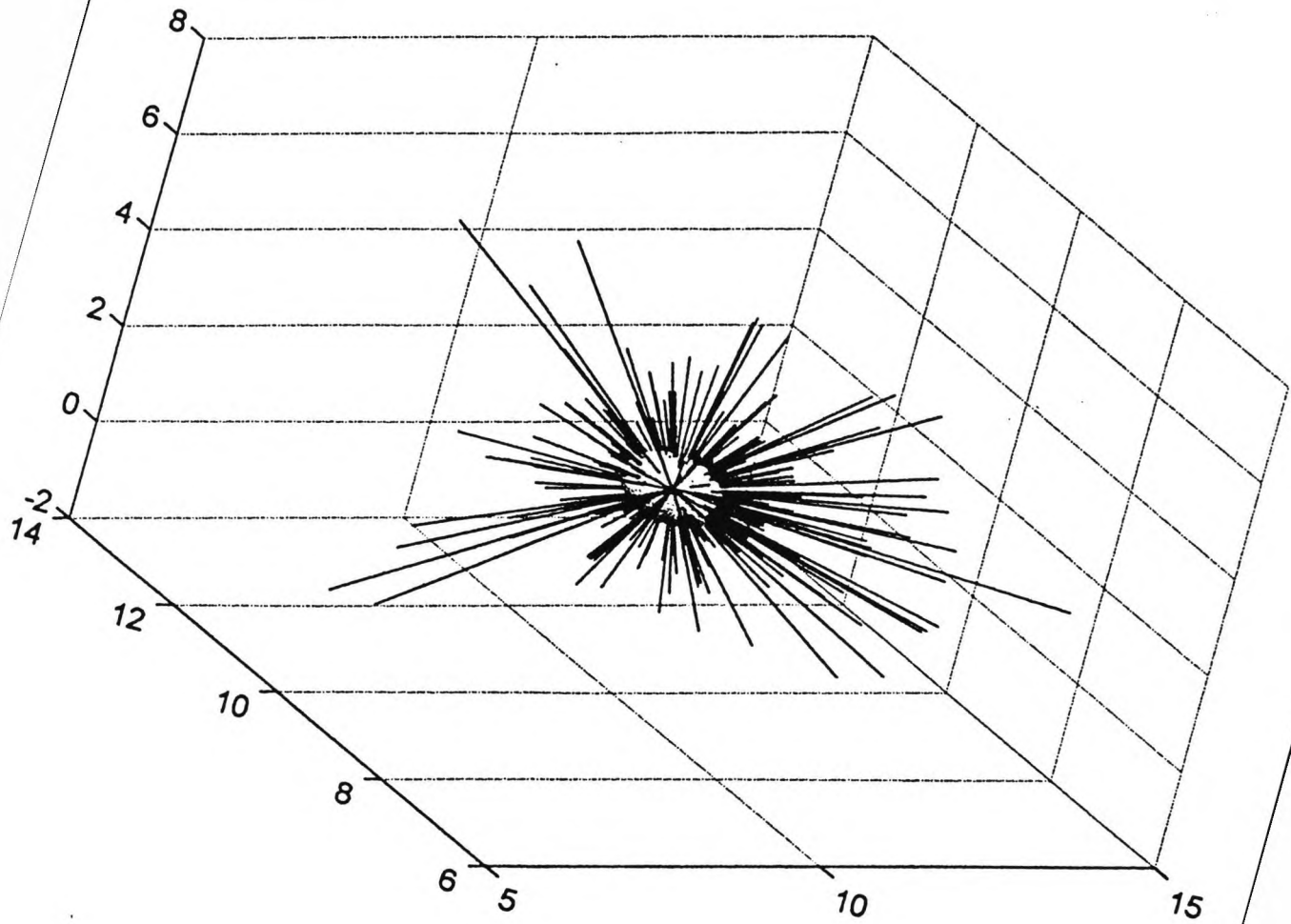


FIGURE 16: RECTANGULAR ROOM CASE, MEAN FREE PATH.

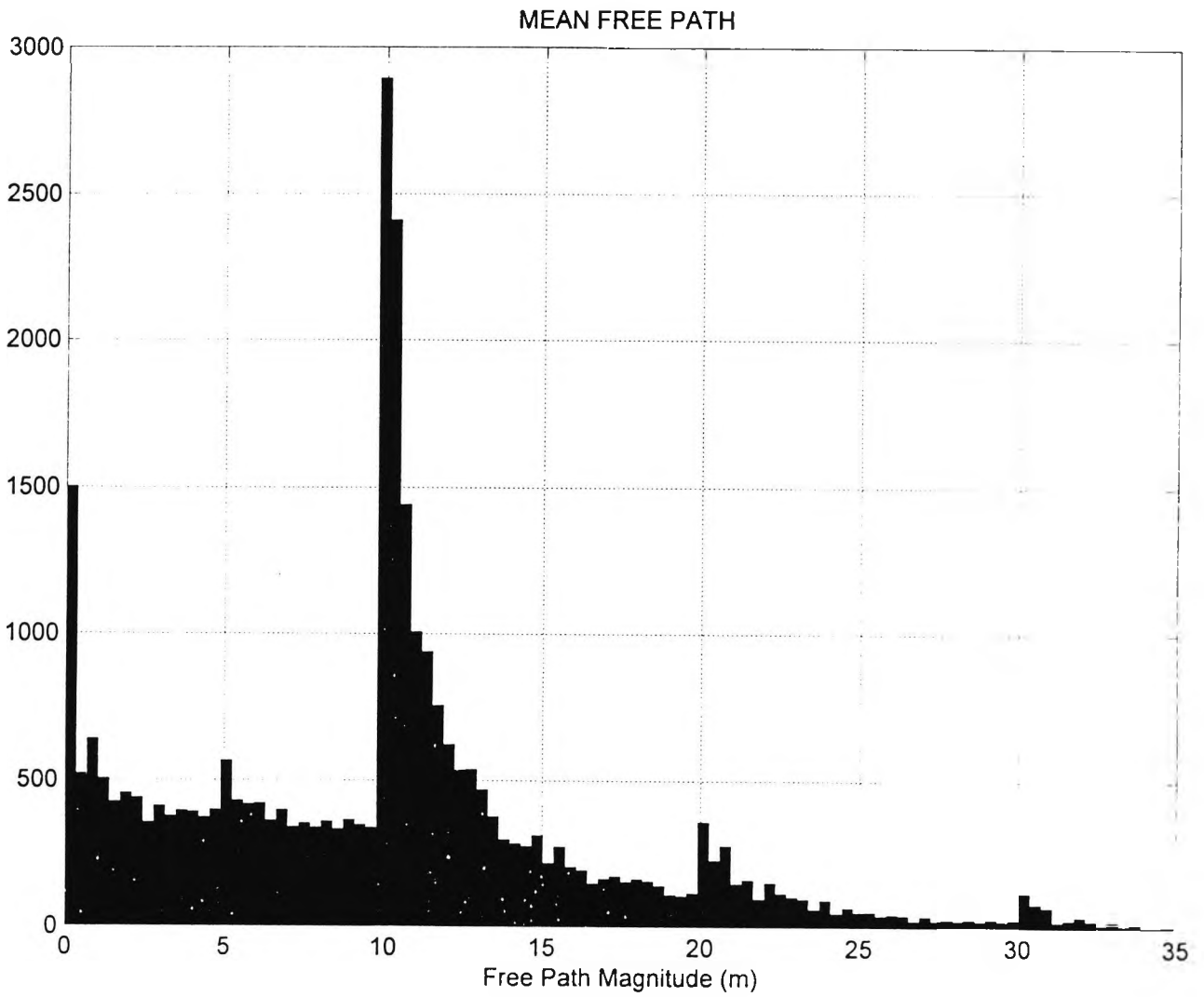


FIGURE 17: RECTANGULAR ROOM CASE, IMPULSE RESPONSE.

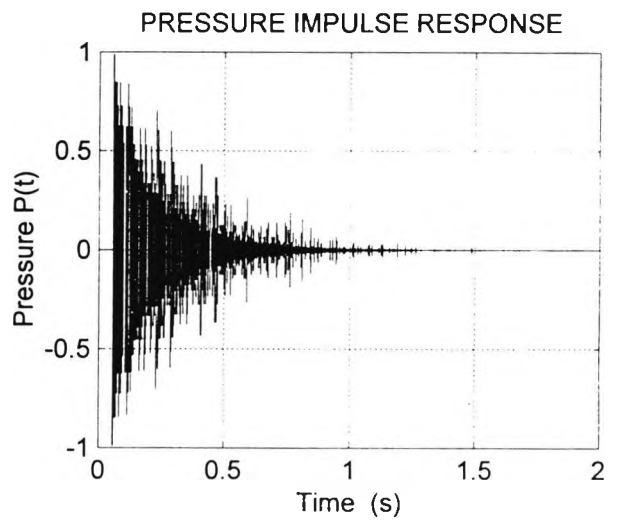
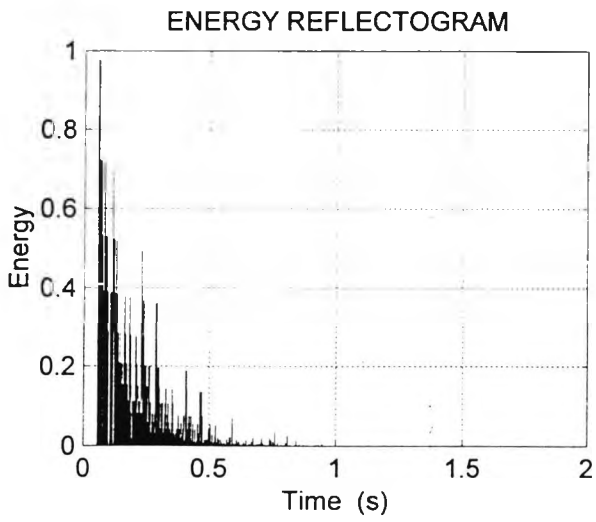
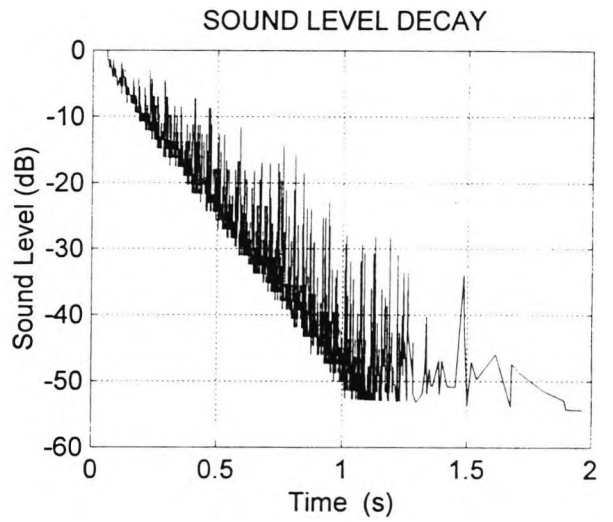
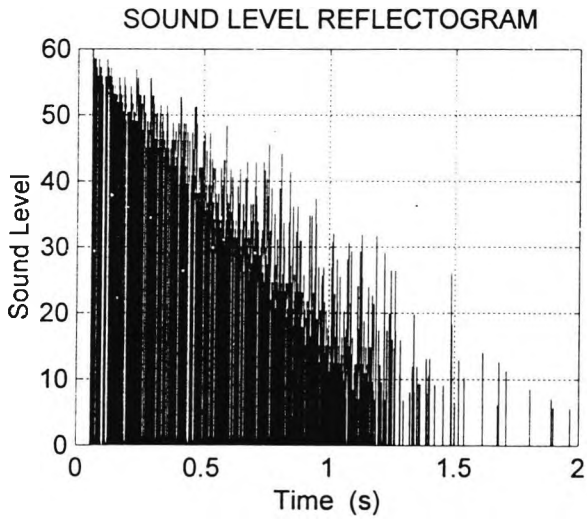
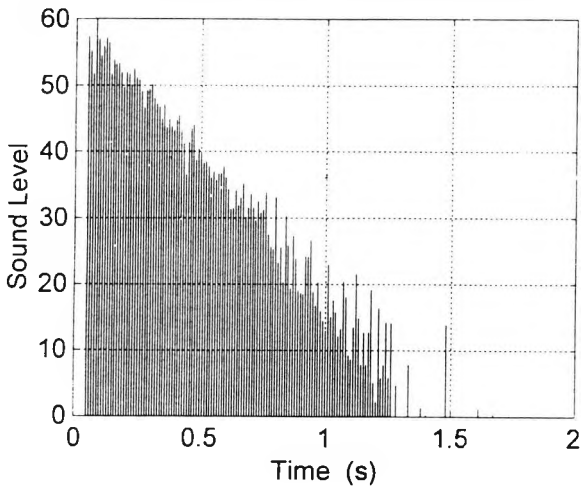
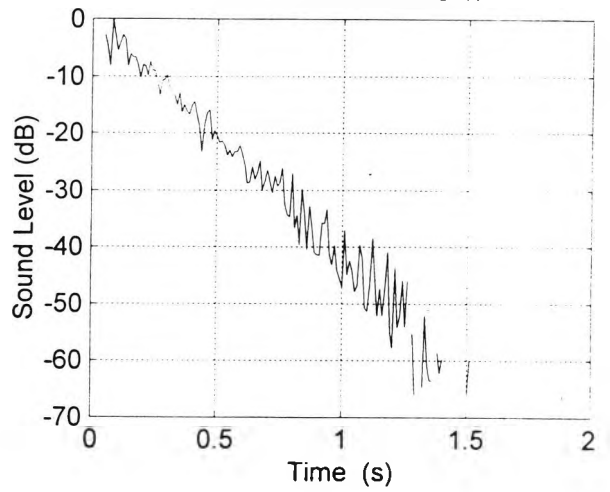


FIGURE 18: RECTANGULAR ROOM CASE, ENERGETIC IMPULSE RESPONSE.

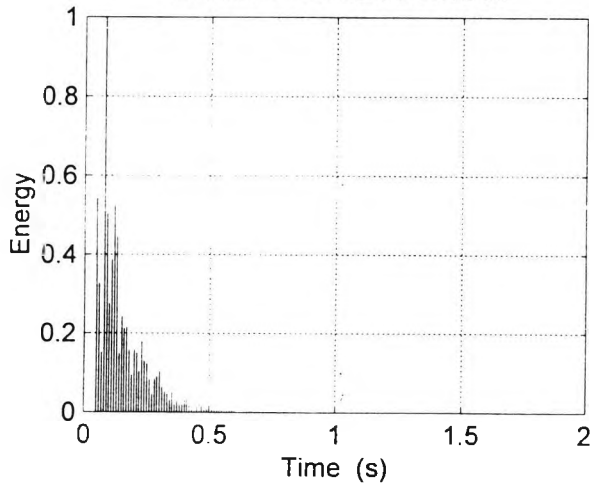
SOUND LEVEL REFLECTOGRAM



SOUND LEVEL DECAY



ENERGY REFLECTOGRAM



PRESSURE IMPULSE RESPONSE

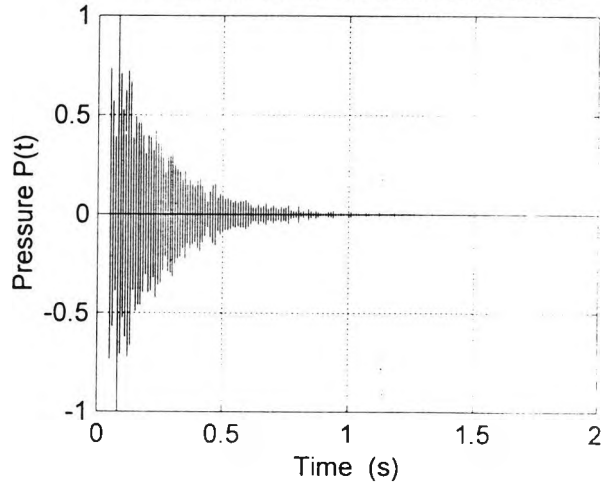


FIGURE 19: RECTANGULAR ROOM CASE, INTEGRATED
IMPULSE RESPONSE.

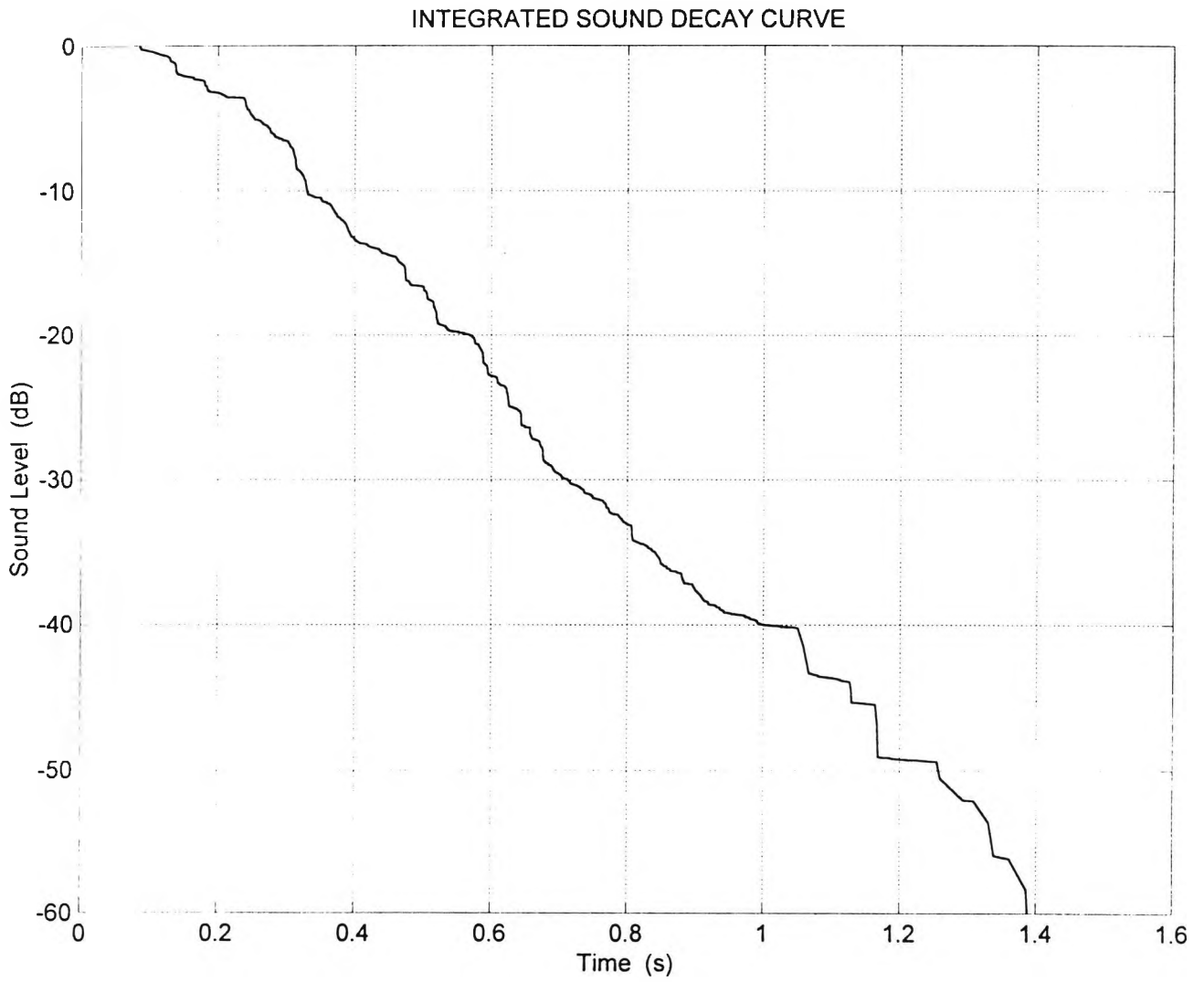


FIGURE 20: RECTANGULAR ROOM CASE, DECIMATED SOUND DECAY CURVE.

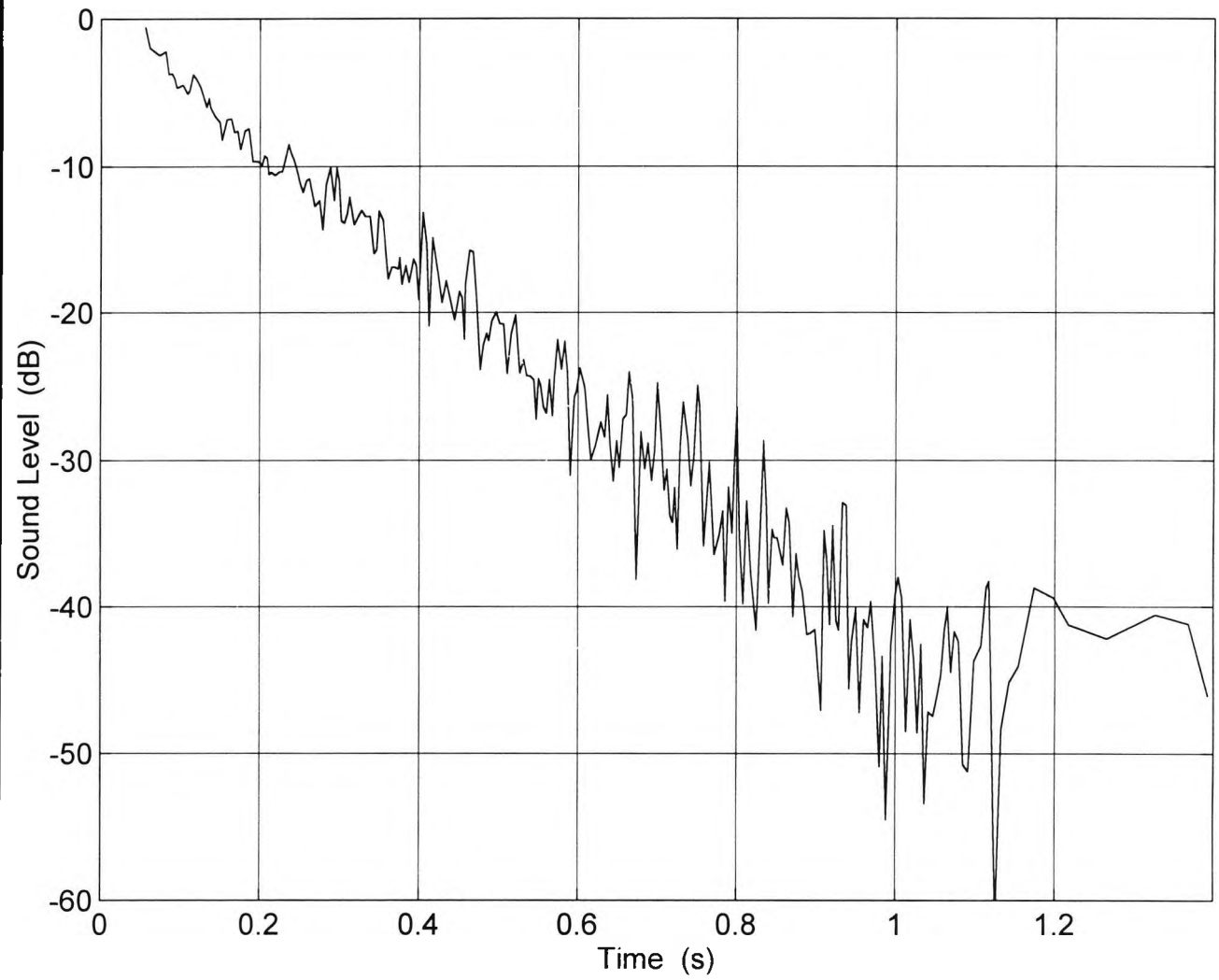


FIGURE 21: RECTANGULAR ROOM CASE, SOUND DECAY CURVE USING REGRESSION ANALYSIS.

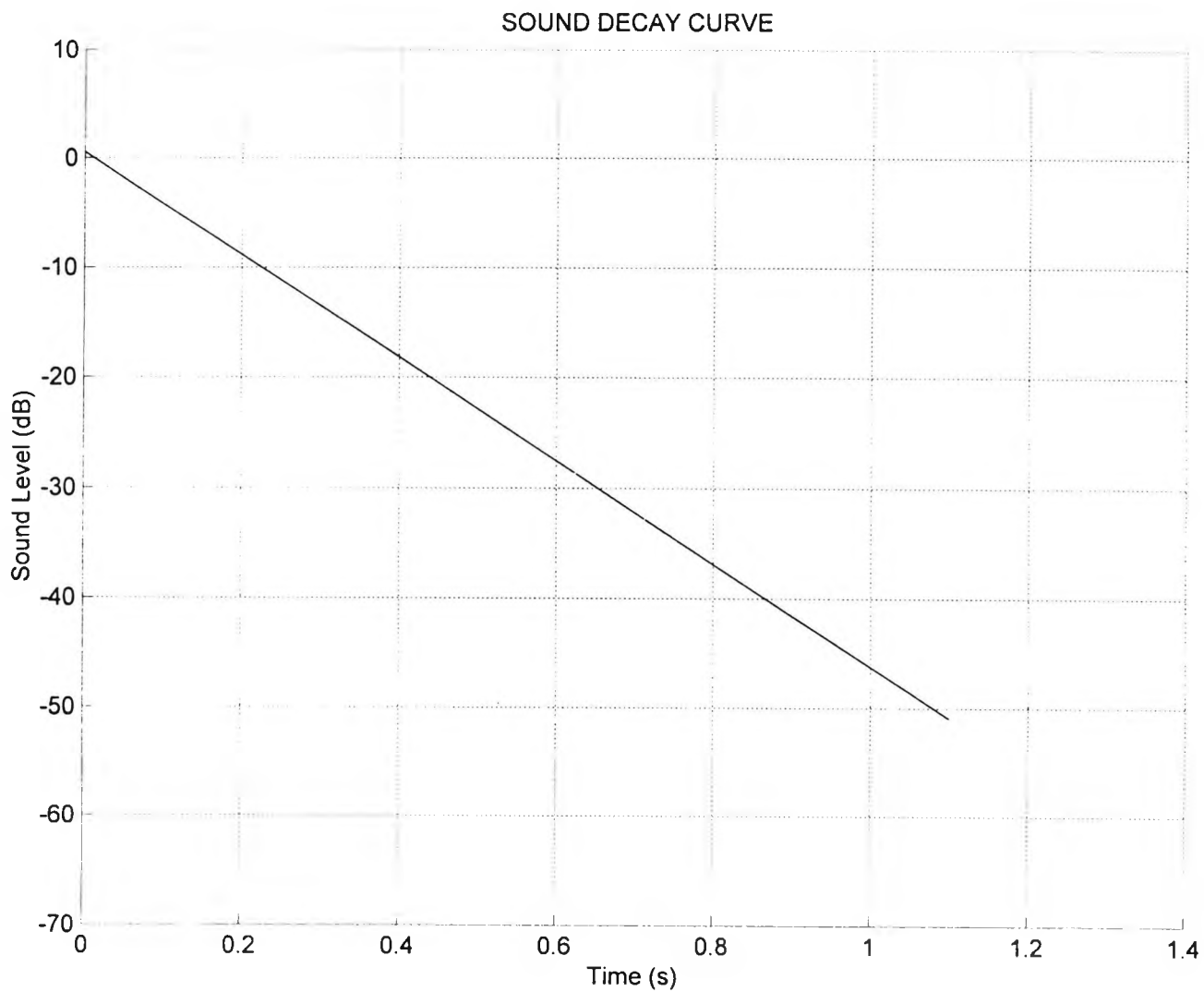


FIGURE 22: RECTANGULAR ROOM CASE, AVERAGE ENERGY DECAY USING ENSEMBLE AVERAGES.

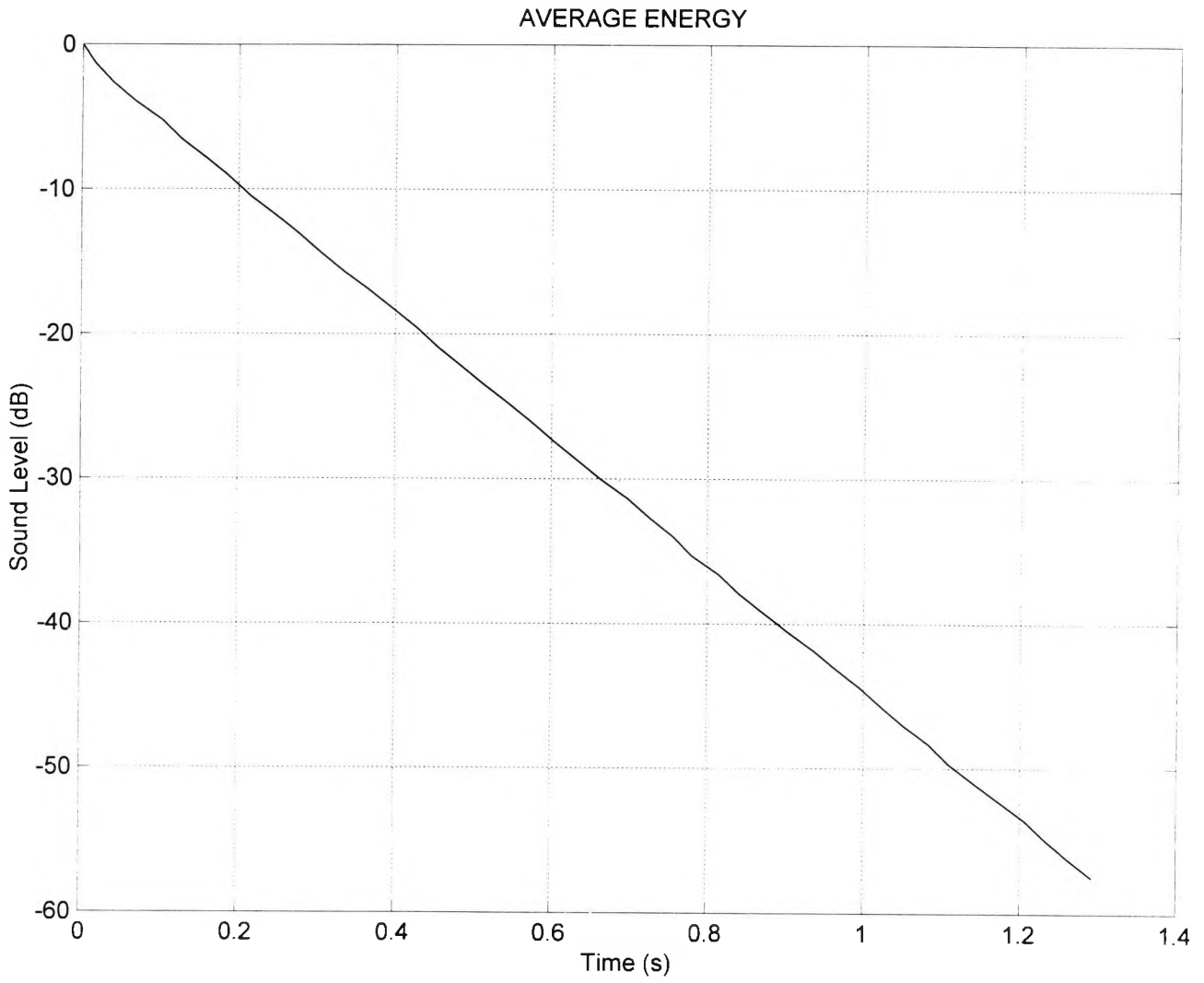


FIGURE 23: TEST ROOM CASE CONFIGURATION (A), SOUND PARTICLE SPATIAL DISTRIBUTION.

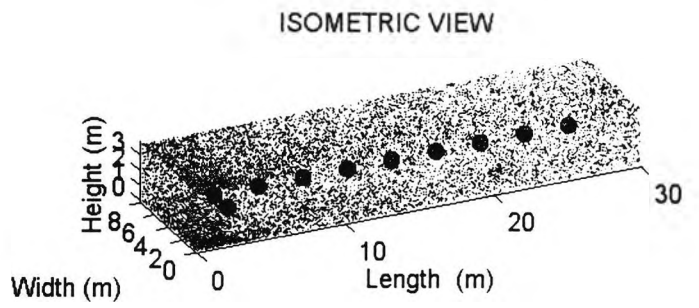
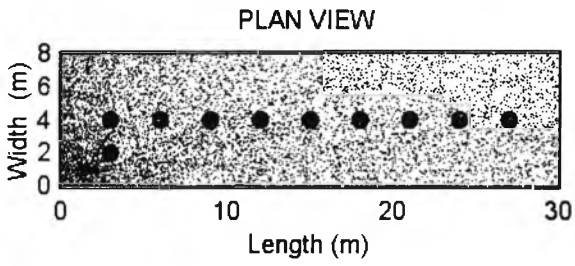
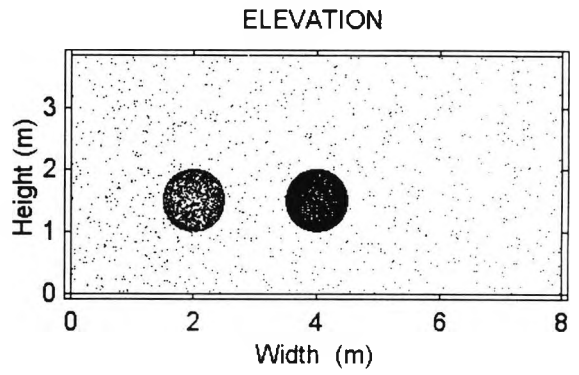
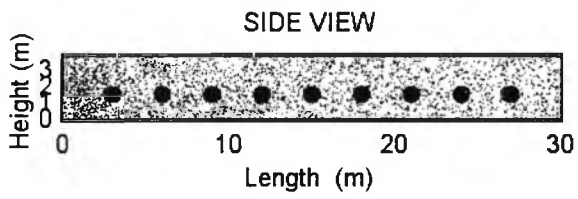


FIGURE 24: TEST ROOM CASE CONFIGURATION (A), 2-D NOISE CONTOUR MAP.

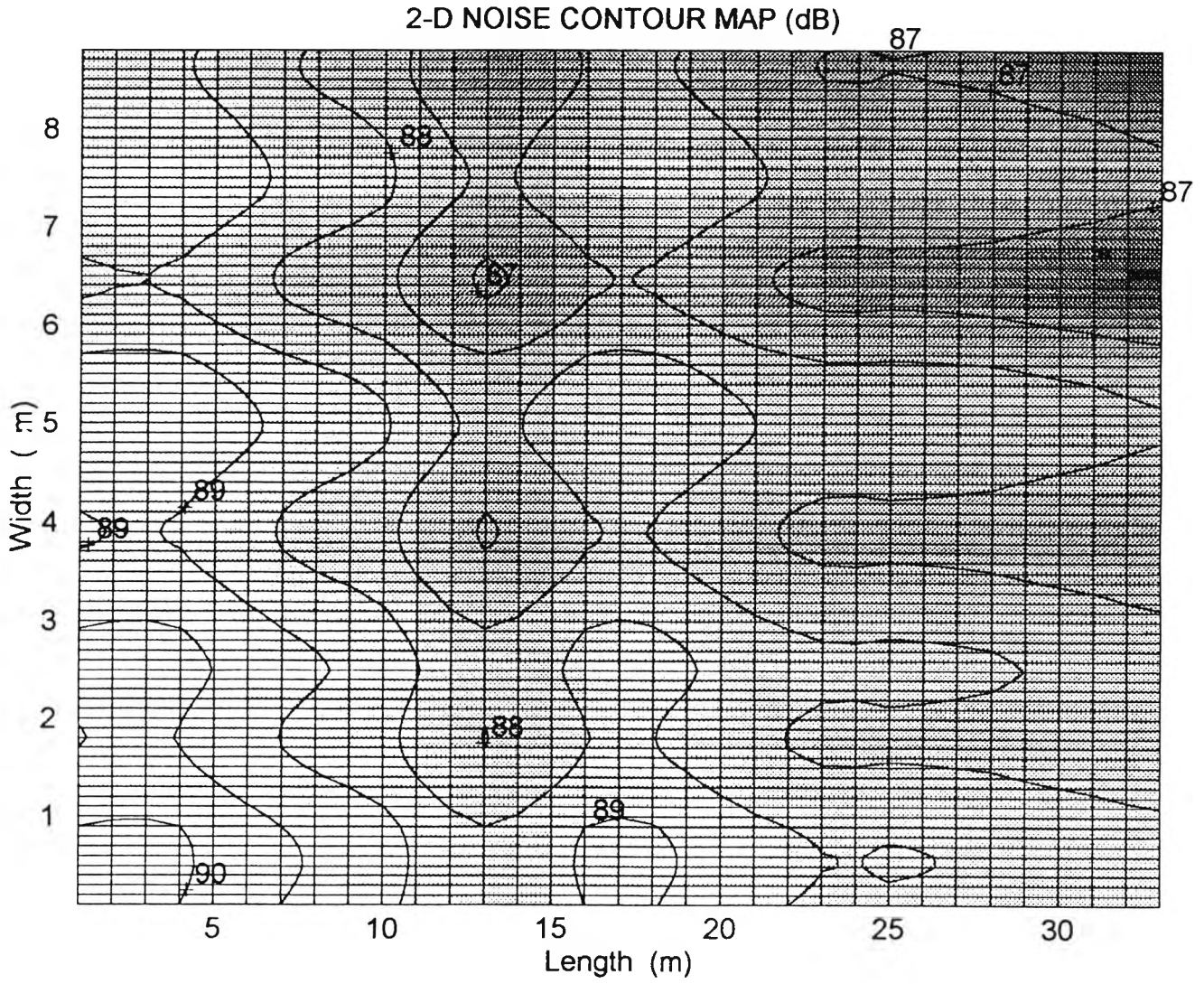


FIGURE 25: TEST ROOM CASE CONFIGURATION (B), SOUND PARTICLE SPATIAL DISTRIBUTION.

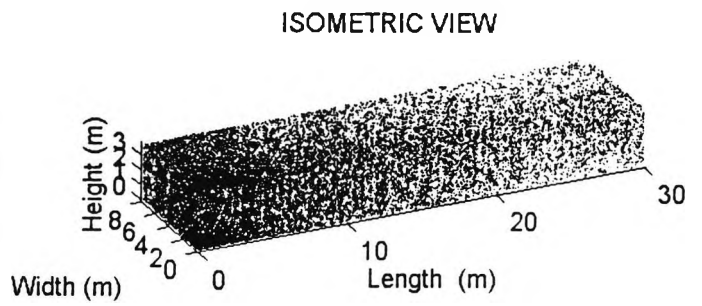
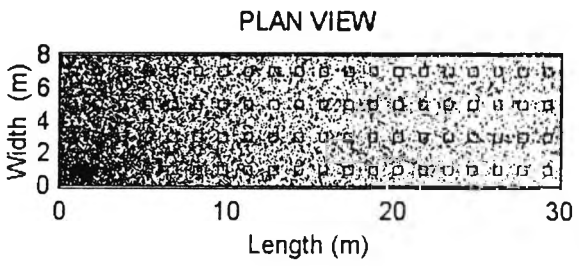
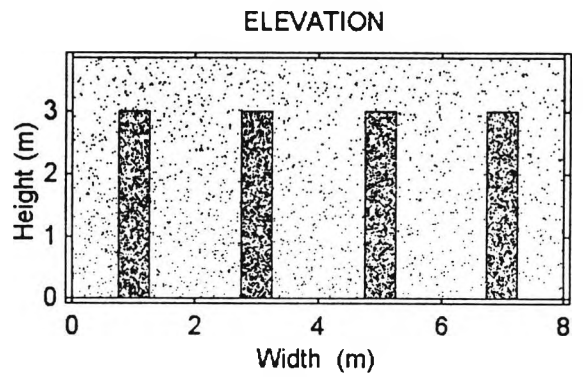
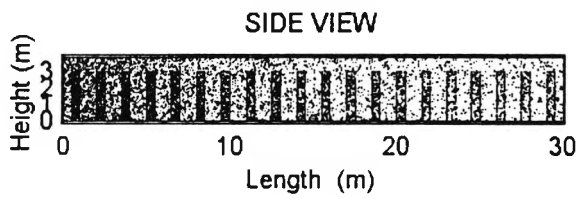


FIGURE 26: TEST ROOM CASE, THE SOUND PRESSURE LEVEL VERSUS RECEIVER POSITION, PREDICTED AND MEASURED RESULTS, (A) EMPTY ROOM, (B) FITTED ROOM.

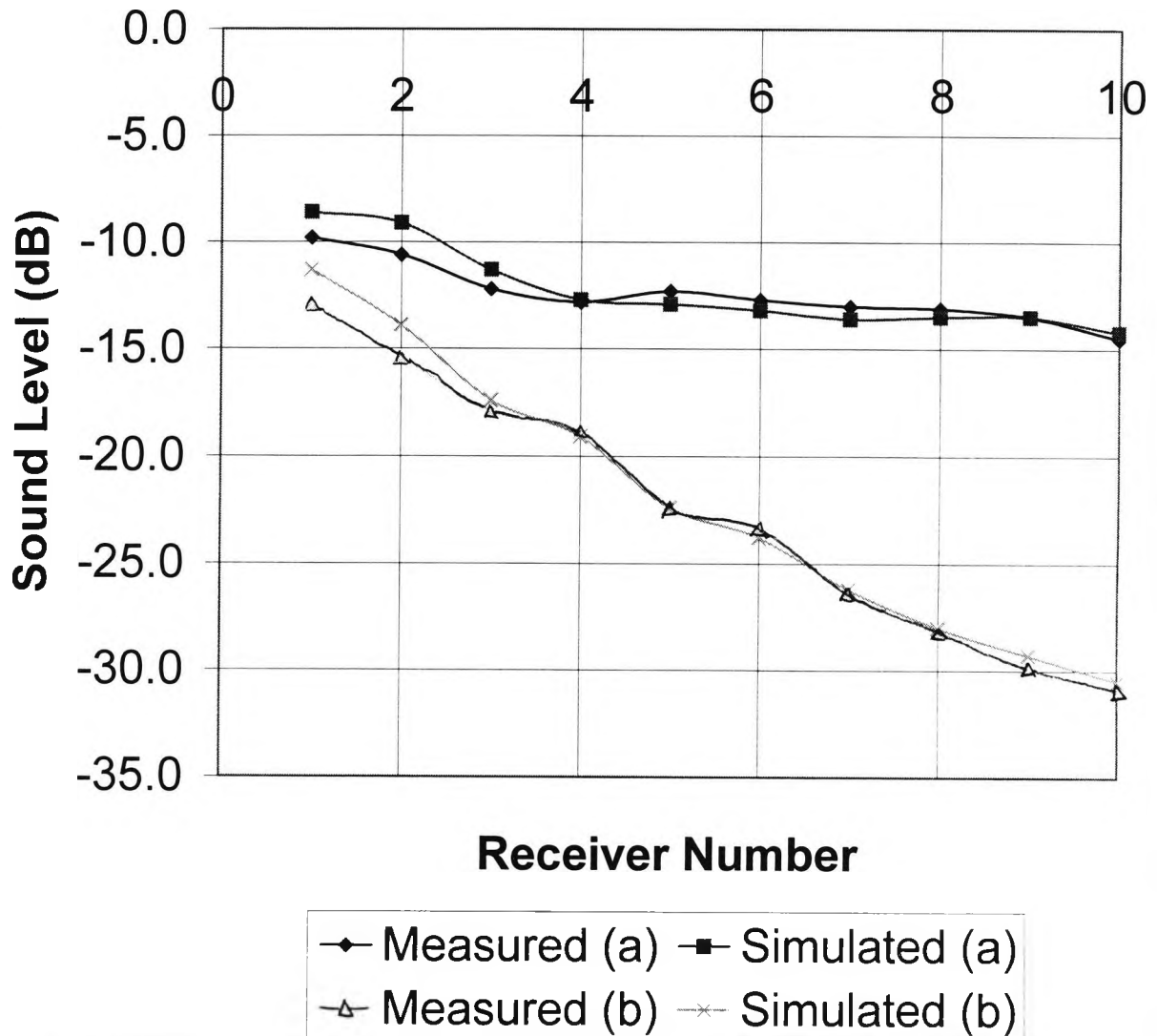


FIGURE 27: CORRIDOR CASE, SOUND PARTICLE SPATIAL DISTRIBUTION AND SOUND PATH ANALYSIS.

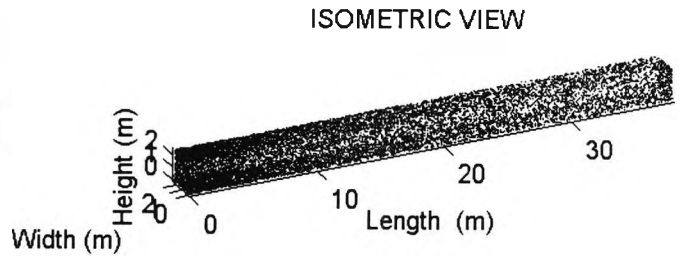
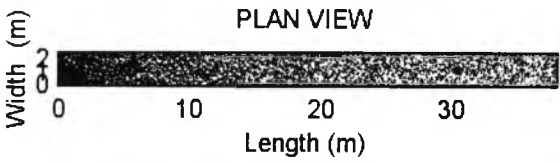
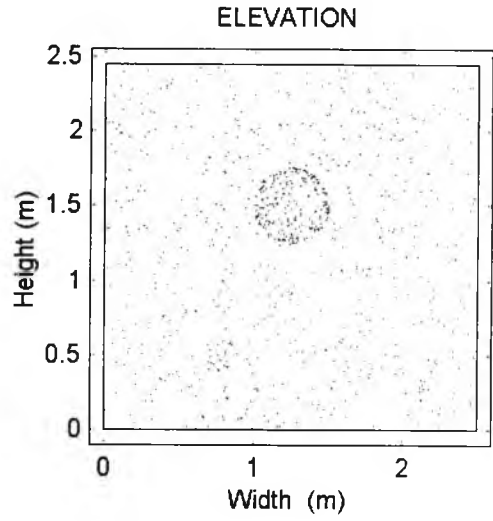
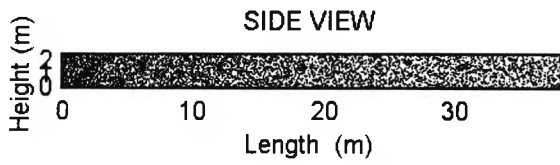


FIGURE 29: CORRIDOR CASE, GRAPHICAL COMPARISON OF SOUND PRESSURE LEVEL BETWEEN COMPUTATIONAL AND EXPERIMENTAL RESULTS.

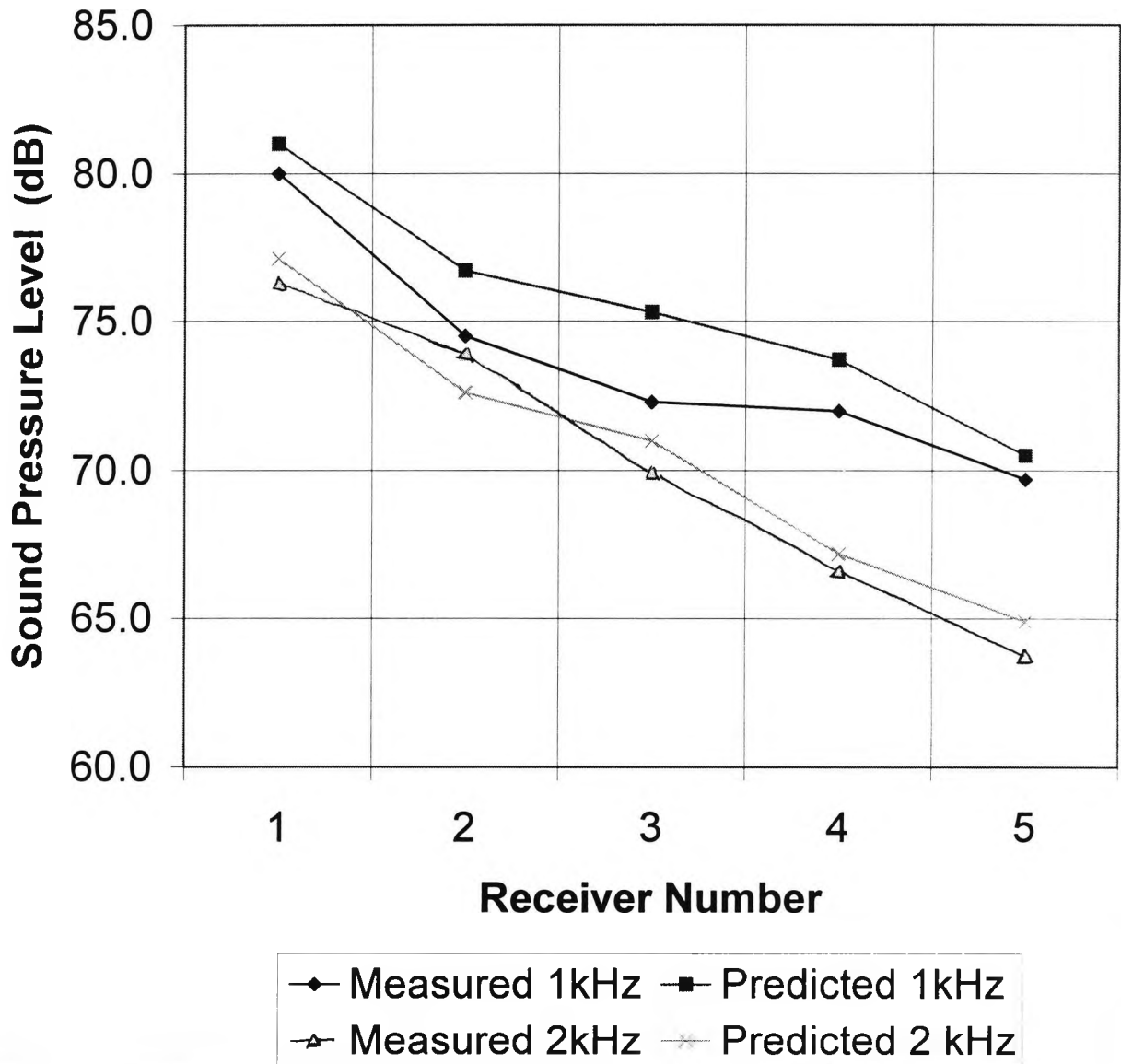


FIGURE 30: CORRIDOR CASE, SIMULATED REVERBERATION TRACE USING SCHROEDER'S BACKWARDS INTEGRATION METHOD.

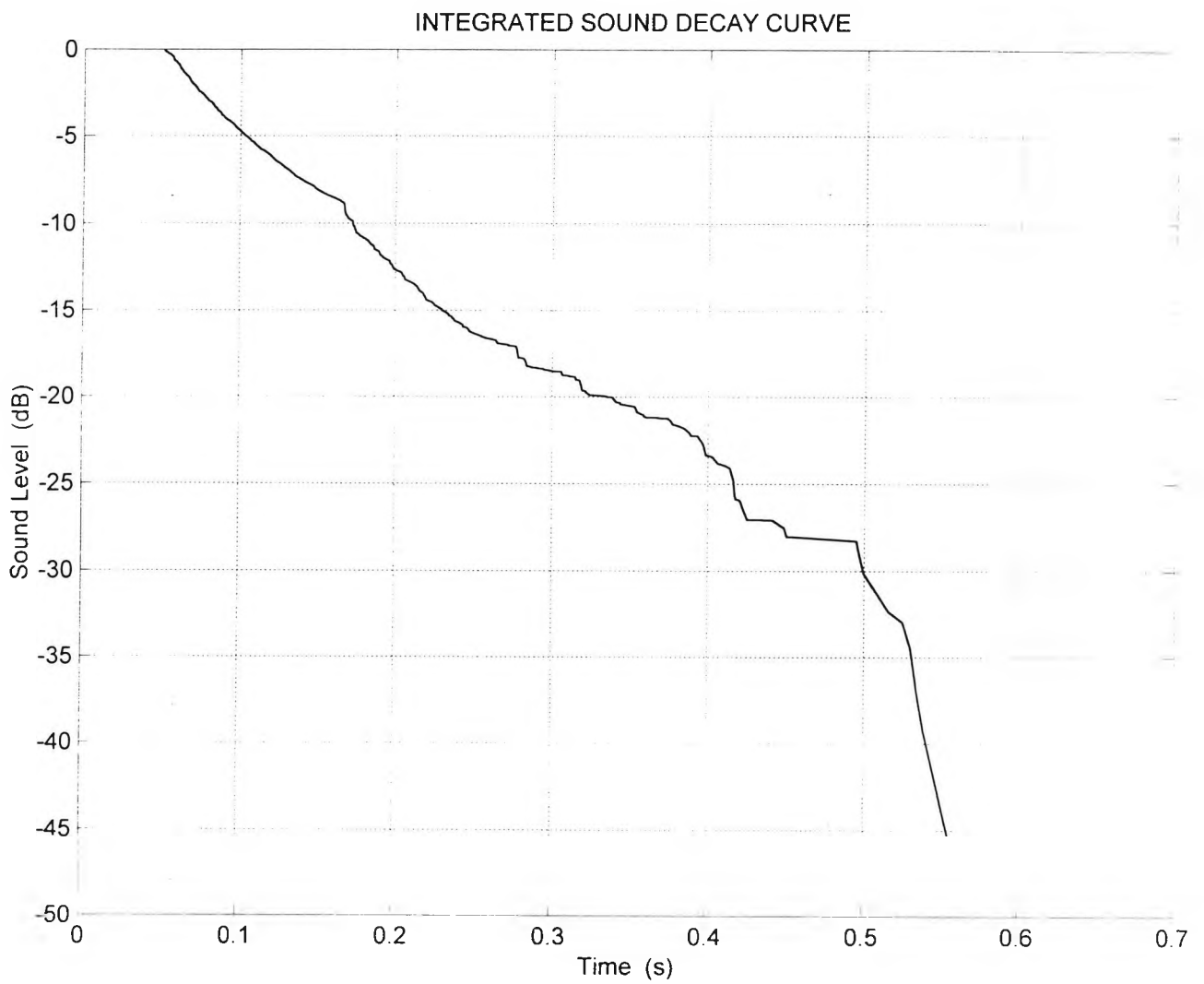


FIGURE 31: CORRIDOR CASE, SPATIAL DIFFUSIVITY AT A RECEIVER POSITION 18.2 M FROM THE SOURCE.

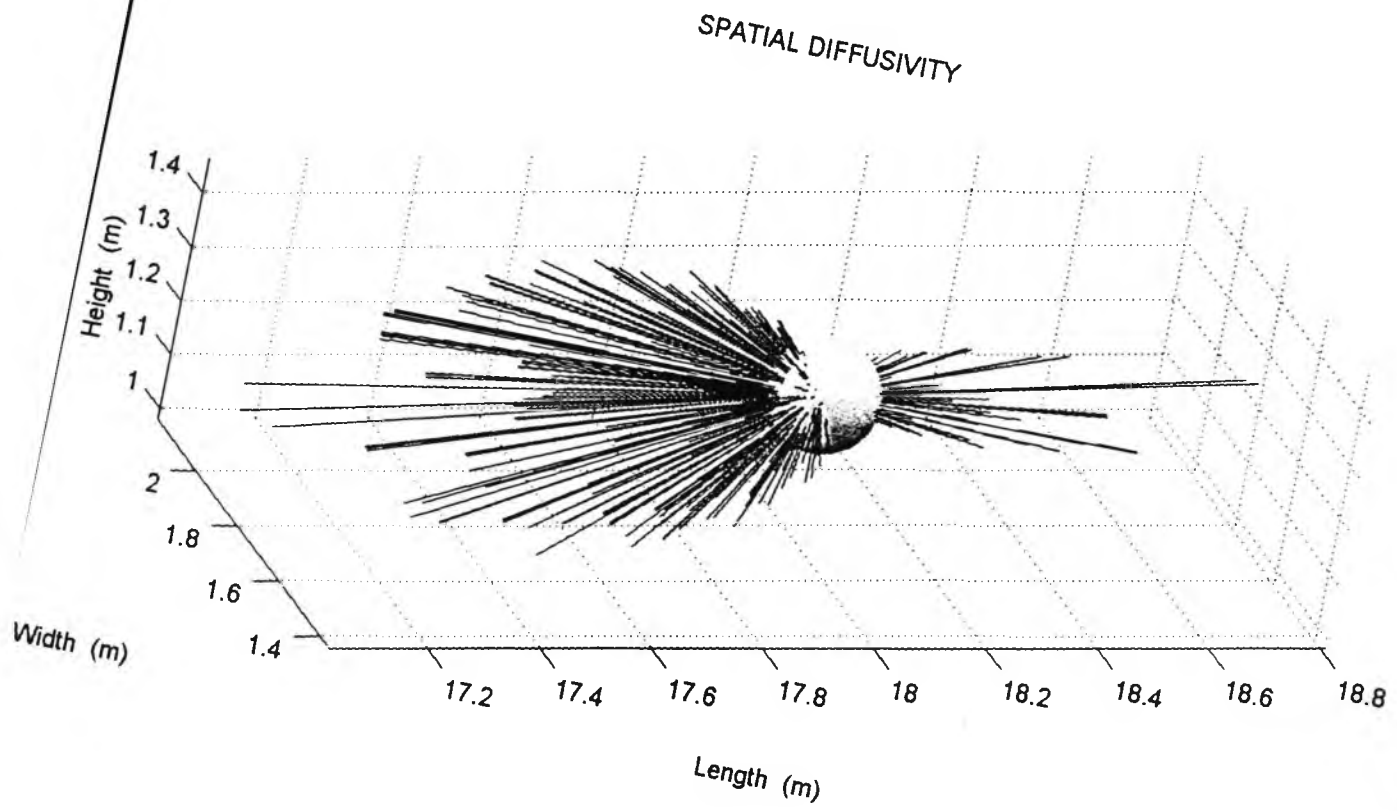
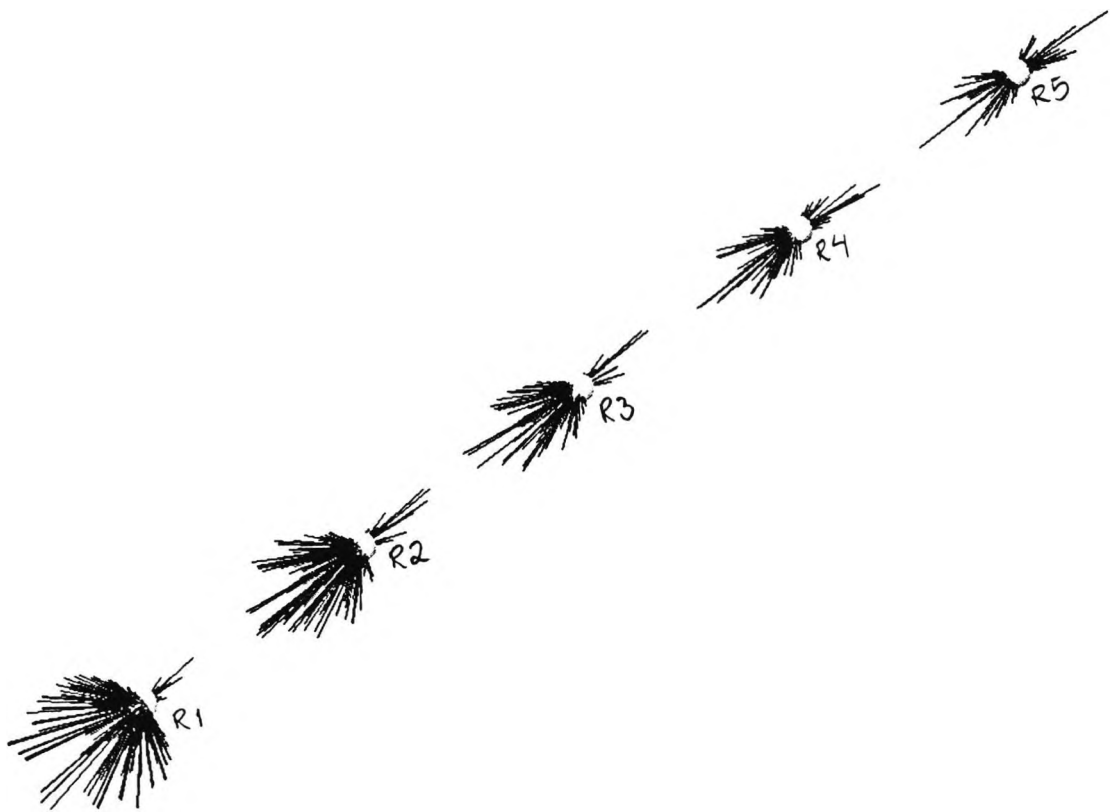


FIGURE 32: CORRIDOR CASE, HEDGEHOG DIAGRAMS
REVEALING THE DIFFUSIVITY OF THE SOUND FIELD
ALONG THE ROOM.

SPATIAL DIFFUSIVITY



* S

FIGURE 33: CORRIDOR CASE, DIFFUSION MAP FOR A RECEIVER 6 M FROM THE SOURCE.

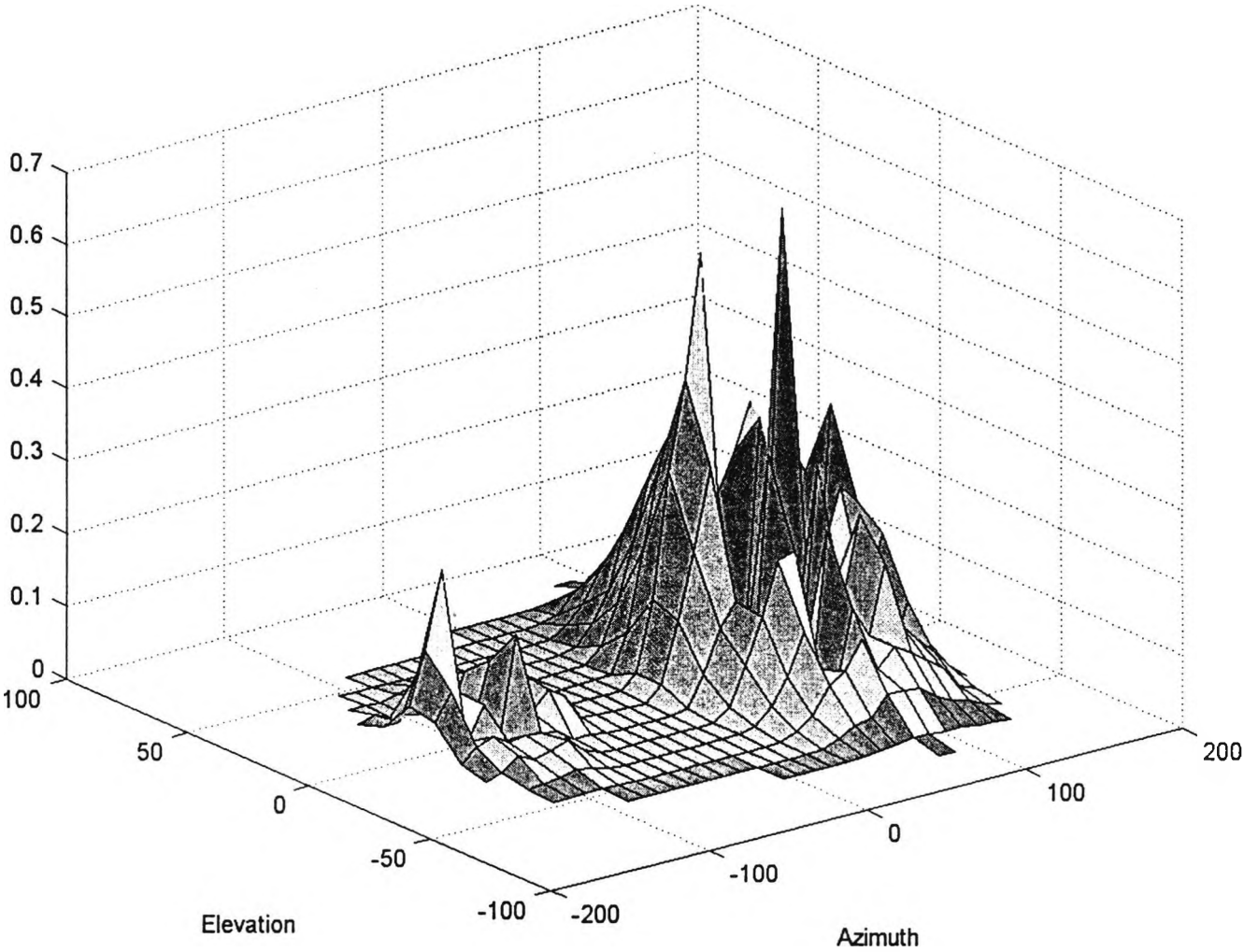


FIGURE 34: CORRIDOR CASE, DIFFUSION MAP FOR A RECEIVER 18 M FROM THE SOURCE.

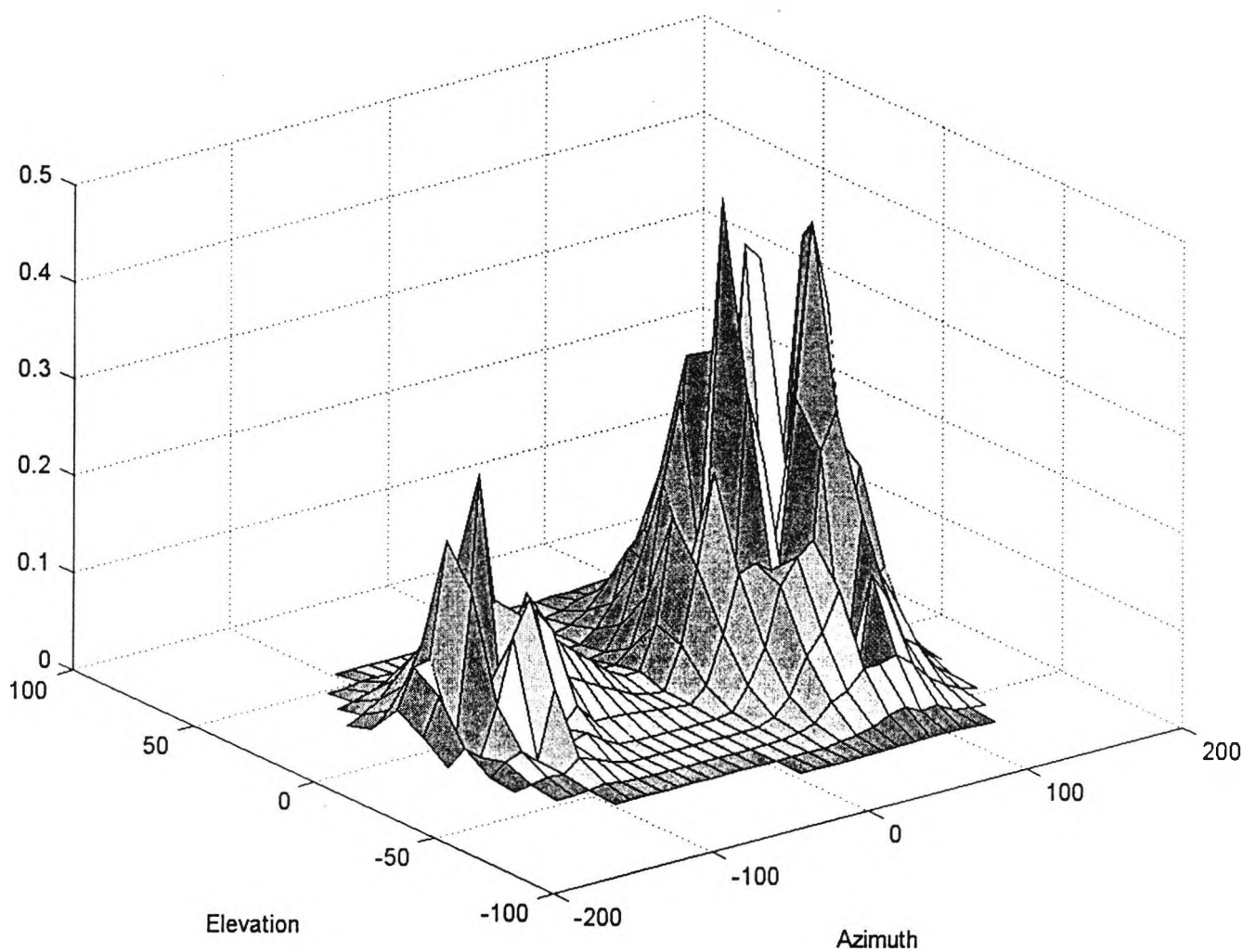
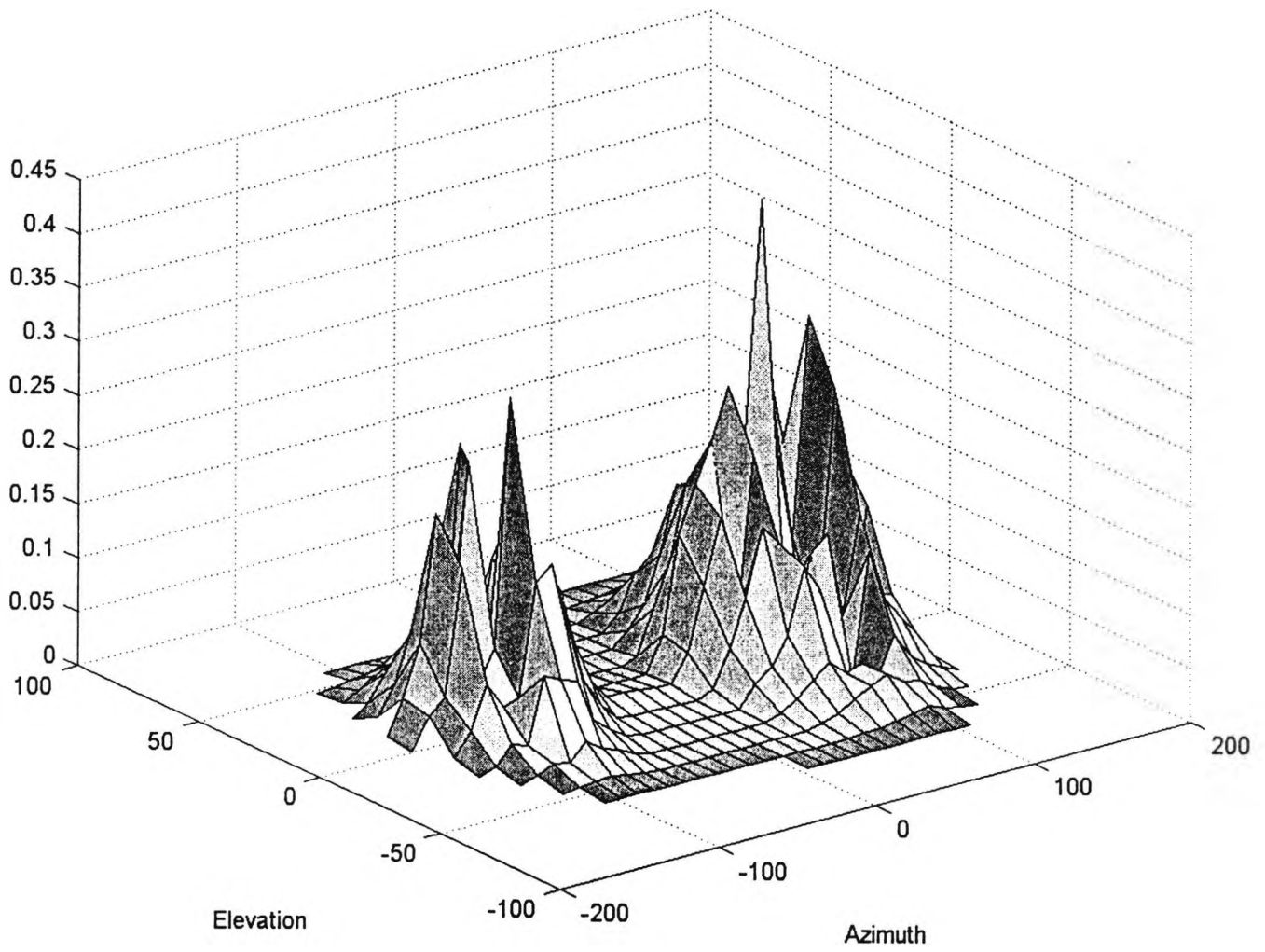
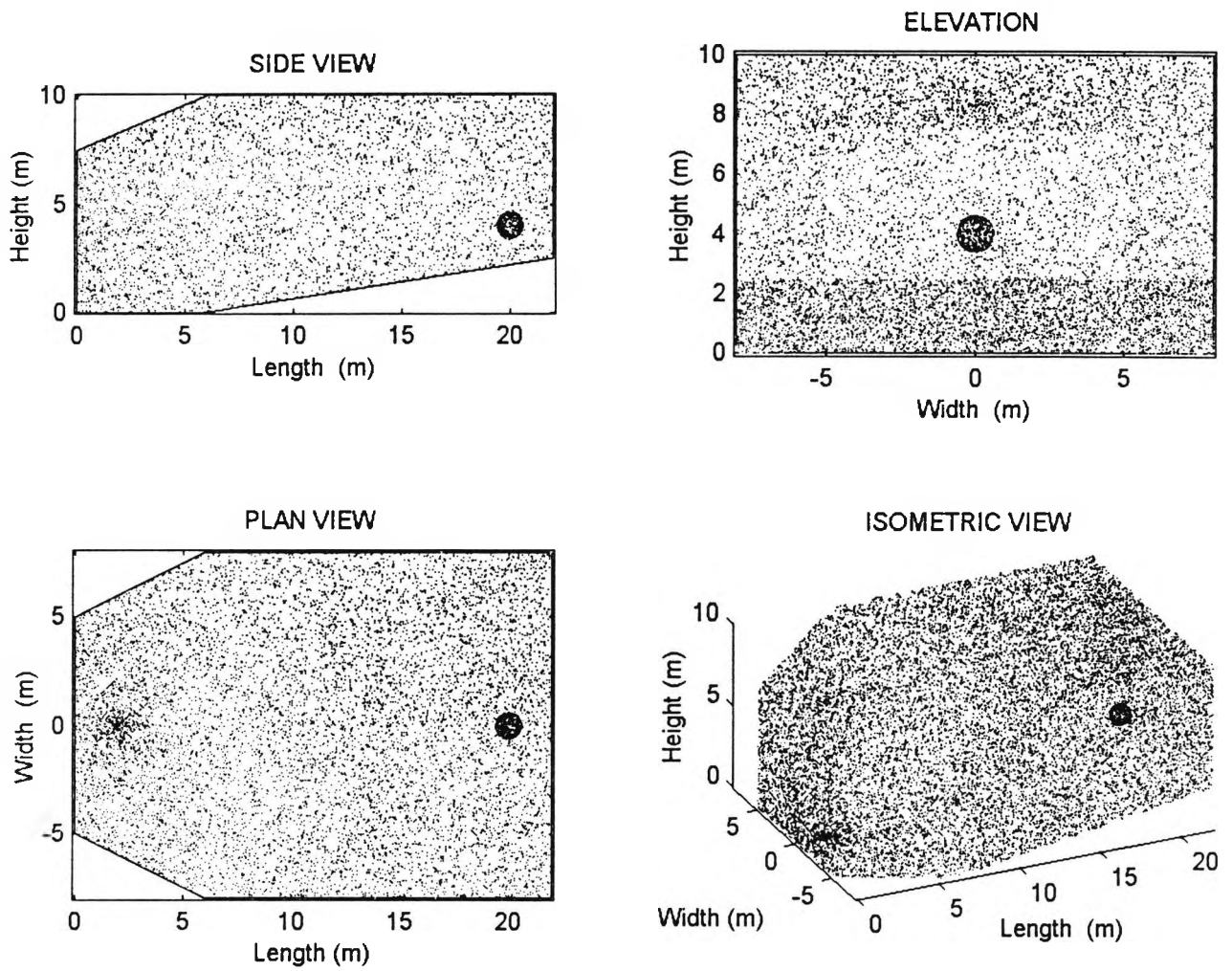


FIGURE 35: CORRIDOR CASE, DIFFUSION MAP FOR A RECEIVER 30 M FROM THE SOURCE.



**FIGURE 36: TYPICAL AUDITORIUM WITH TILTED WALLS
CASE, SOUND PARTICLE SPATIAL DISTRIBUTION.**



**FIGURE 37: AUDITORIUM WITH TILTED WALLS CASE,
SPATIAL DIFFUSIVITY.**

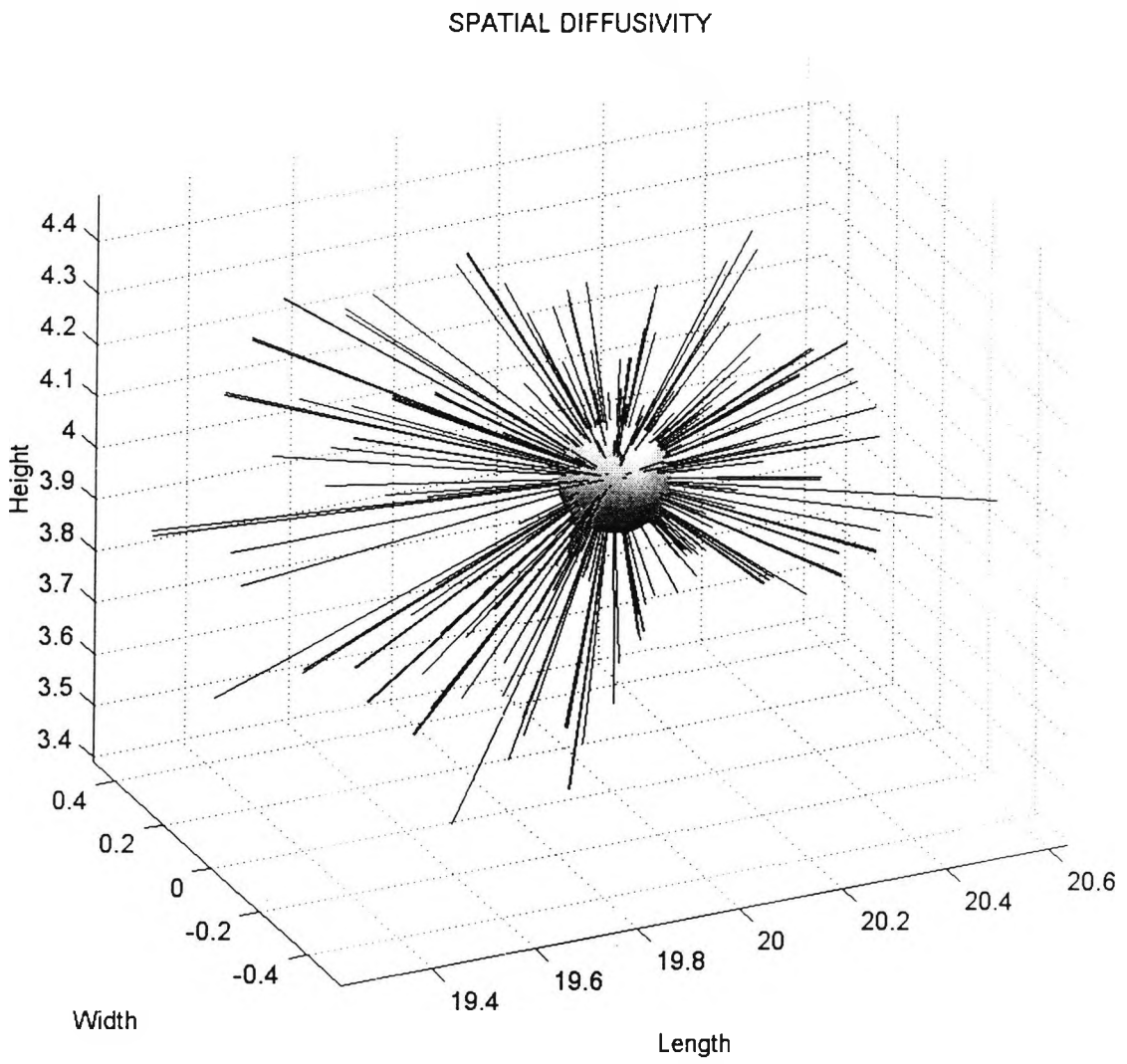


**FIGURE 38: AUDITORIUM WITH TILTED WALLS CASE, MEAN
FREE PATH.**

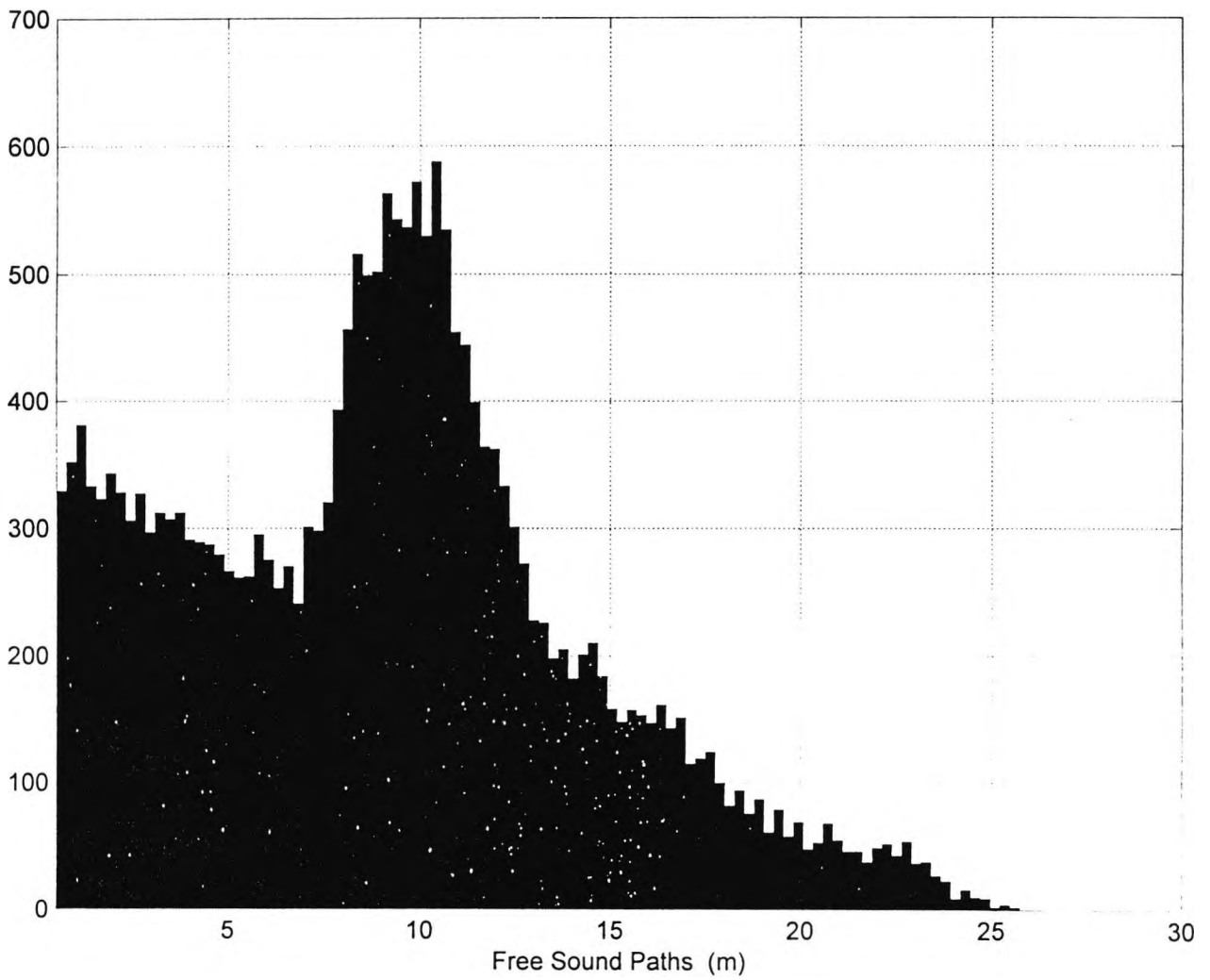


FIGURE 39: AUDITORIUM WITH TILTED WALLS CASE,
ENERGY DECAY USING ENSEMBLE AVERAGES.

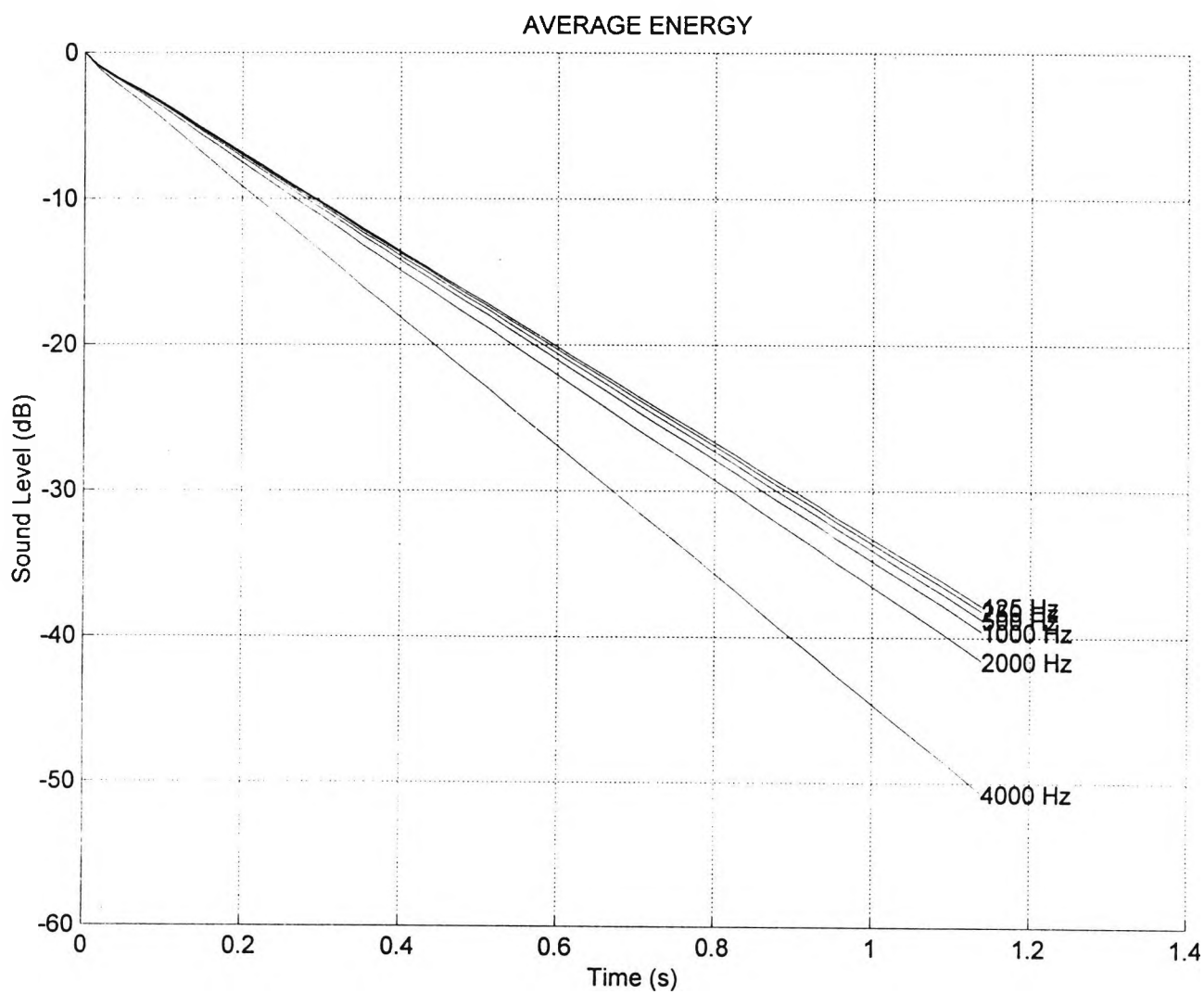


FIGURE 40: AUDITORIUM CASE, INTEGRATED SOUND DECAY CURVE.

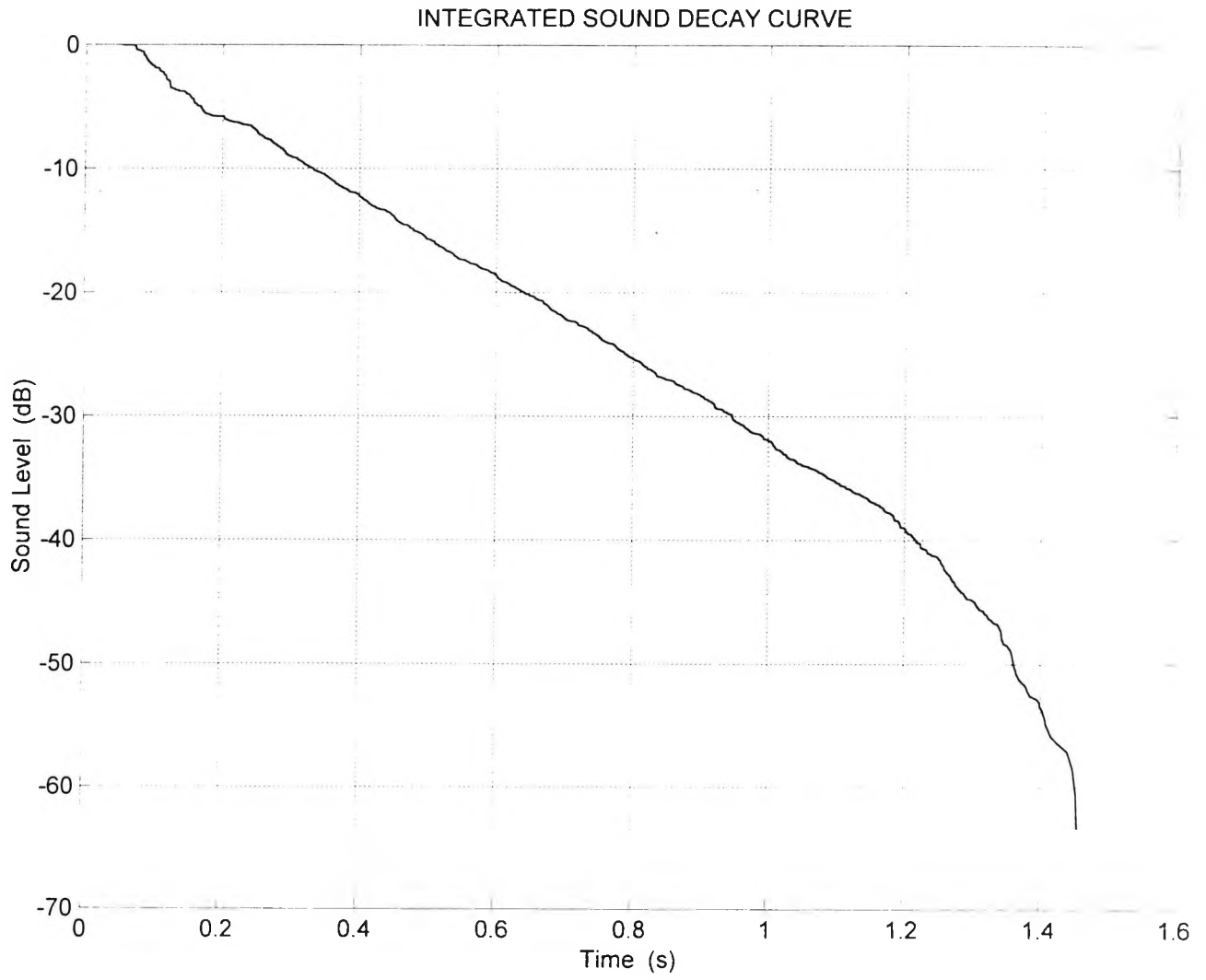


FIGURE 41: COUPLED ROOMS CASE, SOUND PARTICLE SPATIAL DISTRIBUTION.

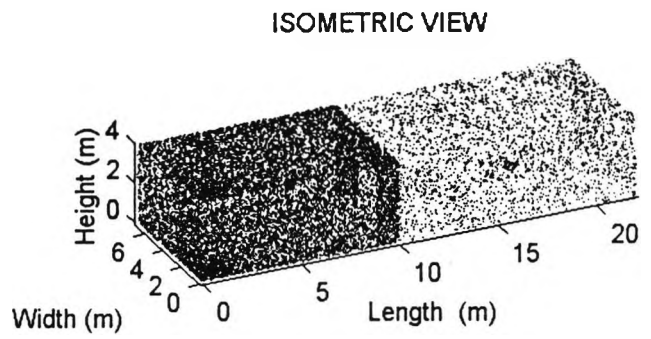
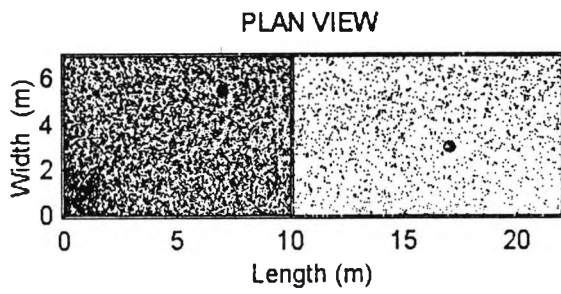
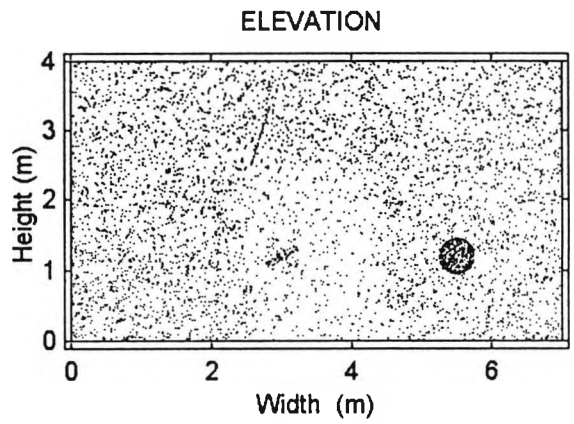
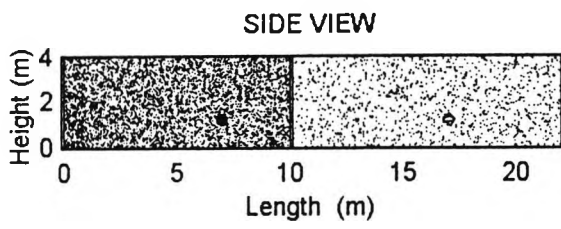


FIGURE 42: COUPLED ROOMS CASE, SOUND DECAY IN THE SOURCE AND ADJACENT ROOMS, THEORETICAL AND PREDICTED RESULTS.

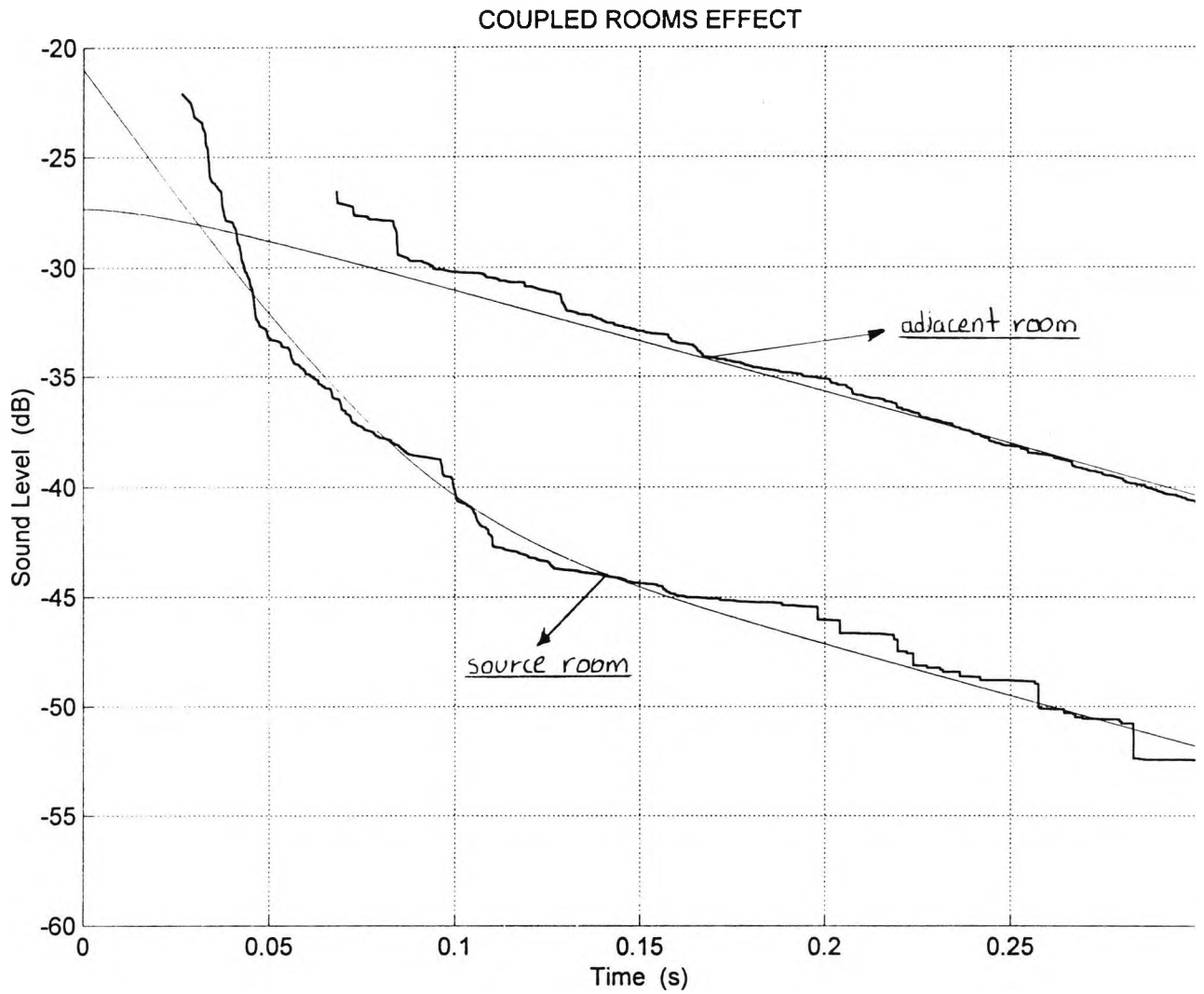
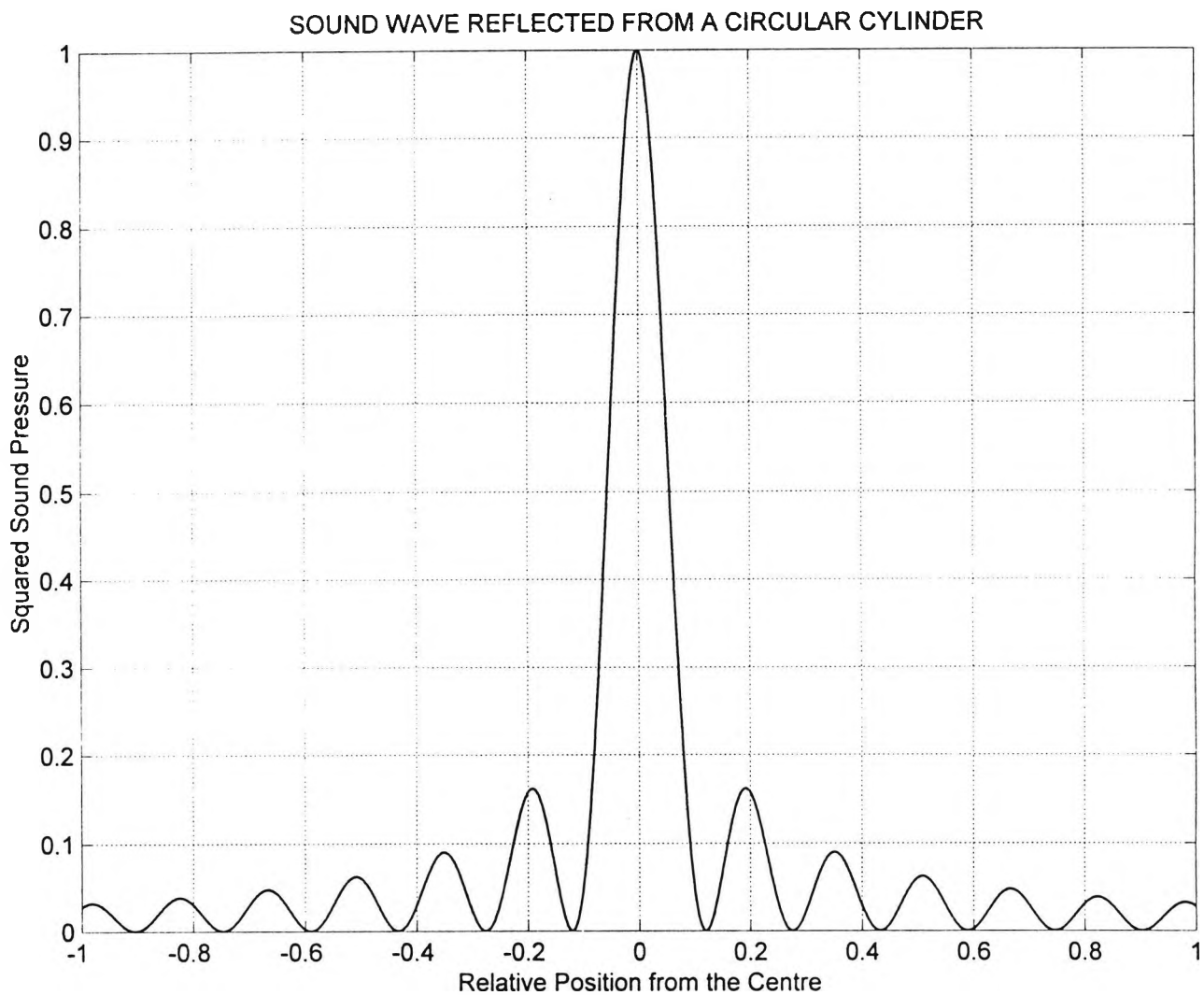
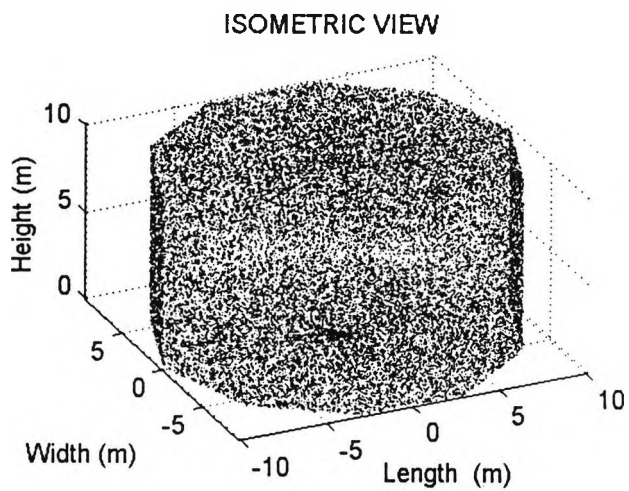
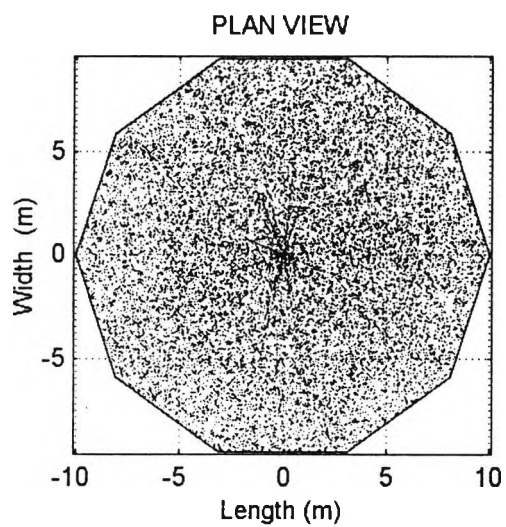
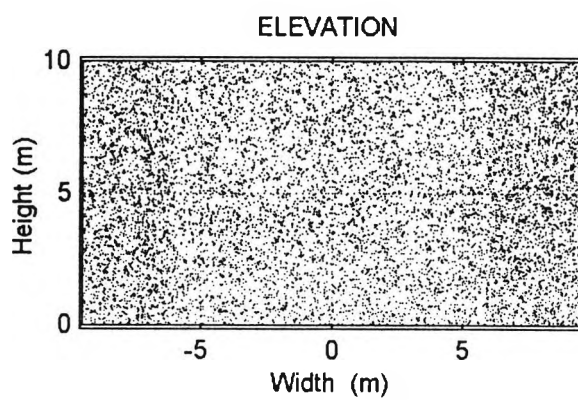
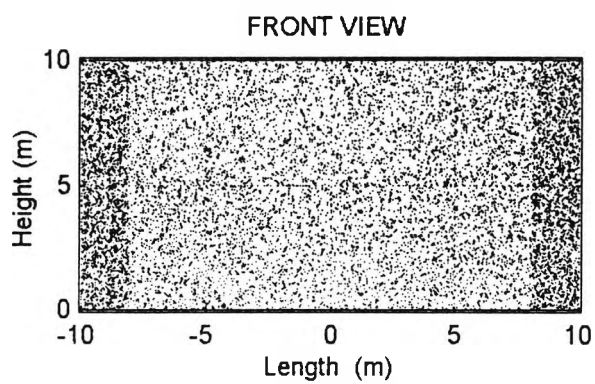


FIGURE 43: CYLINDRICAL BOUNDARY, THEORETICAL RESULTS.



**FIGURE 44: CYLINDRICAL BOUNDARY (FLAT SURFACES),
SOUND PARTICLE SPATIAL DISTRIBUTION.**



**FIGURE 45: CYLINDRICAL BOUNDARY (CURVED SURFACES),
SOUND PARTICLE SPATIAL DISTRIBUTION.**

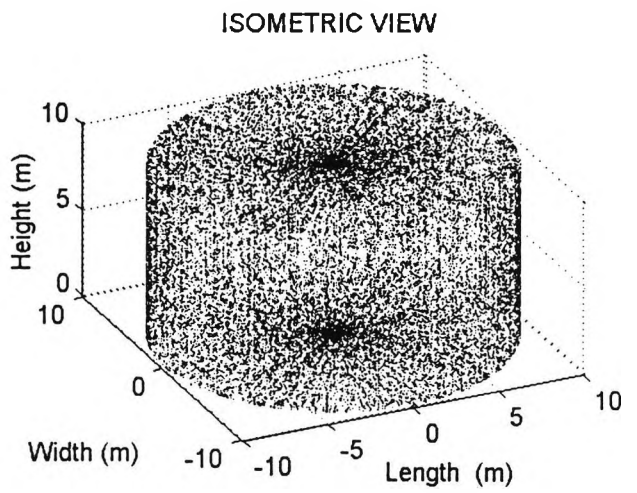
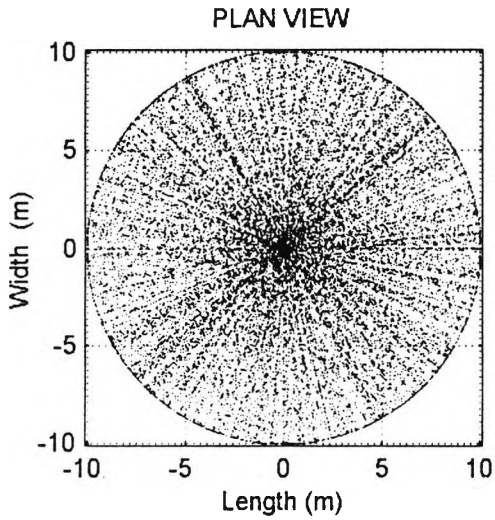
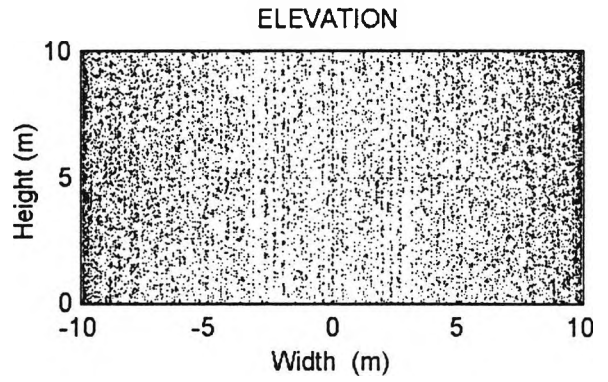
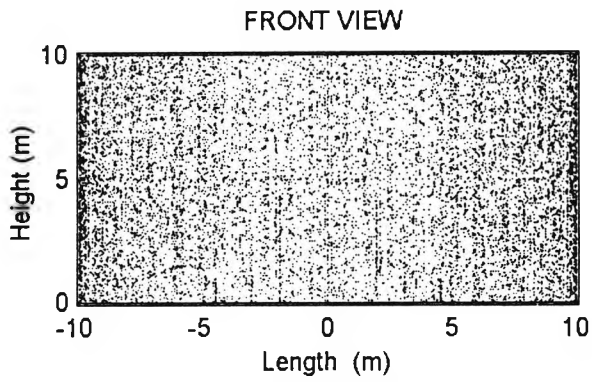


FIGURE 46: CYLINDRICAL BOUNDARY, SOUND ENERGY COMPARISON BETWEEN THE FLAT AND CURVED SURFACE MODELS.

THE CYLINDRICAL BOUNDARY EFFECT

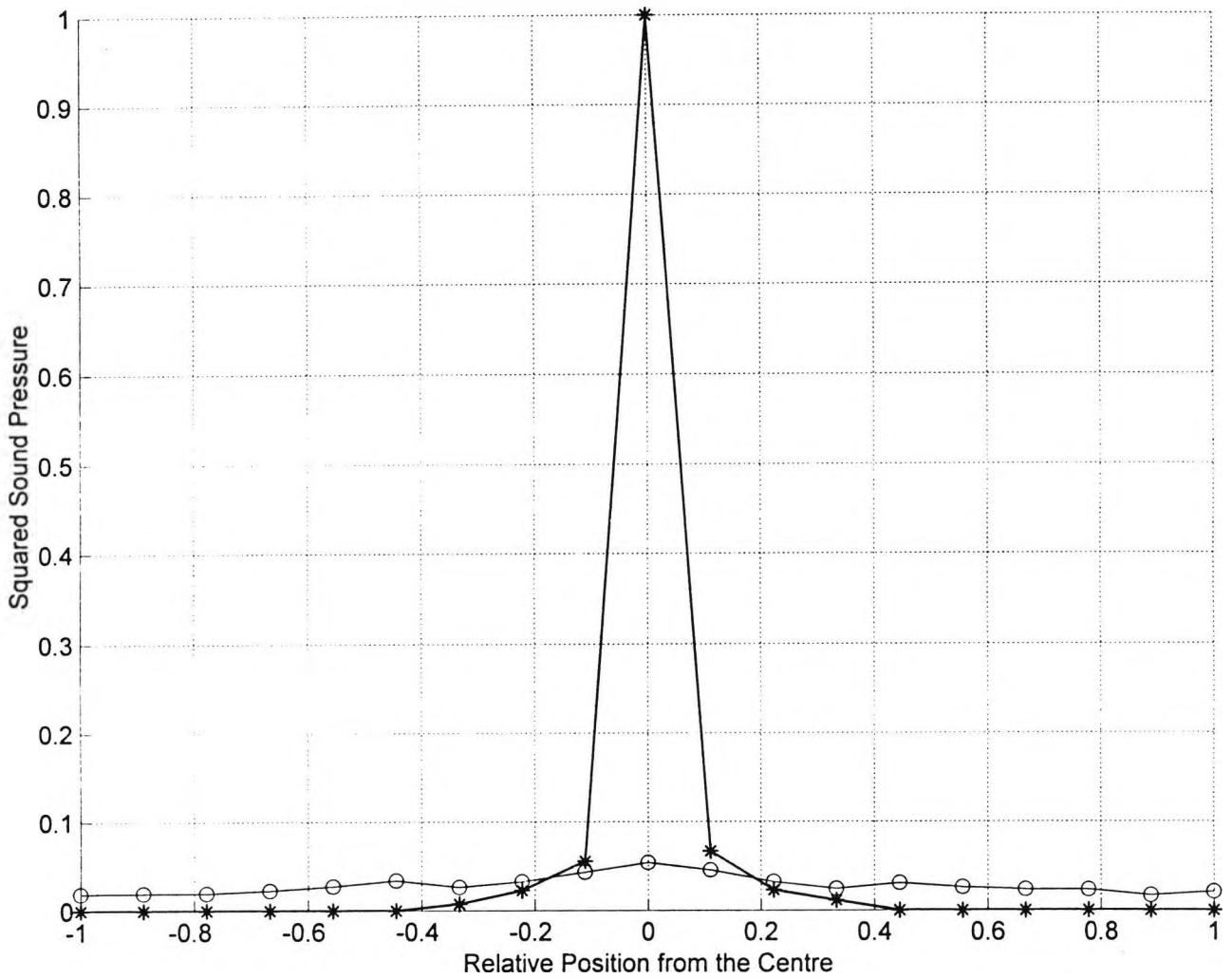


FIGURE 47: BARREL-SHAPED ROOM (FLAT SURFACES),
SOUND PARTICLE SPATIAL DISTRIBUTION.

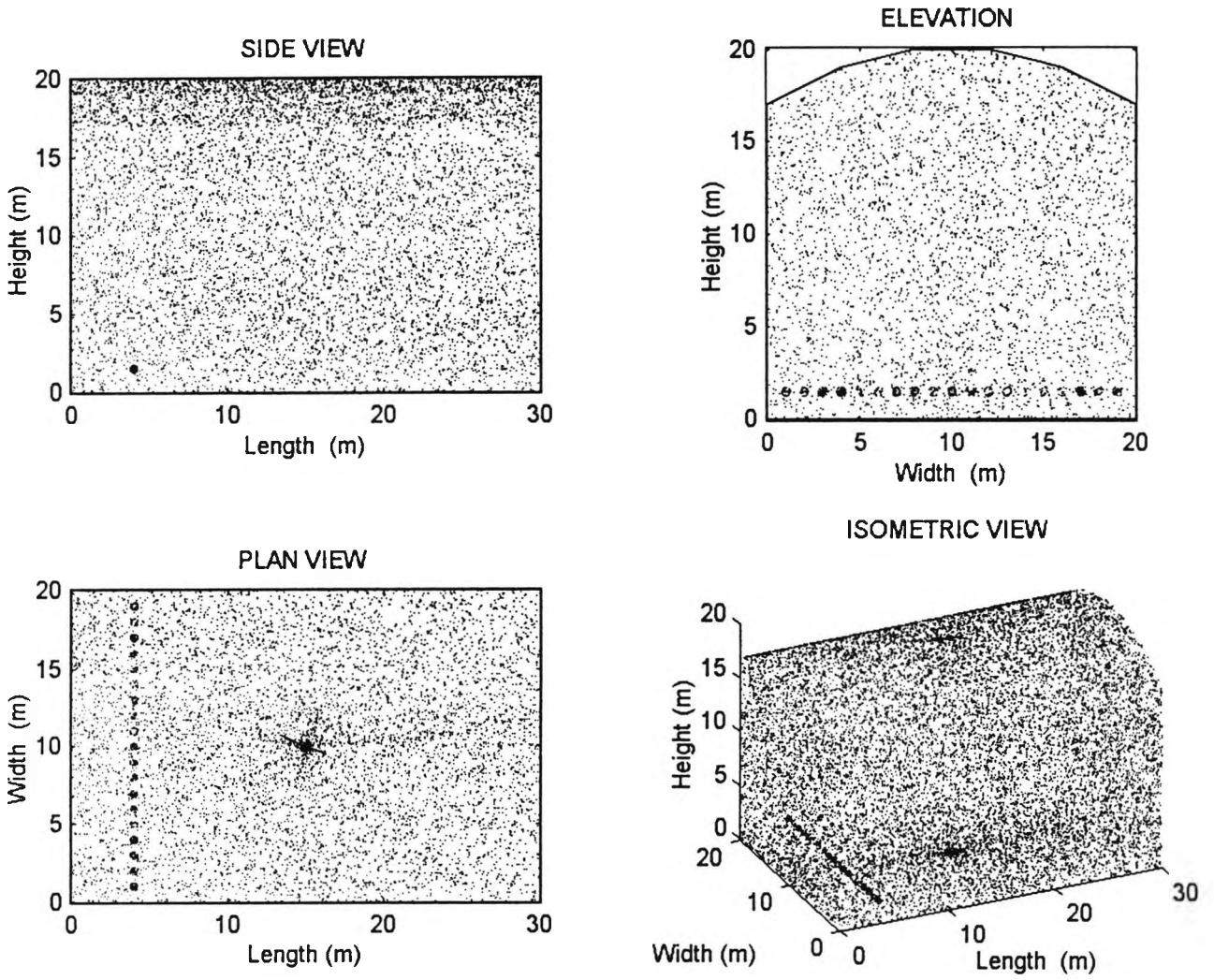
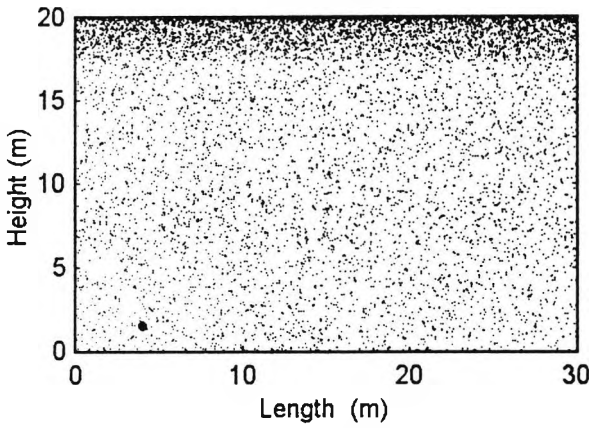
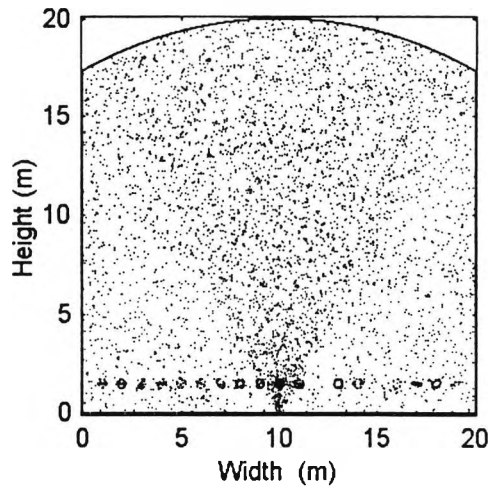


FIGURE 48: BARREL-SHAPED ROOM (CURVED SURFACES),
SOUND PARTICLE SPATIAL DISTRIBUTION.

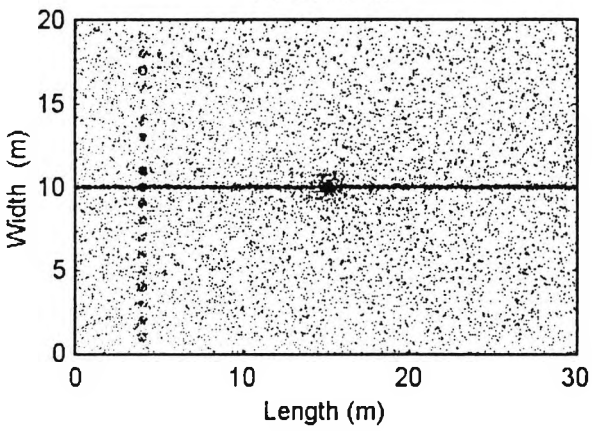
SIDE VIEW



ELEVATION



PLAN VIEW



ISOMETRIC VIEW

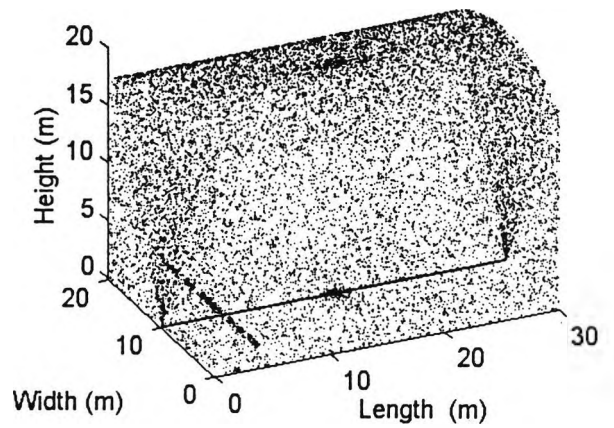


FIGURE 49: BARREL-SHAPED ROOM, SOUND LEVEL COMPARISON BETWEEN THE FLAT AND CURVED SURFACE MODELS.

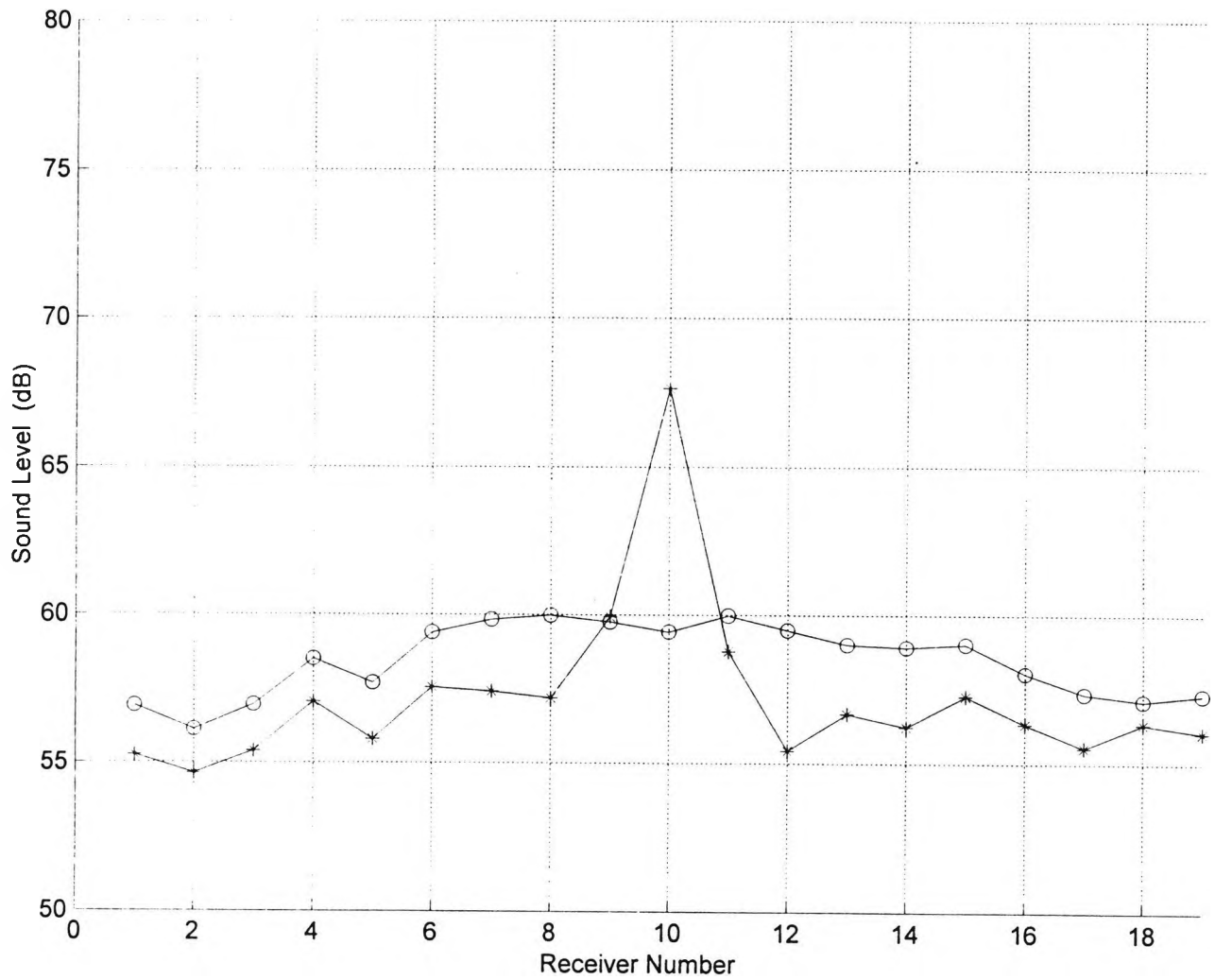


FIGURE 50: ST. PAUL'S CATHEDRAL, CROSS SECTION
LOOKING FROM THE EAST AND ISOMETRIC VIEW.

ST. PAUL'S CATHEDRAL
LONDON

PLATE X

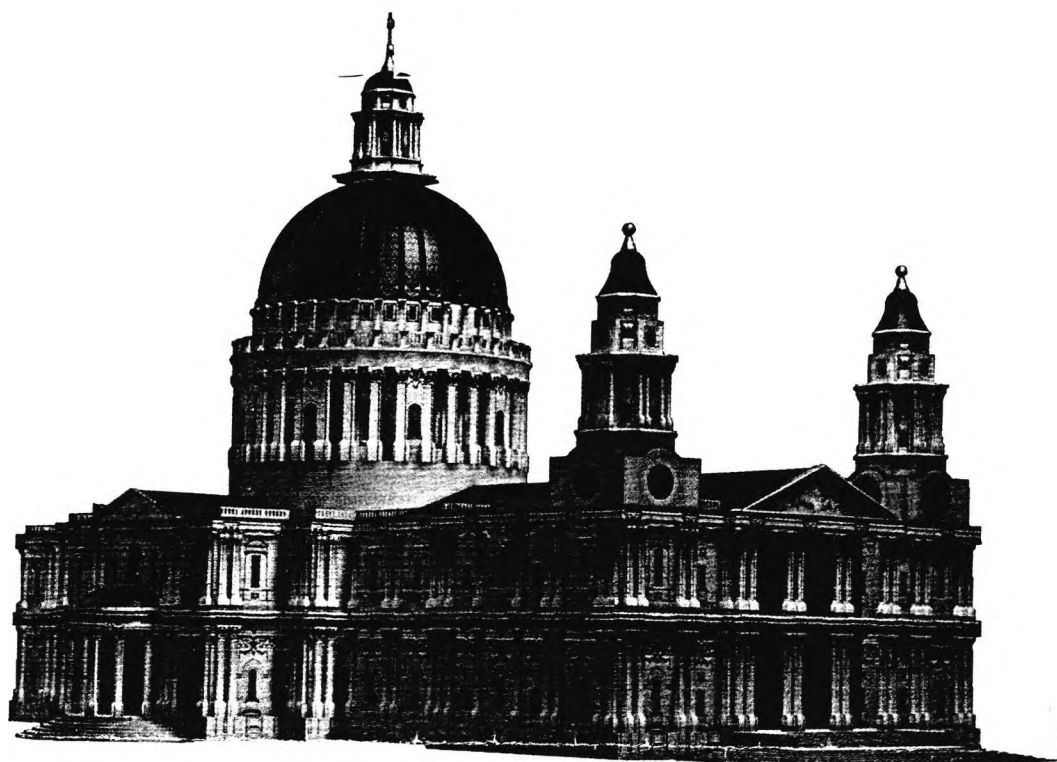
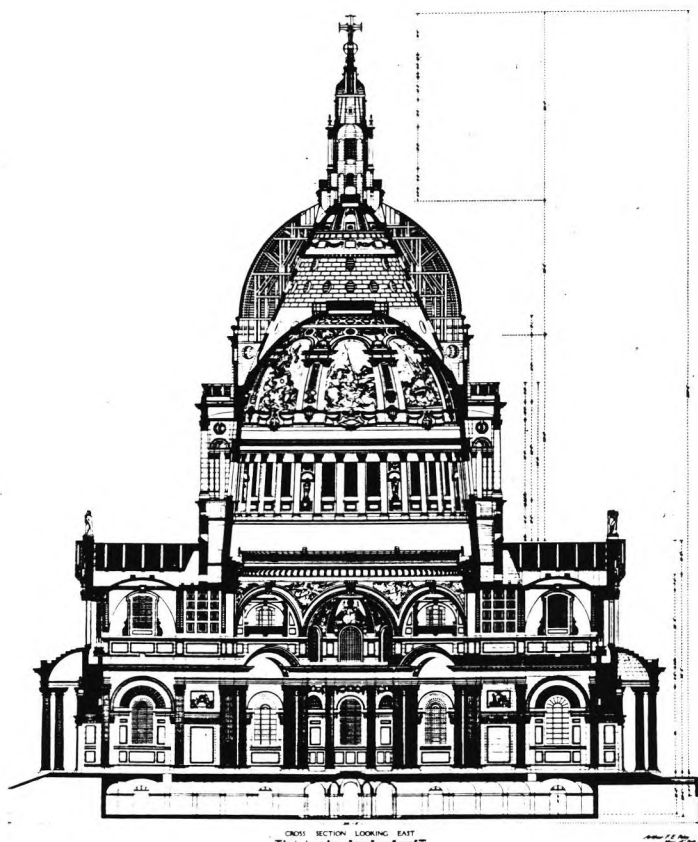


FIGURE 51: ST. PAUL'S CATHEDRAL, SECTIONAL ISOMETRIC VIEW.

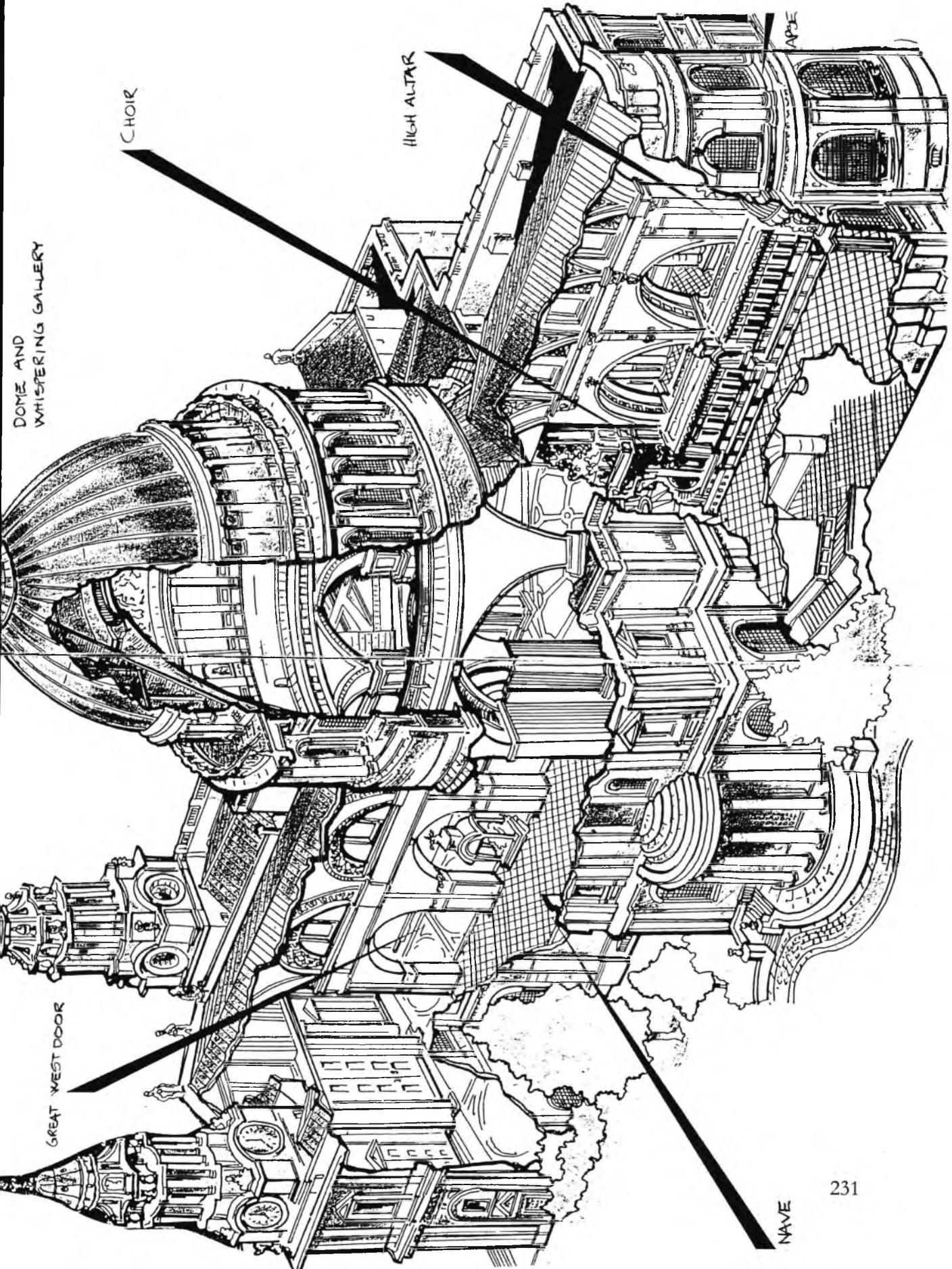
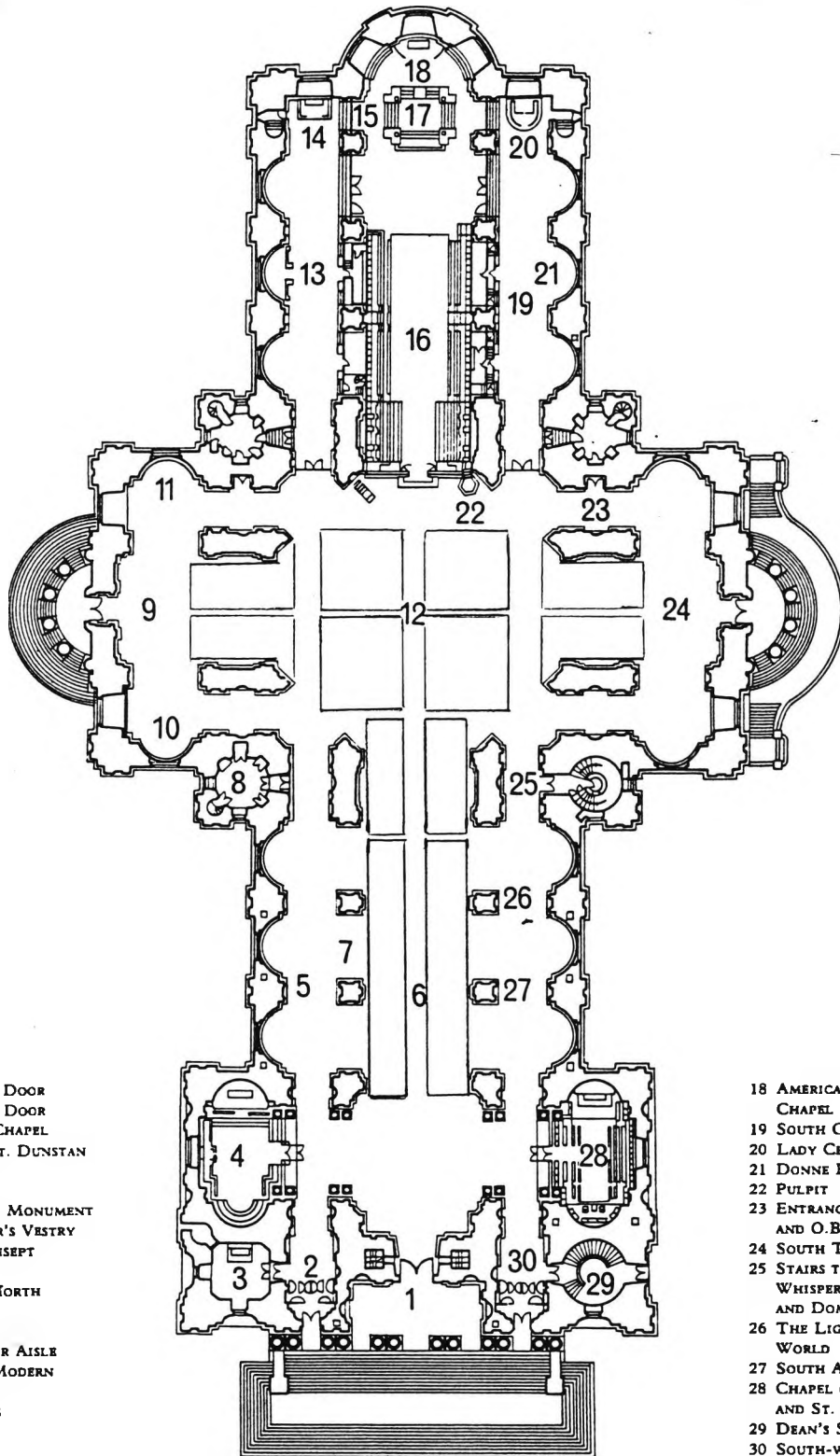


FIGURE 52: ST. PAUL'S CATHEDRAL, PLAN VIEW INDICATING THE VARIOUS PARTS OF THE CATHEDRAL (THE RECTANGLES INDICATE THE SEATING AREAS).



- 1 GREAT WEST DOOR
- 2 NORTH-WEST DOOR
- 3 ALL SOULS' CHAPEL
- 4 CHAPEL OF ST. DUNSTAN
- 5 NORTH AISLE
- 6 NAVE
- 7 WELLINGTON MONUMENT
- 8 LORD MAYOR'S VESTRY
- 9 NORTH TRANSEPT
- 10 THE FONT
- 11 CHAPEL IN NORTH TRANSEPT
- 12 THE DOME
- 13 NORTH CHOIR AISLE
- 14 CHAPEL OF MODERN MARTYRS
- 15 TIJOU GATES
- 16 CHOIR
- 17 HIGH ALTAR

- 18 AMERICAN MEMORIAL CHAPEL
- 19 SOUTH CHOIR AISLE
- 20 LADY CHAPEL
- 21 DONNE EFFIGY
- 22 PULPIT
- 23 ENTRANCE TO CRYPT AND O.B.E. CHAPEL
- 24 SOUTH TRANSEPT
- 25 STAIRS TO LIBRARY, WHISPERING GALLERY AND DOME
- 26 THE LIGHT OF THE WORLD
- 27 SOUTH AISLE
- 28 CHAPEL OF ST. MICHAEL AND ST. GEORGE
- 29 DEAN'S STAIRCASE
- 30 SOUTH-WEST DOOR

FIGURE 53: ST. PAUL'S CATHEDRAL, SOUND PARTICLE SPATIAL DISTRIBUTION.

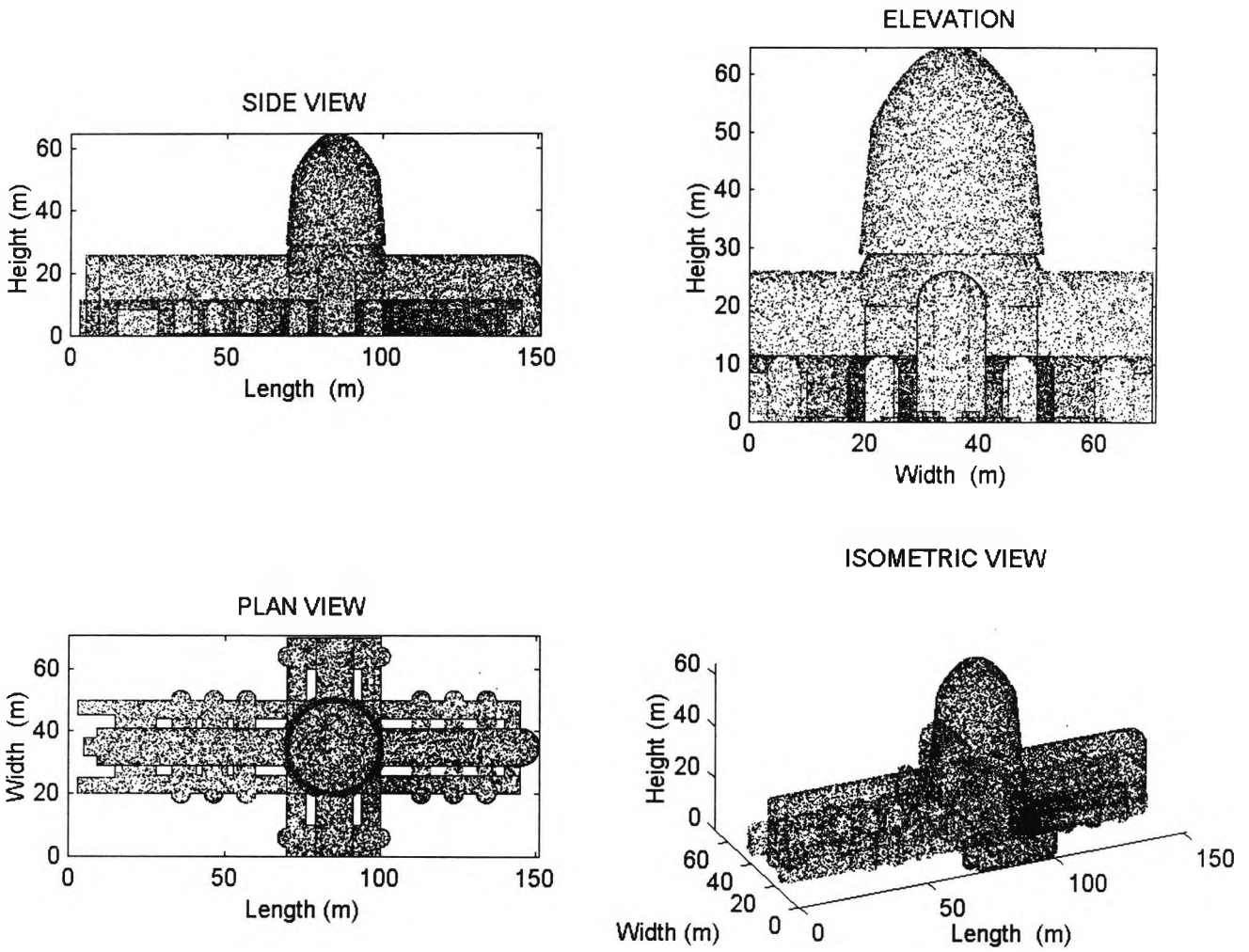


**FIGURE 54: PRELIMINARY MODEL OF ST. PAUL'S CATHEDRAL
MADE IN AUTOCAD.**

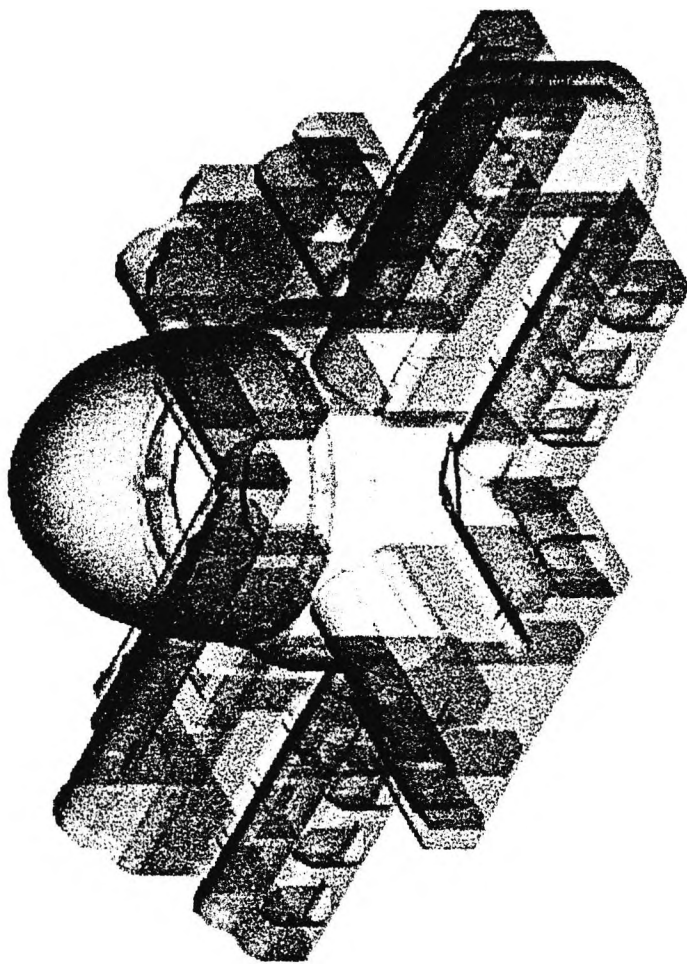


FIGURE 55: ST. PAUL'S CATHEDRAL, SOUND PATH ANALYSIS.

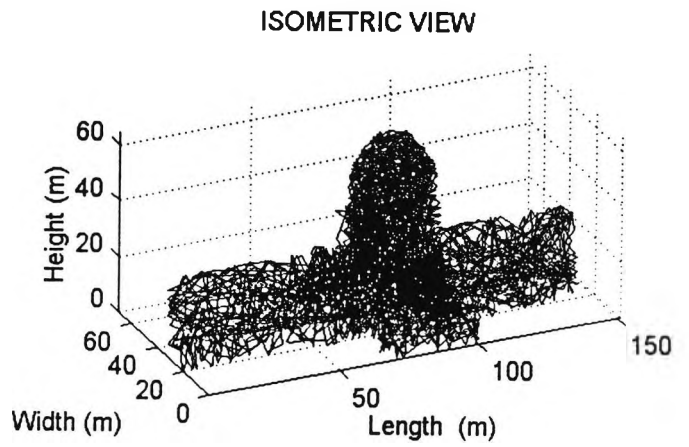
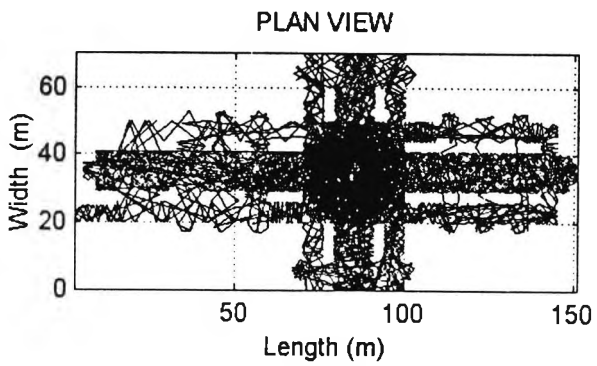
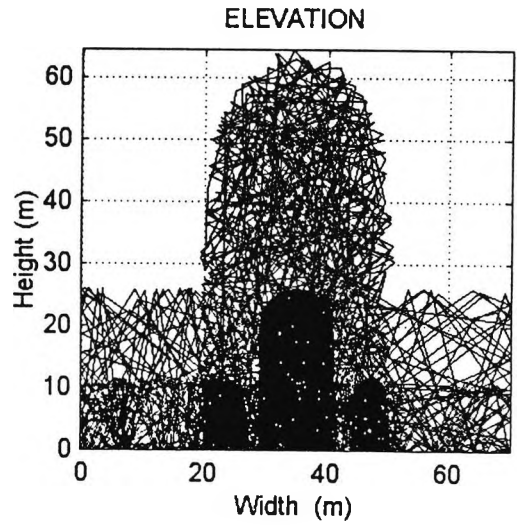
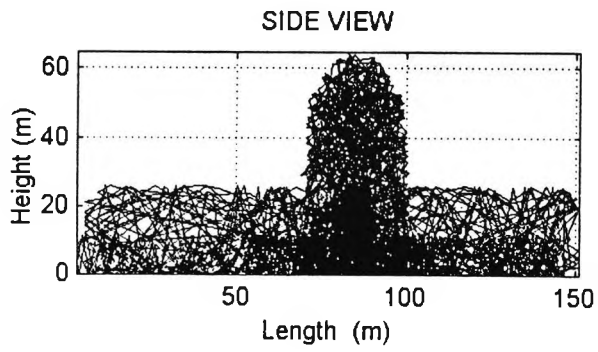


FIGURE 56: ST. PAUL'S CATHEDRAL, AVERAGE ENERGY DECAY WHEN THE CATHEDRAL IS EMPTY.

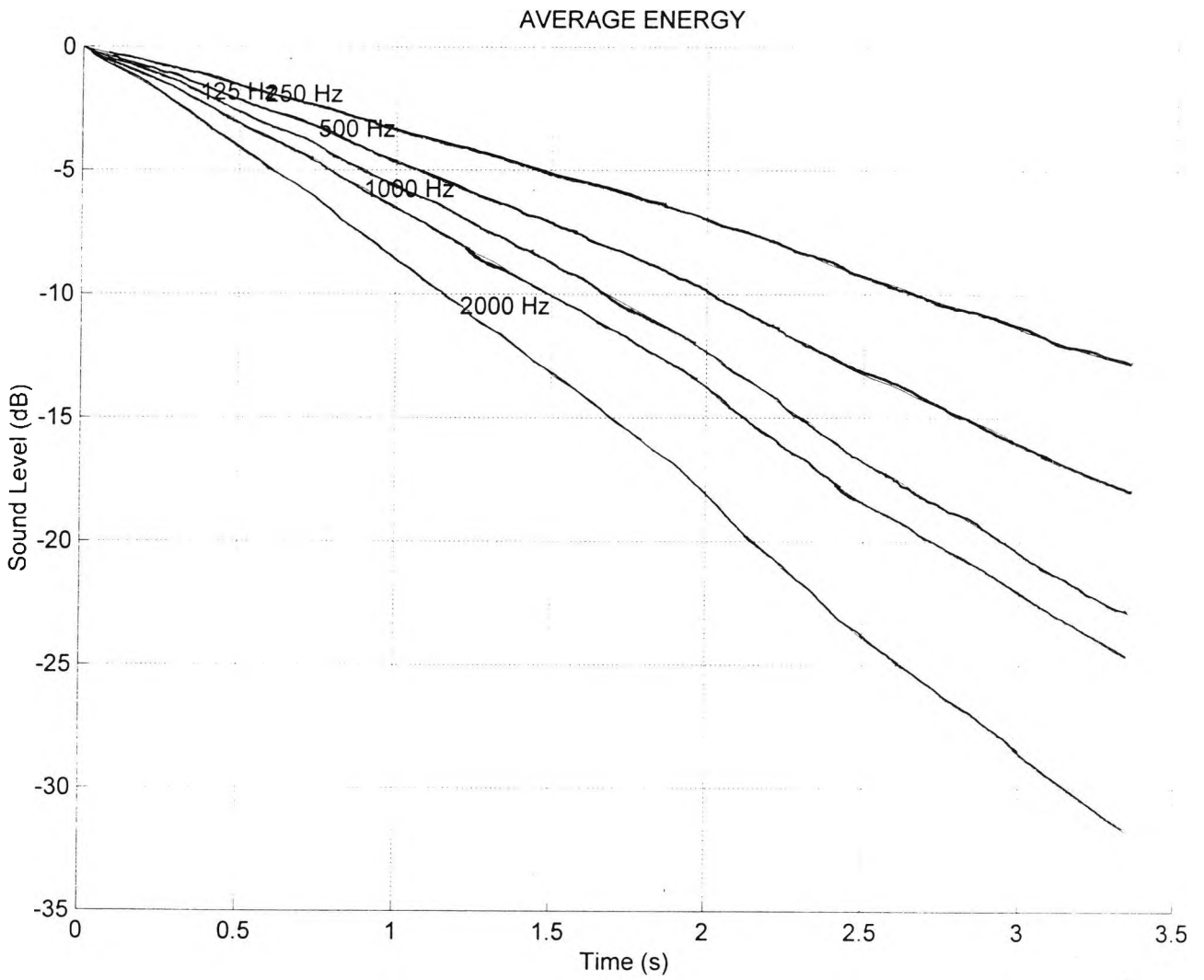


FIGURE 57: ST. PAUL'S CATHEDRAL, AVERAGE ENERGY DECAY WHEN THE CATHEDRAL IS FULL.

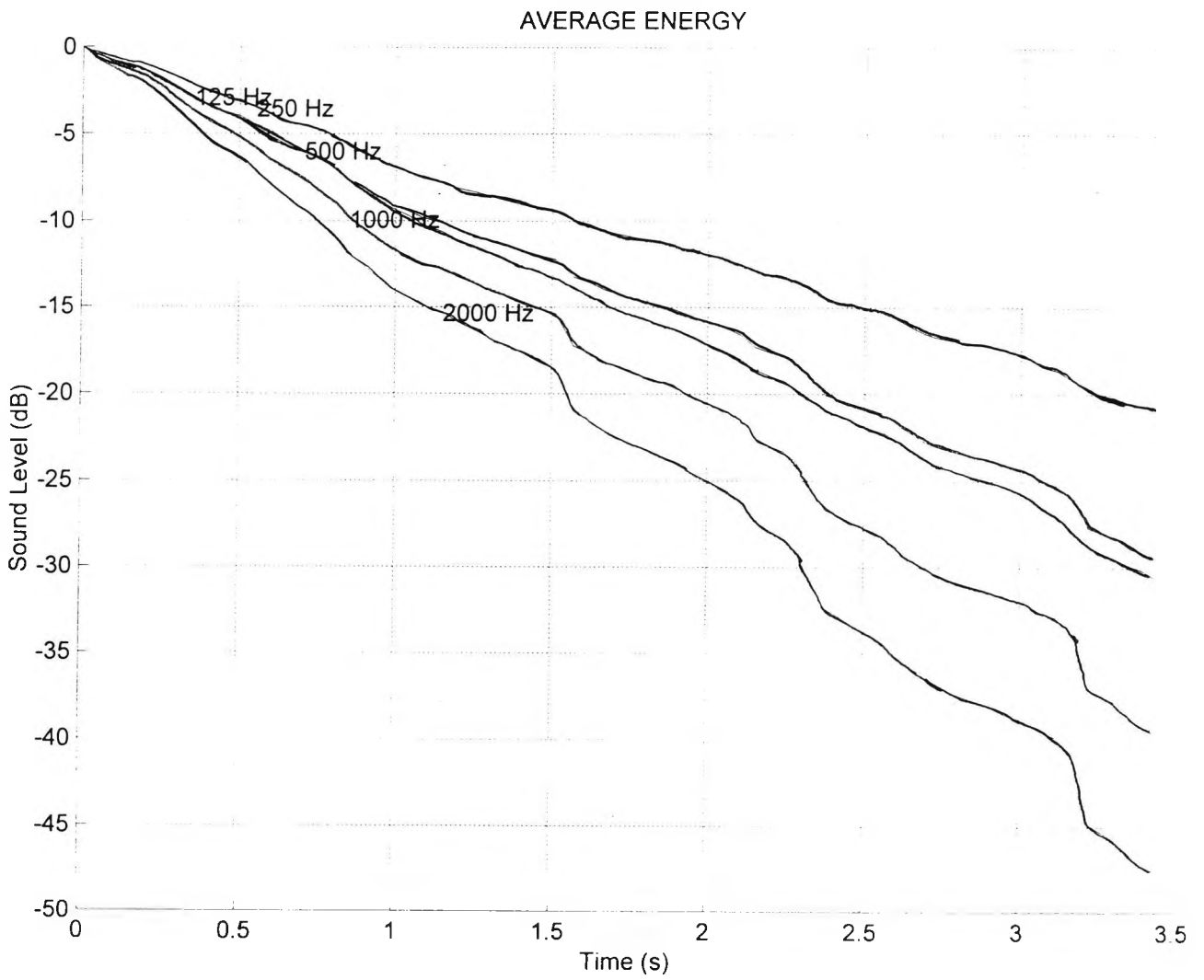


FIGURE 58: ST. PAUL'S CATHEDRAL, COMPARISON BETWEEN SIMULATED AND MEASURED REVERBERATION RESULTS (FULL AND EMPTY).

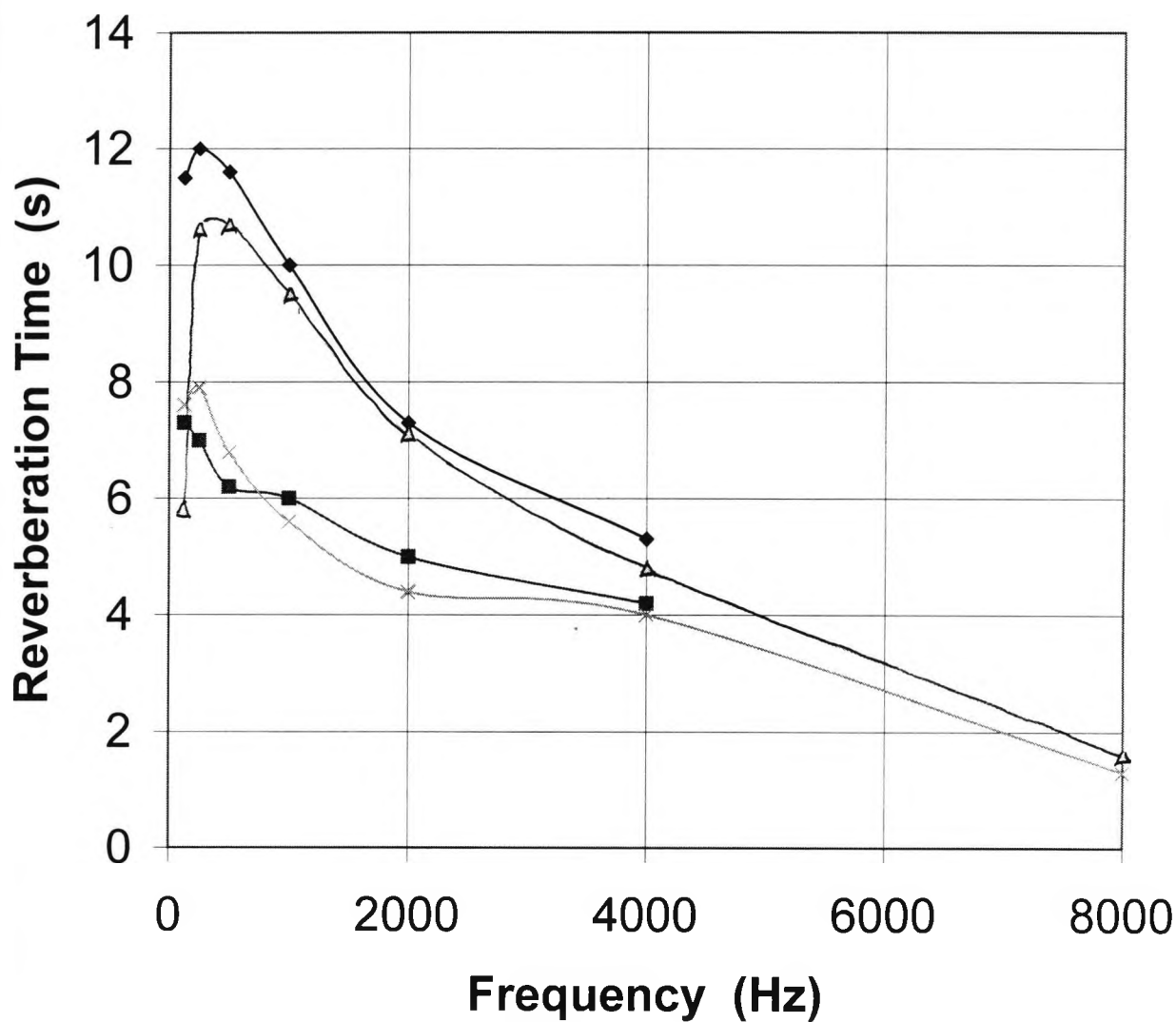


FIGURE 59: ST. PAUL'S CATHEDRAL, SOURCE AND RECEIVER POSITIONS FOR THE REVERBERATION TEST.

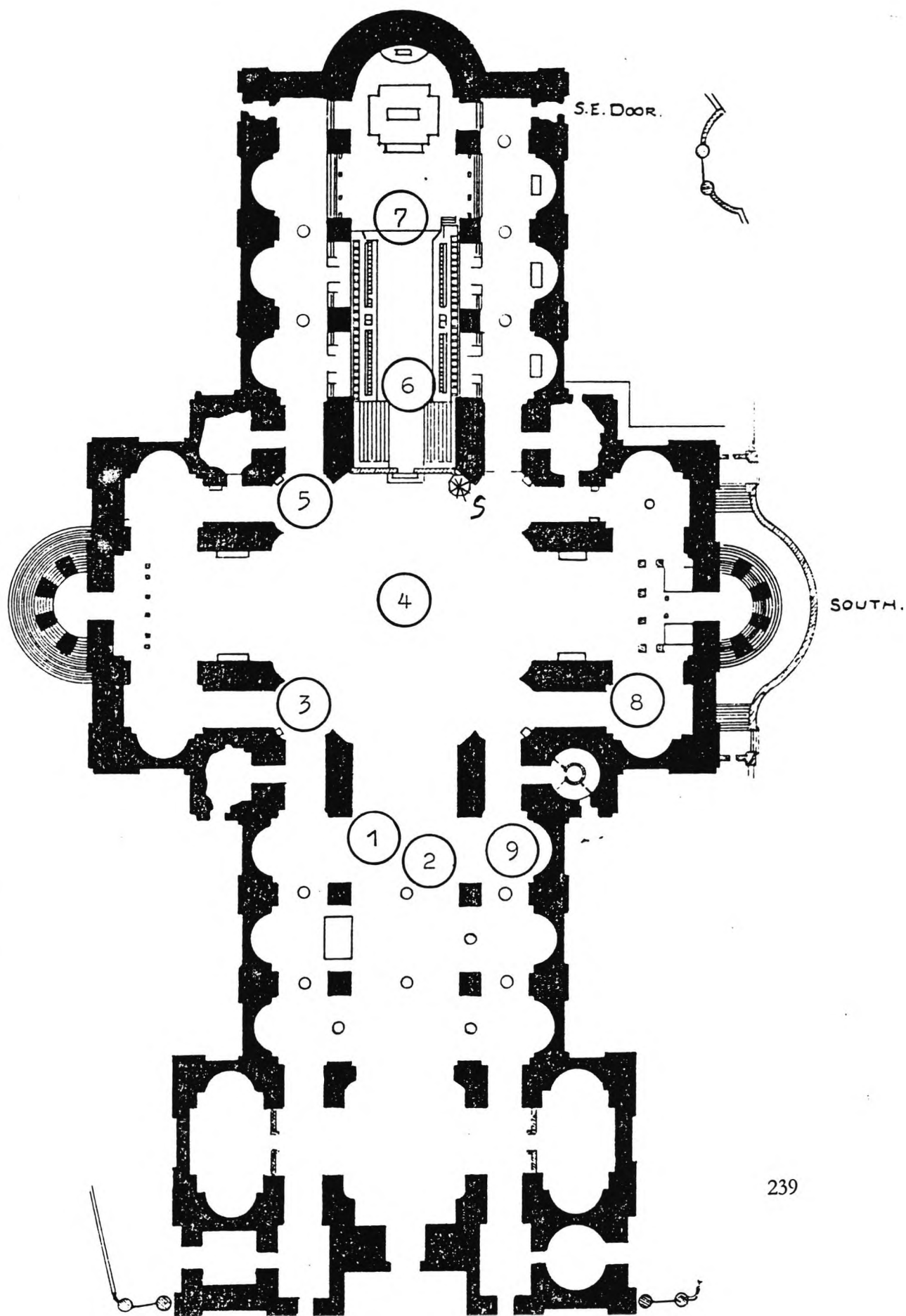


FIGURE 60: ST. PAUL'S CATHEDRAL, SAMPLE MEASURED REVERBERATION TRACES FOR RECEIVER 4 AT 1 KHZ.

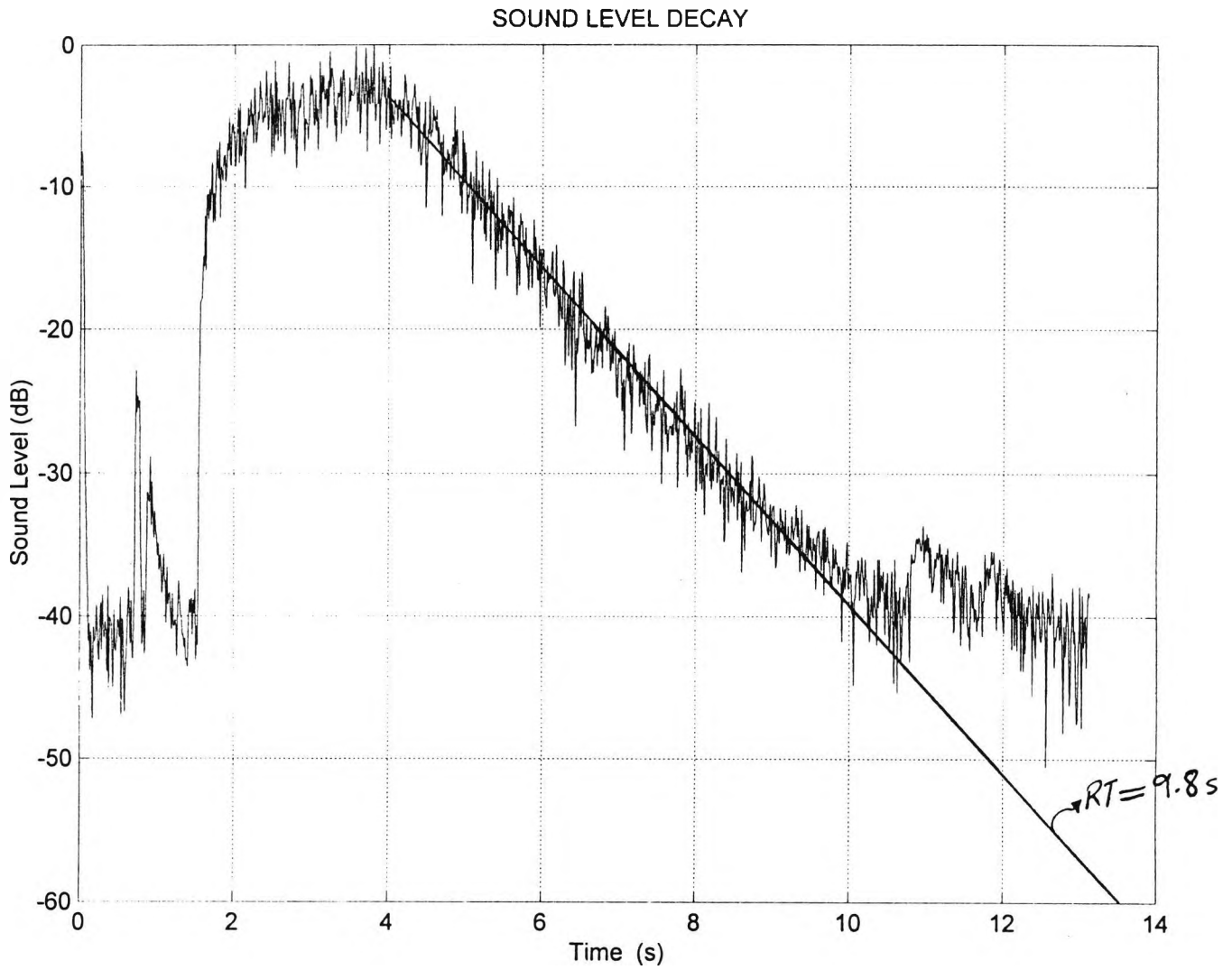
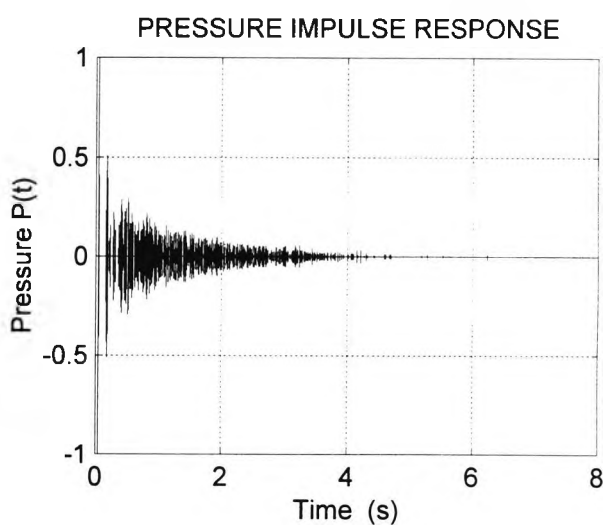
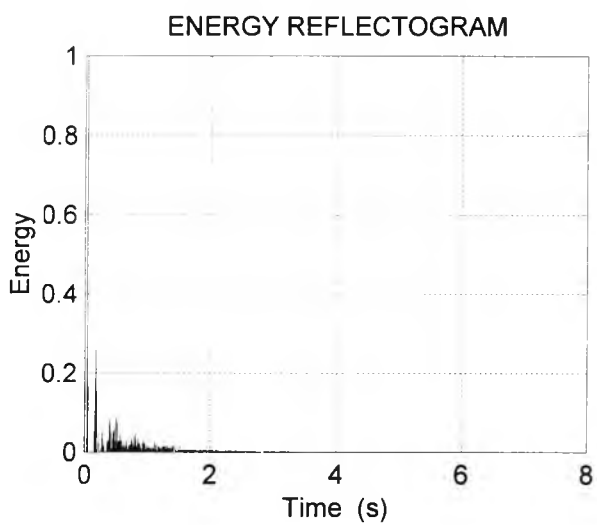
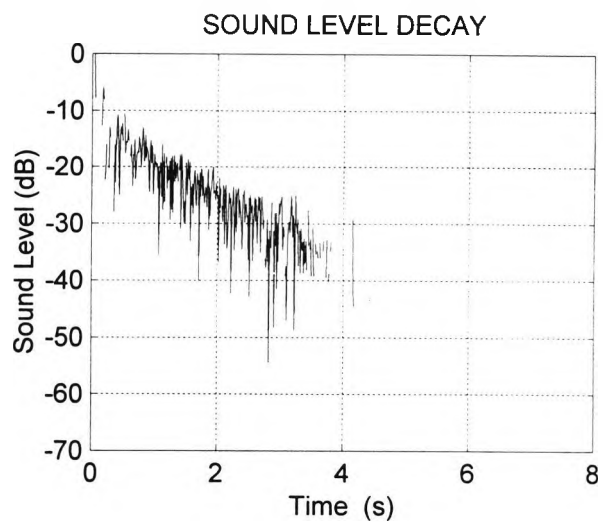
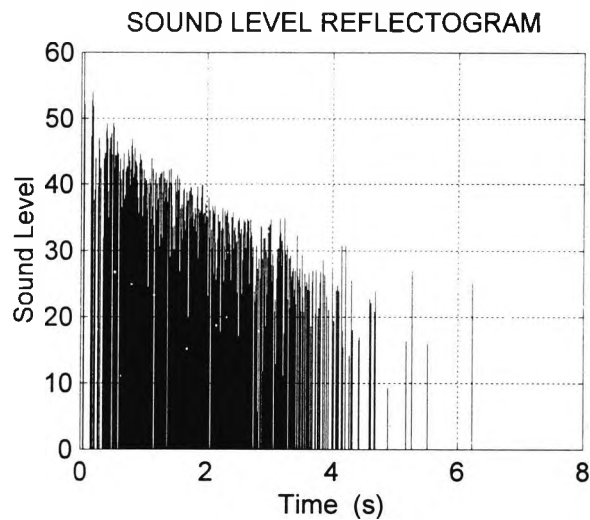


FIGURE 61: ST. PAUL'S CATHEDRAL, PREDICTED RESPONSE FOR RECEIVER 4 AT 1 KHZ.



**FIGURE 62: ST. PAUL'S CATHEDRAL, PREDICTED,
INTEGRATED IMPULSE RESPONSE FOR RECEIVER 4 AT 1
KHZ.**

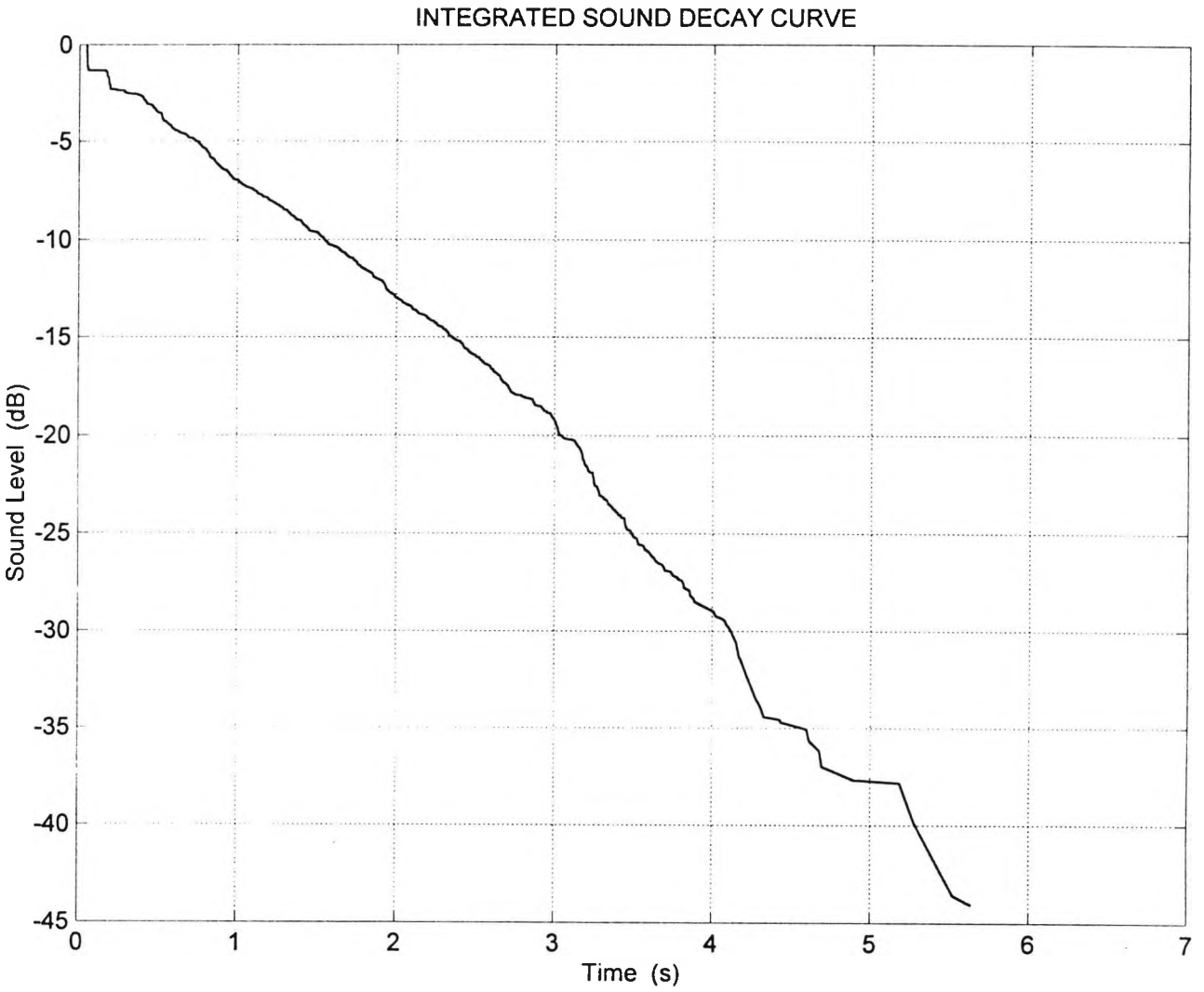


FIGURE 63: ST. PAUL'S CATHEDRAL, SOUNRD DECAy CURVE
USING REGRESSION ANALYSIS FOR RECEIVER 4 AT 2 KHZ.

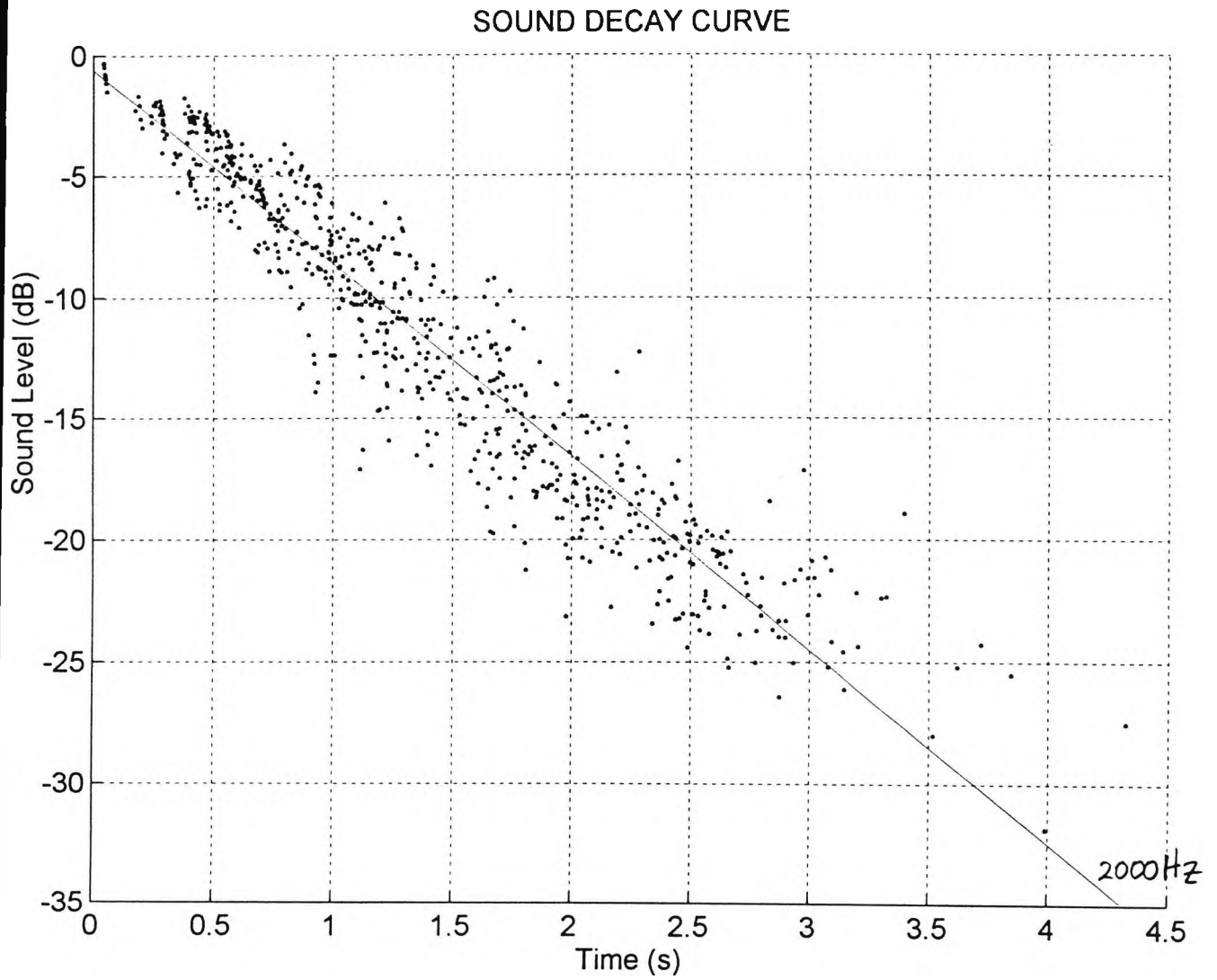


FIGURE 64: ST. PAUL'S CATHEDRAL, REVERBERATION TIME WITH RESPECT TO FREQUENCY FOR RECEIVER 1, MEASURED AND SIMULATED RESULTS.

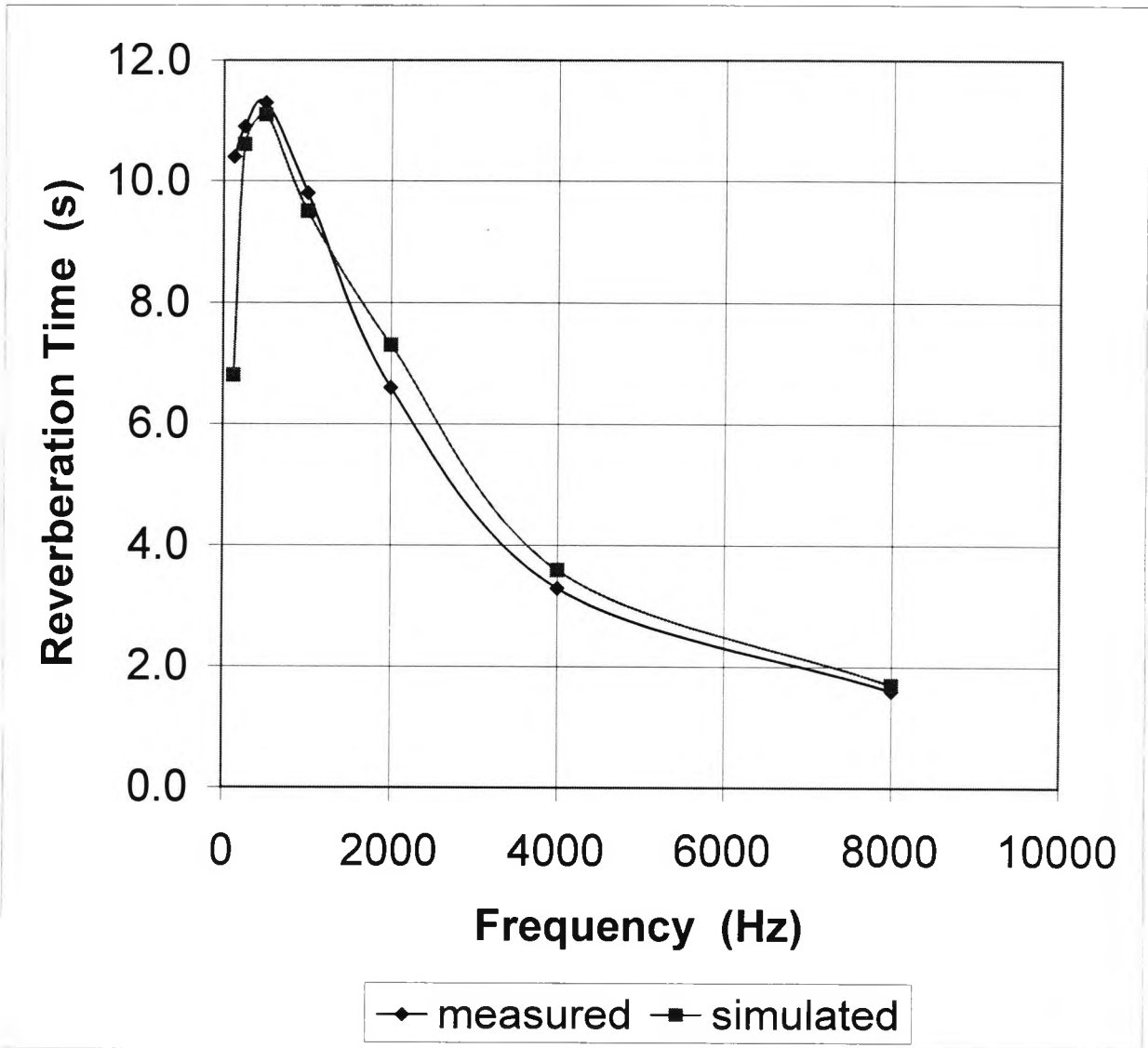


FIGURE 65: ST. PAUL'S CATHEDRAL, REVERBERATION TIME WITH RESPECT TO FREQUENCY FOR RECEIVER 4, MEASURED AND SIMULATED RESULTS.

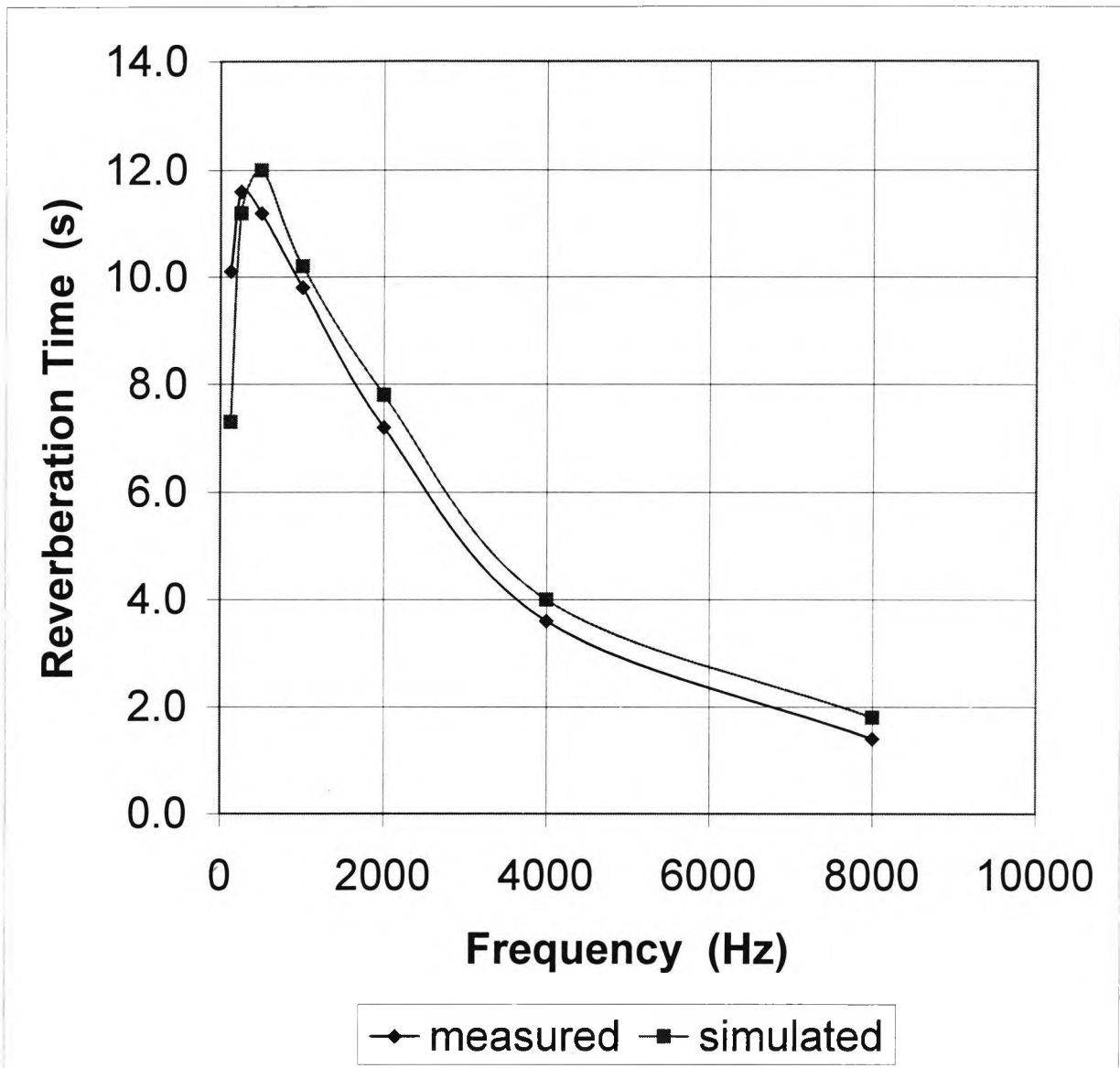


FIGURE 66: ST. PAUL'S CATHEDRAL, SOURCE AND RECEIVER POSITIONS FOR THE SOUND PRESSURE LEVEL TEST.

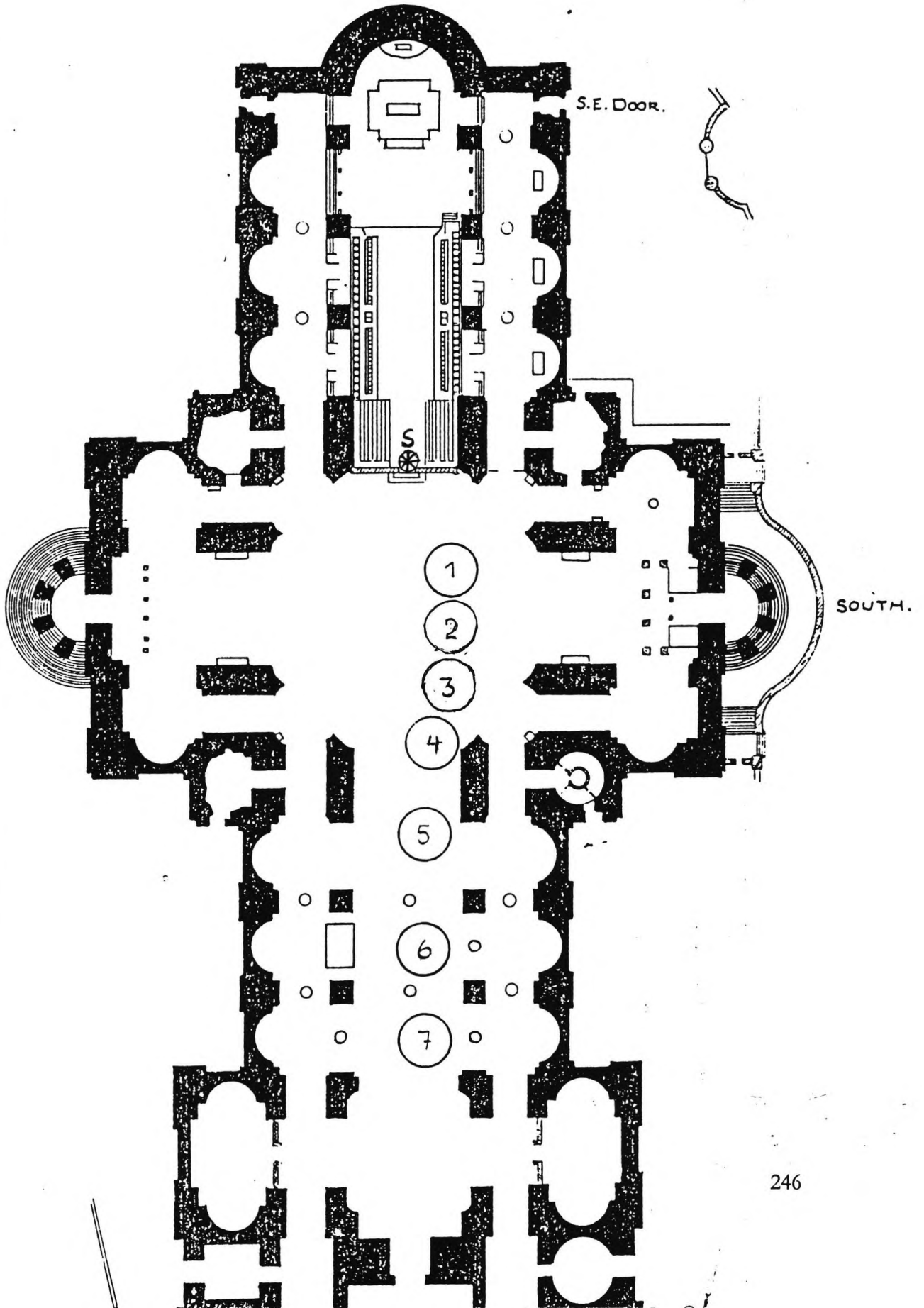


FIGURE 67: ST. PAUL'S CATHEDRAL, MEASURED SOUND PRESSURE LEVEL RESULTS.

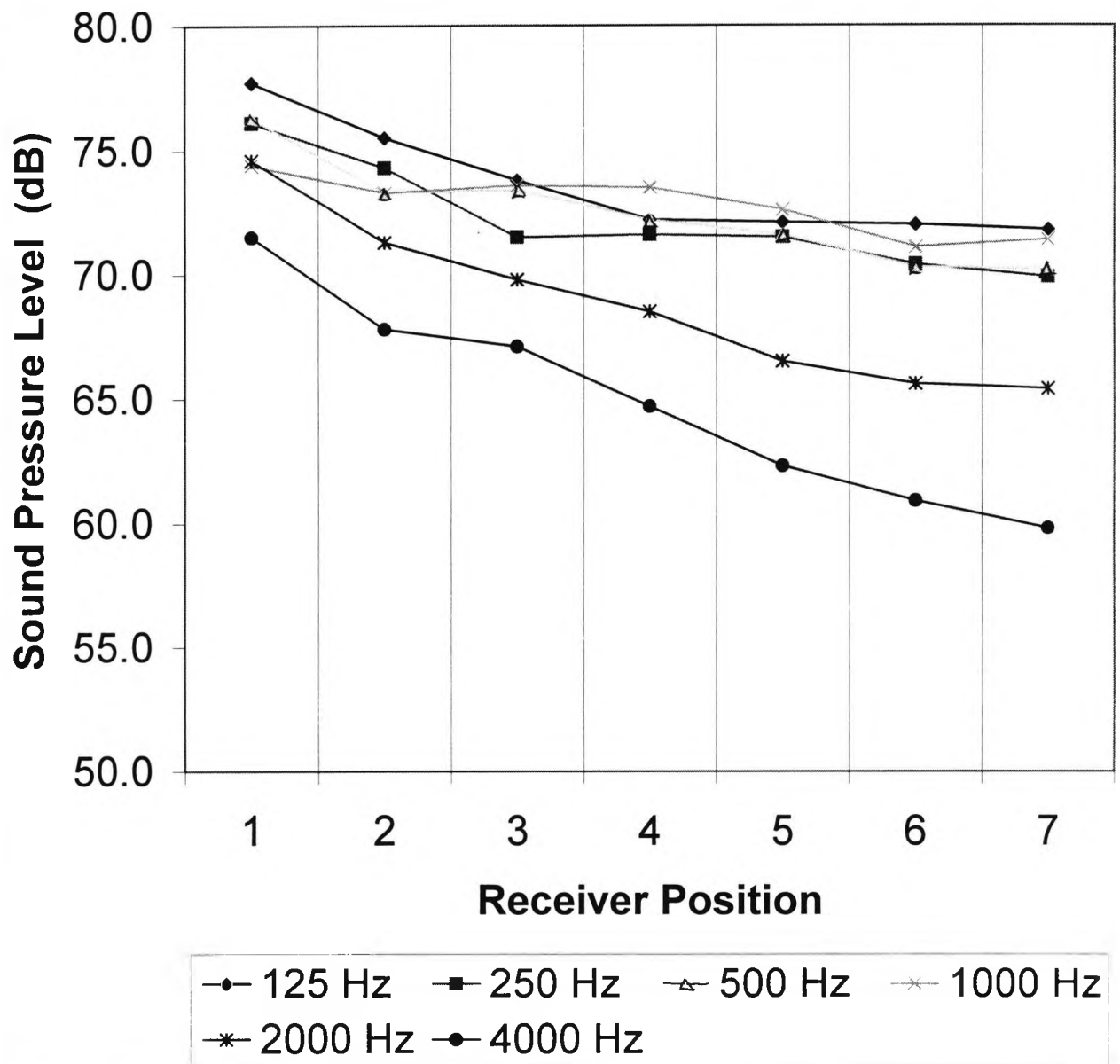


FIGURE 68: ST. PAUL'S CATHEDRAL, PREDICTED SOUND PRESSURE LEVEL RESULTS.

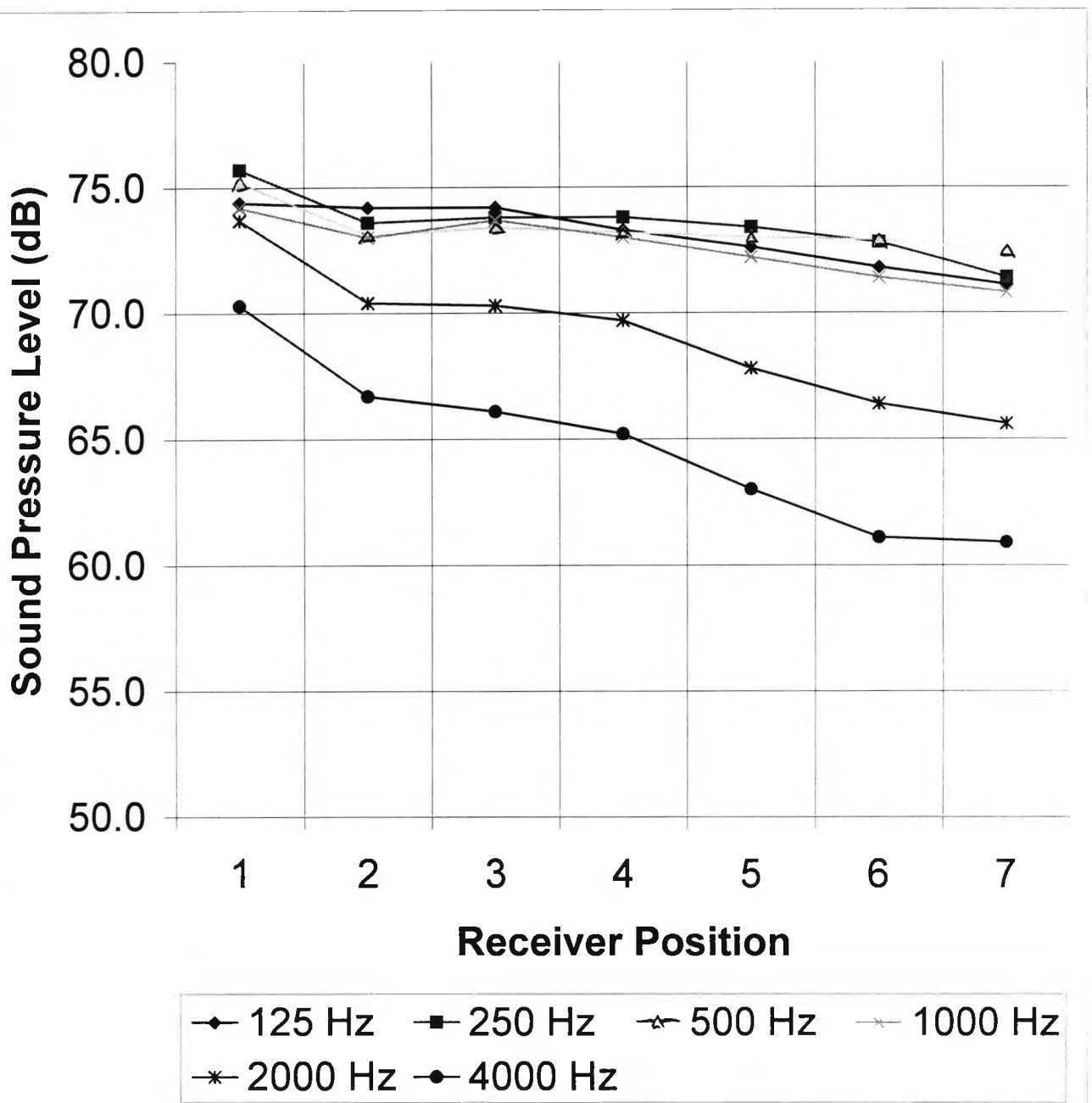


FIGURE 69: ST. PAUL'S CATHEDRAL, SOURCE AND RECEIVER POSITIONS FOR THE SPEECH INTELLIGIBILITY TEST.

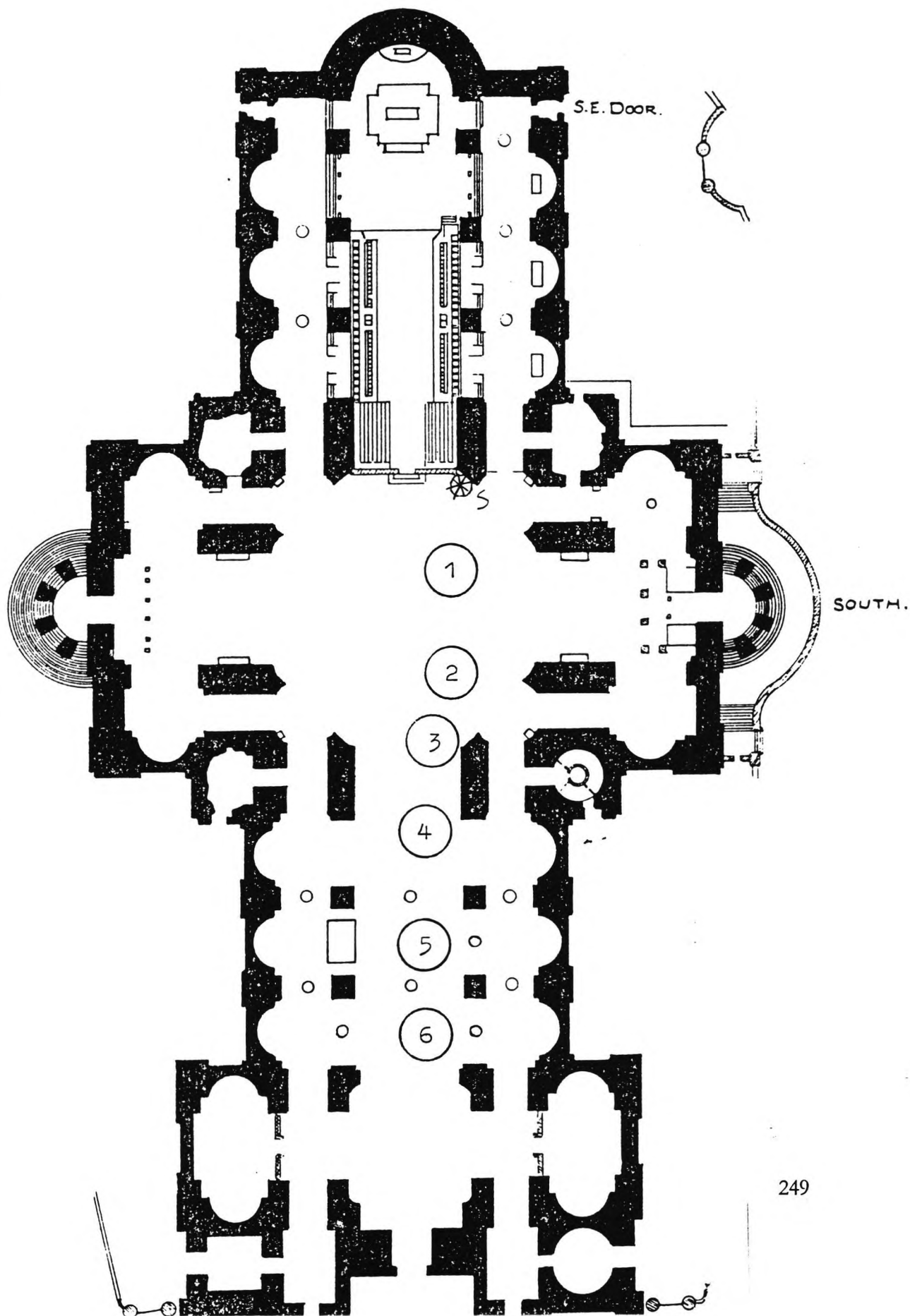


FIGURE 70: ST. PAUL'S CATHEDRAL, SPEECH INTELLIGIBILITY, COMPARISON BETWEEN A SUBJECTIVE TEST, RASTI MEASUREMENTS, AND COMPUTER RESULTS.

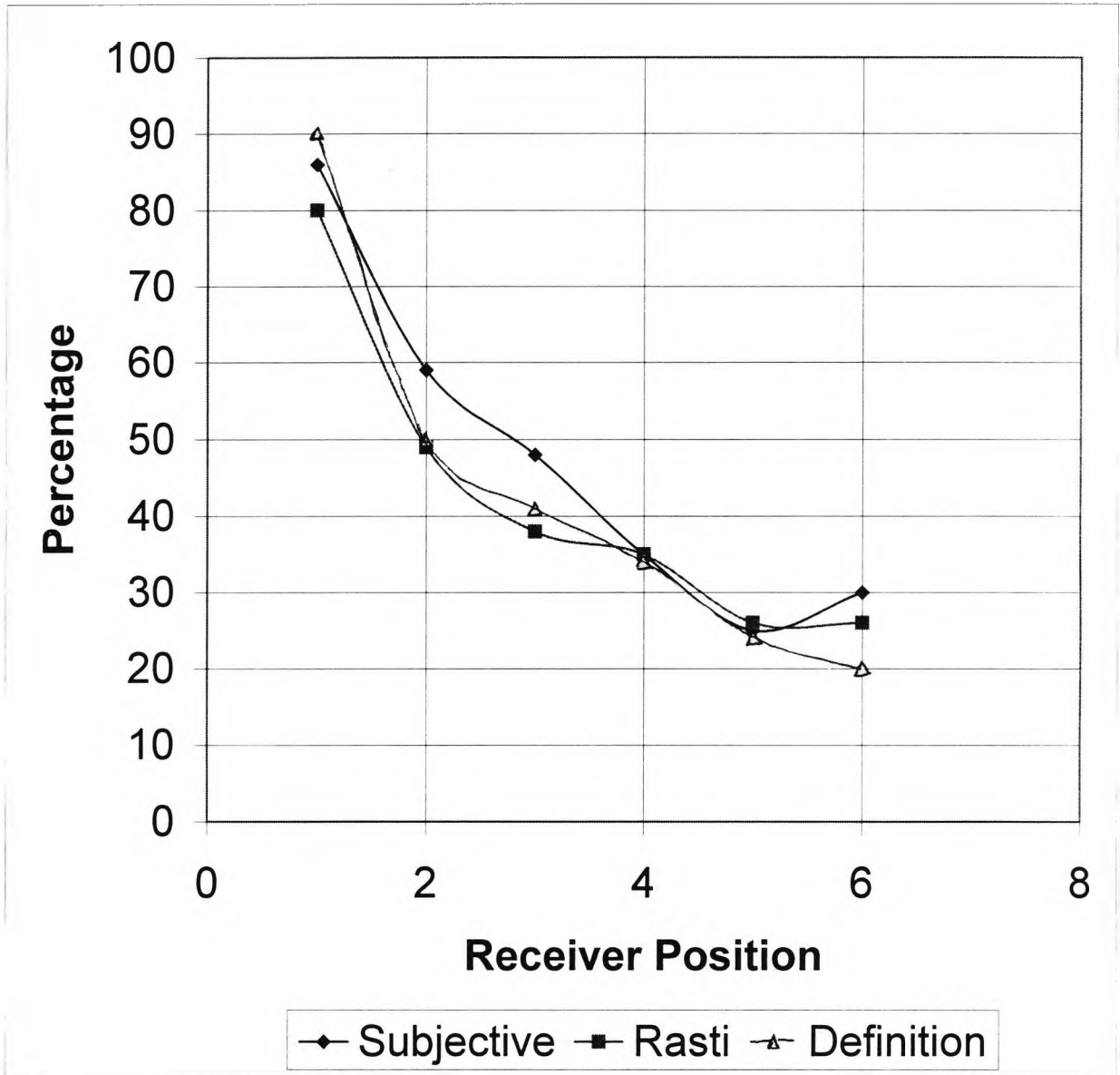


FIGURE 71: ST. PAUL'S CATHEDRAL, SOURCE AND RECEIVER POSITIONS FOR THE COUPLED SPACES TEST.

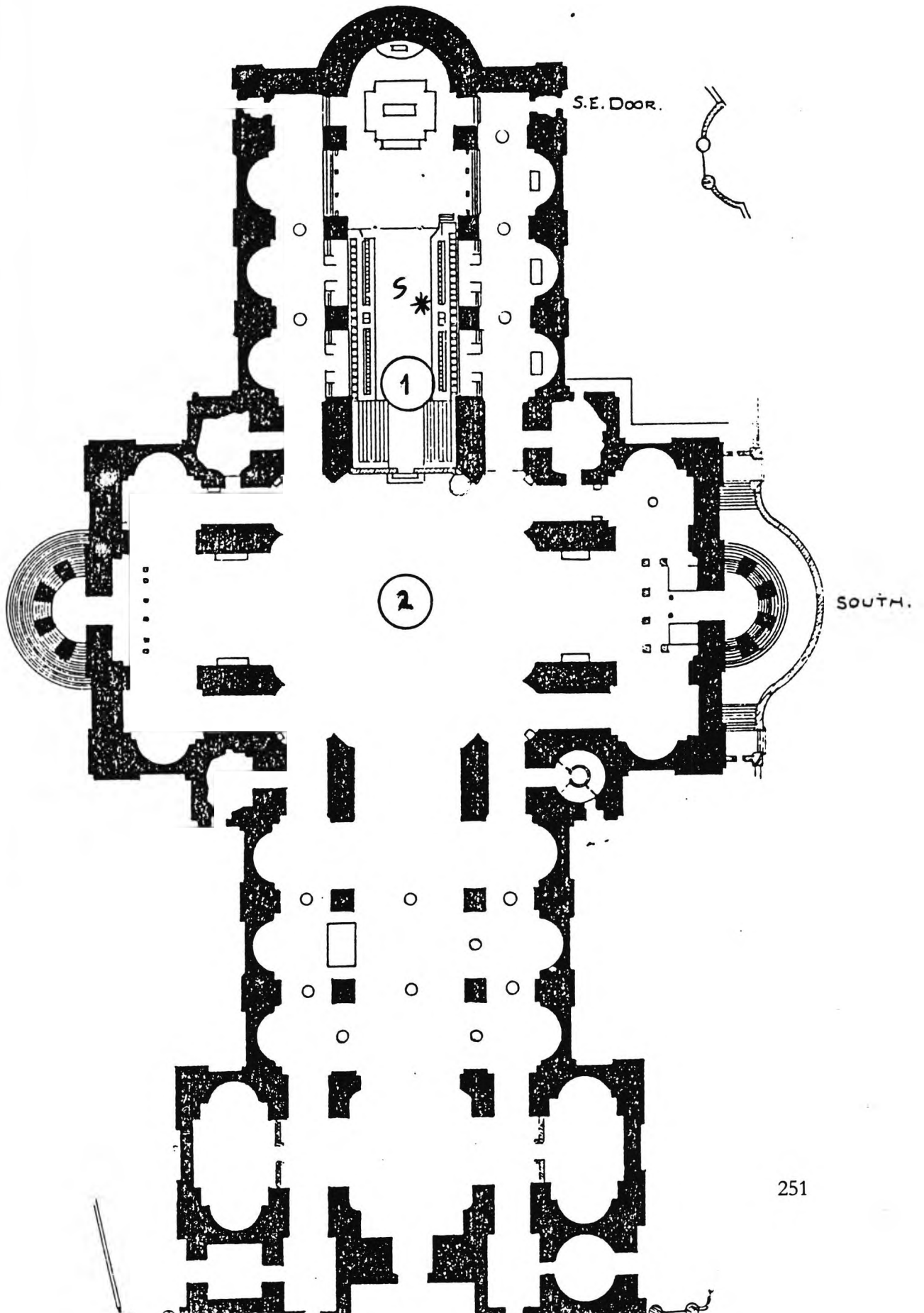


FIGURE 72: ST. PAUL'S CATHEDRAL, MEASURED RESPONSE FOR THE RECEIVER IN THE CHOIR (1 KHZ).

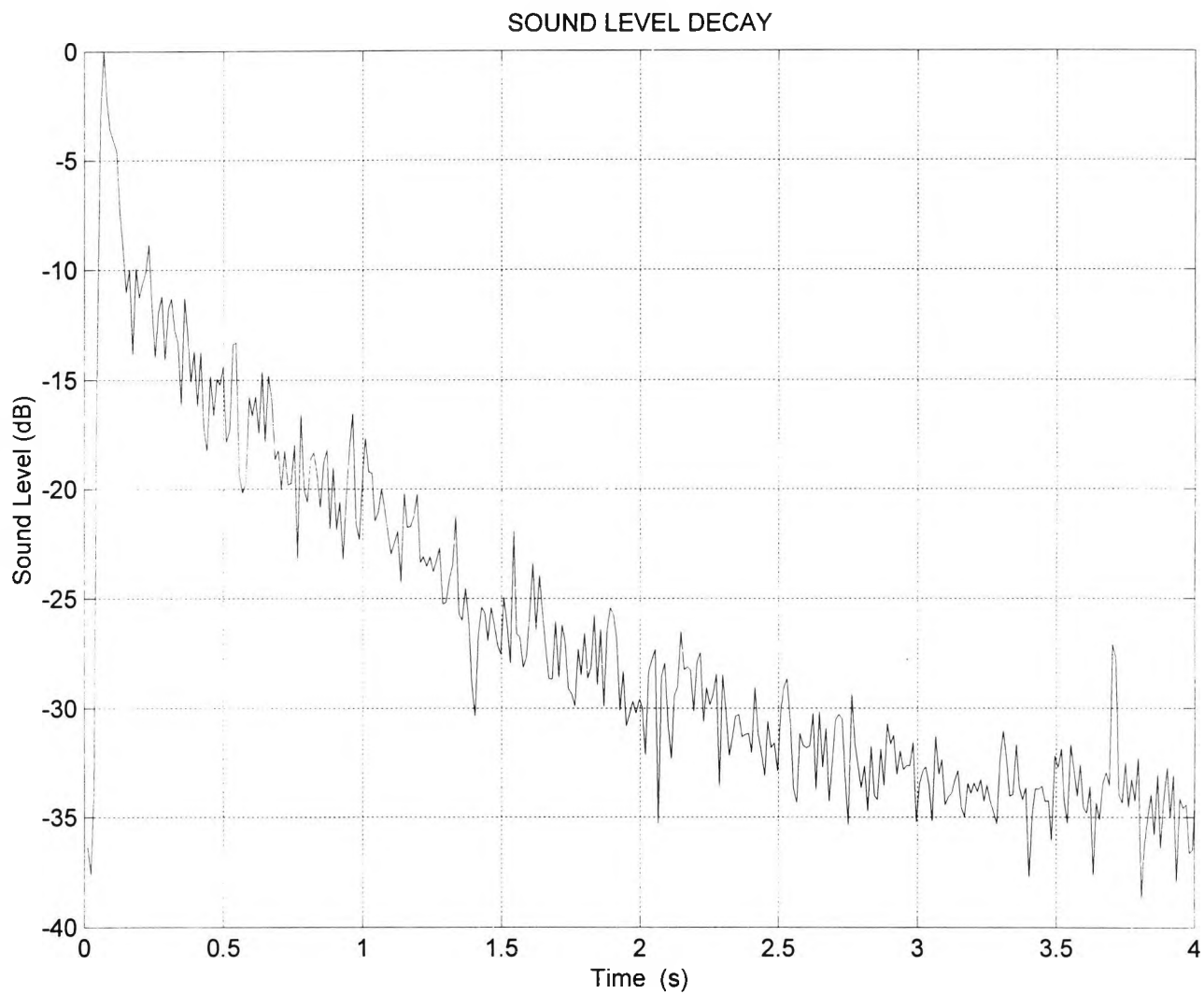


FIGURE 73: ST. PAUL'S CATHEDRAL, MEASURED RESPONSE FOR THE RECEIVER UNDER THE DOME (1 KHZ).

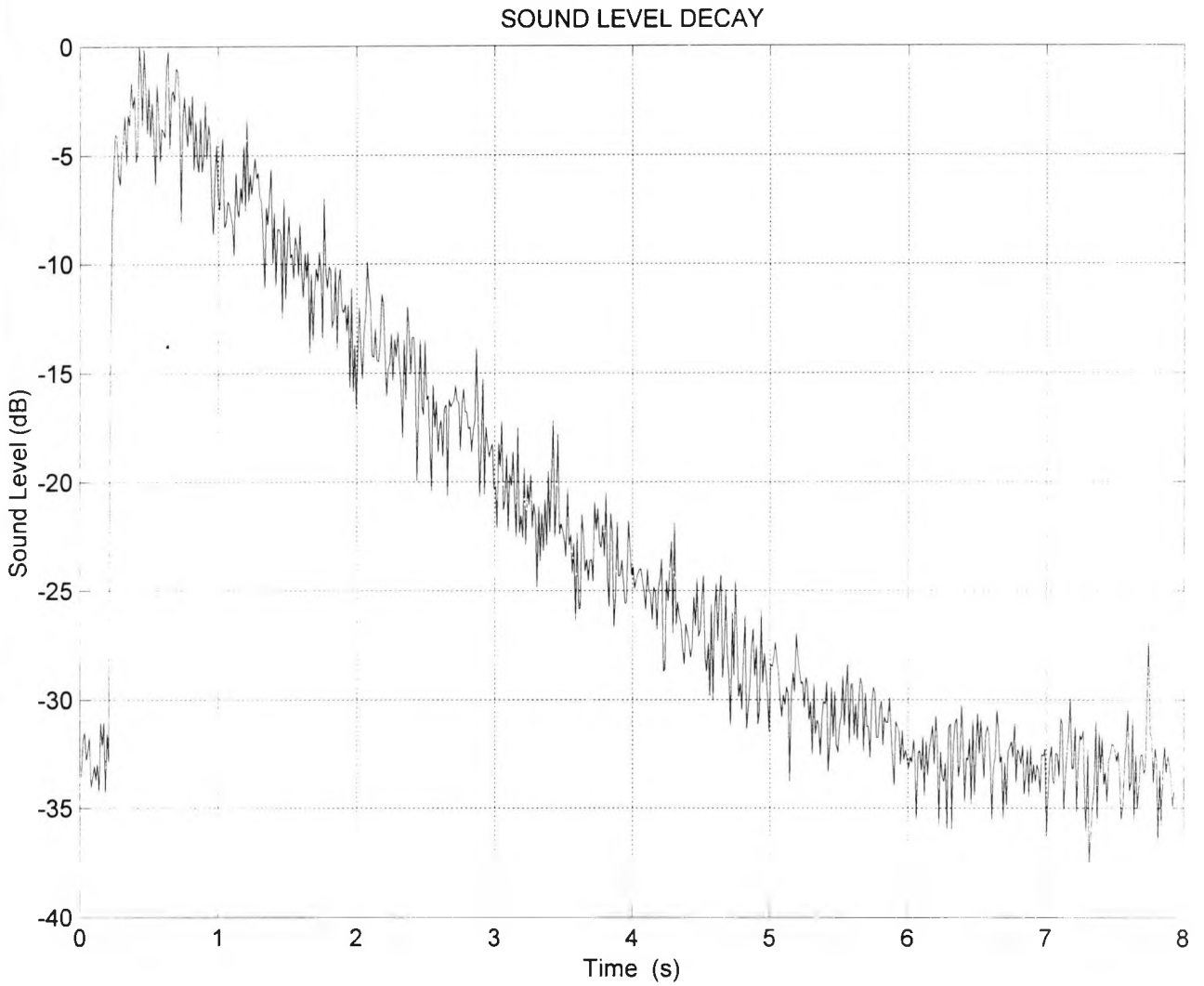


FIGURE 74: ST. PAUL'S CATHEDRAL, COUPLING BETWEEN THE CHOIR AND THE AREA UNDER THE DOME (1 KHZ).

INTEGRATED SOUND DECAY CURVE

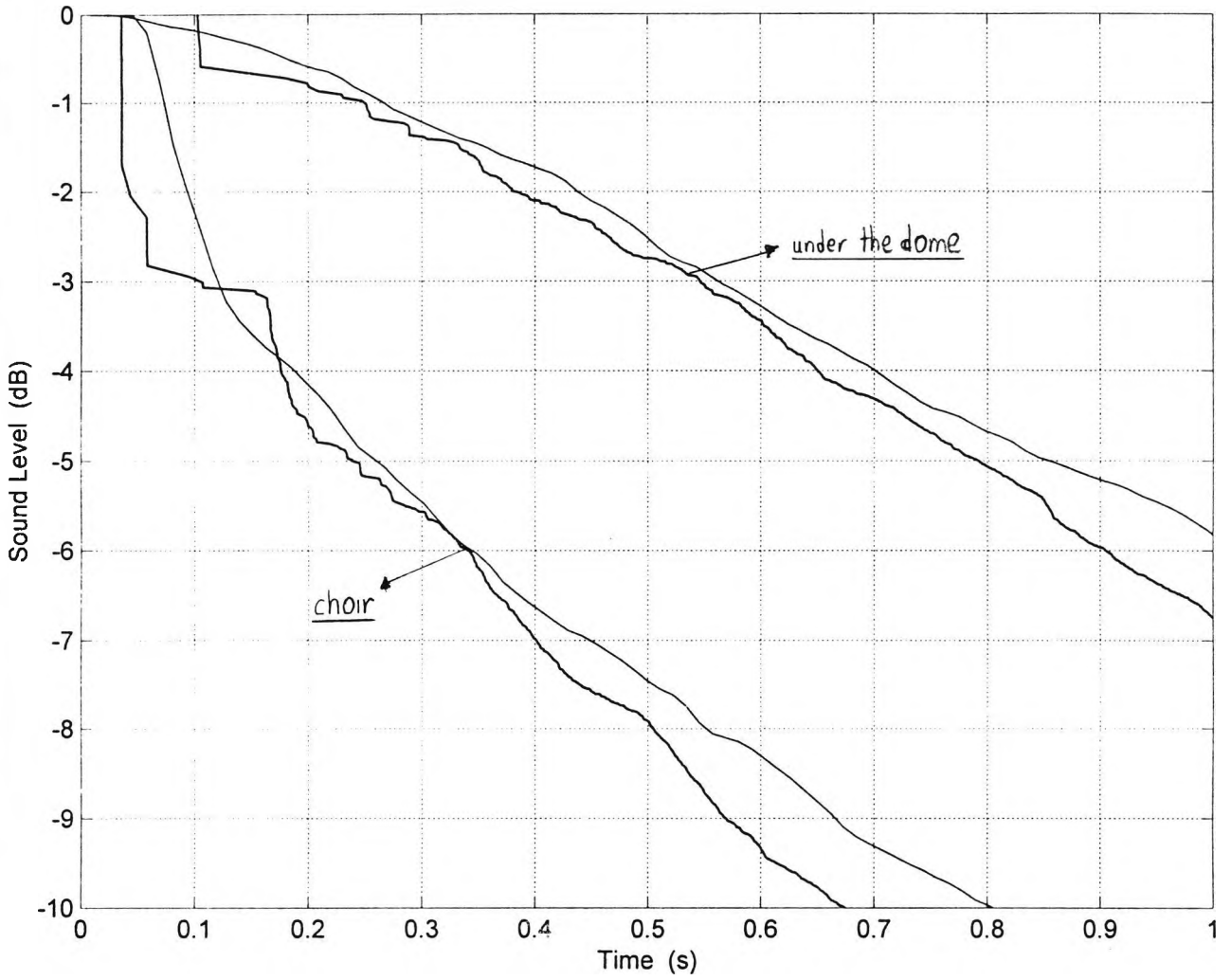
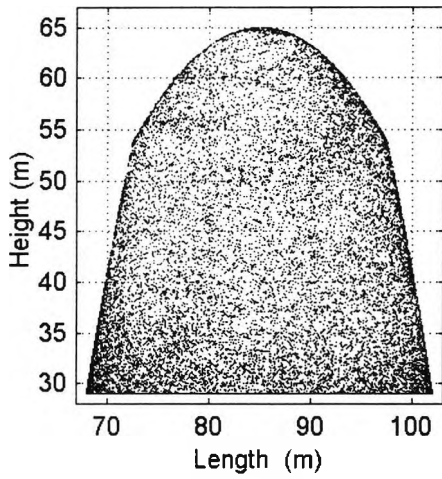
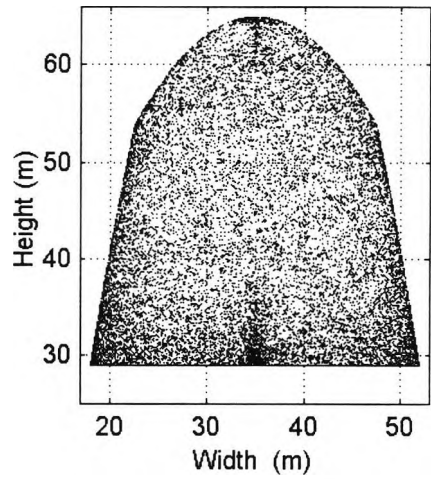


FIGURE 75: WHISPERING GALLERY – DOME, SOUND PARTICLE SPATIAL DISTRIBUTION.

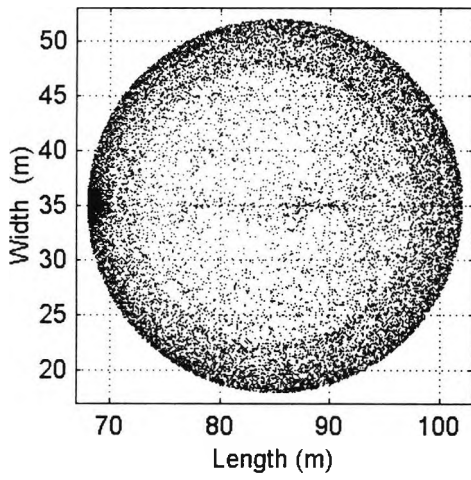
FRONT VIEW



ELEVATION



PLAN VIEW



ISOMETRIC VIEW

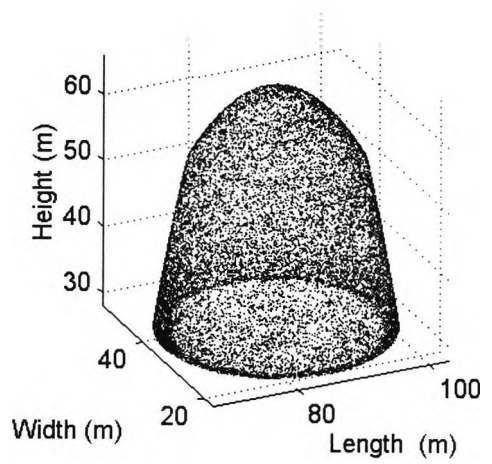


FIGURE 76: WHISPERING GALLERY - DOME, SOUND RAY PATHS (HORIZONTAL VIEW).

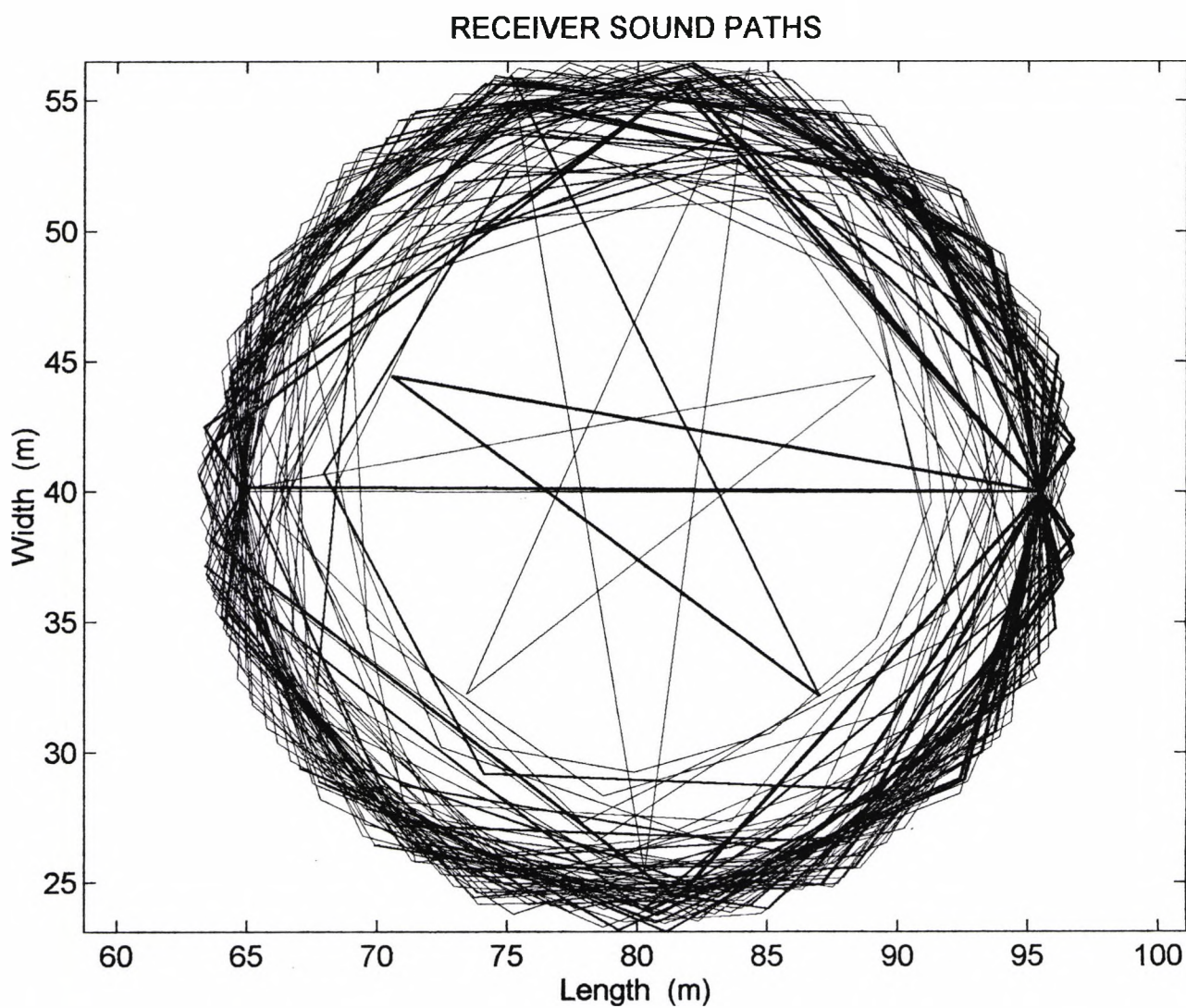
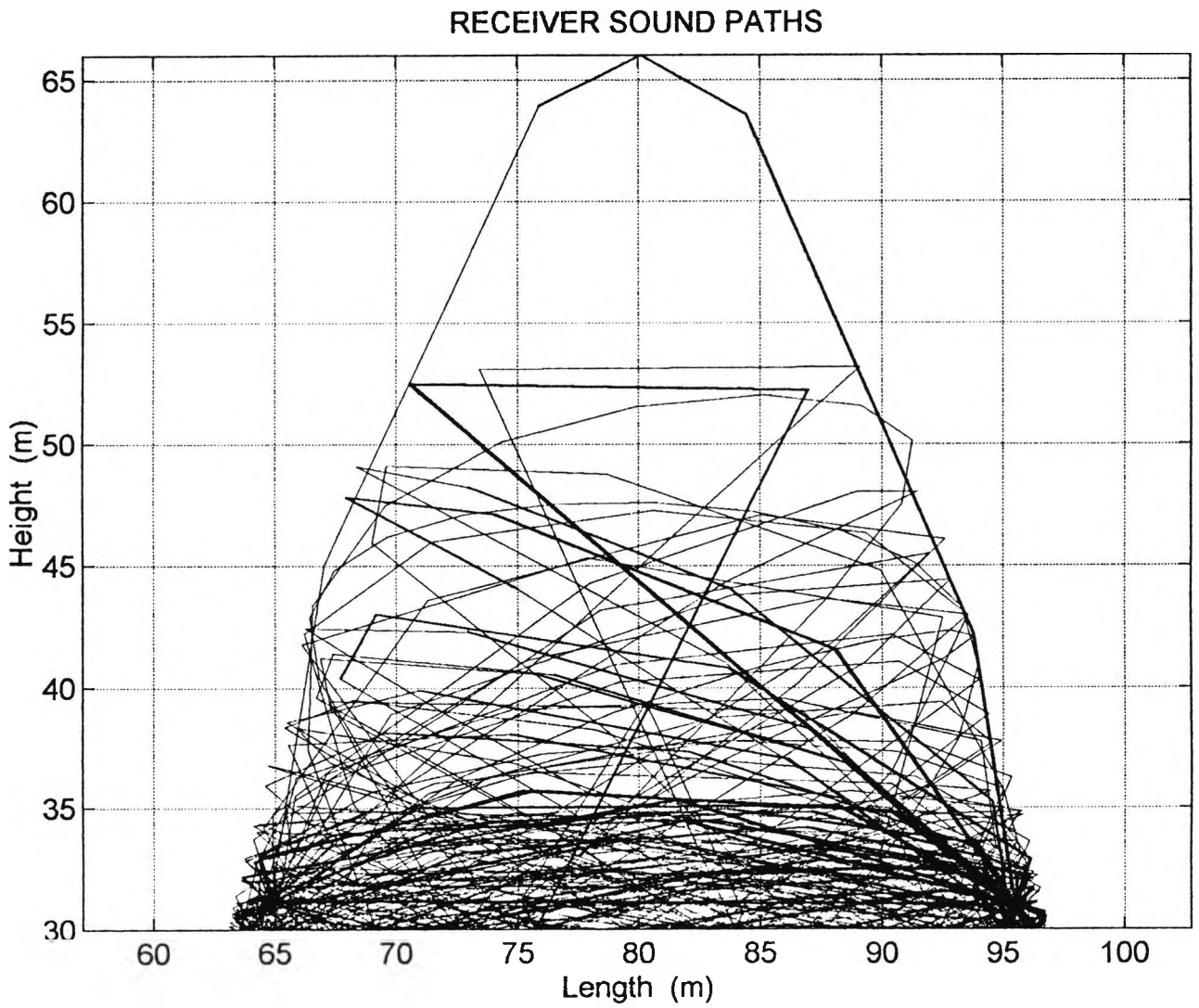


FIGURE 77: WHISPERING GALLERY - DOME, SOUND RAY PATHS (VERTICAL VIEW).



**FIGURE 78: WHISPERING GALLERY, HEDGEHOG DIAGRAM
INDICATING THE DIFFUSIVITY OF THE FIELD.**

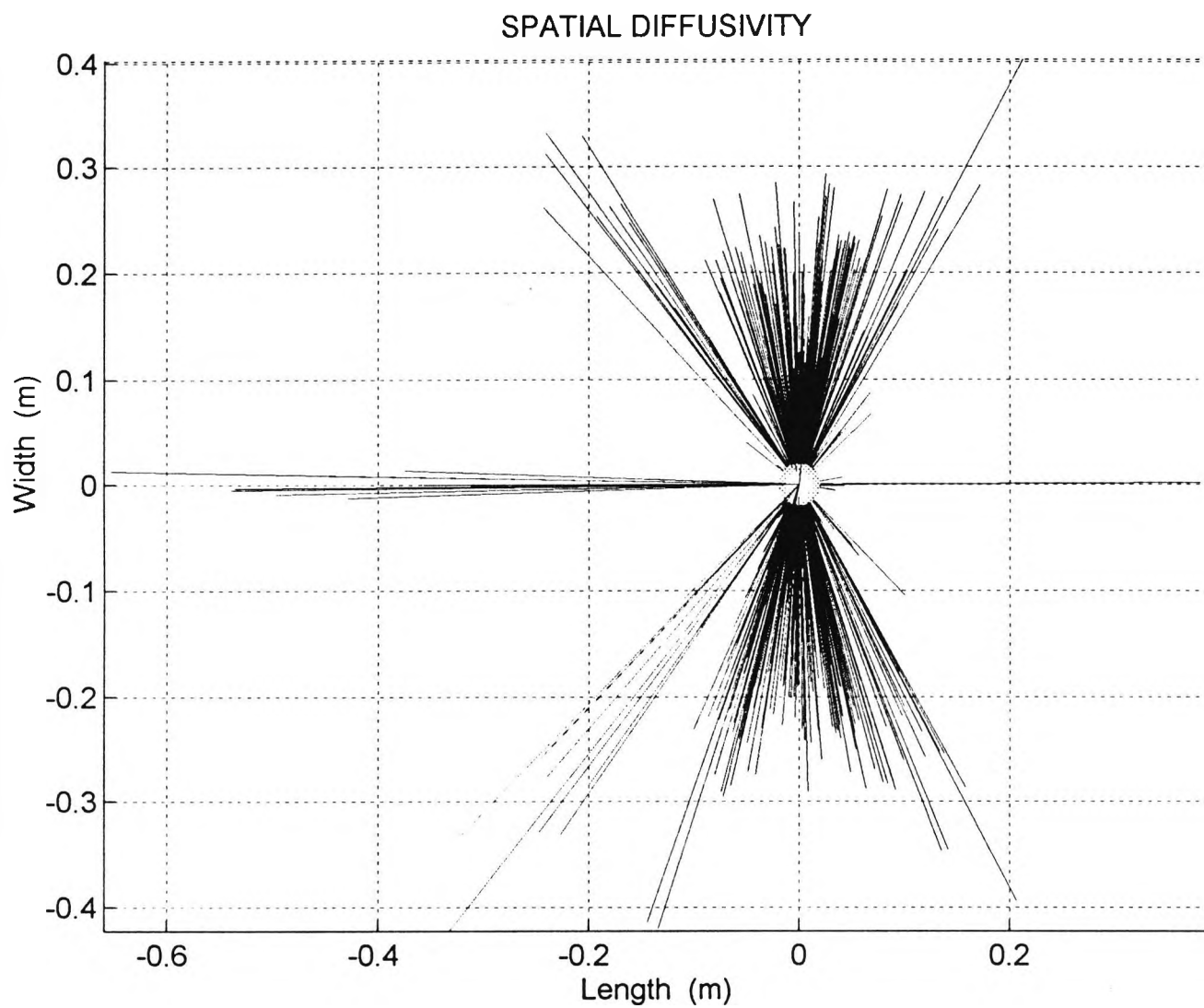


FIGURE 79: WHISPERING GALLERY, DIFFUSION MAP.

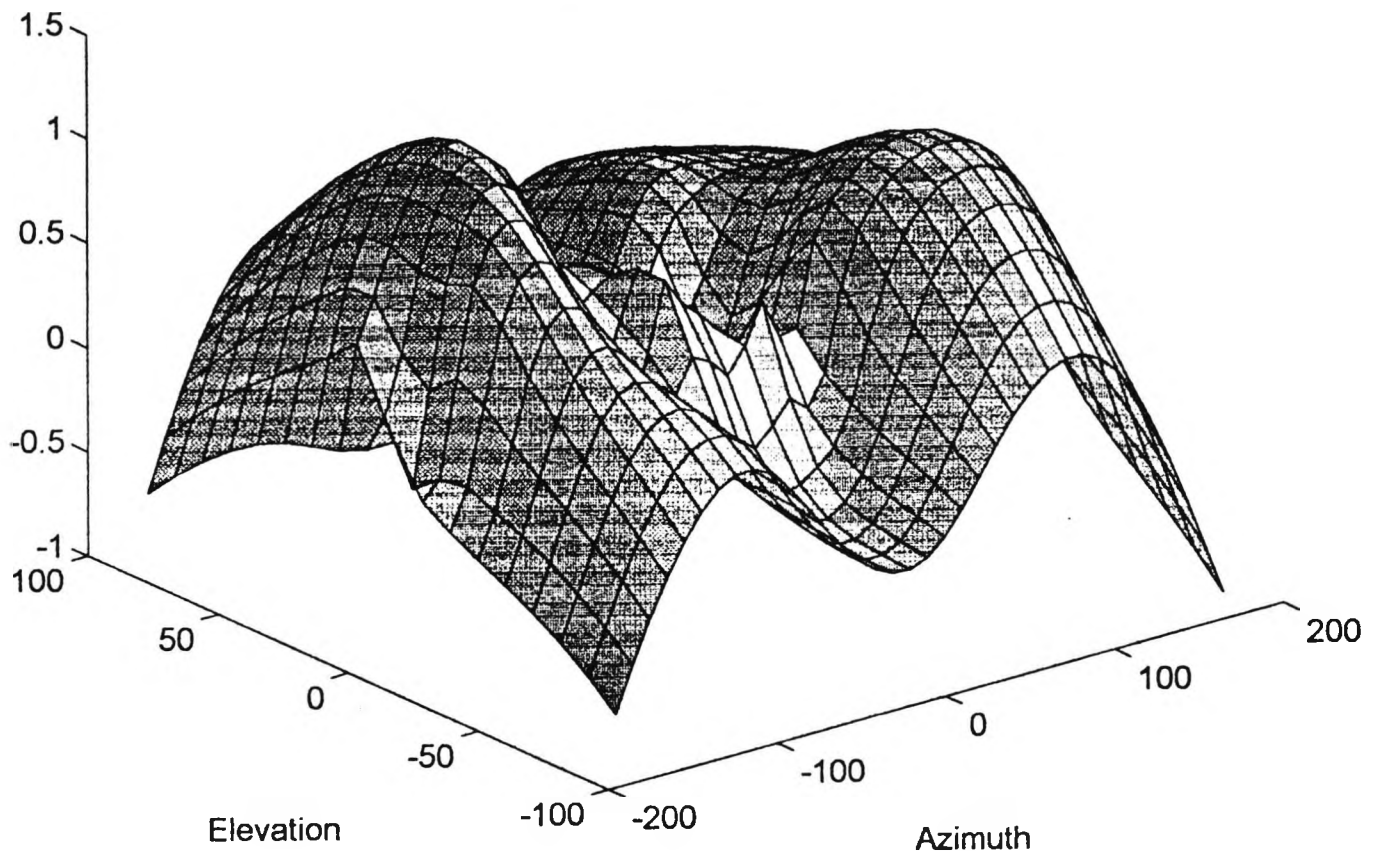


FIGURE 80: WHISPERING GALLERY, COMPARISON BETWEEN THEORETICAL AND SIMULATED RESULTS.

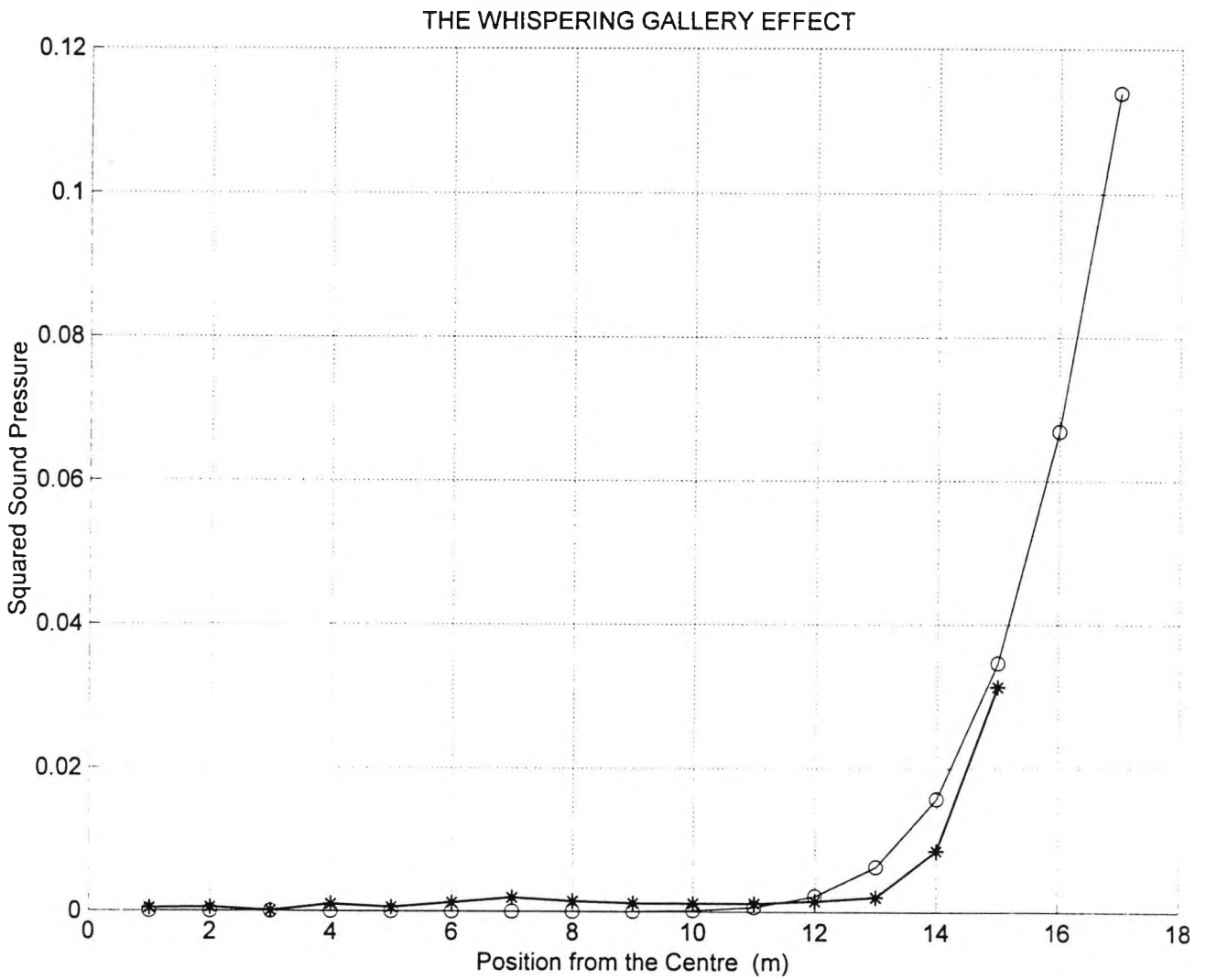
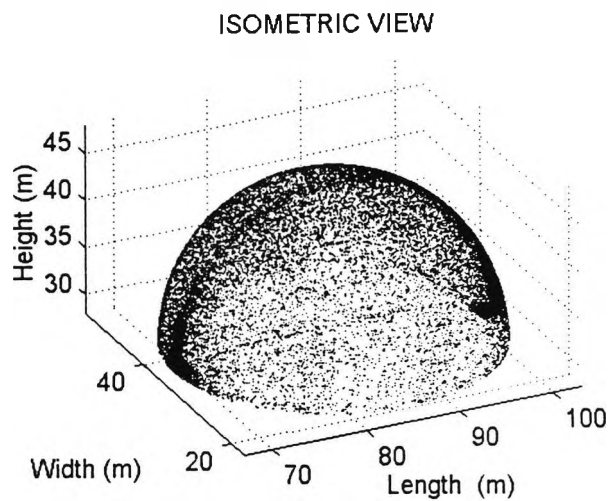
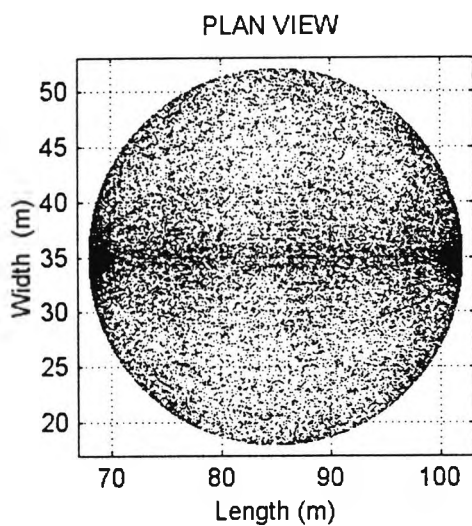
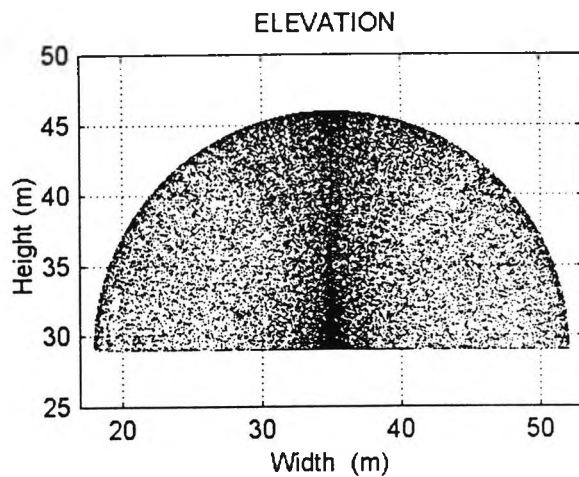
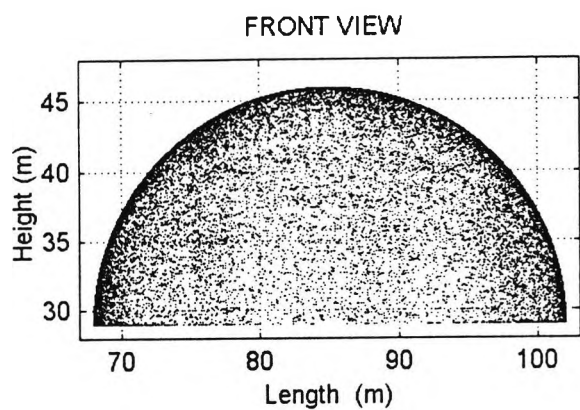


FIGURE 81: WHISPERING GALLERY, THE EFFECT OF HAVING A SPHERICAL DOME.



REFERENCES

-
- ¹ Malecki, I., *Physical Foundations of Technical Acoustics*, Pergamon Press Ltd, Oxford, 1969.
- ² Kleiner, M., Orłowski, R., Kirszenstein, J., A comparison between results from a physical scale model and a computer image source model for architectural acoustics, *Applied Acoustics*, **38** 1993, p.p. 245-67.
- ³ Wright, J.R., An exact model of acoustic radiation in enclosed spaces, *J. Audio Eng. Soc.*, **43**(10) 1995, p.p. 813-820.
- ⁴ Hodgson, M., On the accuracy of models for predicting sound propagation in fitted rooms, *J. Acoust. Soc. Am.*, **88**(2) 1990, p.p. 871-78.
- ⁵ Stephenson, U., Comparison of the image source method with the sound particle simulation method, *Applied Acoustics*, **29** 1990, p.p. 35-72.
- ⁶ Wright, J.R., Acoustic modelling of enclosed spaces, *Acoustics Bulletin*, September/October 1996, p.p. 10-12.
- ⁷ Kuttruff, H., Some remarks on the simulation of Sound reflection from curved walls, *Acustica*, **77** 1992, p.p. 176-82.
- ⁸ Schroeder, M.R., Digital simulation of sound transmission in reverberant spaces, *J. Acoust. Soc. Am.*, **47**(2) 1969, p.p. 424-431.
- ⁹ Papageorgiou, G.N., Computer modelling of sound fields in bounded spatial systems – extension of the ray method to curved surfaces, *Compac* **97**, 1997.
- ¹⁰ Van Rietschote, H.F., Houtgast, T., Steeneken, H.J.M., Predicting speech intelligibility in rooms from the modulation transfer function IV: A ray-tracing computer model, *Acustica*, **49** 1981, p.p. 245-252.
- ¹¹ Kulowski, A., Error investigation for the ray tracing technique, *Applied Acoustics*, **15** 1982, p.p. 263-74.
- ¹² Dance, S.M., The development of computer models for the prediction of sound distribution in fitted non-diffuse spaces, Ph.D Thesis, South Bank University, London, UK, 1993.
- ¹³ Anderson, J.S., Bratos-Anderson, M., *Noise, its measurement, analysis, rating and control*, Avebury Technical, England, UK, 1993.
- ¹⁴ Cremer, L., Muller, H., *Principles and applications of room acoustics*, Applied Science Publishers, London, UK, 1982.
- ¹⁵ Kuttruff, H., *Room Acoustics*, Elsevier Science Publishers, London, UK, 1991.
- ¹⁶ Beranek, L.L., Ver, I.L., *Noise and vibration control engineering, principles and applications*, John Wiley & Sons, Inc., USA, 1992.
- ¹⁷ Pierce, A.D., *Acoustics, an introduction to its physical principles and applications*, McGraw-Hill, Inc., USA, 1981.
- ¹⁸ Kinsler, L.E., Frey, A.R., *Fundamentals of Acoustics*, John Wiley & Sons, Inc., London, 1962.
- ¹⁹ Ando, Y., *Concert Hall Acoustics*, Springer-Verlag, Berlin Heidelberg, 1985.
- ²⁰ Blauert, J., *Spatial Hearing*, MIT Press, Massachusetts, USA, 1997.
- ²¹ Schroeder, M.R., Gerlach, R.E., Diffuse sound reflection by maximum-length sequences, *J. Acoust. Soc. Am.*, **57** 1975, p.p. 149-150.
- ²² Morse, P.M., *Vibration and Sound*, McGraw-Hill, New York, 1948.
- ²³ Rayleigh, J.W.S., *The theory of sound*, Dover Publications, 1945.
- ²⁴ Born, M., Wolf, E., *Principles of Optics*, Pergamon Press, 1975.
- ²⁵ Kennard, E.H., *Kinetic theory of gases with an introduction to statistical mechanics*, McGraw-Hill, New York, 1938.
- ²⁶ Hunt, F.V., Remarks on the mean free path problem, *J. Acoust. Soc. Am.*, **36** 1964, p.p. 556-564.
- ²⁷ Kosten, C.W., The mean free path in room acoustics, *Acustica*, **10** 1960, p.p. 245-250.

- ²⁸ Thiele, R., Richtungsverteilung und Zeitfolge der Schallruckwürfe in Raumen, *Acustica*, **3** 1953, p.p. 291-302.
- ²⁹ Reichardt, W., Alim, D.A., Schmidt, W., Definition und Messgrundlungen eines objektiven Masses zur Ermittlung der Grenze zwischen brauchbarer und unbrauchbarer Durchsichtigkeit bei Musikdarbeitungen, *Acustica*, **32** 1975, p.p. 126-137.
- ³⁰ Jordan, V., *Acoustical Design of Concert Halls and Theatres*, Applied Science Publishers, London, 1980.
- ³¹ Proakis, J.G., Manolakis, D.G., *Introduction to Digital Signal Processing*, Prentice Hall, 1994.
- ³² Kuttruff, K.H., Auralization of impulse responses modelled on the basis of ray tracing results, *J. Audio Eng. Soc.*, **41**(11) 1993, p.p. 876-880.
- ³³ *Programs for Digital Signal Processing*, IEEE, John Wiley & Sons, 1979 Chapter 8.
- ³⁴ *Programs for Digital Signal Processing*, IEEE, John Wiley & Sons, 1979 Algorithm 8.1.
- ³⁵ Schroeder, M.R., A new method of measuring reverberation time, *J. Acoust. Soc. Am.*, **37** 1965, p.p.409-412.
- ³⁶ Kulowski, A., Relationship between impulse response and other types of room acoustical responses, *Applied Acoustics*, **15** 1982, p.p. 3-10.
- ³⁷ Oppenheim, A.V., Schafer, R.W., *Digital Signal Processing*, Prentice-Hall, 1975, p. 556.
- ³⁸ Schroeder, M.R., Kuttruff, K.H., On frequency response curves in rooms. Comparison of experimental, theoretical and Monte Carlo for the average frequency spacing between maxima, *J. Acoust. Soc. Am.*, **34** 1962, p.p. 76-80.
- ³⁹ Kleiner, M., Dalenback, B., Svensson, P., Auralization-an overview, *J. Audio Eng. Soc.*, **41**(11) 1993, p.p. 861-875.
- ⁴⁰ Spandock, F., Akustische Modellversuche, *Ann. Physik V*, **20** 1934, p.p. 345-360.
- ⁴¹ Davis, A.H., Kaye, G.W.C., *The Acoustics of Buildings*, Bell, London, 1927.
- ⁴² Sabine, W.C., *Collected papers on acoustics*, Harvard University Press, Cambridge, Mass., 1922.
- ⁴³ Pinnington, R.J., Nathanail, C.B., Modelling auditorium acoustics with light, *Applied Acoustics*, **37** 1993, p.p. 21-46.
- ⁴⁴ Mackenzie, R. (ED), *Auditorium Acoustics*, Applied Science Publishers Ltd, London, 1975.
- ⁴⁵ Kuttruff, H., Acoustical design of the Chiang Kai Shek cultural centre in Taipei, *Applied Acoustics*, **27** 1989, p.p. 27-46.
- ⁴⁶ Xiang Duanqi, Wang Zheng, Chen Jinjing, Ge Yangang, Acoustic design of Beijing Theater, *Applied Acoustics*, **37** 1992, p.p. 15-30.
- ⁴⁷ Braat-Eggen, P.E., Van Luxemburg, L.C.J., Booy, L.G., A new concert hall for the city of Eindhoven - Design and model tests, *Applied Acoustics*, **40** 1993, p.p. 3-10.
- ⁴⁸ Eyring, C. F., Reverberation time in "dead" rooms, *J. Acoust. Soc. Am.*, **1** 1930, p.p. 217-241.
- ⁴⁹ Allen, J.B., Berkley, D.A., Image method for efficiency simulating small room acoustics, *J. Acoust. Soc. Am.*, **65** 1979, p.p. 943-50.
- ⁵⁰ Barron, M.F.E., The effects of early reflections on subjective acoustical quality in concert halls, Ph.D. thesis, University of Southampton, January 1974.
- ⁵¹ Baxa, D.E., A strategy for the optimum design of acoustic space, Ph.D. thesis, University of Wisconsin-Madison, 1976.
- ⁵² Borish, J., Extension of the image model to arbitrary polyhedra, *J. Acoust. Soc. Am.*, **75** 1984, p.p. 1827-36.
- ⁵³ Vorlander, M., Simulation of the transient and steady state sound propagation in rooms using a new combined ray-tracing/image-source algorithm, *J. Acoust. Soc. Am.*, **86** 1989, p.p. 172-8.

- ⁵⁴Krokstad, A., Strom, S., Sorsdal, S., Calculating the acoustical room response by the use of a ray tracing technique, *J. Sound Vib.*, **8**(1) 1968, p.p.118-25.
- ⁵⁵Vian, J.P., Van Maercke, D., Calculation of room impulse response using a ray tracing method, *12th ICA, Proceedings of the Vancouver Symposium*, 1986, p.p.74-8.
- ⁵⁶Lewers, T., A combined beam tracing and radiant exchange computer model of room acoustics, *Applied Acoustics*, **38** 1993, p.p. 161-79.
- ⁵⁷Allred, J.C., Newhouse, A., Applications of the Monte Carlo method to architectural acoustics, *J. Acoust. Soc. Am.*, **30**(1) 1958 1-3; **30**(10) 1958 903-4.
- ⁵⁸Krokstad, A., Strom, S., Acoustical design of the multipurpose 'Hjertnes' hall in Sandefjord, *Applied Acoustics*, **12** 1979 p.p. 45-63.
- ⁵⁹Krokstad, A., Strom, S., Sorsdal, S., Fifteen years' experience with computerised ray tracing, *Applied Acoustics*, **16** 1983, p.p. 291-312.
- ⁶⁰Strom, S., Dahl, H., Krokstad, A., Eknes, E., Acoustical design of the Grieg Memorial Hall in Bergen, *Applied Acoustics*, **18** 1985, p.p. 127-142.
- ⁶¹Santon, F., Numerical prediction of echograms and of the intelligibility of speech in rooms, *J. Acoust. Soc. Am.*, **59**(6) 1976, p.p. 1399-1405.
- ⁶²Lehnert, H., Systematic errors of the ray-tracing algorithm, *Applied Acoustics*, **38** 1993, p.p. 207-22.
- ⁶³Shield B.M., A computer model for the prediction of factory noise, *Applied Acoustics*, **13** 1980, p.p. 471-486.
- ⁶⁴Mehta, M.L., Mulholland, K.A., Effect of non-uniform distribution of absorption on reverberation time, *J. Sound Vib.*, **46** 1985, p.p. 209-224.
- ⁶⁵Jovicic, S., *Anleitung zur Voraubestimmung des Schallpegels in Betriebsgebäuden* (Muller-BBM GmbH, Plannegg bei Munchen, 1979).
- ⁶⁶Hodgson, M.R., Physical and theoretical models as tools for the study of factory sound fields, Ph.D. dissertation, University of Southampton, 1983.
- ⁶⁷Lindqvist, E.A., Sound attenuation in large factory spaces, *Acoustica*, **50** 1982, p.p. 313-328.
- ⁶⁸Lindqvist, E.A., Noise attenuation in factories, *Applied Acoustics*, **16** 1983, p.p. 183-214.
- ⁶⁹Lemire, G.R., Nicolas, J., *Noise Control Engineering Journal*, **24** 1985, p.p. 58-67.
- ⁷⁰Kurze, U.J., Scattering of sound in industrial spaces, *J. Sound Vib.*, **98** 1985, p.p. 349-364.
- ⁷¹Ondet, A.M., Barby, J.L., Modelling of sound propagation in fitted workshops using ray tracing, *J. Acoust. Soc. Am.*, **85**(2) 1989, p.p. 787-796.
- ⁷²Hodgson, M.R., Factory noise prediction using ray tracing - experimental validation and the effectiveness of noise control measures, *Noise Control Engineering Journal*, **33**(3) 1989, p.p. 97-104.
- ⁷³Moore, G.R., An approach to the analysis of sound in auditoria, Ph.D. Thesis, University of Cambridge, UK, 1984.
- ⁷⁴Farina, A., RAMSETE - A new pyramid tracer for medium and large scale acoustic problems, *Euro-noise'95*, **1** 1995 p.p. 55-60.
- ⁷⁵Stephenson, U.M., SOPRAN - A sound particle program for room acoustics and noise immission - further improvements for the application to factory halls, *Euro-noise'95*, **1** 1995 p.p. 61-66.
- ⁷⁶Ricol, L., Junker, F., A ray tracing software: RAYON2.0, *Euro-noise'95*, **1** 1995 p.p. 49-54.
- ⁷⁷Ondet, A.M., Barby, J.L., Sound propagation in fitted rooms - comparison of different models, *J. Sound Vib.*, **125** 1988, p.p. 137-149.
- ⁷⁸Verbandt, F.J.R., Jonskheere, R.E., Bench-mark of acoustical ray tracing computer programs, *Inter-noise'93*, 1993 p.p. 1531-1534.

- ⁷⁹ Dance, S.M., Shield, B.M., Comparison of three computer models for the prediction of sound propagation in an enclosed space, *Inter-noise'93*, 1993 p.p. 1535-1538.
- ⁸⁰ Rindel, J.H., Room acoustical designing with a computer model and an audio mainframe for auralization, *Western Pacific Regional Acoustic Conference*, Seoul, Korea, August 1994.
- ⁸¹ Rindel, J.H., Naylor, G., Rishoj, K., The use of a digital audio mainframe for room acoustical auralization, *The 96th Convention*, AES, Amsterdam, February 1994.
- ⁸² Naylor, G.M., Odeon-another hybrid room acoustical model, *Applied Acoustics*, **38** 1993, p.p. 131-45.
- ⁸³ Naylor, G., Rindel, J.H., Predicting room acoustical behaviour with the Odeon computer model, *The 124th ASA Meeting*, New Orleans, November 1992.
- ⁸⁴ Klasco, M., JBL's CADP revisited, *Sound & Communications*, September 1990, p.p.66-69.
- ⁸⁵ Staffeldt, H., Modelling of room acoustics and loudspeakers in JBL's Complex Array Design Program CADP2, *Applied Acoustics*, **38** 1993, p.p. 179-94.
- ⁸⁶ Maercke, D., Martin, J., The prediction of echograms and impulse responses within the Epidaure software, *Applied Acoustics*, **38** 1993, p.p. 93-114.
- ⁸⁷ Emerit, M., Martin, J., EBINAUR PC: A software for auralization, *Euro-noise'95*, **1** 1995 p.p. 67-72.
- ⁸⁸ Klasco, M., EASE version 1.0 from Renkus-Heinz, Part I, *Sound & Communications*, February 1991, p.p. 66-69.
- ⁸⁹ Klasco, M., Performance simulations and selecting speakers with EASE, Part II, *Sound & Communications*, April 1991, p.p. 66-69.
- ⁹⁰ Ahnert, W., Kanz, H., EASE JR: Faster, simpler and easier to use, *Sound & Video Contractor*, April 1992, p.p. 68-71.
- ⁹¹ Shaw, N., Acoustical design and auralization, *Sound & Communications*, August 1994, p.p. 66-69.
- ⁹² Klasco, M., Sound system design programs and auralization, *Sound & Communications*, October 1993, p.p. 66-69.
- ⁹³ Klasco, M., BOSE Modeler revisited, *Sound & Communications*, November 1990, p.p. 66-69.
- ⁹⁴ D'antonio, P., The DISC project: directional scattering coefficient determination and auralization of virtual environments, *Noise-Con 93 Proc.*, 1993, p.p. 259-264.
- ⁹⁵ Pleeck, D., De Geest, E., The practical application of a ray tracing program in industrial noise control, *Euro-noise'95*, **1** 1995 p.p. 43-48.
- ⁹⁶ Meng, X.W., De Borger, G., Van Overmeire, M., Numerical simulation of the acoustical behaviour of rooms using RAYNOISE, *Euro-noise'95*, **1** 1995 p.p. 121-26.
- ⁹⁷ De Geest, E., Applications of the conical beam method in architectural industrial and environmental acoustics, *Inter-noise 93*, 1993 p.p. 1539-43.
- ⁹⁸ Gimenez, A., Marin, A., Model of energy calculation of acoustic analysis of closed rooms, *Applied Acoustics*, **26** 1989, p.p. 99-111.
- ⁹⁹ Kulowski, A., Algorithmic representation of the ray tracing technique, *Applied Acoustics*, **18** 1985, p.p. 449-469.
- ¹⁰⁰ Kulowski, A., Optimisation of a point-in-polygon algorithm for computer models of sound field in rooms, *Applied Acoustics*, **35** 1992, p.p. 63-74.
- ¹⁰¹ American National Standard, Method for the calculation of the absorption of sound by the atmosphere, *Published by the American Institute of Physics for the Acoustical Society of America*, ANSI S1.26-1978.
- ¹⁰² Lenhert, H., Blauert, J., Berechnung von langen impulsantworten durch ein schnelles Strahlverfolgungsverfahren (Calculation of long impulse responses with a fast ray-tracing algorithm), *Fortschritte der Akustik, DAGA '91*, DPG-GmbH, Bad Honef, 1991, p.p. 637-640.

-
- ¹⁰³ Dance, S.M., Shield, B.M., The effect of prediction accuracy of reducing the number of rays in a ray tracing model, *Inter-noise 94*, 3 1994, p.p. 2127.
- ¹⁰⁴ Vorlander, M., Revised relation between the sound power and the average pressure level in rooms and consequences for acoustic measurements, *Acustica*, 81 1995, p.p. 332-341.
- ¹⁰⁵ Hanselman, D., Littlefield, B., *Mastering MATLAB*, Prentice-Hall, 1996.
- ¹⁰⁶ McCarthy, T., *AutoCAD for windows express*, Springer-Verlag, 1994.
- ¹⁰⁷ Bramer, B., Bramer, S., *C++ for engineers*, Arnold, 1996.
- ¹⁰⁸ Smith, J.T., *C++ applications guide*, McGraw-Hill, 1993.
- ¹⁰⁹ Rumbaugh, T., *Object-Oriented modelling and design*, Prentice-Hall, 1994.
- ¹¹⁰ Shlaer, S., Mellor, S.J., *Object lifecycles modelling the world in data*, Prentice-Hall, 1993.
- ¹¹¹ Zeid, I., *CAD/CAM theory and practice*, McGraw Hill, 1991.
- ¹¹² Keung, T.W., Behaviour of Sound in Corridors, BSc Dissertation, City University, 1990.
- ¹¹³ Parkin, P.H., Taylor, J.H., Speech reinforcement in St. Paul's Cathedral – experimental system using line-source loudspeakers and time delays, *Wireless World*, 58 1952, p.p.54-57.
- ¹¹⁴ Parkin, P.H., Taylor, J.H., Speech reinforcement in St. Paul's Cathedral – details of the equipment and results of tests, *Wireless World*, 58 1952, p.p. 109-111.
- ¹¹⁵ Poley, St. Paul's Cathedral.
- ¹¹⁶ Lewers, T.H., The acoustics of St. Paul's Cathedral, BSc Dissertation, City University, 1982.
- ¹¹⁷ Anderson, J.S., Jacobsen, T, RASTI Measurements in St. Paul's Cathedral, London, *B&K Application Note*.
- ¹¹⁸ Rayleigh, J.W.S., The problem of the whispering gallery, *Philosophical Magazine*, 20 1910, p.p. 1001-1004.
- ¹¹⁹ Rayleigh, J.W.S., Further applications of Bessel's functions of high order to the whispering gallery and allied problems, *Philosophical Magazine*, 27 1914, p.p. 100-109.